Faculty of Science, Charles University in Prague
Institute of Microbiology, ASCR, v.v.i.

Heat-induced stress granules of *Saccharomyces cerevisiae*

MSc. Tomáš Groušl

PhD Thesis

Supervisor Jiří Hašek, PhD.

Prague 2014

I declare that I wrote the thesis myself, only with a help of referred literature.
The thesis serves only and exclusively for my PhD graduation on Faculty of Science of Charles University in Prague.

Prague, 20.12.2013

Tomáš Groušl

Rád bych na tomto místě poděkoval všem, kteří mi pomáhali a podporovali mě v mém vědeckém úsilí. Speciální díky patří všem členům Laboratoře reprodukce buňky, vedené bezvadným šéfem Jiřím Haškem. Druhé speciální díky patří mé rodině, která to se mnou nejenom celou tu dobu vydržela, ale byla mi vždy oporou. Stejně tak děkuji Martině, která je světlem mého života. Jsem opravdu moc rád, že vás všechny okolo sebe mám.

Can science boldly go where "Star Trek" has already been?

Abstract (*English*)

In response to environmental stresses, cells try to adapt to changed living conditions. Regulation of translation process provides fast-responding and versatile system enabling execution of stress-induced expression program. Messenger ribonucleoprotein complexes (mRNPs) engaged in translation and mRNA turnover are remodelled and may accumulate into higher-order assemblies, in connection to stress-induced translational changes. Stress granules (SGs) and processing bodies (PBs) are examples of such assemblies. Through them, further fate of mRNA molecules and certain translation machinery components is determined. In an effort to better understand the entire role of SGs in cellular metabolism, we performed the analysis of heat-induced SGs in model organism *Saccharomyces cerevisiae*. We contributed to the finding that SGs phenomenon is evolutionary conserved in eukaryotic kingdom proving that SGs are formed also in unicellular yeast *S. cerevisiae* under robust heat stress. The SGs reassemble their counterparts from higher eukaryotes in core composition and proposed functions. However, they possess also unique nature, which seems to be specific to the yeast. We further extended the data about heat-induced SGs, with a focus on additional composition, dynamics, associated proteins and a relation to other cellular structures. One of SGs-associated protein, Mmi1, was characterized in detail. This multifunctional protein was found to be engaged in heat stress response of the yeast, most probably, by its association with both SGs and protein degradation machinery. Taken together, we established model of heat-induced SGs in yeast *S. cerevisiae* and further contributed to the knowledge about SGs phenomenon, which participates in cellular metabolism and stress response. Moreover, in an effort to analyse connection of *Reactive Species*-producers to heat-induced SGs and to cell physiology in general, we extended data about functioning of NOX (NADPH oxidase) enzymes in cell physiology identifying and further characterizing a member of this protein family in yeast *S. cerevisiae*, Yno1 protein. Our evidence about this extramitochondrial *Reactive Species*-producer brings new data about the protein role in the yeast physiology.

Abstrakt (*česky*)

Jedna ze základních charakteristik živých organismů je snaha adaptovat se na měnící se životní podmínky. Regulace translace poskytuje rychlý a široce použitelný mechanismus pro realizaci stresem indukovaných změn. Komplexy mRNA molekul a asociovaných proteinů, které se účastní translace a dalších procesů spojených s mRNA molekulami, podléhají vlivem stresu strukturním změnám. Tyto změny mohou vést k akumulaci zmíněných komplexů do struktur vyššího řádu, jako jsou *stress granules* (stresové granule) nebo *processing bodies*. O dalším osudu mRNA molekul a některých součástí translačního aparátu buňky za stresu, se rozhoduje prostřednictvím právě těchto akumulací. Ve snaze detailně porozumět úloze stresových granulí v buněčném metabolismu, jsme v naší laboratoři blíže analyzovali teplem indukované stresové granule kvasinkového modelového organismu *Saccharomyces cerevisiae*. Zjištěním, že se stresové granule tvoří také v tomto jednobuněčném eukaryotickém organismu, jsme přispěli k poznání, že fenomén stresových granulí je evolučně konzervovaný napříč eukaryotickou říší. Teplem indukované stresové granule kvasinky *S. cerevisiae* se podobají stresovým granulím evolučně vyšších eukaryot složením a v navrhovaných metabolických funkcích. Nicméně, tyto granule jsou také v některých ohledech jedinečné a tvoří tak kvasinkově specifický typ stresových granulí. Analýzou jejich složení, dynamiky, asociovaných proteinů a vztahu k dalším buněčným strukturám, jsme je dále detailněji charakterizovali. Následně jsme se zaměřili na jeden z jejich asociovaných proteinů, na protein Mmi1. Navrhli jsme možnou úlohu tohoto multifunkčního proteinu v buněčné odpovědi na stress, ve spojitosti s jeho asociací s teplem indukovanými stresovými granulemi a degradačním systémem proteinů za teplotního stresu. V souhrnu, jsme zavedením a bližším charakterizováním modelu teplem indukovaných stresových granulí kvasinky *S. cerevisiae* přispěli k detailnějšímu pochopení fenoménu stresových granulí, který hraje roli v odpovědi na stress a buněčném metabolismu obecně. Ve snaze analyzovat vliv buněčných producentů *Reactive Species* (volných radikálů) na teplem indukované stresové granule a na fyziologický stav buňky obecně, jsme přispěli k bližšímu pochopení funkce zástupce NOX (NADPH oxidázových) enzymů a zároveň nemitochondriálního producenta volných radikálů u kvasinky *S. cerevisiae*, proteinu Yno1, v buněčném metabolismu. Identifikováním a bližší charakterizací zástupce této proteinové rodiny u kvasinky *S. cerevisiae*, jsme napomohli k detailnějšímu pochopení úlohy NOX enzymů v metabolických procesech buňky.

Table of contents

List of abbreviations

ASCR	- Academy of Sciences of the Czech Republic
DNA	- deoxy-ribonucleic acid
ERAD	- endoplasmic reticulum-associated protein degradation
GFP	- green fluorescent protein
GTP	- Guanosine-5'-triphosphate
H_2O_2	- hydrogen peroxide
IF	- impact factor
mRNA	- messenger ribonucleic acid
NADPH	- nicotinamide adenine dinucleotide phosphate
PMID	- PubMed identifier
RFP	- red fluorescent protein
rRNA	- ribosomal ribonucleic acid
tRNA	- transfer ribonucleic acid
UTR	- untranslated region
WoS	- Web of Science

1. Introduction

Yeasts are surely ones of the most utilized organisms in biological and medical research and in industrial applications. The yeast cells come along with the mankind for a very long time. Primarily, yeasts were used for such processes as are those linked to food production. Along with a development of the biological science, they became to be priceless tool for a research of the eukaryotic cell. As a mostly single eukaryotic cell, yeasts provide view to nearly all basic cellular processes, mechanisms and structures. Along with the sophisticated arsenal of molecular biology and genetics techniques, yeasts are well established and still promising model organisms.

Nowadays, people try to deal with broad range of biological treats, as are viral and bacterial illnesses, prion and neurodegenerative diseases and cancer. All of these pathologies represent a kind of stress for an organism. A discovery and a better understanding of cellular processes accompanying a stress response help people in an effort to cope with mentioned pathologies. Considering this, yeasts are useful model for a study of stress impact on eukaryotic cell physiology. The research in Laboratory of Cell Reproduction of the Institute of Microbiology of ASCR focuses on heat stress response of *Saccharomyces cerevisiae* regarding translation and mRNA metabolism. In this respect, two major types of stress-responsive intracellular entities are engaged. Those are stress granules and processing bodies.

Stress granules (SGs) appear inside cells upon influence of various stresses. Their appearance reflects alteration in dynamics of translation process. Whilst translation is slow down or completely shut off, certain components of its machinery and up to that time translated mRNA molecules are sequestered into SGs. However, SGs seem to play more diverse role in cellular physiology under a stress, than only as accumulations of translation components. They have been shown to modulate cellular signalling pathways and other processes of the cell participating thus actively on regulation of entire cellular metabolism and cell fate decision. Therefore, SGs are possibly interconnecting sites which link signals between translation and cell metabolism under a stress. Nevertheless, besides beneficial role of SGs, they are also given in the context with certain pathologies, for example, with neurodegenerative and other *unfolded protein* diseases.

In Laboratory of Cell Reproduction, I and my colleagues focused on heat-induced stress granules of yeast *S. cerevisiae*. Despite the presence of SGs was for some time unsure in yeasts, we and others proved that yeast SGs exist and thus that the SGs phenomenon seems

to be evolutionary conserved among eukaryotes. The core composition of the yeast heat-induced SGs reflects constitution of their higher eukaryotes‘ counterparts. However, there is even unique nature of yeast SGs concerning their additional composition and also dynamics. It may suggest evolutionary older and possibly more versatile mechanisms of SGs functioning and translation control under a stress. Nevertheless, we believe that a research on yeast SGs will contribute even to better understanding of functions, dynamics and possible relation to various pathologies of higher eukaryotes‘ SGs, including those of mammals.

Moreover, we additionally focused on cellular *Reactive Species*-producers and their relation to heat-induced SGs and to cell physiology in general. In an effort to link heat-induced stress granules with other cellular processes and structures, we analysed a proposed interconnection between the SGs and the mitochondria. Despite we did not prove that the mitochondria-interacting and the SGs-associated protein Mmi1 is directly engaged in localization of the SGs onto the organelle, we proposed a role for this protein in heat stress response of the yeast cell. Finally, the evidence and new data about extramitochondrial *Reactive Species*-producer and NOX (NADPH oxidase) enzyme, Yno1, help in elucidating of the protein functions in the yeast cell metabolism. Since Yno1 NOX enzyme seems to maintain similar roles in the yeast as are those of NOX enzymes in higher eukaryotes, we believe that further research on Yno1 protein will contribute even in an effort to undercover missing parts in NOX enzymes functioning in cells of higher eukaryotes.

2. Aims of the thesis

I. Analyse effects of heat stress on translation of *Saccharomyces cerevisiae* regarding heat-induced accumulations of messenger ribonucleoprotein complexes (mRNPs).

II. Define spatial and propose functional link between *the microtubule and mitochondria interacting protein 1* (Mmi1) and heat-induced stress granules of *S. cerevisiae*.

III. Analyse impacts of extramitochondrial *Reactive Species*-producer, Yno1 protein, on selected aspects of the yeast physiology.

3. Review of literature

One of basic characteristics of living organisms is adaptability to the environment. Cells try to deal with changing environmental conditions by various mechanisms. In general, an adaptation is primarily mediated by differential gene expression. Every environmental change can be viewed as a kind of stress. With the respect to the intensity and the type of a stress, an expression of gene groups is repressed, while transcription and translation of other gene groups are induced. Common feature of the adaptation is also saving cell resources and energy. On the level of proteosynthesis, it is achieved by selective translation of mRNA molecules. The unneeded ones are stored or degraded and new ones are engaged in translation in order to finally confer appropriate changes in the cell metabolism. Stress granules (SGs) are assemblies of messenger ribonucleoprotein complexes (mRNPs), which are formed in response to stress-induced alterations of mRNA metabolism. Upon severe stress conditions when global translation is inhibited, certain components of translation machinery are assembled into SGs to be sorted, stored or further forwarded to other subcellular locations. Thus, SGs link cellular stress response and translation, or, in better words, they are executors of stress response on the level of translation. In an effort to described stress granules in detail in the thesis, a basic review of translation process and its regulation upon a stress follows firstly. Secondly, the chapter about mRNPs in general and in yeast continues focusing on heat stress-induced stress granules of *S. cerevisiae*. Then, the stress granule-associated protein Mmi1 and its protein family are described. Finally, a brief overview about *Reactive Species*, as mediators of oxidative and also heat stress, and about one of their producers, Yno1 protein, completes the Review of literature.

3.1 Translation

Translation is a multistep process which results in a synthesis of new protein. This stage of gene expression enables, with the help of genetic code, to “translate” a sequence stored in mRNA molecule into sequence of amino acids in the protein. The process is catalysed by various protein factors and RNA molecules and can be generally divided into four stages. They are translation initiation, elongation, termination and the recycling step. Translation initiation of eukaryotic cellular mRNA molecules begins, in most cases, with a protein complex assembly on the mRNA 5'-capped end. In the search for translation start

codon, the formed ribonucleoprotein complex scans the mRNA molecule until proper, usually AUG, codon is reached. The selection of the right start codon is facilitated by unique nucleotide sequence (Kozak consensus sequence) situated around the codon. After a location of translation start side, the 80S ribosome is formed and protein synthesis continues by elongation stage of translation. Translation elongation concerns repeating creation of polypeptide bond by the action of the ribosome, aminoacyl-tRNA molecules, translation elongation factors and other associated molecules. When the translation termination codon is reached, the newly synthesized protein is released with the help of translation release factors. The final step of translation is detaching of ribosome from mRNA molecule and recycling of ribosomal subunits for a new round of translation. According to a current view on the translation process, it is generally believed that multiple ribosomes are positioned on one mRNA molecule at a time and translation efficiency is increased by the "closed loop" mRNA molecule architecture (adapted from Darnell et al., Molecular Cell Biology, 5th edition).

3.1.1 Translation initiation

In general and for majority of eukaryotic cellular mRNA molecules, the process of translation initiation begins when the initiator ternary complex binds to small ribosomal subunit (40S) and all together is loaded to mRNA molecule on its 5′ end. The ternary complex consists of initiator methionyl-tRNA and GTP-bound form of eukaryotic translation initiator factor 2 (eIF2). The eIF2 factor plays important role not only in an initiation of translation, but also in regulation of entire translation process. The alpha subunit of the factor can be phosphorylated in response to various conditions, which do not favour general and efficient translation, leading to global translation inhibition (for a review see (Proud 2005)). A joining of 40S ribosomal subunit with the ternary complex is mediated by translational initiator factors eIF1, eIF1A, eIF3 and eIF5. The sum of them creates translational pre-initiation complex (43S).

Subsequently, the 43S complex binds to mRNA on the mRNA cap structure by an action of eIF3, Pab1 (PABP), eIF4B, eIF4H (in mammals) and eIF4F forming 48S pre-initiation complex. The eIF4F complex is composed of the cap-binding protein eIF4E, eIF4G factor and RNA helicase eIF4A. eIF4G factor binds together Pab1 (PABP), eIF4E, eIF4A (plus eIF3 in mammals) and mRNA molecule. Thus, it facilitates establishing of

the “closed loop“ structure of mRNA molecule (Fig. I) (Wells, Hillner et al. 1998). At least two models for an exact mechanism of the 43S complex recruitment onto mRNA („activated mRNP“ and „holoPIC“) exist (for a review see (Hinnebusch and Lorsch 2012)).

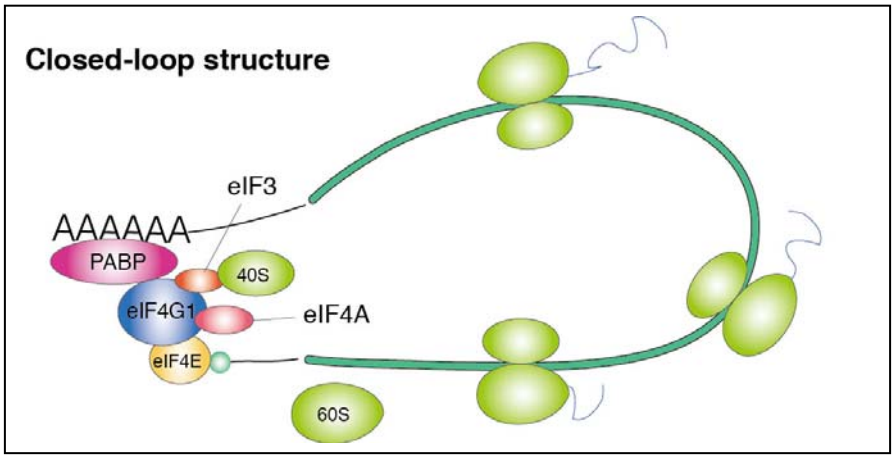

Figure I – mRNA closed loop structure (MBL Life Science; http://www.mblintl.com/)

The next step in translation initiation process is “scanning“ of mRNA molecule by newly formed 48S complex. When start codon is reached, GTP on eIF2 is hydrolyzed, with the help of eIF5 factor. Simultaneously, eIF2 and others are detached and 60S ribosomal subunit assembles with 40S to form 80S ribosome and translational initiation complex. A process of the joining is catalyzed by eIF5B factor. In this state, the ribosome is prepared to be engaged in an elongation phase of translation.

Nevertheless, the eukaryotic cells use even alternative mechanisms for translation initiation when general cap-dependent mechanism is somehow compromised. It should be stressed that these ways of beginning protein synthesis are in majority applied during periods of stress. In that time, a significant fraction of eIF2 is usually in phosphorylated form, thus translation incompetent. In the respect to stress response-induced translation, it is noteworthy to mention a mechanism, which is utilized across eukaryotic kingdom from yeast to mammals. With the use of sequential structured 5´ UTR of mRNA, which contains regulatory upstream open reading frames (uORFs), it is possible to driven synthesis of stress-specific proteins. The exact mechanism utilizes lower availability of translation competent form of eIF2 factor. It results in repression of the inhibition function of certain uORFs and rather preferential translation of the protein ORF. The process is well documented for translation of yeast *gcn4* mRNA or mammalian *atf4* mRNA (for reviews see (Hood, Neafsey et al. 2009) and (Hinnebusch 2005)). As well as prokaryotes have Shine-Delgardo sequence-dependent and independent mechanisms for initiation of translation, eukaryotes have alternatives to

trigger process of translation independently of the cap-mRNA structure. Beside a possibility to initiate translation directly on the start codon in so called "leaderless" mechanisms, another alternative to cap-dependent translation initiation lies in utilization of the internal ribosome entry sites (IRES). These special mRNA conformation structures located in 5' UTR of mRNA molecule enable, with the help of canonical and non-canonical translation factors, load translation pre-initiation complexes on the mRNA without help of the cap structure (for a review see (Malys and McCarthy 2011)).

3.1.2 Translation - continuation

After the translation initiation complex is, in any way, formed on mRNA molecule, translation continues with the elongation phase. Translational elongation factors have, besides ribosome itself, the central role in translation elongation. eEF1 class factors bring aminoacyl-tRNA molecules to ribosomes and eEF2 class factors mediate „translocation“ of the ribosome. The mentioned eukaryotic factors have their counterparts (orthologs) even in prokaryotic kingdom. The third evolutionary conserved class of translation elongation factors seems to be represented by bacterial EFP and eukaryotic eIF5A proteins. The latter was firstly though to be rather translation initiator factor, but contemporary results show that eIF5A has unique role in translation elongation (Gregio, Cano et al. 2009) (Saini, Eyler et al. 2009) (Gutierrez, Shin et al. 2013). This uniquely post-translationally modified (hypusinated) protein plays role in promotion of peptide bond formation on consecutive proline residues. Consistently, the protein depletion abolishes translation of polyproline-containing proteins (Gutierrez, Shin et al. 2013). In addition to aforementioned evolutionary conserved translation elongation proteins, there exists also additional and fungal-specific translational elongation factor eEF3 (Chakraburtty 2001). In *S. cerevisiae*, this factor (Yef3) stimulates the binding of aminoacyl-tRNA to the ribosome in eEF1α-dependent manner, probably by facilitating release of (“empty”) eEF1α factor from the ribosome (Kamath and Chakraburtty 1989). Possible role for eEF3 (Yef3) in recycling of translation post-termination complexes (see below) has also been suggested (Kurata, Nielsen et al. 2010; Pisarev, Skabkin et al. 2010). Multiplicity of translation elongation factors-operation is further documented by various observed functions of these factors outside translation. eEF1A is probably the number one in this matter. It has been reported that the factor is directly engaged in cellular processes, as are regulation of actin and microtubule cytoskeleton dynamics, nuclear export, protein degradation, apoptosis

and viral infection (for a review see (Mateyak and Kinzy 2010)). Similarly to eIF1A, a connection between eIF5A and the yeast actin cytoskeleton has been observed. Certain eIF5A mutants, which display also translation defects, show altered actin cytoskeleton dynamics upon a heat stress (our unpublished data and Avaca-Crusca J.S. personal communication).

The next and the third stage in the order of "translation cycle" is translation termination step. Once the termination codon enters into A-site inside the ribosome, two eukaryotic translation release factors (eRF1 and eRF3) finish a synthesis of the protein. Whereas eRF1 recognises termination codon, eRF3 is a GTP binding protein and both factors together stimulate release of newly synthesized protein from the ribosome. However, the ribosome is then still bound to mRNA, along with deaminoacetylated tRNA, eRF1 and possibly also with eRF3 (Pisarev, Skabkin et al. 2010). The components of resulted post-termination complex must be recycled before a re-use in another or in the same mRNA molecule translation.

Thus, the final step of translation is recycling of translation post-termination complexes. Whereas in prokaryotic kingdom the translation post-termination step is mediated by specialized ribosome recycling factor RRF, together with translation elongation factor G (Zavialov, Hauryliuk et al. 2005), further analyses of recycling mechanism are still required for detailed understanding the process in eukaryotic kingdom. A couple of hypotheses, based mainly on in vitro experiments, have been proposed. According to current view, the final step of translation slightly differs between yeast and higher eukaryotes. However, in both cases, the role of ATP binding cassettes containing-protein ABCE1/Yef3/Rli1 seems to be essential. A participation of eRF1 and eRF3 in the recycling step has also been suggested (Kurata, Nielsen et al. 2010; Pisarev, Skabkin et al. 2010). In the light of these data, it is noteworthy to mention that heat-induced stress granules of *S. cerevisiae* contain both eEF3 (Yef3) so eRF1 with eRF3 (Grousl, Ivanov et al. 2013). It may suggest that the stress granules contain translation post-termination complexes (see below and *Discussion*).

3.2 Translation under a stress

In the terms of stress response, translation regulation offers fast-responding and versatile system, how to reduce both energy- and source-consuming global protein synthesis under stress conditions and simultaneously engage stress-specific translation program. This chapter focuses on translation initiation, as on main regulatory step of entire translation, and

concurrently describes basic mechanisms, how translation initiation can be regulated upon certain stresses. In addition, the effect of heat stress on yeast translation process and individual components of translation machinery is described.

3.2.1 Regulation of translation initiation

Although translation can be affected in many ways, translation initiation seems to be the key step in a regulation of the entire process. One possibility how to regulate the rate of translation initiation is modulation of the initiator ternary complex availability. Under certain conditions, eIF2α is phosphorylated by its kinases in higher eukaryotes or by its exclusive kinase in yeast *S. cerevisiae*, Gcn2 (for a review see (Proud 2005)). Since the phosphorylated form of eIF2 factor has higher binding affinity to its nucleotide exchange factor eIF2B than non-phosphorylated form of eIF2 (Pavitt, Ramaiah et al. 1998) (Hinnebusch 2005), a capacity of eIF2B enzyme to regenerate non-phosphorylated and translation competent form of eIF2 factor is depleted. Consequently, the availability of the initiator ternary complex drops down and translation initiation is globally repressed. This phenomenon is commonly linked to stress granule assembly (see below and for a review see (Anderson and Kedersha 2002)). An alternative mechanism how to decrease the ternary complex availability and abolish translation initiation is direct inhibition of eIF2B factor. It reassembles an effect of eIF2α phosphorylation, but, in this case, eIF2B factor is primary engaged. It was shown that fusel alcohols directly target yeast eIF2B factor and inhibit its enzyme activity (Ashe, Slaven et al. 2001).

Besides modulation of the ternary complex availability, translation initiation can be regulated on the level of eIF4F complex formation. eIF4E-binding proteins (eIF4E BPs) compete with mRNA cap structure for association with eIF4E factor. These competitive inhibitors of eIF4E can thus sequestrate the factor, which leads, in a consequence, to less efficient eIF4F complex formation and reduction of translation initiation process. In mammalian cells, eIF4E BPs association with eIF4E is regulated by TOR (Target of Rapamycin) pathway. However in the yeast, the regulation is not so clear and is still not completely understood (for a review see (Simpson and Ashe 2012)).

The next possible way how to regulate translation initiation process concerns eIF4A helicase and its function in “scanning” of mRNA molecule. It was shown that drugs inhibiting function of eIF4A helicase provoke inhibition of translation and subsequent stress granules

formation in mammalian cells (Dang, Kedersha et al. 2006) (Mazroui, Sukarieh et al. 2006). Similarly, glucose depletion leads to release of eIF4A factor from translation pre-initiation complexes and inhibition of translation initiation in the yeast (Castelli, Lui et al. 2011). In general, it can be summarized that translation initiation is regulated by, at least, three main mechanisms. Those include either functionality of eIF2B factor, which can be influenced either directly or via eIF2 phosphorylation, eIF4A helicase or eIF4E and its binding proteins (Fig. II) (for a review see (Simpson and Ashe 2012)).

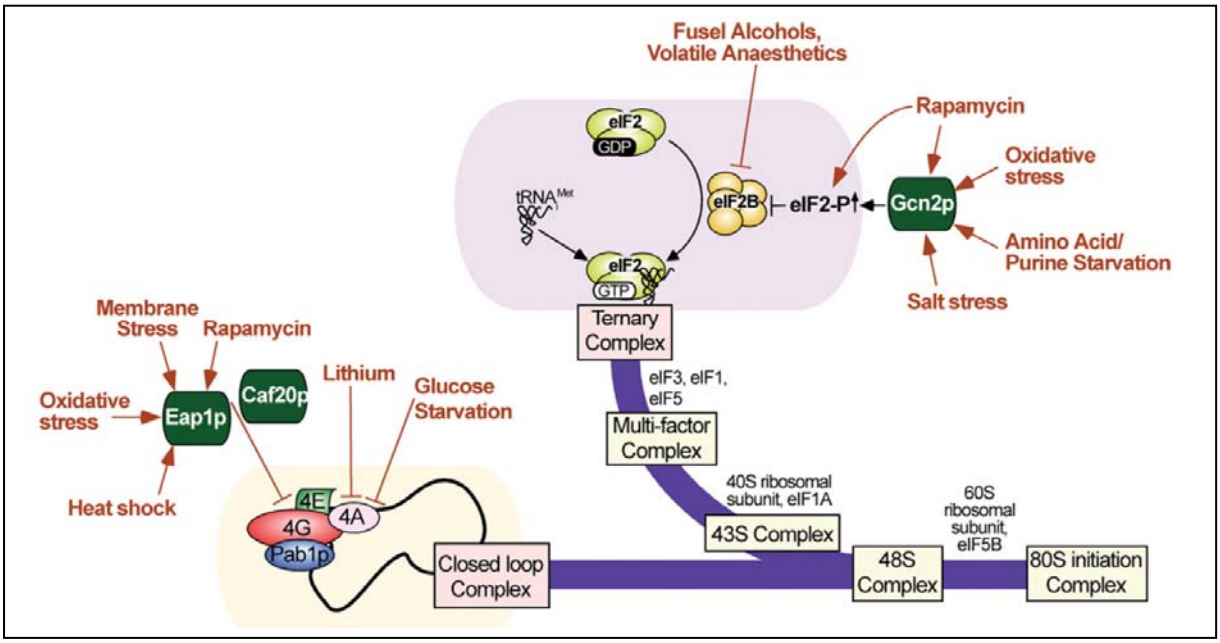

Figure II – Translation initiation regulatory mechanisms in *S. cerevisiae* ((Simpson and Ashe 2012)

3.2.2 Yeast translation upon a heat stress

Concerning process of translation and RNA turnover, yeast cells react to heat stress by different mechanisms depending on the intensity and duration of the stress. Exact mechanism or mechanisms how translation is regulated upon a heat stress are still not completely understood. Nevertheless, currently-known data point to complex regulatory system which encompasses multiple aspects of protein synthesis.

The yeast translation is temporary slowed under mild heat stress at 37°C, as is shown by both protein incorporation assays and polysome profile analyses (Meier, Deloche et al. 2006). Whereas inhibitory effect of mild heat stress at 37°C on translation process is minor and translation early recovers to and even up to initial rate, exposition to higher temperatures

seems to result in more severe alterations of translation process. However, the detailed analysis of translation dynamics upon these elevated temperatures is missing. It has been only shown that polysome fraction, which usually refers to efficient running of translation, is continually diminished corresponding to increasing temperature (Grousl, Ivanov et al. 2009; Cowart, Gandy et al. 2010; Grousl, Ivanov et al. 2013). It equally suggests that translation initiation is a regulatory point in charge under these conditions. Despite these analyses imply that translation is preferentially modulated on the level of the initiation upon severe heat stresses, an accumulation of translation elongation and termination factors in the yeast stress granules and eIF2α factor phosphorylation-independence of the SGs formation open a possibility that translation is also and rather primarily regulated on the post-initiation levels under these conditions (see below and *Discussion*).

In addition to translation process *per se*, heat stress, as well as other stresses, influences stability, integrity and subcellular localization of yeast translation machinery components and mRNA molecules (mRNAs). Nuclear export of maturated mRNAs of housekeeping genes is inhibited upon cultivation at temperature of 42°C and upper (Saavedra, Tung et al. 1996). On the contrary, heat shock mRNAs are actively exported from nucleus under these conditions to ensure proper heat stress response. It is obvious that heat shock mRNAs must utilize different exporting way(s) to reach cytoplasm. Indeed, it has been shown that their export is not mediated by GTPase Ran/Gsp1, which is necessary for a majority of cellular mRNAs, but it is rather coupled to nucleoporin-related protein Rip1 (Saavedra, Hammell et al. 1997).

Heat and other stresses influence also stability and integrity of tRNA and rRNA molecules. A cleavage of tRNA, preferentially in its anticodon loop, by Rny1 nuclease has been observed upon heat stress and also under other stresses in *S. cerevisiae* cells (for a review see (Thompson and Parker 2009)). These tRNA fragments seem to origin from maturated tRNA molecules and thus do not represent by-products of aberrant tRNA molecules decay. While the cleavage of tRNA is observed even in unstressed cells, this process is potentiated upon a stress (Thompson, Lu et al. 2008). It is proposed that these heat-induced tRNA fragments have physiological ("signalling") function. Moreover, although tRNA fragments-mediated stress response seems to be evolutionary conserved, it is restricted only to certain stresses ((Thompson, Lu et al. 2008) and for a review see (Thompson and Parker 2009)). The tRNA molecules are not only cleavaged upon a stress, but they are also subjected to retrograde transport to the nucleus. A couple of hypotheses were suggested for a reason of this phenomenon. One of them tells that a depletion of tRNA molecules from

cytoplasm inhibits translation under a stress. It is analogy to a sequestration of mRNA molecules within stress granules and processing bodies during translation unfavourable conditions (see the *3.3 Stress granules and processing bodies* chapter). Nevertheless, to elucidate exact roles either for stress-induced tRNA fragments or for retrograde transport of tRNA molecules upon a stress will surely need further research.

During periods of reprogramming cellular expression profile upon a stress, cells usually inhibit energy- and resources-consuming synthesis of ribosomal proteins and rRNA. It was shown that, in *S. cerevisiae*, expression of genes encoding ribosomal proteins is primary regulated on the transcription level and that rates of transcription of individual ribosomal genes are co-ordinated (for a review see (Planta 1997)). It was also shown that upon a mild heat stress, levels of mRNAs for ribosomal proteins rapidly, co-ordinately and temporary decrease (Herruer, Mager et al. 1988). The decline was later shown to be mainly caused by inhibition of their transcription (Li, Nierras et al. 1999). Interestingly, unlike tRNA fragments, rRNA fragments were not detected upon a heat stress, yet they have been observed in oxidative-stressed cells (Thompson, Lu et al. 2008).

Finally, under heat stress conditions, the fate of already translated mRNA molecules and certain translation machinery protein components, as are translation factors and ribosomal subunits, is determined according to intensity and duration of the stress. A detailed view on this phenomenon, which includes also a formation of stress granules and processing bodies, is described in the next, *3.3 Stress granules and processing bodies*, chapter.

3.3 Stress granules and processing bodies

In response to various stresses, cells try to adapt to changed living conditions. Concerning translation phase of gene expression, global translation is often reduced or completely shut down. On the contrary, translation of stress responsive genes is triggered. Stress-induced messenger ribonucleoprotein complexes (mRNPs) are formed in distinct cellular compartments, through which the fate of translation machinery components and mRNA molecules is determined. Two major types of cytoplasmic mRNPs accumulations formed upon a stress are stress granules (SGs) and processing bodies (PBs). Discovery of these entities in cells from yeasts to mammals suggests that SGs and PBs belong to universal and evolutionary conserved part of cellular stress response.

3.3.1 Processing bodies

Under growth-favorable and non-stress conditions, global translation is running to supply cells with protein demands. Certain messenger ribonucleoprotein complexes (mRNPs) are formed as translation process goes through its particular steps (see the *3.1 Translation* chapter). No more needed or damaged mRNA molecules (mRNAs) are continually degraded. In general, two strategies of eukaryotic mRNA degradation exist. The process usually begins with the poly(A)-end shortening and subsequent decapping of mRNA 5′ end. After that, mRNA molecule is begun to be degraded by exoribonuclease in 5′ end to 3′ end direction. Alternatively, mRNA can be degraded after de-adenylation in oppose way (3′ end to 5′ end) by the exosome (for a review see (Balagopal, Fluch et al. 2012)).

The mRNA decapping and degradation enzymes, together with translation repressors, are concentrated in form of mRNPs in cellular entities, called processing bodies. Since mRNA degradation occurs in the cell even under non-stress conditions, PBs are present also in unstressed cells. Originally, in accordance with the fact that PBs contain mainly mRNA decapping and mRNA degradation enzymes, PBs were described as sites where mRNA decay actually occurs (Sheth and Parker 2003). Nowadays, it is more and more evident that a function of PBs is not limited only to mRNA decay. They have also been connected to translation repression, mRNA storage, mRNA quality control and even to other functions (Brengues, Teixeira et al. 2005; Balagopal and Parker 2009; Arribere, Doudna et al. 2011; Parker 2012). However, an entire role of PBs in mRNA metabolism is still not completely understood (for a review see (Balagopal, Fluch et al. 2012)).

Formation of processing bodies is enhanced by such stresses which force the cell to reprogram gene expression and translation profile to confer adaptation. In connection, the no more needed mRNAs cease translation cycle and are sequestered in PBs to be degraded. After engaging stress-specific translation profile and adaptation, PBs mostly disappear. However, when the stress is more severe and the cells are not able to adapt to it, PBs persist and may be remodelled to SGs.

3.3.2 Stress granules

Whereas processing bodies (PBs) exist in the cell even under permissive conditions and their formation is enhanced by a stress, stress granules (SGs) are assembled in cells only

upon restrictive conditions. Despite of still not completely understood functions of SGs in cellular metabolism, it is obviously evident that they fulfil evolutionary conserved roles in regulation of translation, mRNA turnover and cellular signalling. The primary role of SGs seems to consist in regulation of translation under a stress, in sorting and storage of mRNA molecules (mRNAs) and in preservation of certain translation machinery components (Anderson and Kedersha 2002) (Anderson and Kedersha 2008) (Balagopal and Parker 2009). In connection, SGs thus help the cells to minimize the impact of a stress on translation apparatus and they are also proposed to ensure efficient translation recovery after a stress (Parker and Sheth 2007) (Grousl, Ivanov et al. 2013). Moreover, along with the fact that SGs may also sequestrate proteins engaged in cellular signalling pathways and other factors and, in connection, confer cell survival upon a stress, it is likely that SGs regulate not solely translation upon stress conditions, but they also actively participate on regulation or modulation of entire cellular metabolism and cell fate decision ((Kwon, Zhang et al. 2007) (Arimoto, Fukuda et al. 2008) (Kim, Cooke et al. 2012) and for reviews see (Anderson and Kedersha 2008) (Kedersha and Anderson 2009)).

Stress granules or SG-like bodies were found, besides yeasts (see below), across eukaryotic kingdom, in *Aspergilus oryzae* (Huang, Maruyama et al. 2013), *Trypanosoma brucei* (Kramer, Queiroz et al. 2008), *Drosophila melanogaster* (Farny, Kedersha et al. 2009), *Caenorhabditis elegans* (Jud, Czerwinski et al. 2008), *Brachionus manjavacas* (Rotifera) (Jones, Vanloozen et al. 2013), plant cells (Weber, Nover et al. 2008) and mammalian cells (Kedersha, Gupta et al. 1999). Moreover, SGs were observed in chloroplasts of *Chlamydomonas reinhardtii* suggesting that similar entities may be formed even in prokaryotes (Uniacke and Zerges 2008).

The composition of SGs is closely connected with the mechanism of their assembly. It is widely accepted that SGs are composed mainly by stalled translation pre-initiation complexes (Kedersha, Chen et al. 2002; Kimball, Horetsky et al. 2003). These complexes are formed in response to alteration of translation initiation kinetics. The best characterized mechanism of their formation, so far, is stress responsive phosphorylation of translation initiation factor 2 alpha subunit (eIF2α) (Anderson and Kedersha 2002) (Anderson and Kedersha 2008). The phosphorylation leads to reduction of the initiator ternary complex availability (see the *3.2 Translation under a stress* chapter). This reduction of ternary complex availability is linked to translation repression and SGs assembly. However, eIF2α-phosphorylation independent mechanisms of SGs formation, e.g. an alteration of mRNA cap-recognition complex dynamics, were also documented (see the *3.2 Translation under a stress*

chapter and for reviews (Anderson and Kedersha 2008) (Simpson and Ashe 2012)). Possible alternative ways of SGs assembly may mean that these accumulations of mRNPs could be formed also in response to other stimuli than primary inhibition of translation initiation. An example of SGs formed independently on eIF2α phosphorylation and proposed to be primarily modulated on the level of translation elongation are heat-induced SGs of *S. cerevisiae* (see below and *Discussion*) (Grousl, Ivanov et al. 2009) (Grousl, Ivanov et al. 2013).

In addition to stalled translation pre-initiation complexes, as "core" constituents of SGs, SGs contain even other protein components. Among these, RNA-binding proteins engaged in regulation of translation, mRNA stability or mRNA processing are present. Some of them, as are TIA-1 and Ataxin-2 in mammalian cells, influence dynamics of SGs (Kedersha, Gupta et al. 1999; Gilks, Kedersha et al. 2004; Nonhoff, Ralser et al. 2007). Moreover, SGs can associates with several other proteins which lack direct connection to RNA metabolism (for a review see (Anderson and Kedersha 2008)).

Despite multiplicity of SGs functions, they are not the only stress-induced mRNPs accumulations in the cell. Equally, SGs are not the only stress-induced mRNPs assemblies participating on translation regulation and mRNAs turnover during a stress. SGs usually act in co-operation with PBs in this matter. Therefore, these two cellular entities are spatially and compositionally intertwined. The interconnection of both entities and active translation is described by the usage of the proposed "mRNA cycle" model.

3.3.3 The "mRNA cycle"

There is an increasing body of evidence that mRNA molecules (mRNAs) can shuttle between polysomes (active translation) and processing bodies (PBs) (decay and possibly other functions). This mRNA movement can be complemented by stress granules (SGs) (triage, storage, signalling) when even SGs are formed. Cycloheximide-based experiments show that mRNAs are in dynamic equilibrium between polysomes and PBs and between polysomes and SGs (Brengues, Teixeira et al. 2005) (Kedersha, Cho et al. 2000). It suggests that mRNAs can be sent back to active translation from SGs or PBs during a stress relief or even just upon a stress. However, the phenomenon seems not to be universal, at least for PBs where only limited number of specific mRNAs has been shown to be able to return to active translation from PBs (Arribere, Doudna et al. 2011). Nevertheless, it is generally accepted that mRNA

molecules and even protein components can migrate between SGs and PBs and vice versa. Moreover, it has been shown that PBs directly promote assembly of SGs in yeasts, as well as in higher eukaryotes ((Buchan, Muhlrad et al. 2008); (Grousl, Ivanov et al. 2009) and for a review see (Anderson and Kedersha 2008)).

With the usage of model organism *S. cerevisiae*, the precise "mRNA cycle" model is tried to be established. In general, two major hypotheses about the mRNA movement from active translation to PBs, SGs and back to translation exist. According to the one, it is believed that SGs serve as transient stage on the mRNA route from PBs back to active translation (Brengues and Parker 2007; Buchan, Yoon et al. 2011). It anticipates that PBs are always formed first and mRNA leaving active translation firstly accumulates in them. Afterwards, the mRNA can be sent back to translation either directly or via remodelling of PBs to SGs and subsequently forwarding SGs components to active translation. On the other hand, the second hypothesis assumes that SGs are formed independently on PBs and serve as transient storage sites for mRNA molecules and mRNP complexes during period of stress (Hoyle, Castelli et al. 2007; Shah, Zhang et al. 2013). Regardless the case, stress granules and processing bodies thus represent two distinct cellular entities, which concurrently and in co-operation orchestrated cell stress response on the level of translation and mRNA metabolism. The current knowledge about yeast stress granules, with the focus on heat stress-induced SGs of *S. cerevisiae*, is described in the next chapter.

3.3.4 Yeast stress granules

Discovery of stress granules (SGs) in yeasts together with growing evidence about SGs from new and new organisms support the hypothesis that SGs are evolutionary conserved stress-response phenomenon. In yeasts, stress granules have been discovered and described relatively recently. They were observed either in budding yeast *Saccharomyces cerevisiae* (Brengues and Parker 2007; Hoyle, Castelli et al. 2007; Buchan, Muhlrad et al. 2008; Grousl, Ivanov et al. 2009; Buchan, Yoon et al. 2011; Kato, Yamamoto et al. 2011; Hofmann, Cherkasova et al. 2012; Iwaki, Kawai et al. 2013; Iwaki, Ohnuki et al. 2013; Shah, Zhang et al. 2013; Yamamoto and Izawa 2013), or in fission yeast *Schizosaccharomyces pombe* (Dunand-Sauthier, Walker et al. 2002; Wen, Stevenson et al. 2010; Nilsson and Sunnerhagen 2011).

In general, yeast SGs seem to be analogous to SGs of higher eukaryotes in composition and proposed functions. As well as their counterparts from higher eukaryotes, yeast SGs contain components of translation initiation machinery. Typical examples of budding yeast stress granules are those induced by robust heat shock (Grousl, Ivanov et al. 2009), ethanol (Kato, Yamamoto et al. 2011) or sodium azide (Buchan, Yoon et al. 2011). However, yeast SGs possess even unique nature concerning additional constituents or missing of otherwise core SGs components. In this respect, only SGs observed in heat-stressed, ethanol-stressed or the combined stressed cells contain small ribosomal subunit (40S)[1] (Grousl, Ivanov et al. 2009; Kato, Yamamoto et al. 2011; Yamamoto and Izawa 2013). The only other case of SGs containing small ribosomal subunit are those induced by accumulation of yeast metabolite furfural (Iwaki, Kawai et al. 2013). Heat stress-induced SGs also harbour additional protein components, as are mRNA decay enzymes Dcp2 and Dhh1 or translation elongation and termination factors (Grousl, Ivanov et al. 2009) (Grousl, Ivanov et al. 2013). On the other hand, ethanol-induced SGs contain only the one protein (Nip1/eIF3c) of entire translation initiation complex eIF3 and SGs (EGP bodies) of glucose-deprived cells do not harbour this complex at all (Hoyle, Castelli et al. 2007) (Brengues and Parker 2007) (Buchan, Muhlrad et al. 2008). To complete a list of, so far, documented *S. cerevisiae* SGs, it has to be mentioned that they are formed even under cold stress (Hofmann, Cherkasova et al. 2012), in stationary phase of growth (Shah, Zhang et al. 2013) or in presence of lignin-degradation product vanillin (Iwaki, Ohnuki et al. 2013).

What distinguishes, in essence, lower eukaryotes‘ SGs from the majority of higher eukaryotes‘ SGs is signalling which controls their assembly. Whereas mammalian SGs are formed mainly is response to phosphorylation of eIF2α factor (Anderson and Kedersha 2002) and for a review see (Anderson and Kedersha 2008), an assembly of yeast SGs seems to be independent on this signalling pathway. All of, up today, known *S. cerevisiae* SGs, which were analysed in this way, are formed independently on eIF2α phosphorylation (Grousl, Ivanov et al. 2009; Buchan, Yoon et al. 2011; Kato, Yamamoto et al. 2011). Only SGs of *S. cerevisiae* glucose-deprived cells are, at least, potentiated by eIF2α phosphorylation (Buchan, Muhlrad et al. 2008). However, it has been recently shown that assembly of glucose deprivation-triggered SGs is mainly driven by releasing of eIF4A helicase from 48S pre-initiation complex and subsequent alterations in the complex dynamics (Castelli, Lui et al. 2011). Despite other alternative mechanisms for higher eukaryotes‘ SGs assembly were

[1] Despite this widely believed evidence, the presence of small ribosomal subunit in heat-induced SGs has been recently impeached (Cherkasov et al., 2013).

described (Dang, Kedersha et al. 2006; Mazroui, Sukarieh et al. 2006; Ohn, Kedersha et al. 2008; Li, Ohn et al. 2010) and several mechanisms of translation inhibition upon stresses were characterized in yeasts (for a review see (Simpson and Ashe 2012)), processes which lead to formation of a majority of yeast SGs are still largely unknown.

Since eIF2α phosphorylation-independent mechanism for SGs assembly prevails in yeasts and even in other lower eukaryotes (*Trypanosoma brucei, Drosophila melanogaster*), it seems to be evolutionary older than that of mammals (Kramer, Queiroz et al. 2008; Farny, Kedersha et al. 2009). The clue for elucidation of the mechanism(s) may be provided by heat-induced stress granules of *S. cerevisiae*. Whereas heat stress triggers phosphorylation of eIF2α factor, formation of the SGs is independent on it. Moreover, an accumulation of translation elongation and termination factor in the SGs may suggest that the SGs assembly is primarily regulated by the post-initial level of translation (Grousl, Ivanov et al. 2009; Grousl, Ivanov et al. 2013).

Heat stress-induced SGs are formed in response to robust heat-shock at 46°C (Grousl, Ivanov et al. 2009) and are preformed just under heat stress at 42°C (Grousl, Ivanov et al. 2013). It is believed that they are engaged in the same roles, as are those of higher eukaryotes‘ SGs, regarding sorting and storage of certain mRNA molecules and translation factors upon a stress and providing help in efficient recovery of translation after a stress relief. Similarly to higher eukaryotes‘ SGs, heat shock-induced SGs of *S. cerevisiae* contain stalled translation pre-initiation complexes represented by small ribosomal subunit (40S), mRNA molecules, certain translation initiation factors and other mRNA binding proteins. In addition, they possess even unique components, as are proteins of processing bodies (PBs) or translation elongation and termination factors. As mentioned earlier, an accumulation of yeast heat-induced SGs, as well as other yeast‘s SGs, has been shown to be independent on eIF2α phosphorylation. Along with the evidence about unique composition of yeast heat-induced SGs (especially presence of translation elongation and termination factors), it suggests that process of yeast SGs assembly may be mediated by affecting other translation stages than only translation initiation. Such a type of translation regulation seems to be engaged, for example, during nutrient deprivation or oxidative stress (for details see *Discussion*). Alteration of translation post-termination phase (recycling step) provide another possibility, how translation can be regulated upon robust heat stress. In this step of translation, ribosome subunits are released from mRNA molecule (and from the last deacetyled-tRNA molecule) by the action of translation termination factors (eRF1, eRF3) and translation elongation factor (eEF3) (see *3.1.2 Translation – continuation* chapter). With the respect to the fact that all

these factors are accumulated in the heat-induced SGs, it can be anticipated that just this phase of translation cycle is influenced by robust heat stress (for details see *Discussion*). Despite translation elongation and termination factors have never been observed to be components of any SGs from any organism, the termination factors were found to be associated with PBs (Dori and Choder 2007; Buchan, Muhlrad et al. 2008). Those authors suggested that their presence in PBs is somehow coupled to PBs assembly. A similar role can be assigned to translation elongation and termination factors concerning heat-induced SGs. In accordance, some of these factors were found to accumulate just upon lower temperature than those at which genuine SGs are formed and most probably prepare a platform for the SGs assembly (Grousl, Ivanov et al. 2013). Recently, it has been documented that heat-induced SGs also associate with molecular chaperons and co-accumulate with misfolded protein aggregates (Cherkasov, Hofmann et al. 2013). Since formation of these aggregates precedes assembly of the SGs, those authors believed that the aggregates serve as a scaffold for a docking of the SGs. The main reason for the co-accumulation of the SGs and misfolded protein aggregates is, however, declared to be co-regulation of heat stress response of the cell (for details see *Discussion*).

Finally, heat-induced SGs were proposed to be sites where translation efficiently recovers after a stress relief. This statement is also based on an observation that α-subunit of key translation initiation factor eIF2 (Sui2) is enriched on dissolving SGs during recovery from a stress (Grousl, Ivanov et al. 2013). It is in a consistence with an earlier finding that presence of SGs upon heat stress supports cell recovery during a period of stress relief (Grousl, Ivanov et al. 2009).

The unique components of heat-induced SGs of *S. cerevisiae* can be either directly involved in translation repression and the SGs assembly or their accumulation in the SGs is only a consequence of these processes. Regardless the case, it can be anticipated that the protein accumulation in SGs surely impacts all of processes in which the protein is engaged. One such an example may be given by a sequestration of the target of rapamycin complex 1 (TORC1) in SGs upon heat stress in mammalian cells (Takahara and Maeda 2012). Those authors conclude that a deposition of the complex in SGs during a period of the stress and thus an inactivation of the signalling cascade may finally result in less damage caused by the stress. Another evidence of SGs influence on cellular signalling cascades is a repression of apoptosis via deposition of RACK1 protein in SGs upon certain stresses (Arimoto, Fukuda et al. 2008). The mentioned examples of protein sequestration in SGs point to inter-connection of SGs with other cellular processes than only with translation and also with certain signalling

pathways. That is also the case of the protein, about which the next chapter dissertates. It is microtubule and mitochondria interacting protein 1 (Mmi1) of *S. cerevisiae*.

3.4 Mmi1 / TCTP protein family

Mmi1 (microtubule and mitochondria interacting protein 1) or also Tma19 (translation machinery associated protein 19) is *S. cerevisiae* ortholog of mammalian TCTP (translationally controlled tumor protein). These proteins, along with their counterparts from other organisms, belong to evolutionary conserved, but structurally unique, protein family (for a review see (Hinojosa-Moya, Xoconostle-Cazares et al. 2008)). The predicted protein structure from *Sch. pombe* shows three distinct domains within the protein (Thaw, Baxter et al. 2001). The flexible loop and the helical domains are Mmi1 / TCTP protein family specific, whereas the β-stranded core domain is similar to those of Mss4/Dss4 proteins. The schematic view on an arrangement of these domains is shown in Fig. III (Bommer and Thiele 2004). Despite highly conserved protein structure, particular members of the family slightly differ among each other. For example, in *Plasmodium knowlesi*, the protein has one extra α-helix in its structure (for a review see (Hinojosa-Moya, Xoconostle-Cazares et al. 2008)).

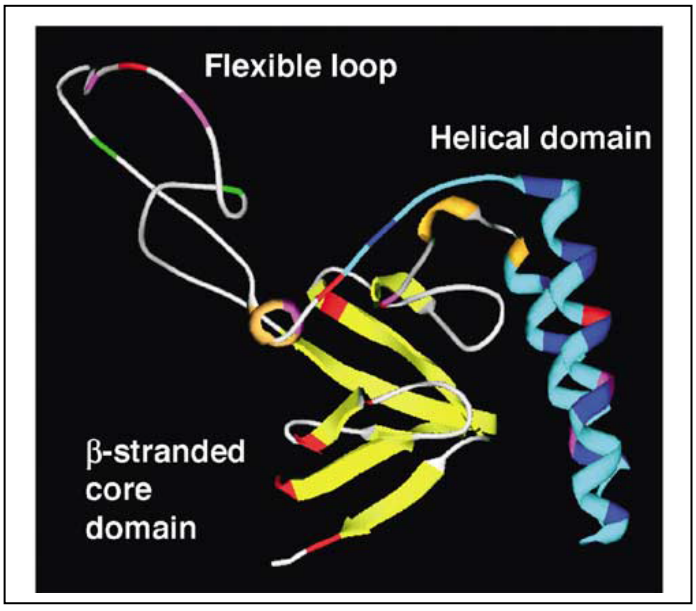

Fig. III – The predicted structure of Mmi1 / TCTP family proteins ((Bommer and Thiele 2004))

The TCTP protein displays variety of cellular functions. It is engaged in cell division control, regulation of growth and translation. In connection with that, it has been documented to have stress-response regulatory and anti-apoptotic features. Moreover, the protein binds tubulin and actin and it is also a calcium binding protein. Possible function as a chaperon has also been suggested. Finally, TCTP serves as histamine-release factor in non-classical secretion in mammals (for a review see (Bommer 2012)). However, the detailed and complex understanding of TCTP / Mmi1 cellular function is still not complete.

3.4.1 Yeast members of Mmi1 / TCTP protein family

Members of Mmi1 / TCTP family have been identified also across fungi kingdom. They are present in commonly used model organisms, as are yeasts *S. cerevisiae* or *Sch. pombe*. In addition to them, a corresponding gene has been identified in *Candida glabrata*, *Cryptococcus neoformans*, *Yarrowia lipolytica* and even others (for a review see (Hinojosa-Moya, Xoconostle-Cazares et al. 2008)).

S. cerevisiae Mmi1 / Tma19 protein was first described as translation machinery associated protein. Deletion of *mmi1* gene alters polysome profile of the cell and confers decrease in protein synthesis rate (Fleischer, Weaver et al. 2006). However, the detailed analysis of particular Mmi1 / Tma19 function(s) in translation is still missing. Additionally, Mmi1 has been shown to be stress-response modulator of the cell. In this respect, strains with a deletion of *mmi1* displays resistance to oxidative stress induced by H_2O_2 and resistance to robust heat stress (Rinnerthaler, Jarolim et al. 2006) (Rinnerthaler, Lejskova et al. 2013). Moreover, Mmi1 has been identified as a regulator of the proteasomal activity. Finally, it has been found in an association with de-ubiquitination system and also with heat-induced stress granules, under a heat stress (see the next chapter) (Rinnerthaler, Lejskova et al. 2013).

3.4.2 Mmi1 in the time of heat stress

It was shown that cells which harbour *mmi1* deletion are on the one hand more sensitive to moderate heat stress (37°C) and on the other hand more resistant to robust heat stresses (46°C), than the wild type cells (Sinha, David et al. 2008) (Rinnerthaler, Lejskova et al. 2013). These contradictory phenotypes may arise from a qualitatively different cellular response to milder or severe heat stress (for details see *Discussion*). Rinnerthaler et al. showed

that cells carrying *mmi1* deletion better survive prolonged treatment under conditions of robust heat stress (46°C) in comparison to the wild type cells. The same situation was described for the mutant upon an oxidative stress. While, under an oxidative stress, Mmi1 becomes to be enriched on the mitochondria and thus can influence mitochondria-related stress-responsive pathways, under robust heat stress, no such an accumulation has been observed (Rinnerthaler, Jarolim et al. 2006) (Rinnerthaler, Lejskova et al. 2013). However, the protein translocates to the nuclear region and accumulates in cytoplasmic granules upon the heat stress. The Mmi1 granules formed in the cytoplasm of heat-shocked cells were found to co-localize with stress granule marker protein Rpg1 (eIF3a) (Rinnerthaler, Lejskova et al. 2013). Subsequent analysis revealed that the Mmi1 accumulation is reversible and partially influenced by cycloheximide. This drug blocks translation by inhibiting the peptidyl-transferase activity of ribosome (Campbell, Hoyle et al. 2005), thus "freezing" mRNA molecules on polysomes. Consequently, it prevents assembly of stress granules in general and thus also assembly of heat-induced stress granules of *S. cerevisiae* (Grousl, Ivanov et al. 2009). For above mentioned reasons, Mmi1 has been assigned as a heat stress-induced stress granules associating protein (Rinnerthaler, Lejskova et al. 2013). In addition to that, the link between the protein degradation system and Mmi1 was established in relation to the heat stress. In other words, Mmi1 was co-localized with the proteasome in the nuclear region and also with components of de-ubiquitination machinery upon the stress. The link between Mmi1 and protein degradation system is further supported by the finding that Mmi1 associates with Cdc48 chaperon under robust heat shock. Finally, the proteasomal activity was found to be altered (increased) when Mmi1 is missing in the cell suggesting that Mmi1 itself may be an inhibitor of the proteasome function (Rinnerthaler, Lejskova et al. 2013).

Inter-connection of heat-induced SGs and protein degradation system mediated by Mmi1 reflects also global heat stress-induced changes in protein homeostasis *per se*. The protein conformation, stability and integrity are influenced by heat stress, as well as by some other kinds of cellular stresses. One such a protein damaging-condition is represented by oxidative stress and its mediators *Reactive Species* (RS). Heat stress is inter-twined with oxidative stress on multiple levels and RS were shown to be engaged in deleterious effects of heat on the eukaryotic cells ((Davidson, Whyte et al. 1996) and references therein). The last chapter is thus focused on RS and their particular producers in the cell – NOX (NADPH oxidase) enzymes.

3.5 Reactive species and NOX enzymes

In response to various stresses, cellular proteins and other cellular constituents are usually subjected to altered physical and chemical conditions. To alleviate these noxious effects on cell homeostasis, cells developed certain protective mechanisms. These mechanisms comprise expression of stress-responsive proteins as well as non-protean-based protective mechanisms, which together help to keep protein homeostasis balanced.

Reactive species (RS) are large group of agents which endanger cellular redox balance, when escaping cellular antioxidant defence. The well-known members of those are reactive oxygen species (ROS). However, other reactive agents as are nitrogen (RNS) and sulphur species (RSS) also exist. All of them are mediators of oxidative stress, since they are able to either oxidize others due to their own reactivity or can be metabolized to such a molecule. In the class of RS, we can find inorganic molecules as are superoxide anion, hydrogen peroxide, hydroxyl anion or nitric oxide and also organic metabolites as are reactive thiol groups or organic hydroperoxides. It is widely believed that main source of ROS and eventually other RS in aerobically living eukaryotic cell arises from mitochondrial respiration (Murphy 2009). Additional "producers" of ROS are endoplasmic reticulum, β-oxidation pathway in peroxisomes, oxidative deamination of amino acids and even others (for a review see (Morano, Grant et al. 2012)). Besides intracellular generated RS, cells may be challenged either to external RS exposition, such as immune reaction against pathogens, or to RS-generating stimuli, as are UV and ionizing radiation, xenobiotics or heavy metal exposure. On the other hand, RS production is not linked only to stress conditions. Enzymes generating RS and RS themselves have even its physiological functions. Thus, RS are not only unwanted by-products of cell metabolism, but they also actively participate in cellular metabolism and signalling pathways. Such an example of enzymes generating ROS is NOX (NADPH oxidases) protein family. The next chapter deals with NOX enzymes, with a focus on yeast NOX enzyme - Yno1.

3.5.1 NOX enzymes and Yno1 of *S. cerevisiae*

A catalytic component of phagocytic NADPH oxidase - gp91phox (NOX2) served as a starting point to identify additional members of NOX enzyme family. Up today, the other six NADPH oxidases have been defined according to sequence homology with NOX2 in higher

eukaryotes. All of them, as well as NOX2, generate superoxide anion (O_2^-), by electron transfer from NADPH through two heme groups to final acceptor, oxygen molecule. However, in the case of Duox class, a production of (O_2^-) is still under a debate. All of these enzymes possess transmembrane domains, but they differ in their overall structure. NOX5, Duox1 and Duox2 have additional calcium-dependent regulatory domain and Duox class has also extracellular domain with predicted peroxidase activity (for a review see (Nauseef 2008)). A structure organization of NOX enzymes is depicted in the Fig. IV (Nauseef 2008). Variety of NOX-generated ROS physiological functions encompasses participation in innate immunity, cell differentiation, mitogenic regulation and others. Nevertheless, activity of NOX enzymes and ROS production is also interconnected with various pathologies. These include mainly age-related diseases as are atherosclerosis, hypertension, cardiovascular or neurodegenerative diseases (for a review see (Lambeth 2007)). NOX enzymes do not operate alone, but associate with several binding partners. These associated factors influence the enzyme activity. NOX1 to NOX4, that those which do not harbour calcium binding regulatory domain, form heterodimer with p22phox protein. This protein is not catalytically active, but it is necessary for proper function of the NOX enzymes (Yu, Quinn et al. 1998) (DeLeo, Burritt et al. 2000). Moreover, NOX organizing (NOXO1) and NOX activating (NOXA1) proteins exist ((Nauseef 2008) and references therein). Finally, in addition to calcium ions, an activity of the protein family members is regulated by direct phosphorylation or by small GTPases (for a review see (Lambeth, Kawahara et al. 2007)).

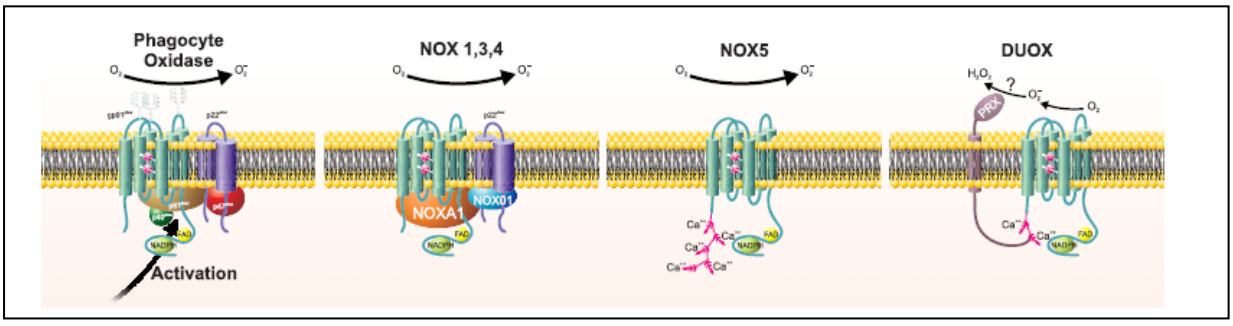

Figure IV – Structure organization of NOX protein family members (Nauseef 2008)

Recently, endoplasmic reticulum-localized member of NOX (NADPH oxidase) enzyme family and ROS producer, Yno1 protein, has been identified in yeast *S. cerevisiae* (Rinnerthaler, Buttner et al. 2012). Yno1 protein was first identified in a screen for homologs of ferric reductases Fre1 and Fre2 and concurrently proposed to possess electron transport capacity (Finegold, Shatwell et al. 1996). Despite the gene was assigned as an iron / copper

reductase-related gene, it was found that its expression is not regulated by an iron or copper availability (Georgatsou and Alexandraki 1999). In connection, Rinnerthaler et al. proved that Yno1 / Aim14 does not have ferric reductase activity and instead, they showed that Yno1 has NADPH oxidase activity. In another screen, the protein was shown to be involved in mitochondria inheritance and was named Aim14, for altered inheritance of mitochondria protein 14 (Hess, Myers et al. 2009).

According to sequence similarity of Yno1 catalytic subunit with human NADPH oxidase NOX2, Yno1 was being identified and later on confirmed as an endoplasmic reticulum-localized yeast NADPH oxidase. Moreover, in the search for *yno1*Δ-associated phenotypes, it was found that the deletion confers both, sensitivity to actin-destabilizing drugs and less sensitivity to apoptotic stimuli (Rinnerthaler, Buttner et al. 2012). Production of ROS (superoxide) by Yno1 was also shown to take part in inhibition of mitochondrial respiration under presence of glucose. The process, mediated by superoxide dismutase enzyme Sod1, leads to stabilization of certain casein kinases which, in turn, participate on repression of mitochondrial respiration (Reddi and Culotta 2013). On the other hand, ROS production mediated by Yno1 has been shown to be altered when mitochondrial cytochrome c oxidase activity is compromised (Leadsham, Sanders et al. 2013). Leadsham et al. identified Yno1 as a major source of ROS production when mitochondria are not functional. The dysfunctional organelle accumulates Ras2 signalling protein on its outer membrane and it consequently leads to suppression of ERAD-mediated degradation of Yno1 and thus aberrant production of ROS.

Despite an identification of Yno1 protein as a first member of NOX enzyme family in hemiascomycetous yeasts is promising for further research of pleiotropic functions of the protein family members and RS in the cell, the detailed role of Yno1 in cellular metabolism needs to be primarily established.

4. Methods

For a purpose of a performance of experimental procedures, all of yeast cultures were cultivated in liquid or on solid media using generally, either yeast pepton dextrose (YPD) medium or synthetic complete (SC) medium.

Bacterial cultures used for propagation of plasmids and DNA cloning were cultivated in liquid lysogeny broth (LB) medium or on corresponding solid medium.

The classical genetic and molecular biology methods, including the whole cell manipulations (yeast mating, sporulation of diploids, spore dissection, selections for auxotrophies), DNA manipulations (isolation of DNA, restriction of DNA by restriction endonucleases, polymerase chain reaction – PCR, electroforetic separation of DNA) and protein manipulations (protein isolation, electroforetic separation of proteins, Western blot analysis) were used in appropriate analyses or to create and verify required strains. Alternatively, the strains were prepared through direct genetic manipulations as are a transformation and an integration of deletion or fusion DNA cassettes into yeast cells and their genomes.

Live cell imaging fluorescence microscopy was one of prominent methods used through the research papers in the thesis. For these experiments, strains with GFP/RFP/mCherry-fused gene(s) of interest or treated with specific chemical compounds were engaged. Upright or inverted, adequately equipped, visible light and fluorescence microscopes enabled to perform mentioned experiments. Using additional equipment, the Onix Microfluidic System (Millipore), the time-lapse heat-shock experiment described in *Grousl et al., 2013* was done.

Polysome profile analysis allows monitoring translation profile of cells. Briefly, this method includes preparation of a lysate from cycloheximide-treated cells, fractionating of the lysate, a separation on sucrose gradient and a measurement of certain light absorbance of the sample.

Proteasome activity assay enables to quantified activity of the proteasome on the basis of a fluorescence measurement. Briefly, fluorogenic substrate in combination with cell lysate generates light, which can be measured, and activity of the proteasome is determined according to the light intensity.

Other methods, as are mass spectrometry, electron microscopy and immunogold labelling, protein structure prediction, iron and ROS detection assays, microsomes

purification and phylogenetic analyses, are also mentioned in the research papers of the thesis. However, these methods have not been done in our laboratory and I have participated on their performance only partially or not at all.

List of Methods

(methods that have not been done in our laboratory are written in italic)

Yeast and bacteria cells cultivation
DNA cloning
Genetic modification of yeast cells
Live cell fluorescence microscopy
Polysome profile analysis
Protein purification
Western blot analysis
Proteasome activity assay
Electron microscopy and immunogold labelling
In-gel protein digestion and mass spectrometry
Protein structure prediction
Iron and ROS detection assays
Microsomes purification
Phylogenetic analyses

5. Presented publications

Paper 1

Robust heat shock induces eIF2alpha-phosphorylation-independent assembly of stress granules containing eIF3 and 40S ribosomal subunits in budding yeast, *Saccharomyces cerevisiae*.

Grousl T, Ivanov P, Frydlova I, Vasicova P, Janda F, Vojtova J, Malinska K, Malcova I, Novakova L, Janoskova D, Valasek L, Hasek J.

J Cell Sci. 2009 Jun 15;122(Pt 12):2078-88.

PMID:19470581

IF_{2012} 5,877

Number of citations: 56 (WoS; 2013-12-18)

Contribution of the author: Tomas Grousl contributed to the designing of the experiments, performed some of the experiments, analysed the data and contributed to the writing of the publication.

Paper 2

Heat shock-induced accumulation of translation elongation and termination factors precedes assembly of stress granules in *S. cerevisiae*.

Grousl T, Ivanov P, Malcova I, Pompach P, Frydlova I, Slaba R, Senohrabkova L, Novakova L, Hasek J.

PLoS One. 2013;8(2):e57083.

PMID:23451152

IF_{2012} 3,730

Number of citations: 1 (WoS; 2013-12-13)

Contribution of the author: Tomas Grousl conceived and designed the experiments, performed a majority of experiments, analysed the data and co-wrote the publication.

Paper 3

Mmi1, the yeast homologue of Mammalian TCTP, associates with stress granules in heat-shocked cells and modulates proteasome activity.

Rinnerthaler M, Lejskova R, **Grousl T**, Stradalova V, Heeren G, Richter K, Breitenbach-Koller L, Malinsky J, Hasek J, Breitenbach M.

PLoS One. 2013 Oct 28;8(10):e77791.

PMID:24204967

IF_{2012} 3,730

Number of citations: 0 (WoS; 2013-12-18)

Contribution of the author: Tomas Grousl contributed to the designing of the experiments, performed some of the experiments and analysed the data.

Paper 4

Yno1p/Aim14p, a NADPH-oxidase ortholog, controls extramitochondrial reactive oxygen species generation, apoptosis, and actin cable formation in yeast.

Rinnerthaler M, Buttner S, Laun P, Heeren G, Felder TK, Klinger H, Weinberger M, Stolze K, **Grousl T**, Hasek J, Benada O, Frydlova I, Klocker A, Simon-Nobbe B, Jansko B, Breitenbach-Koller H, Eisenberg T, Gourlay CW, Madeo F, Burhans WC, Breitenbach M.

Proc Natl Acad Sci U S A. 2012 May 29;109(22):8658-63

PMID:22586098

IF_{2012} 9,737

Number of citations: 10 (WoS; 2013-12-18)

Contribution of the author: Tomas Grousl contributed to the experimental part.

I declare that the contribution of Tomáš Groušl to the presented results in Grousl et al., JCS, 2009 and Grousl et al., PlosOne, 2013, as stated in "Presented publications" chapter, is true.

Prague, 25.11.2013

Jiří Hašek

I declare that the contribution of Tomáš Groušl to the presented results in Rinnerthaler et al., PNAS, 2012 and Rinnerthaler et al., PlosOne, 2013, as stated in "Presented publications" chapter, is true.

Prague, 25.11.2013

Mark Rinnerthaler

Paper 1

The paper *Robust heat shock induces eIF2-phosphorylation independent assembly of stress granules containing eIF3 and 40S ribosomal subunits in budding yeast, Saccharomyces cerevisiae* by Grousl et al. focuses on a description and analyses of heat-induced stress granules (SGs) of *Saccharomyces cerevisiae*.

The main message of the paper is identification and characterization of yeast SGs induced by robust heat shock. These SGs are in composition and in proposed functions analogous to SGs of higher eukaryotes. Generally, stress granules are formed in a response to environmental stresses. Their formation is one possible way, how to regulate translation upon a stress. It is thought that SGs represent sites where certain translation machinery components are sorted and subsequently stored or sent back to translation or designed for a degradation.

SGs are characterized by a presence of stalled translation pre-initiation complexes represented by certain translation initiation factors, small ribosomal subunits (40S), mRNA molecules and mRNA binding proteins. A presence of other constituents should vary depending on the type and the intensity of a stress and the cell type. Indeed, heat-induced SGs of *S. cerevisiae* were shown to contain, besides mentioned factors, also unique components as are mRNA decay proteins. A formation of yeast heat-induced SGs is reversible and energy-dependent process. In contrast to a majority of higher eukaryotes‘ SGs, their assembly is not triggered by phosphorylation of translation initiation factor eIF2α. Authors of the paper also compare heat-induced SGs with, in that time, only known SGs in *S. cerevisiae*, with glucose deprivation-induced stress granules. It was shown that unlike SGs in glucose deprived cells, heat-induced ones require different scaffolding proteins and have even different composition, which more reassembles a composition of higher eukaryotes‘ SGs. The characterization is, so far, completed with a comparison of heat-induced SGs with processing bodies. Processing bodies (PBs) are another type of stress response-induced accumulations of ribonucleoprotein complexes. They were originally characterized as sites where mRNA decay occurs. However, their role in cell metabolism seems to be far more complex. Despite heat-induced SGs contain components of PBs and PBs promote the SGs formation, the SGs are based on different scaffolding proteins and represent separate and unique entities.

Authors of the paper performed variety of methodologies including live cell fluorescence microscopy, polysome profile analyses and also certain genetic and biochemical methods.

The paper summarizes the data about newly discovered heat-induced stress granules in *S. cerevisiae*. These granules possess similar dynamics and composition as their counterparts from higher eukaryotes. Despite certain differences between yeast SGs and SGs of evolutionary higher organisms, the first ones can offer valuable tool for a research of the second ones.

JCS ePress online publication date 26 May 2009

Robust heat shock induces eIF2α-phosphorylation-independent assembly of stress granules containing eIF3 and 40S ribosomal subunits in budding yeast, *Saccharomyces cerevisiae*

Tomáš Grousl[1], Pavel Ivanov[1,*], Ivana Frýdlová[1], Pavla Vašicová[1], Filip Janda[1], Jana Vojtová[1], Kateřina Malínská[1], Ivana Malcová[1], Lenka Nováková[1], Dana Janošková[1], Leoš Valášek[2] and Jiří Hašek[1,‡]

[1]Laboratory of Cell Reproduction, Institute of Microbiology of the AS CR, v.v.i., Prague, Czech Republic
[2]Laboratory of Regulation of Gene Expression, Institute of Microbiology of the AS CR, v.v.i., Prague, Czech Republic
*Present address: A.N. Belozersky Institute of Physico-Chemical Biology MSU, Moscow, Russia
‡Author for correspondence (e-mail: hasek@biomed.cas.cz)

Accepted 18 March 2009
Journal of Cell Science 122, 2078-2088 Published by The Company of Biologists 2009
doi:10.1242/jcs.045104

Summary

Environmental stresses inducing translation arrest are accompanied by the deposition of translational components into stress granules (SGs) serving as mRNA triage sites. It has recently been reported that, in *Saccharomyces cerevisiae*, formation of SGs occurs as a result of a prolonged glucose starvation. However, these SGs did not contain eIF3, one of hallmarks of mammalian SGs. We have analyzed the effect of robust heat shock on distribution of eIF3a/Tif32p/Rpg1p and showed that it results in the formation of eIF3a accumulations containing other eIF3 subunits, known yeast SG components and small but not large ribosomal subunits and eIF2α/Sui2p. Interestingly, under these conditions, Dcp2p and Dhh1p P-body markers also colocalized with eIF3a. Microscopic analyses of the *edc3*Δ*lsm4*ΔC mutant demonstrated that different scaffolding proteins are required to induce SGs upon robust heat shock as opposed to glucose deprivation. Even though eIF2α became phosphorylated under these stress conditions, the decrease in polysomes and formation of SGs occurred independently of phosphorylation of eIF2α. We conclude that under specific stress conditions, such as robust heat shock, yeast SGs do contain eIF3 and 40S ribosomes and utilize alternative routes for their assembly.

Key words: P-bodies, Stress granules, Yeast

Introduction

Intracellular compartmentalization of specific mRNAs and components of the translation machinery is an important mode of regulation for gene expression in eukaryotic cells. In this respect, formation of various mRNA-containing assemblies, such as stress granules (SGs) or processing bodies (P-bodies), is a striking illustration of this regulation (Anderson and Kedersha, 2008; Bond, 2006; Parker and Sheth, 2007).

Various stresses cause a fast and transient redistribution of nontranslated mRNAs into SGs in mammalian as well as plant cells. This effect is a result of a rapid repression of general translation initiation, often mediated through phosphorylation of the alpha subunit of the translation initiation factor 2 (eIF2) (Holcik and Sonenberg, 2005; Kedersha et al., 1999). Therefore mammalian SGs are thought to represent abortive 48S complexes that include mRNA linked to poly(A)-binding protein 1, translation initiation factors (e.g. eIF3, eIF4A, eIF4G) and 40S ribosomal subunits (Anderson and Kedersha, 2008; Kedersha et al., 2002). SGs persist in equilibrium with polysomes and this can be affected by translation inhibitors, which either stabilize or destabilize the polysomes. It has been proposed that the SGs serve as triage sites redirecting mRNA to either translation, storage or degradation (Anderson and Kedersha, 2008). Interestingly, SG-like structures, containing eIF3, have been found in heat-shocked fission yeast *Schizosacchomyces pombe* (Dunand-Sauthier et al., 2002), but have not yet been reported in *Saccharomyces cerevisiae*.

P-bodies were originally described as sites of mRNA decapping and decay, which mainly contain the mRNA degradation machinery components including the decapping enzyme complex (Brengues et al., 2005). P-bodies and SGs share some proteins and mRNA components, but also contain a number of unique markers specific to each structure (Kedersha and Anderson, 2007). Unlike SGs, P-bodies are present even under non-stress conditions (Mollet et al., 2008) and never contain eIF3 and 40S ribosomal subunits (Anderson and Kedersha, 2008; Brengues and Parker, 2007; Parker and Sheth, 2007; Sheth and Parker, 2003; Sheth and Parker, 2006). P-bodies are therefore believed to be structurally distinct from SGs; however, their simultaneous appearance in stressed mammalian cells showed a close spatial connection perhaps indicating an intimate mutual communication (Kedersha et al., 2005; Wilczynska et al., 2005). In addition, because of these interactions, a role for pre-existing P-bodies in the nucleation of SG assembly has been suggested recently (Buchan et al., 2008; Mollet et al., 2008).

In the budding yeast *S. cerevisiae*, a number of small cytosolic foci of accumulated Dcp2p can be observed also in normal proliferating cells (Brengues et al., 2005; Teixeira et al., 2005). Under various stresses, e.g. glucose starvation, hyperosmotic stress and heat stress at 37°C, these foci increase in size to form enlarged P-bodies (Brengues et al., 2005). Recently, novel mRNA assemblies called EGP-bodies (for eIF4E, eIF4G and Pab1p) that are distinct from P-bodies were found to form under prolonged glucose

starvation in *S. cerevisiae* (Hoyle et al., 2007). While this manuscript was under a review process in this journal, additional markers of mammalian SGs were identified within EGP-bodies that led the authors to rename them 'yeast stress granules' (Buchan et al., 2008). In sharp contrast to mammalian SGs, however, the reported yeast SGs of glucose-deprived yeast cells do not contain eIF3 and 40S ribosomal subunits (Buchan et al., 2008; Hoyle et al., 2007).

In *S. cerevisiae*, numerous stresses including hyperosmolarity, glucose deprivation and robust heat shock at 46°C were demonstrated to stabilize many mRNAs (Hilgers et al., 2006). Whereas the impact of hyperosmolarity on formation of P-bodies seems to be identical to that of glucose deprivation (Brengues et al., 2005), it is not known whether robust heat shock also elicits similar effects. In this report, we show that robust heat shock at 46°C for 10 minutes applied to aerobically cultivated yeast cells results in formation of accumulations containing eIF3 subunits, mRNA, eIF4G2, Pab1p, Ngr1p, Pub1p, 40S ribosomal subunits and also typical P-body proteins such as Dcp2p and Dhh1p. Assembly of these transient protein accumulations is eIF2α-phosphorylation independent. We also demonstrate that they are not formed in cycloheximide-treated and energy-depleted cells. Because of their composition, irregular shapes and requirement for different scaffolding proteins than are those needed for P-bodies, we posit that these protein accumulations are yeast SGs specific for the robust heat shock. We further propose that they can only be detected in *S. cerevisiae* when transient severe stresses such as robust heat shock are applied and the period of yeast mRNA triage is relatively prolonged.

Results

Robust heat shock induces transient formation of eIF3-containing SGs

We showed previously that eIF3a/Tif32p/Rpg1p colocalized with cytoplasmic microtubules in the fixed yeast cells (Hasek et al., 2000). In order to examine intracellular distribution of eIF3a in living cells, we constructed wild-type strains expressing eIF3a fused either with RFP or GFP from its chromosomal locus. In accord with previously published data (Brengues et al., 2005), we found that distribution of both fluorescing eIF3a fusions is uniformly cytosolic in cells cultivated in complete YPD medium at 30°C (Fig. 1A). In addition, this localization pattern was not affected by a mild heat shock at 42°C for 10 minutes (data not shown), which has been used to induce formation of SGs in fission yeast *S. pombe* (Dunand-Sauthier et al., 2002). However, we found that raising the temperature of the heat shock to over 42°C has a dramatic effect on the eIF3a distribution. In particular, incubation of cells in YPD medium at 46°C for 10 minutes resulted in formation of distinct eIF3a accumulations (Fig. 1B). We observed that this rearrangement of eIF3a was transient and reversible (Fig. 1C), since the eIF3a became uniformly cytosolic after cultivation of heat-shocked cells in YPD medium at 30°C for 30 minutes.

To investigate whether these protein accumulations are limited to eIF3a in isolation or whether it is a common characteristic of components of the eIF3 complex, we prepared strains coexpressing eIF3a-GFP with either eIF3b/Prt1p-RFP or eIF3c/Nip1p-RFP fusions from their chromosomal loci. As shown in Fig. 1D, the eIF3a-GFP foci always colocalized with the other eIF3 subunits, strongly suggesting that protein accumulations induced by robust heat shock contain core components of the eIF3 complex. As confirmed by high values of the Pearson's correlation coefficient (Rr), over 0.9 (see Materials and Methods), distribution for both eIF3b and eIF3c signals almost completely matched that of eIF3a.

In living yeast, accumulation of mRNA in P-bodies has been assessed using a specific *PGK1* reporter mRNA containing multiple U1A-specific binding sites in its 3′ untranslated region to which U1A-GFP fusion protein binds (Brengues et al., 2005; Teixeira et al., 2005). We employed this detection system in order to find out if mRNA also accumulates in the eIF3a foci after robust heat shock. As shown in Fig. 1E, the *PGK1* mRNA in unstressed cells was distributed across the cytosol, as has previously been observed (Brengues et al., 2005). In cells heat-shocked in a complete medium at 46°C for 10 minutes, the cytoplasmic GFP signal corresponding to the accumulated *PGK1* mRNA significantly overlapped with that of eIF3a foci. Weak background fluorescence was observed in the cytoplasm of control cells expressing the U1A-GFP fusion protein only, without *PGK1* mRNA under all tested conditions (data not shown).

eIF3a foci contain typical components of the mammalian SGs

Stalled 48S pre-initiation complexes containing mRNA, eIF3, eIF4G, PABP and 40S, but not 60S ribosomal subunits and eIF2, are the core constituents of the mammalian SGs (Kedersha et al., 2002). To determine whether yeast eIF3 foci are related to mammalian SGs, we constructed strains coexpressing various RFP and GFP fusion proteins, exposed the exponentially growing cells to robust heat shock in YPD medium at 46°C for 10 minutes and analyzed the distribution of fusion proteins using the Olympus Cell R microscopic system.

First, we found that in the heat-shocked cells eIF3a colocalized with eIF4G2 and Pab1p (Fig. 2A). Very high values of Pearson's correlation coefficient (Rr), over 0.8, confirmed a high degree of colocalization. In addition, we also analyzed changes in the distribution of Rps30A-GFP fusion protein that we used as a marker of the 40S ribosomal subunit. We found that robust heat shock induced formation of Rps30A-GFP foci, which clearly colocalized with eIF3a-RFP as illustrated by a high Rr (Fig. 2B). By contrast, exposing cells to robust heat shock did not induce accumulation of Rpl25-GFP that was used as a marker of the 60S ribosomal subunit (Fig. 2C). Consistently, the frequency scatter plot analysis as well as a small value of Rr confirmed a very weak colocalization of Rpl25p with eIF3a. These results imply that, in contrast to the 40S ribosomal subunit, the 60S subunit is not actually accumulated within the eIF3a foci. No fluorescent foci were observed in heat-shocked strains expressing eIF2α-RFP (Sui2p-RFP), GFP alone or GFP fusions of the cytosolic metabolic enzymes Pgk1, Pfk1 and Pfk2 (Fig. 2D). Thus, we conclude that cytosolic accumulations of eIF3a, induced by robust heat shock in *S. cerevisiae*, contain components typical of mammalian SGs. Therefore we refer to them as SGs throughout the rest of this study.

P-body proteins colocalize with eIF3a-containing SGs in heat-shocked cells

Glucose deprivation and mildly elevated temperature (37°C) were shown to induce formation of enlarged cytosolic P-bodies (Brengues et al., 2005). Despite the fact that no eIF3a accumulations were observed upon glucose deprivation, we decided to investigate the relationship of the SGs with P-bodies upon robust heat shock. To do this, we constructed yeast strains coexpressing eIF3a-RFP together with GFP fusions of known P-body proteins from their chromosomal loci. First, we analyzed

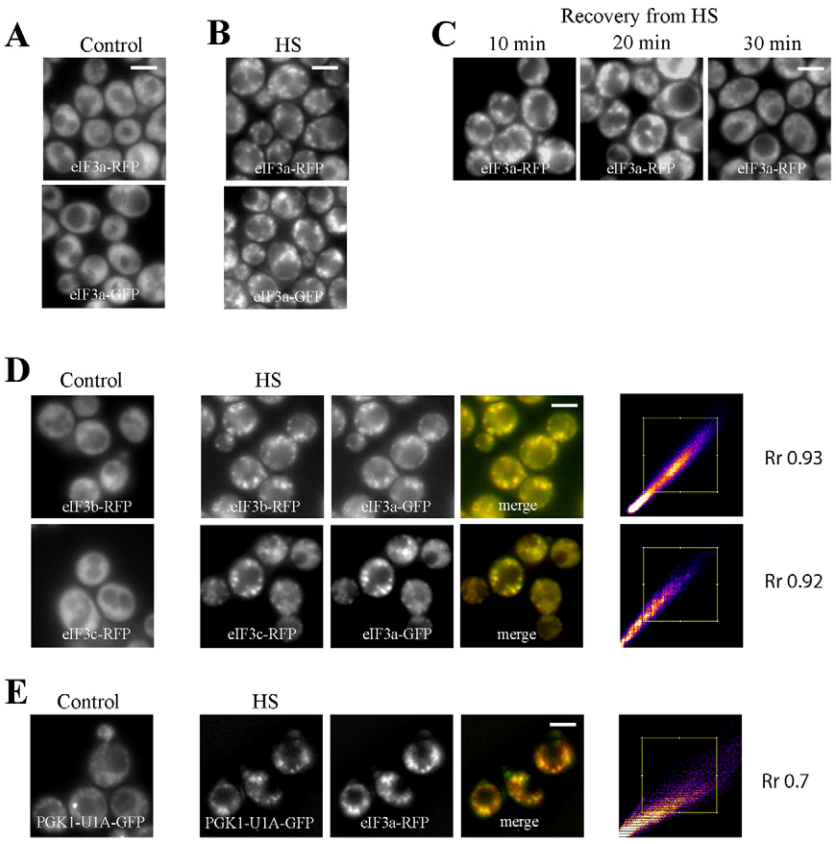

Fig. 1. Robust heat shock results in formation of the eIF3-mRNA colocalizing foci in yeast cells. (A) Distribution of either GFP or RFP fusion of eIF3a/Tif32p/Rpg1p is cytosolic at 30°C (strains CRY204, CRY255). (B) Upon robust heat shock (46°C, 10 minutes), both eIF3a fluorescent fusions accumulated in discrete foci. (C) eIF3a foci are transient assemblies and the eIF3a-RFP signal becomes uniformly cytosolic after a subsequent 30 minute cultivation of heat-shocked cells (strain CRY255) in YPD medium at 30°C on a rotary shaker. (D) Control: Distribution of RFP fusions of eIF3b/Prt1p and eIF3c/Nip1p is uniformly cytosolic at 30°C (strains CRY344, CRY346). HS: In cells heat-shocked at 46°C for 10 minutes in YPD medium, eIF3b and eIF3c fusions colocalize with eIF3a foci with the high Pearson's correlation coefficient (Rr). (E) Control: PGK1 reporter mRNA (via U1A-GFP) is uniformly distributed in cells cultivated at 30°C. HS: In cells heat-shocked at 46°C for 10 minutes, *PGK1* mRNA accumulates in foci colocalizing with aggregates of eIF3a-RFP (strains CRY774, CRY775). Scale bars: 5 μm.

colocalization of eIF3a and the decapping enzyme Dcp2p that is a core component of P-bodies. In contrast to uniform cytosolic distribution of eIF3a, Dcp2p accumulated in small cytosolic foci in control cells cultivated in YPD medium at 30°C (Fig. 3A, control) as described previously (Brengues et al., 2005). Surprisingly, when these cells were heat-shocked in YPD medium at 46°C for 10 minutes, Dcp2p colocalization with eIF3a in multiple enlarged cytosolic foci (Fig. 3A, HS). The very high degree of colocalization of these fusion proteins in heat-shocked cells was exemplified by high Rr values of over 0.8. A similar pattern of colocalization in heat-shocked cells was also obtained for another P-body-specific marker Dhh1p (Fig. 3B). These findings thus suggest that components of SGs and P-bodies form joint accumulations when the fermenting cells are exposed to robust heat shock.

Differential centrifugation confirmed localization data from microscopic examination

To confirm the in vivo localization data biochemically, we performed immunochemical analyses of samples prepared from control and the heat-shocked cells by differential centrifugation using a protocol described elsewhere (Teixeira et al., 2005). Protein accumulations from the non-stressed versus heat-shocked cells were collected from the lysates as pellets and together with the corresponding supernatants subjected to western blotting (see the Materials and Methods). As shown in Fig. 4, the pellet from the heat-shocked cells was specifically enriched for eIF3a, Dcp2p, eIF4G2 and Pab1p, as expected from our fluorescence microscopy data. In addition, we also confirmed the presence of 40S ribosomal subunits (Rps30Ap) in the pellets and the absence of 60S ribosomal subunits (Rpl25p). Similarly, eIF2α, Pgk1p and Pfk1p, which did not occur in the SGs, were not pelleted from lysates of the heat-shocked cells. Hence, these biochemical data fully comply with our microscopic observations.

Inhibition of translation initiation and formation of SGs upon robust heat shock is Gcn2p independent

It is well known that inhibition of general translation upon various types of stress is mediated by phosphorylation of eIF2α, which is sufficient for formation of mammalian SGs under various stress conditions (Kedersha et al., 1999). In *S. cerevisiae*, Gcn2p is the only eIF2α kinase (Proud, 2005). Interestingly, it was previously shown that formation of P-bodies is independent of eIF2α phosphorylation (Kedersha et al., 2005). Thus we next decided to examine whether eIF2α phosphorylation is required for the formation of SGs in heat-shocked cells. As shown in Fig. 5A, incubation of fermenting wild-type *GCN2*$^{+}$ cells at 46°C for 10 minutes (HS) resulted in marked phosphorylation of the α-subunit of eIF2 in contrast to the heat-shocked *gcn2*Δ cells. Accordingly, the *GCN2*$^{+}$ cells incubated at 46°C for 10 minutes (HS) displayed a dramatic polysome run-off, resulting in accumulation of the 80S ribosomal species called monosomes (Fig. 5B). This redistribution of ribosomes from polysomes to monosomes serves as a hallmark of inhibition of translation initiation (Hartwell and McLaughlin, 1969). Strikingly, robust heat shock (HS) inhibited translation initiation in *gcn2*Δ cells (unable to phosphorylate eIF2α) to the same extent as in the wild-type *GCN2*$^{+}$ cells. In agreement with the translational arrest induced by robust heat shock in *gcn2*Δ cells, formation of SGs was also found to be independent of the Gcn2 kinase (Fig. 5C). To conclude, our results indicate that in *S.*

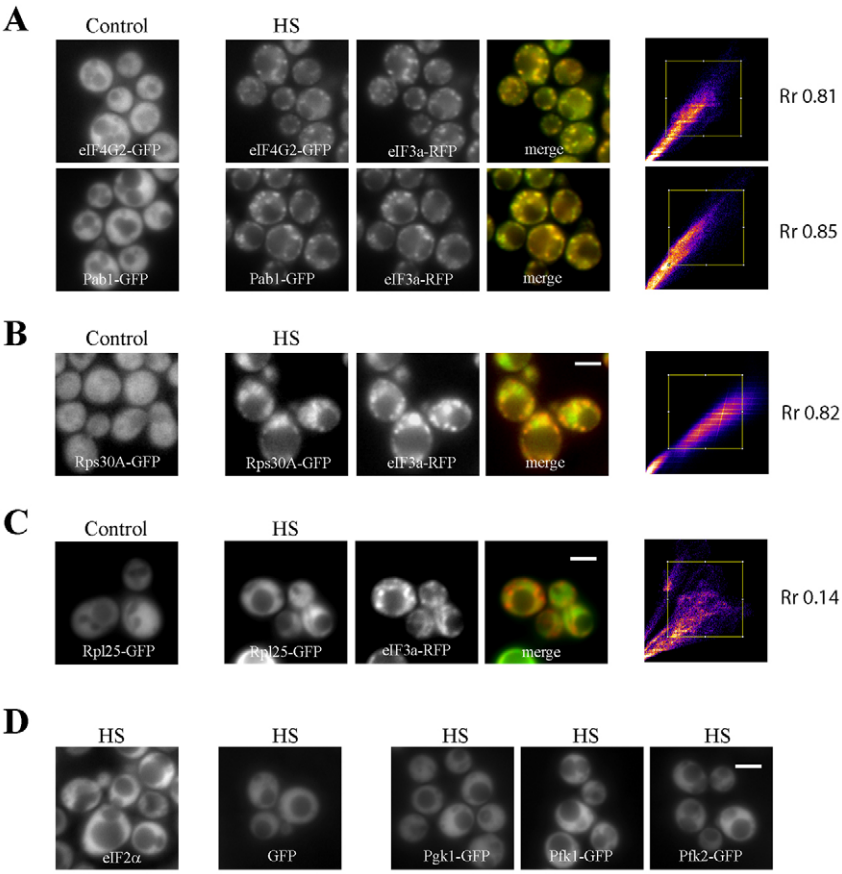

Fig. 2. Robust heat shock-induced eIF3 foci contain numerous translational components with the exception of eIF2 and the 60S ribosomal subunits. (A) Control: Distribution of GFP fusions of eIF4G2 and Pab1p is uniformly cytosolic in fermenting cells at 30°C (strains CRY340, CRY527). HS: Upon robust heat shock, both fusion proteins colocalize with the foci of eIF3a. (B) Uniform distribution of the 40S ribosomal marker Rps30Ap in fermenting cells at 30°C (Control) becomes condensed (HS) and clearly colocalizes with eIF3a foci upon heat treatment (strain CRY887). (C) Distribution of the 60S ribosomal marker Rpl25p remains uniform in both, fermenting (Control) or heat-shocked (HS) cells (strain CRY837). The very low Rr value further illustrates that 60S ribosomes do not accumulate within the eIF3a foci in heat-shocked cells. (D) Robust heat shock did not induce accumulation of eIF2α/Sui2-RFP (strain CRY334), GFP alone (strain CRY836) or metabolic enzymes Pgk1p, Pfk1p and Pfk2p (strains CRY431, CRY490, CRY491). Scale bars: 5 μm.

cerevisiae, the inhibition of translation initiation and formation of SGs triggered by robust heat shock are independent of eIF2α phosphorylation.

Cycloheximide prevents assembly of SGs in heat-shocked cells

Cycloheximide (CYH) causes stalling of polyribosomes on mRNA and as such has been shown to prevent formation of SGs in mammalian cells (Kedersha et al., 1999) and assembly of P-bodies or SGs in yeast cells starved of glucose (Brengues et al., 2005; Buchan et al., 2008). Therefore we also analyzed its effect on assembly of SGs during robust heat shock using the strain coexpressing eIF3a-RFP and Dcp2p-GFP from their chromosomal loci. We treated exponentially growing cells with CYH (50 μg/ml) in YPD medium at 30°C for 10 minutes before glucose deprivation or robust heat shock. In accordance with previously published data (Brengues et al., 2005), we observed the CYH-related inhibition of the P-body assembly in glucose-deprived cells (Fig. 6A). Similarly, no enlarged accumulations of either eIF3a or Dcp2p were formed when the culture of CYH-treated cells was subsequently heat-shocked in YPD at 46°C for 10 minutes (Fig. 6B). Assuming that CYH prevented formation of SGs by sequestration of mRNAs into polysomes, these results suggest that the protein as well as mRNA composition of SGs of heat-shocked cells is dynamic, similar to P-

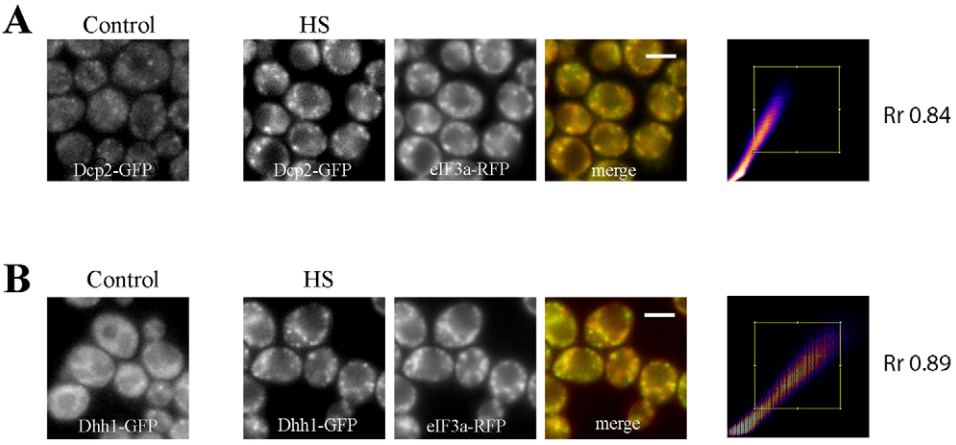

Fig. 3. P-body markers, Dcp2p (A) and Dhh1p (B), colocalize with SGs in wild-type cells after robust heat shock. In fermenting cells grown at 30°C, Dcp2p-GFP and Dhh1p-GFP were uniformly distributed (Control), whereas upon robust heat shock (HS) they were accumulated in enlarged cytosolic foci closely colocalizing with eIF3a-RFP (strains CRY522, CRY564). Scale bars: 5 μm.

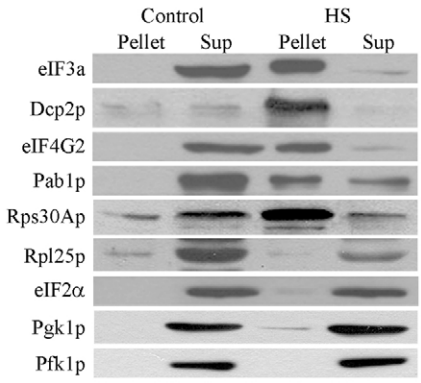

Fig. 4. Biochemical characterization of SGs confirms microscopic observations. Samples containing SG components were prepared according to a protocol described previously (Teixeira et al., 2005). Western blot analyses show that eIF3a, eIF4G2, Pab1p as well as Rps30Ap (40S ribosomal subunit) and Dcp2p are enriched in the pellet of the lysate prepared from the heat-shocked cells (46°C, 10 minutes). Cell debris were pelleted at 2296 × ***g*** for 10 minutes and the supernatant was spun down at 18,000 × ***g*** for 10 minutes (for the source of antibodies, please see the Materials and Methods). By contrast, eIF2α/Sui2p, Rpl25p (60S ribosomal subunit), as well as metabolic enzymes Pgk1p and Pfk1p remained predominantly in the supernatant of heat-shocked cells (strains CRY336, CRY411, CRY423, CRY431, CRY490, CRY837 and CRY887).

bodies and SGs of glucose-deprived yeast cells (Buchan et al., 2008; Sheth and Parker, 2003) and mammalian SGs (Kedersha et al., 2000) and, moreover, that their core components are also in equilibrium with polysomes.

Assembly of SGs upon robust heat shock is an energy-dependent process

To examine whether formation of heat shock-induced SGs in *S. cerevisiae* depends on the energy supply, we analyzed changes in distribution of Dcp2p and eIF3a upon robust heat shock in energy-depleted cells. Energy depletion was achieved by inhibiting both glycolysis by 2-deoxy-D-glucose (Franzusoff and Cirillo, 1982), and oxidative phosphorylation, by sodium-azide that blocks cytochrome C oxidase (Duncan and Mackler, 1966). Under normal conditions in fermenting cells, Dcp2p was localized into small cytosolic foci and eIF3a was uniformly cytosolic (Fig. 7A; control). We found that simultaneous treatment of these cells with 20 mM 2-deoxy-D-glucose and 20 mM sodium azide for 20 minutes did not significantly affect distribution of eIF3a; however, small cytosolic foci of Dcp2p enlarged into obvious P-bodies (Fig. 7A, ED). In contrast to heat-shocked fermenting cells in which there is colocalization of foci of Dcp2p and eIF3a (Fig. 7B, HS), the energy-depleted and subsequently heat-shocked cells (Fig. 7B, ED and HS) were unable to form SGs, but they displayed enlarged P-bodies characterized by accumulated Dcp2p. Interestingly, growth rate analyses of the cells recovering from the robust heat shock revealed that the outgrowth of ED/HS cells was significantly delayed by several hours when compared with cells that were only heat-shocked (Fig. 7C). These striking findings suggest that assembly of SGs in heat-shocked *S. cerevisiae* is, in contrast to P-bodies, an active process that requires energy. In addition, depletion of the ATP and/or GTP pool in living cells significantly delays the recovery phase of heat-shocked cells hinting that SGs could play a key role in the adaptation and resilience of yeast to robust heat shock.

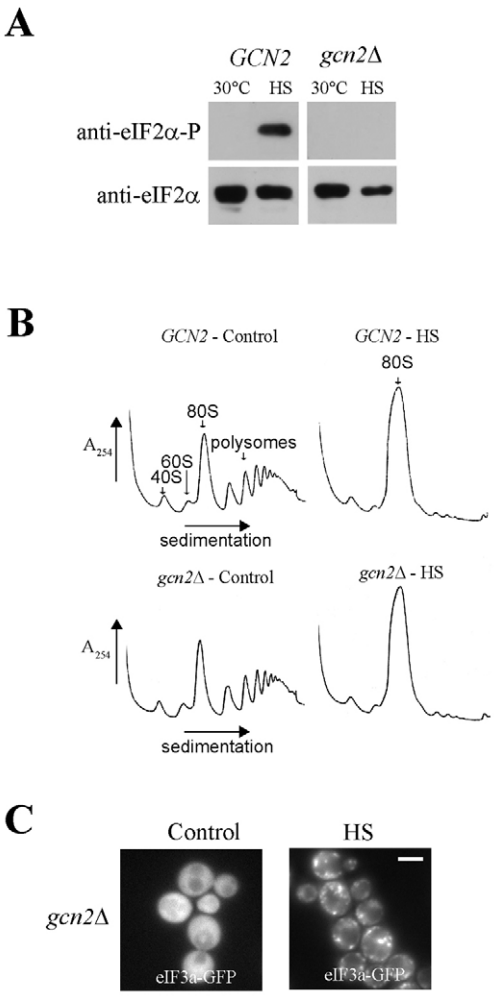

Fig. 5. eIF2α phosphorylation is not required for the polysome run-off and SG assembly upon robust heat shock. (A) Robust heat shock at 46°C for 10 minutes (HS) induces the Gcn2p kinase-mediated phosphorylation of eIF2α in wild-type cells (*GCN2*; strain BY 4741) that is not detected in the *gcn2*Δ mutant (strain CRY309). (B) Nevertheless, robust heat shock (HS) does result in a polysome run-off with commensurate increase in the amount of monosomes in both wild-type cells (*GCN2*; strain BY4741) as well as in the *gcn2*Δ mutant (strain CRY309), indicating that translation is inhibited in a Gcn2p-independent manner. (C) SGs are also assembled in heat-shocked (46°C, 10 minutes) *gcn2*Δ cells (HS; strain CRY569). Scale bar: 5 μm.

Robust heat shock elicits formation of Dcp2p accumulations even in the absence of typical P-body scaffolding proteins Edc3p and Lsm4p that overlap with eIF3-containing SGs

The fact that eIF3a and Dcp2p colocalize, prompted us to elucidate whether formation of SGs in cells upon robust heat shock depends on the same scaffolding proteins as P-bodies. To this end, in a strain coexpressing eIF3a-RFP and Dcp2p-GFP from their chromosomal loci, we generated *edc3*Δ and *lsm4*ΔC mutations. The deletion of the *EDC3* gene and the deletion of 97 amino acids from the C-terminal part of Lsm4p have been previously shown to prevent formation of P-bodies (Decker et al., 2007) and SGs (Buchan et al., 2008) in glucose-deprived yeast cells. Consistently, we found that glucose starvation of cells at 30°C resulted in formation of several enlarged P-bodies in wild-type cells but not in the mutant cells (Fig. 8A, top panels). The *edc3*Δ *lsm4*ΔC mutant cells had a stronger Dcp2-GFP signal in the cytosol as well as an obvious accumulation

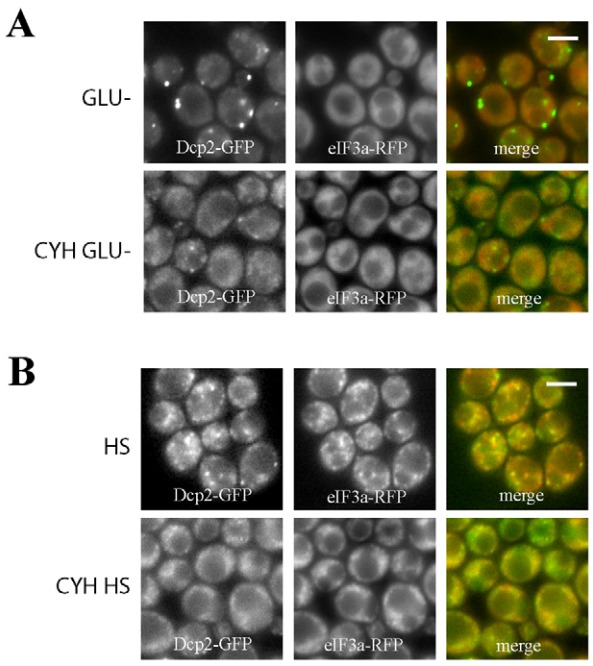

Fig. 6. Cycloheximide (CYH) prevents formation of P-bodies (A) and SGs (B). The cells coexpressing eIF3a-RFP and Dcp2p-GFP (strain CRY564) were grown in YPD at 30°C to an exponential phase and treated with CYH (50 µg/ml) for 10 minutes before the medium was replaced with YP lacking glucose (A; CYH GLU-); or prior the heat shock at 46°C for 10 minutes in the YPD medium (B; CYH HS). Scale bars: 5 µm.

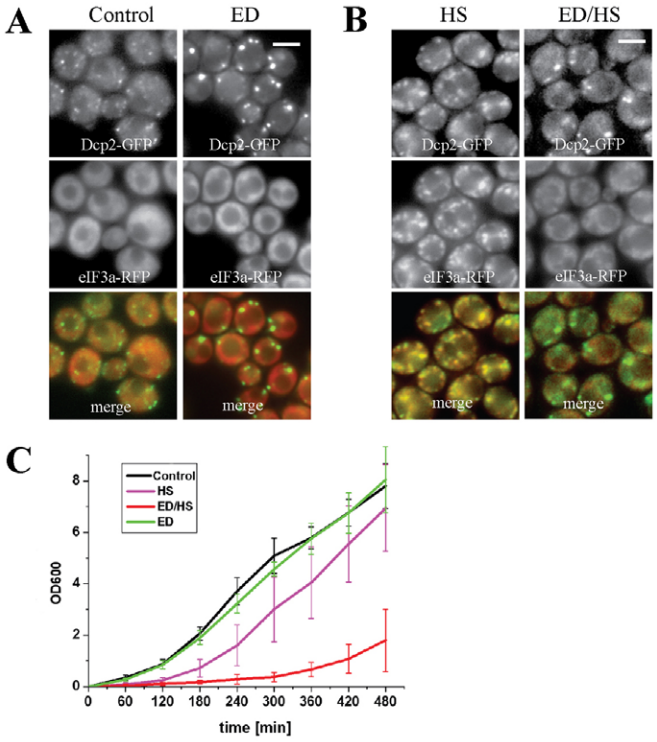

Fig. 7. Energy depletion preceding the robust heat shock prevents SG assembly and delays the subsequent recovery phase (strain CRY564). (A) In exponentially growing cells, Dcp2p forms small foci and eIF3a is uniformly cytosolic (Control). When a pool of energy was depleted by the simultaneous treatment of wild-type cells with 2-D-deoxyglucose (20 mM) and sodium azide (20 mM) for 20 minutes, Dcp2p accumulated in enlarged P-bodies but the eIF3a distribution remained uniform (ED). (B) Heat-shocked cells (HS) show accumulation of Dcp2p in SGs as shown above; however, energy depletion applied before robust heat shock (ED/HS) prevented formation of YSGs and Dcp2p accumulated in enlarged P-bodies. (C) Outgrowth of cells during the recovery from energy depletion followed by robust heat shock was delayed several hours compared to heat shock or energy depletion alone; values are mean ± s.e.m. Scale bars: 5 µm.

of Dcp2-GFP in the nuclear region. As expected, distribution of eIF3a-RFP was uniformly cytosolic in both strains starved of glucose for 30 minutes (Fig. 8A, middle panels). In the presence of glucose, wild-type fermenting cells had small cytosolic foci of Dcp2p-GFP, as expected (Fig. 8B, left-handed top panel), whereas the *edc3*Δ *lsm4*ΔC mutant cells showed a dominant accumulation of the Dcp2-GFP signal in the nuclear region (Fig. 8B, right-handed top panel). Distribution of eIF3a-RFP was again uniformly cytosolic in both strains grown in glucose as expected (Fig. 8B, middle panels). Strikingly, when both strains were first starved of glucose for 30 minutes and subsequently heat-shocked at 46°C for 10 minutes in the YP medium (in the absence of glucose), mainly enlarged P-bodies developed in the wild-type cells (Fig. 8C, left-handed top panel), whereas in the *edc3*Δ *lsm4*ΔC mutant cells there were only distinct accumulations of Dcp2-GFP in the vicinity of nuclei (Fig. 8C, right-handed top panel). In both strains, eIF3a-RFP clearly colocalized with Dcp2-GFP accumulations (Fig. 8C, middle panel). This novel and rather surprising finding indicates that the robust heat shock induces formation of Dcp2p accumulations qualitatively distinct from P-bodies, at least with respect to scaffolding proteins, which overlap with eIF3a-containing SGs. In perfect agreement, Dcp2p-GFP accumulations readily formed also in fermenting *edc3*Δ*lsm4*ΔC mutant cells (in the presence of glucose) subjected to robust heat shock (Fig. 8D, right-handed top panel).

Assembly of SGs upon robust heat shock requires different scaffolding proteins than assembly of SGs in glucose-deprived cells

Recently, it has been shown that a prolonged glucose starvation results in assembly of yeast SGs that do not contain eIF3 and 40S ribosomal subunits (Buchan et al., 2008). In fact, these SGs were proposed to be identical to previously described accumulations called EGP bodies (Hoyle et al., 2007). To compare SGs assembled in glucose-deprived cells with eIF3-containing accumulations evoked by robust heat shock we constructed several strains coexpressing known yeast TIAR and TIA protein orthologs that were shown to constitute yeast SGs such as Ngr1-GFP or Pub1-GFP with eIF3a-RFP (Buchan et al., 2008). We found that both of these yeast SG markers expressed from their chromosomal loci colocalized with eIF3a in cells exposed to robust heat shock at 46°C in YPD medium for 10 minutes (Fig. 9A). As confirmed by high values of the Pearson's correlation coefficient of over 0.8, distribution of both Ngr1-GFP and Pub1-GFP signals almost completely matched that of eIF3a-RFP. Interestingly, in addition to that, both yeast SG markers were also enriched in the nuclear region of the stressed cells.

To test whether deletions of the P-body scaffolding proteins Lsm4 and Edc3 would or would not have an effect on the accumulation of Ngr1p into robust heat shock-induced SGs (the deletions do not affect accumulation of eIF3a), we generated the *edc3*Δ *lsm4*Δ*C* double-deletion strain coexpressing eIF3a-RFP with Ngr1-GFP from chromosomal loci. As predicted, we found

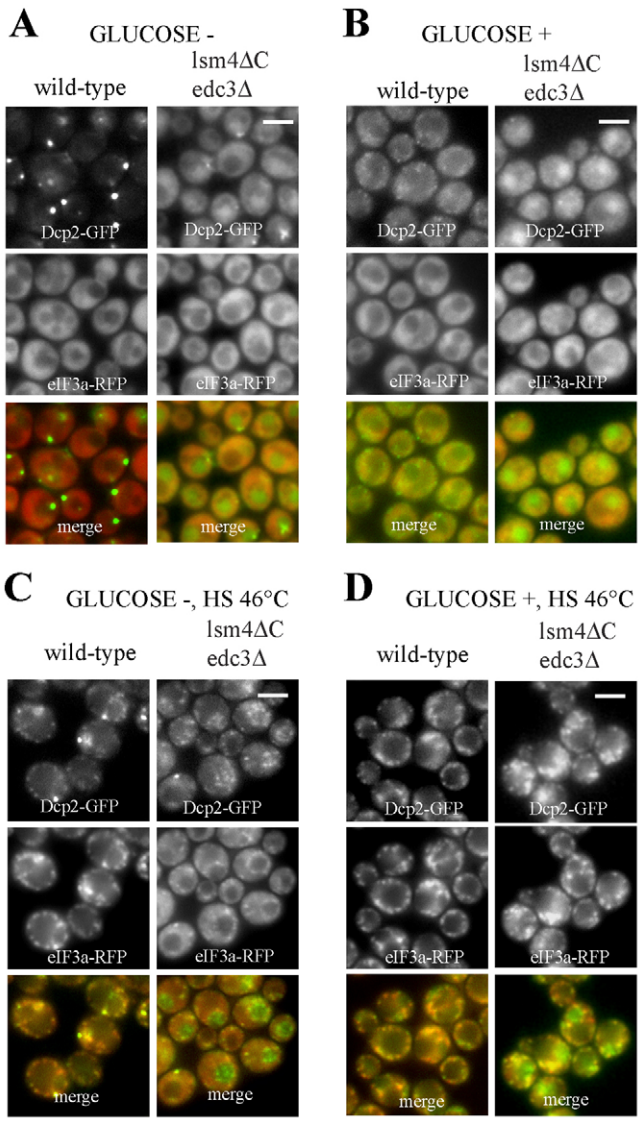

Fig. 8. Wild-type and the *edc3*Δ *lsm4*ΔC mutant cells coexpressing Dcp2p-GFP and eIF3a-RFP (strains CRY564 and CRY977) reveal a different requirement of eIF3-containing SGs for scaffolding proteins. (A) Wild-type cells starved for glucose in YP medium at 30°C for 30 minutes show enlarged P-bodies (accumulation of Dcp2p) unlike the *edc3*Δ *lsm4*ΔC mutant cells. Distribution of eIF3a remains uniform under glucose starvation in both wild-type and mutant cells. (B) Wild-type and *edc3*Δ *lsm4*ΔC mutant cells exponentially grown in YPD medium at 30°C have Dcp2-GFP distributed in small cytosolic foci. In addition, the mutant cells also accumulate the Dcp2-GFP signal in the nuclear region. Distribution of eIF3a-RFP is uniformly cytosolic in both wild-type and mutant fermenting cells. (C) Cells starved for glucose at 30°C in the YP medium for 30 minutes were subsequently heat-shocked at 46°C in YP medium for 10 minutes. There was colocalization of Dcp2-GFP and eIF3a-RFP in multiple cytosolic protein accumulations in both wild-type and *edc3*Δ *lsm4*ΔC cells. (D) The cells exponentially growing in YPD medium at 30°C were heat-shocked at 46°C for 10 minutes. Both wild-type and the mutant cells show accumulation of the Dcp2p signal in cytosolic SGs. In addition, the mutant cells show an obvious accumulation of the Dcp2-GFP signal in the nuclear region. Scale bars: 5 μm.

that the heat-shocked *edc3*Δ *lsm4*Δ*C* mutant cells accumulated Ngr1-GFP in the eIF3-containing SGs (Fig. 9B). In addition to this colocalization pattern, we also observed cells with the Ngr1-GFP signal in the nuclear region. This may suggest an increased level of degradation of this yeast SG marker upon robust heat shock.

Pub1p but not Ngr1p was implicated in playing a crucial role in yeast SG formation under glucose deprivation (Buchan et al., 2008). To examine the role of Ngr1 and Pub1 proteins in the assembly of SG upon robust heat shock, we deleted the *NGR1* and *PUB1* genes in the strain coexpressing Dcp2-GFP and eIF3a-RFP from the chromosomal loci. As shown in Fig. 9C, both heat-shocked mutants displayed unchanged colocalization pattern of Dcp2-GFP foci with eIF3a-RFP accumulations when compared with wild-type cells (see Fig. 3A) suggesting that neither Pub1p nor Ngr1 are required for assembly of yeast SGs upon robust heat shock, in contrast to glucose-deprivation-induced SGs (Buchan et al., 2008).

Glucose starvation of heat shocked cells results in separation of the Dcp2-GFP signal from eIF3a-containing SGs

The fact that formation of eIF3 accumulations in fermenting cells upon robust heat shock requires different scaffolding proteins than assembly of P-bodies and SGs in glucose-deprived cells prompted us to investigate links between eIF3-containing SGs in glucose-fed fermenting cells and P-bodies and/or SGs formed in glucose-deprived cells. To do that, we used the strains coexpressing eIF3a-RFP and Dcp2-GFP or Pab1-GFP from their chromosomal loci. We first exposed the exponentially growing cells to robust heat shock at 46°C for 10 minutes in the YPD medium, washed them once with YP medium without glucose and cultured them in YP medium at 30°C for an additional 90 minutes. In sharp contrast to recovery after heat shock in the presence of glucose (see Fig. 1C), the absence of glucose in the medium prevented dissolution of eIF3a accumulations (Fig. 10). In these cells, the Dcp2-GFP signal did not overlap with the persistent eIF3a accumulations after cultivation for 30 minutes in the absence of glucose (Fig. 10A). By contrast, the marker of the yeast SGs, Pab1-GFP, remained closely colocalized with eIF3a-RFP even after 90 minutes of subsequent cultivation (Fig. 10B). Therefore our results provide strong support for the idea that SGs and P-bodies are intertwined but distinct accumulations (Mollet et al., 2008).

Discussion

In stressed eukaryotic cells, non-translating mRNAs are sequestered into various transient granules or bodies depending on the type of stress condition that the cells are subjected to and the cell type (Anderson and Kedersha, 2008; Bond, 2006; Brengues et al., 2005; Buchan et al., 2008; Hoyle et al., 2007; Kedersha and Anderson, 2007; Malagon and Jensen, 2008; Mollet et al., 2008; Parker and Sheth, 2007). In this investigation we analyzed the impact of a robust heat shock and employed live cell imaging fluorescence microscopy to demonstrate for the first time that robust heat shock in budding yeast, *S. cerevisiae*, induces assembly of SGs more similar in their content to mammalian SGs than those that were described in glucose-deprived *S. cerevisiae* (Buchan et al., 2008) while this manuscript was under editorial review.

It should be emphasized that all tested proteins that were fused to either green fluorescent protein (GFP) or red fluorescent protein (RFP), were the only forms of those proteins expressed in the test cells and they fully supported growth. In control experiments, neither GFP alone nor GFP fusions of several cytosolic enzymes formed any visible aggregates or accumulations upon robust heat shock, indicating that the formation of large fluorescent foci is not a general phenomenon of protein aggregation resulting from intense heat treatment. Hence, we consider the ability of translational

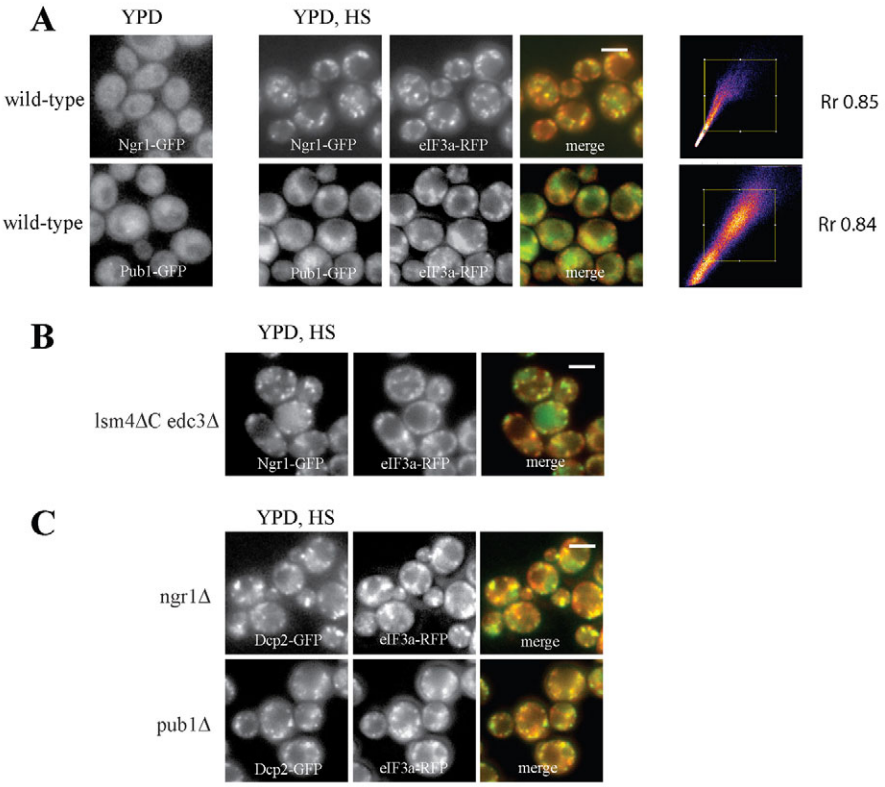

Fig. 9. Yeast TIAR and TIA protein orthologs, Ngr1 and Pub1, colocalize with eIF3a-containing SGs but their absence does not affect SG assembly upon robust heat shock. (A) Uniform distribution of Ngr1-GFP or Pub1-GFP in fermenting cells at 30°C (YPD) becomes condensed and both fusion proteins colocalize with eIF3a foci upon robust heat shock (YPD, HS; strains CRY1017, CRY1021). (B) Ngr1-GFP accumulated at eIF3a-RFP foci also in the heat-shocked *edc3*Δ *lsm4*ΔC mutant cells (strain CRY1036). (C) Deletion mutant strains *ngr1*Δ and *pub1*Δ coexpressing Dcp2p-GFP and eIF3a-RFP (strains CRY1027 and CRY1028) that were heat-shocked at 46°C for 10 minutes displayed similar distribution of both markers as wild-type cells (see Fig. 3A). Scale bars: 5 µm.

components to accumulate in detectable accumulations to be part of their function in translational control of stressed cells. Whereas studies on mammalian cells showed that SGs can be either deficient in eIF2α (Kedersha et al., 2002) or not (Kimball et al., 2003), the fact that eIF2α is not part of SGs in heat-shocked cells of *S. cerevisiae* clearly indicates that SGs are not the same as the heat shock granules containing eIF2α that were found as a result of prolonged heat treatment (60 minutes) in plant cells (Weber et al., 2008). In accord with the logic applied by Buchan et al. (Buchan et al., 2008), we assume that eIF2α does not accumulate with eIF3-containing SGs because it is believed to form yeast-specific structures with its GTP/GDP exchange factor eIF2B under certain stress conditions (Campbell et al., 2005).

In agreement with previously published data (Brengues et al., 2005), *PGK1* mRNA was found uniformly distributed in the cytosol of unstressed exponentially growing cells. However, upon robust heat shock this mRNA clearly accumulated in eIF3 foci. Consistent with this, cycloheximide prevents formation of SGs upon robust heat shock in a similar way to that described for the formation of P-bodies (Brengues et al., 2005) and SGs in glucose-deprived yeast cells (Buchan et al., 2008). This suggests that mRNA may be an essential component in the formation of SGs upon robust heat shock, presumably by decreasing its availability. This conclusion is in keeping with the idea that under robust heat shock, at least some yeast mRNAs are protected in sub-cellular structures that are inaccessible to deadenylases, retaining a portion of the cytoplasmic mRNA pool for later use during recovery from the stress (Hilgers et al., 2006).

SGs of mammalian cells have already been shown to interact with P-bodies suggesting they are distinct but closely intertwined assemblies sharing components, depending on cell type and type of stress (Kedersha et al., 2005; Mollet et al., 2008; Wilczynska et al., 2005). In addition, preexisting P-bodies have been only recently shown to directly promote assembly of SGs in glucose-deprived *S. cerevisiae* cells (Buchan et al., 2008). We show here that in contrast to glucose deprivation, robust heat shock does not result in formation of typical enlarged P-bodies but rather in multiple small Dcp2p-GFP accumulations containing other P-body markers as well. The key question is whether these accumulations of Dcp2-GFP in heat-shocked cells can still technically be considered as a different form of P-bodies? We observed that both formations in question depend on the availability of mRNA, but can be easily distinguished by

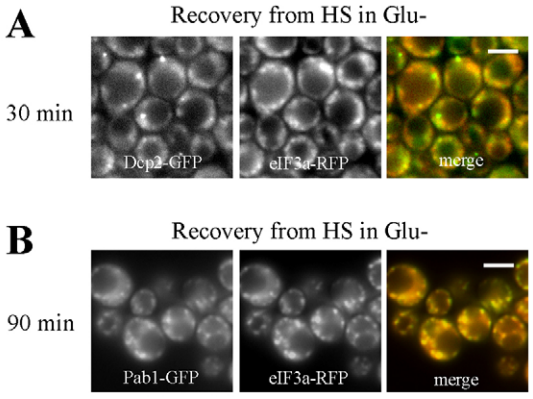

Fig. 10. (A) Heat-shocked wild-type cells starved of glucose for 30 minutes following the robust heat shock show separation of the P-body marker Dcp2-GFP from the eIF3a-RFP accumulations (strain CRY564). (B) By contrast, the SG marker Pab1-GFP remained colocalized with eIF3a-RFP, even after 90 minutes of glucose deprivation (strain CRY527). Scale bars: 5 µm.

their requirement for different scaffolding proteins; Edc3p and Lsm4p are required for P-body formation in glucose-deprived cells but not for the formation of Dcp2p accumulations upon robust heat shock (see Fig. 8). Interestingly, similar requirements were also found in glucose-deprivation-induced SGs (Buchan et al., 2008) but not by SGs elicited by robust heat shock. Finally, it is also worth noting that eIF3-containing SGs in heat-shocked cells had distinct morphologies and a different requirement for energy than P-bodies, and that we observed a separation of Dcp2p and eIF3a signals in heat-shocked cells recovering in the glucose-free medium. Taken together, the results presented herein clearly indicate that Dcp2p accumulations and eIF3-containing SGs induced by robust heat-shock are also two discrete but closely intertwined assemblies similar to but differing substantially from the P-bodies and SGs induced by glucose deprivation as shown previously (Buchan et al., 2008). Since SGs and P-bodies are generally considered to be dynamic assemblies of mRNA-protein systems (mRNPs) (Brengues et al., 2005; Hoyle et al., 2007), we suggest that these apparent differences most probably reflect distinctions in the rate-limiting steps in a given mRNP transition process that probably changes under various stress conditions.

In keeping with this suggestion, assembly of mammalian SGs was shown to be dependent on the RNA binding protein TIA-1. Its overexpression induces SG formation without stress. Moreover, the absence of TIA-1 results in a strong impairment of SG formation under various stresses (Gilks et al., 2004). *S. cerevisiae* contains potential TIA, TIAR and ATXN2 orthologs, namely Pub1p, Ngr1p and Pbp1p, respectively. Whereas *pub1*Δ and *ngr1*Δ strains showed a strong decrease in the number of SGs in glucose-deprived cells (Buchan et al., 2008), we found that the absence of either Pub1p or Ngr1p had no significant impact on the assembly eIF3-containing SGs following robust heat shock. These findings thus may suggest that either the function of the latter proteins is more redundant under robust heat shock conditions or that other non-homologous scaffolding proteins are involved.

Despite the fact that yeast SGs that are formed upon robust heat shock seem to contain most if not all components of mammalian SGs, their formation is eIF2α-phosphorylation independent in the budding yeast, unlike the situation in mammals (Kedersha et al., 1999). Actually, in this respect, yeast SGs formed in heat-shocked cells more closely resemble P-bodies of glucose-deprived cells, the assembly of which also does not require phosphorylation of eIF2 (Kedersha et al., 2005). Nevertheless, the most recent observation from trypanosomes showing that assembly of SGs in response to heat shock was also found to be independent of phosphorylation of eIF2α (Kramer et al., 2008) might indicate that either the biochemistry of the SG assembly induced by heat shock differs substantially from that induced by other stresses (perhaps in involvement of heat shock proteins) or that higher eukaryotes acquired some novel aspect(s) of this control mechanism that has imposed a need for eIF2α-phosphorylation. Since interfering with the activity of eIF4G (Mazroui et al., 2006) or eIF4A (Dang et al., 2006; Mazroui et al., 2006) seems to trigger SG formation independently of eIF2α phosphorylation also in mammalian cells, these factors could play some role in this process.

Along these lines, it was only recently shown that several components of the hexosamine biosynthetic pathway, which reversibly modifies proteins with O-linked *N*-acetylglucosamine (O-GlcNAc) in response to stress, are required for accumulation of untranslated messenger ribonucleoproteins in SGs in mammalian cells (Ohn et al., 2008). However, the hexosamine biosynthetic enzymes are lacking in budding yeast and the authors suggested that this fact may contribute to differences between mammalian SGs and their closest relatives known in yeast so far, the SGs without eIF3 and 40S ribosomal subunits. Hence, in analogy, it could be proposed that the absence of these proteins makes the yeast translational machinery somewhat more resistant to mild stresses, explaining why accumulation of eIF3a was not previously observed in *S. cerevisiae* cells heat-shocked at 42°C, or subjected to hyperosmotic stress (Brengues et al., 2005) or glucose deprivation (Buchan et al., 2008). It will be intriguing in the future to investigate what differentiates yeast cells from other cell types that produce typical SGs in response to robust heat shock, and what roles these accumulations play in stress survival.

Materials and Methods

Yeast strains and growth conditions

S. cerevisiae strains used in this study were derived either from the BY4742 background, S288C background (Huh et al., 2003) or SEY6210 background (Scott Emr, Cornell University, Ithaca, NY) and are listed in Table 1. Yeast cultures were grown in YPD medium (1% yeast extract, 2% peptone, 2% glucose) or SC medium (0.17% yeast nitrogen base medium without amino acids and ammonium sulfate, 0.5% ammonium sulfate, 2% glucose, supplemented with a complete or a strain-specific mixture of amino acids) at 30°C. Solid media contained 2% agar. Standard methods were used for all DNA manipulations (Sambrook and Russell, 2001). The cells coexpressing U1A-GFP and PGK1 mRNA from the corresponding plasmids were pre-cultured in an appropriate SC medium after several inoculation steps (1:10) followed by an 8-hour culture to increase the homogeneity of the U1A-GFP distribution pattern within the cell population. To subject yeast strains to robust heat shock, cells were resuspended in YPD medium preheated to 46°C and incubated for an additional 10 minutes while shaking. Cells were always washed with SC medium before being mounted for microscopic inspection. Cycloheximide (Sigma) was added at a final concentration of 50 μg/ml. Inhibitors 2-deoxy-D-glucose (Sigma) and sodium azide (Sigma) were added as stock aqueous solutions to a final concentration of 20 mM into cultivation media.

Construction of strains with chromosome-derived expression of GFP or RFP fusions

Integrative cassettes containing various RFP or GFP fusions were created by PCR using template DNA pRFPKanMX or pGFPKanMX, respectively, as described elsewhere (Malinska et al., 2003). Purified PCR fragments were transformed into SEY6210 wild-type cells and the corresponding transformants were selected on YPD plates containing 200 μg/ml of G418. The correct integration of the RFP or GFP fusions was confirmed by PCR. The strains were generated by mating, subsequent sporulation in liquid Fowel medium and spore dissection using the Singer micromanipulator.

The mutant strain *edc1*Δ *lsm4*Δ*C* expressing DCP-GFP and eIF3a-RFP from chromosomal sites was constructed by the repeated one-step gene disruption technique (Rothstein, 1991). The deletion cassettes loxP-*URA3*-loxP and loxP-*LEU2*-loxP were amplified from pUG72 and pUG73, respectively (Gueldener et al., 2002), using the ORF-specific primers. The *lsm4*Δ*C* designates a partial deletion of the C-terminal 97 amino acids of the Lsm4p (Decker et al., 2007).

Polysome profile analyses

Cells were grown to an OD_{600}. Approximately 1 and 50 μg/ml cycloheximide (Sigma) was added to a culture 5 minutes before harvesting. Cells were chilled and washed in GA buffer (20 mM Tris-HCl pH 7.5, 50 mM KCl, 10 mM $MgCl_2$, 1 mM DTT, 5 mM NaF) containing 50 μg/ml cycloheximide. Lysates were prepared in GA buffer (supplemented with 1 tablet/10 ml of Complete Mini Protease Inhibitor Mix EDTA-free (Roche) and 50 μg/ml cycloheximide) using glass beads and Fastprep Bio101 at speed 5 for 20 seconds. Lysates were pre-cleared twice by centrifugation at 826 × ***g*** for 5 minutes and 15,520 × ***g***, for 15 minutes (Jouan AB 2.14, France) and loaded onto 5-45% sucrose gradient. Gradients were ultracentrifuged in a SW41 rotor for 2.5 hours at 260,000 × ***g*** at 4°C. Gradients were collected from the bottom and A_{254} was recorded. Fractions of the sucrose gradient were precipitated with trichloroacetic acid, washed several times with ethanol and used for western blot analysis.

Analyses of protein accumulations

Exponentially growing cells were heat-shocked at 46°C for 10 minutes and harvested. Cells were washed and re-suspended in the lysis buffer (Teixeira et al., 2005) containing 50 mM Tris-HCl (pH 7.6), 50 mM NaCl, 5 mM $MgCl_2$, 0.1% NP-40, 1 mM β-mercaptoethanol and 1 tablet/10 ml of Complete Mini Protease Inhibitor Mix EDTA-free (Roche). Disruption of cells was carried out in Fastprep (Bio101-Thermo Savant, Savant Instruments, Waltham, MA) twice at speed 4 for 20 seconds. Cell debris were pelleted at 2296 × ***g*** for 10 minutes at 4°C. Supernatant was

Table 1. Yeast strains used in this study

Strain	Genotype	Source
SEY6210	*MAT***a** *leu2-3112 ura3-52 his3-Δ200 trp1-Δ901 lys2–801 suc2-Δ9*	(Robinson et al., 1988)
SEY6210.1	*MATα leu2-3112 ura3-52 his3-Δ200 trp1-Δ901 lys2–801 suc2-Δ9*	(Robinson et al., 1988)
S288C	*MATα SUC2 gal2 mal mel flo1 flo8-1 hap1 ho bio1 bio6*	(Mortimer and Johnston, 1986)
BY4741	*MAT***a** *his3Δ1 leu2Δ0 met15Δ0 ura3Δ0*	EUROSCARF
CRY204	Sey6210; *MAT***a** *RPG1::GFP::KanMX*	This study
CRY255	Sey6210.1; *MATα RPG1::RFP::KanMX*	This study
CRY309	BY4741; *MAT***a** *gcn2::KanMX*	EUROSCARF
CRY334	Sey6210; *MAT***a** *SUI2::RFP::KanMX*	This study
CRY336	Sey6210; *MAT***a** *TIF4632::GFP::KanMX*	This study
CRY340	Sey6210×Sey6210.1; *MAT***a** *RPG1::RFP::KanMX TIF4632::GFP::KanMX*	This study
CRY344	Sey6210×Sey6210.1; *MAT***a** *RPG1::GFP::KanMX NIP1::RFP::KanMX*	This study
CRY346	Sey6210×Sey6210.1; *MAT***a** *RPG1::GFP::KanMX PRT1::RFP::KanMX*	This study
CRY411	S288C; *MAT***a** *DCP2::GFP::HIS3MX*	(Huh et al., 2003)
CRY423	S288C; *MAT***a** *PAB1::GFP::HIS3MX*	(Huh et al., 2003)
CRY431	S288C; *MAT***a** *PGK1::GFP::HIS3MX*	(Huh et al., 2003)
CRY490	S288C; *MAT***a** *PFK1::GFP::HIS3MX*	(Huh et al., 2003)
CRY491	S288C; *MAT***a** *PFK2::GFP::HIS3MX*	(Huh et al., 2003)
CRY522	Sey6210.1×S288C; *MAT***a** *RPG1::RFP::KanMX DHH1::GFP::HIS3MX*	This study
CRY527	Sey6210.1×S288C; *MAT***a** *RPG1::RFP::KanMX PAB1::GFP::HIS3MX*	This study
CRY564	Sey6210.1×S288C; *MAT***a** *RPG1::RFP::KanMX DCP2::GFP::HIS3MX*	This study
CRY569	BY4741×S288C; *MAT***a** *RPG1::GFP::HIS3MX gcn2::KanMX*	This study
CRY836	BY4741; *MAT***a** + pUG23 (HIS+)	This study
CRY837	Sey6210; *MAT***a** *RPG1::RFP::KanMX* + pRS316-L25e-GFP (URA+)	This study
CRY774	Sey6210; *MAT***a** *RPG1::RFP::KanMX* + pRP1187 (TRP+) + pPS2037(URA+)	This study
CRY775	Sey6210; *MAT***a** *RPG1::RFP:: KanMX* + pRP1187 (TRP+)	This study
CRY887	Sey6210.1×S288C; *MAT*a *RPG1::RFP::KanMX RPS30A::GFP::HIS3MX*	This study
CRY977	CRY564; *MAT***a** *RPG1::RFP::KanMX DCP2::GFP::HIS3MX lsm4ΔC::LEU2 edc3::URA3*	This study
CRY1017	Sey6210.1×S288C; *MAT***a** *RPG1::RFP::KanMX PUB1::GFP::HIS3MX*	This study
CRY1021	Sey6210.1×S288C; *MATα RPG1::RFP::KanMX NGR1::GFP::HIS3MX*	This study
CRY1027	CRY564; *MAT***a** *RPG1::RFP::KanMX DCP2::GFP::HIS3MX pub1::URA3*	This study
CRY1028	CRY564; *MAT***a** *RPG1::RFP::KanMX DCP2::GFP::HIS3MX ngr1::LEU2*	This study
CRY1036	CRY1021; *MATα RPG1::RFP::KanMX NGR1::GFP::HISMX lsm4ΔC::LEU2 edc3::URA3*	This study

centrifuged at 18,000 × ***g*** (Jouan AB 2.14, Saint-Herblain, France) for 10 minutes at 4°C. Pellets and supernatants were analyzed by western blotting for the presence of translation factors and P-body markers.

Western blot analyses

Except for detection of eIF2α phosphorylation, whole cell lysates for western blot analyses with various antibodies were prepared according to a protocol as described elsewhere (Riezman et al., 1983). Proteins resolved by SDS-PAGE were transferred to Protran (Sigma) nitrocellulose membranes. The membrane blots were blocked with 5% non-fat dried milk and incubated overnight with the antibodies. The antibodies used were: mouse monoclonal anti-Rpg1 antibody PK1 (Jirincova et al., 1998) at 1:10,000; mouse monoclonal anti-GFP antibody (Unifect, Moscow, Russia) at 1:2000; rabbit anti-eIF2α/Sui2p antibody (kindly provided by Thomas Dever, NICHHD, Bethesda, MD) at 1:1000. As a secondary antibody, goat anti-mouse IgG antibodies or goat anti-rabbit IgG antibodies conjugated with a horseradish peroxidase (Amersham Pharmacia Biotech, Uppsala, Sweden) were used.

To detect eIF2α phoshorylation, cells were grown to mid-logarithmic phase (OD_{600} ~0.5) in YPD medium and either kept at the permissive temperature or exposed to heat shock at 46°C for 10 minutes. Subsequently, the cells were collected by centrifugation, re-suspended in ice-cold breaking buffer (100 mM Tris-HCl, pH 8.0, 20% glycerol, 1 mM 2-mercaptoethanol, protease inhibitors (Complete Mini Protease Inhibitor Mix plus EDTA; Roche) and phosphatase inhibitors (Inhibitor Cocktail I and II, Sigma)) and lysed using glass beads in Fastprep (Bio101-Thermo Savant) at speed 5, four times 20 seconds at 4°C. Lysates were then pre-cleared at 2000 × ***g*** to remove glass beads and cell debris and centrifuged at 15,000 × ***g*** for 30 minutes at 4°C. Supernatants were collected and separated by electrophoresis on 12% acrylamide SDS-PAGE gels and transferred to PVDF membranes. Western blot analyses were carried out using the rabbit polyclonal phosphospecific antibody against eIF2α (Biosource, Invitrogen) and the rabbit anti-eIF2α antibody (kindly provided by T. Dever).

Microscopy

The cells were inspected after washing with SC or SC-glucose medium, mounting on coverslips and coating with a slice of 1% agarose in appropriate medium. Distribution of GFP and RFP fusion proteins was analyzed with a 100× PlanApochromat objective (NA 1.4) using an Olympus IX-71 inverted microscope equipped with a Hammamatsu Orca/ER digital camera and the Olympus Cell R detection and analyzing system (GFP filter block U-MGFPHQ, exc. max. 488, em. max. 507; RFP filter block U-MWIY2, exc. max. 545-580, em. max. 610). Images were processed and merged using Olympus Cell-R and Adobe CS2 software. The quantitative colocalization analyses were performed using the NIH ImageJ software with the Colocalization Finder plugin, available at http://rsb.info.nih.gov/ij/plugins/. This software was used to determination the Rr, which describes the extent of overlap between image pairs. It is a value between –1 and +1, with –1 being no overlap and +1 being perfect overlap of two images.

We are grateful to Mark Ashe, Anna Koffer and Michael Breitenbach for critical reading of manuscript and helpful comments. The technical assistance by J. Serbouskova and M. Spryngar is also gratefully acknowledged. The plasmid used for the PCR preparation of particular RFP integrative cassettes was kindly provided by Roger Tsien (Howard Hughes Medical Institute, University of California, San Diego, CA). The plasmid pRS316-L25e-GFP is a kind gift from Eduard Hurt (University of Heidelberg, Heidelberg, Germany); plasmids pRP2037 and pRP1187 for the PGK1 mRNA detection were kind gifts from Roy Parker (University of Arizona, Tuscon, AZ). The plasmid pUG23 was kindly provided by Johannes Hegemann (Heinrich Heine University, Düsseldorf, Germany). This work was supported by grants from the Czech Science Foundation 204/02/1424, 204/05/0838 and 204/09/1924, L545 (MSMT), ME 939, and also by the Institutional Research Concept No. AV0Z50200510. P.I. was supported by grant INTAS 05-109-4807 and L.V. was supported by a Jan E. Purkyne Fellowship from Academy of Sciences of the Czech Republic.

References

Anderson, P. and Kedersha, N. (2008). Stress granules: the Tao of RNA triage. *Trends Biochem. Sci.* **33**, 141-150.

Bond, U. (2006). Stressed out! Effects of environmental stress on mRNA metabolism. *FEMS Yeast Res.* **6**, 160-170.

Brengues, M. and Parker, R. (2007). Accumulation of polyadenylated mRNA, Pab1p, eIF4E, and eIF4G with P-bodies in Saccharomyces cerevisiae. *Mol. Biol. Cell* **18**, 2592-2602.

Brengues, M., Teixeira, D. and Parker, R. (2005). Movement of eukaryotic mRNAs between polysomes and cytoplasmic processing bodies. *Science* **310**, 486-489.

Buchan, J. R., Muhlrad, D. and Parker, R. (2008). P bodies promote stress granule assembly in Saccharomyces cerevisiae. *J. Cell Biol.* **183**, 441-455.
Campbell, S. G., Hoyle, N. P. and Ashe, M. P. (2005). Dynamic cycling of eIF2 through a large eIF2B-containing cytoplasmic body: implications for translation control. *J. Cell Biol.* **170**, 925-934.
Dang, Y., Kedersha, N., Low, W. K., Romo, D., Gorospe, M., Kaufman, R., Anderson, P. and Liu, J. O. (2006). Eukaryotic initiation factor 2alpha-independent pathway of stress granule induction by the natural product pateamine A. *J. Biol. Chem.* **281**, 32870-32878.
Decker, C. J., Teixeira, D. and Parker, R. (2007). Edc3p and a glutamine/asparagine-rich domain of Lsm4p function in processing body assembly in Saccharomyces cerevisiae. *J. Cell Biol.* **179**, 437-449.
Dunand-Sauthier, I., Walker, C., Wilkinson, C., Gordon, C., Crane, R., Norbury, C. and Humphrey, T. (2002). Sum1, a component of the fission yeast eIF3 translation initiation complex, is rapidly relocalized during environmental stress and interacts with components of the 26S proteasome. *Mol. Biol. Cell* **13**, 1626-1640.
Duncan, H. M. and Mackler, B. (1966). Electron transport systems of yeast. 3. Preparation and properties of cytochrome oxidase. *J. Biol. Chem.* **241**, 1694-1697.
Franzusoff, A. and Cirillo, V. P. (1982). Uptake and phosphorylation of 2-deoxy-D-glucose by wild-type and single-kinase strains of Saccharomyces cerevisiae. *Biochim. Biophys. Acta* **688**, 295-304.
Gilks, N., Kedersha, N., Ayodele, M., Shen, L., Stoecklin, G., Dember, L. M. and Anderson, P. (2004). Stress granule assembly is mediated by prion-like aggregation of TIA-1. *Mol. Biol. Cell* **15**, 5383-5398.
Gueldener, U., Heinisch, J., Koehler, G. J., Voss, D. and Hegemann, J. H. (2002). A second set of loxP marker cassettes for Cre-mediated multiple gene knockouts in budding yeast. *Nucleic Acids Res.* **30**, e23.
Hartwell, L. H. and McLaughlin, C. S. (1969). A mutant of yeast apparently defective in the initiation of protein synthesis. *Proc. Natl. Acad. Sci. USA* **62**, 468-474.
Hasek, J., Kovarik, P., Valasek, L., Malinska, K., Schneider, J., Kohlwein, S. D. and Ruis, H. (2000). Rpg1p, the subunit of the Saccharomyces cerevisiae eIF3 core complex, is a microtubule-interacting protein. *Cell Motil. Cytoskeleton* **45**, 235-246.
Hilgers, V., Teixeira, D. and Parker, R. (2006). Translation-independent inhibition of mRNA deadenylation during stress in Saccharomyces cerevisiae. *RNA* **12**, 1835-1845.
Holcik, M. and Sonenberg, N. (2005). Translational control in stress and apoptosis. *Nat. Rev. Mol. Cell. Biol.* **6**, 318-327.
Hoyle, N. P., Castelli, L. M., Campbell, S. G., Holmes, L. E. and Ashe, M. P. (2007). Stress-dependent relocalization of translationally primed mRNPs to cytoplasmic granules that are kinetically and spatially distinct from P-bodies. *J. Cell Biol.* **179**, 65-74.
Huh, W. K., Falvo, J. V., Gerke, L. C., Carroll, A. S., Howson, R. W., Weissman, J. S. and O'Shea, E. K. (2003). Global analysis of protein localization in budding yeast. *Nature* **425**, 686-691.
Jirincova, H., Vavrickova, P., Palecek, J. and Hasek, J. (1998). A new monoclonal antibody against Rpg1p. *Folia Biol. (Praha)* **44**, 73.
Kedersha, N. and Anderson, P. (2007). Mammalian stress granules and processing bodies. *Methods Enzymol.* **431**, 61-81.
Kedersha, N. L., Gupta, M., Li, W., Miller, I. and Anderson, P. (1999). RNA-binding proteins TIA-1 and TIAR link the phosphorylation of eIF-2 alpha to the assembly of mammalian stress granules. *J. Cell Biol.* **147**, 1431-1442.
Kedersha, N., Cho, M. R., Li, W., Yacono, P. W., Chen, S., Gilks, N., Golan, D. E. and Anderson, P. (2000). Dynamic shuttling of TIA-1 accompanies the recruitment of mRNA to mammalian stress granules. *J. Cell Biol.* **151**, 1257-1268.
Kedersha, N., Chen, S., Gilks, N., Li, W., Miller, I. J., Stahl, J. and Anderson, P. (2002). Evidence that ternary complex (eIF2-GTP-tRNA(i)(Met))-deficient preinitiation complexes are core constituents of mammalian stress granules. *Mol. Biol. Cell* **13**, 195-210.
Kedersha, N., Stoecklin, G., Ayodele, M., Yacono, P., Lykke-Andersen, J., Fritzler, M. J., Scheuner, D., Kaufman, R. J., Golan, D. E. and Anderson, P. (2005). Stress granules and processing bodies are dynamically linked sites of mRNP remodeling. *J. Cell Biol.* **169**, 871-884.
Kimball, S. R., Horetsky, R. L., Ron, D., Jefferson, L. S. and Harding, H. P. (2003). Mammalian stress granules represent sites of accumulation of stalled translation initiation complexes. *Am. J. Physiol. Cell Physiol.* **284**, C273-C284.
Kramer, S., Queiroz, R., Ellis, L., Webb, H., Hoheisel, J. D., Clayton, C. and Carrington, M. (2008). Heat shock causes a decrease in polysomes and the appearance of stress granules in trypanosomes independently of eIF2{alpha} phosphorylation at Thr169. *J. Cell Sci.* **121**, 3002-3014.
Malagon, F. and Jensen, T. H. (2008). The T body, a new cytoplasmic RNA granule in Saccharomyces cerevisiae. *Mol. Cell. Biol.* **28**, 6022-6032.
Malinska, K., Malinsky, J., Opekarova, M. and Tanner, W. (2003). Visualization of protein compartmentation within the plasma membrane of living yeast cells. *Mol. Biol. Cell* **14**, 4427-4436.
Mazroui, R., Sukarieh, R., Bordeleau, M. E., Kaufman, R. J., Northcote, P., Tanaka, J., Gallouzi, I. and Pelletier, J. (2006). Inhibition of ribosome recruitment induces stress granule formation independently of eukaryotic initiation factor 2alpha phosphorylation. *Mol. Biol. Cell* **17**, 4212-4219.
Mollet, S., Cougot, N., Wilczynska, A., Dautry, F., Kress, M., Bertrand, E. and Weil, D. (2008). Translationally repressed mRNA transiently cycles through stress granules during stress. *Mol. Biol. Cell* **19**, 4469-4479.
Mortimer, R. K. and Johnston, J. R. (1986). Genealogy of principal strains of the yeast genetic stock center. *Genetics* **113**, 35-43.
Ohn, T., Kedersha, N., Hickman, T., Tisdale, S. and Anderson, P. (2008). A functional RNAi screen links O-GlcNAc modification of ribosomal proteins to stress granule and processing body assembly. *Nat. Cell Biol.* **10**, 1224-1231.
Parker, R. and Sheth, U. (2007). P bodies and the control of mRNA translation and degradation. *Mol. Cell* **25**, 635-646.
Proud, C. G. (2005). eIF2 and the control of cell physiology (Invited review). *Semin. Cell Dev. Biol.* **16**, 3-12.
Riezman, H., Hase, T., van Loon, A. P., Grivell, L. A., Suda, K. and Schatz, G. (1983). Import of proteins into mitochondria: a 70 kilodalton outer membrane protein with a large carboxy-terminal deletion is still transported to the outer membrane. *EMBO J.* **2**, 2161-2168.
Robinson, J. S., Klionsky, D. J., Banta, L. M. and Emr, S. D. (1988). Protein sorting in Saccharomyces cerevisiae: isolation of mutants defective in the delivery and processing of multiple vacuolar hydrolases. *Mol. Cell. Biol.* **8**, 4936-4948.
Rothstein, R. (1991). Targeting, disruption, replacement, and allele rescue: integrative DNA transformation in yeast. *Methods Enzymol.* **194**, 281-301.
Sambrook, J. and Russell, D. W. (2001). *Molecular Cloning: A Laboratory Manual*. 3rd edn. Cold Spring Harbor, NY: Cold Spring Harbor Laboratory Press.
Sheth, U. and Parker, R. (2003). Decapping and decay of messenger RNA occur in cytoplasmic processing bodies. *Science* **300**, 805-808.
Sheth, U. and Parker, R. (2006). Targeting of aberrant mRNAs to cytoplasmic processing bodies. *Cell* **125**, 1095-1109.
Teixeira, D., Sheth, U., Valencia-Sanchez, M. A., Brengues, M. and Parker, R. (2005). Processing bodies require RNA for assembly and contain nontranslating mRNAs. *RNA* **11**, 371-382.
Weber, C., Nover, L. and Fauth, M. (2008). Plant stress granules and mRNA processing bodies are distinct from heat stress granules. *Plant J.* **56**, 517-530.
Wilczynska, A., Aigueperse, C., Kress, M., Dautry, F. and Weil, D. (2005). The translational regulator CPEB1 provides a link between dcp1 bodies and stress granules. *J. Cell Sci.* **118**, 981-992.

Paper 2

The paper *Heat Shock-Induced Accumulation of Translation Elongation and Termination Factors Precedes Assembly of Stress Granules in S. cerevisiae* by Grousl et al., focuses on new data obtained from analyses of heat-induced stress granules (SGs) of *Saccharomyces cerevisiae*.

The main message of the paper is a discovery of new components of heat-induced SGs and detailed analysis of the SGs dynamics resulting in proposition of hypothesis about the SGs function. The paper builds on the paper *Grousl et al., 2009*. The data upgrade the information about previously established SGs of robust heat shocked cells. In an effort to more characterize the SGs, new components of them were discovered. These are translation elongation and translation termination factors. Among them, a potential yeast prion protein is present. A presence of translation elongation and termination factors within any SGs has not yet been recorded. Concurrently, it was shown that heat-induced SGs begin to being assembled just upon milder heat shock at 42°C (robust heat shock occurs at 46°C). These pre-formed ribonucleoprotein accumulations consist of only some of genuine SGs components. Nevertheless, they possess the same dynamics as robust heat shock-induced SGs and can develop into proper SGs when a temperature of a heat shock is increased. Taken together, these data can help in explaining of both, mechanisms of SGs assembly and cellular signals leading to SGs formation. Finally, based on particular findings, authors support hypothesis which defines SGs as sites required for efficient translation recovery after the stress.

Authors of the paper performed variety of methodologies including live cell imaging fluorescence microscopy, mass spectrometry analyses, polysome profile analyses and certain genetic and biochemical methods.

The paper extends the knowledge about heat-induced stress granules of *Saccharomyces cerevisiae*. The data about composition, dynamics and function of the SGs were enriched. The new components of those can illuminate the mechanism of the SGs formation. Simultaneously, the proposed function of the SGs, as sites of translation machinery components storage and as sites of translation re-initiation after a stress, was experimentally supported.

OPEN ACCESS Freely available online

PLOS ONE

Heat Shock-Induced Accumulation of Translation Elongation and Termination Factors Precedes Assembly of Stress Granules in *S. cerevisiae*

Tomas Grousl, Pavel Ivanov¤, Ivana Malcova, Petr Pompach, Ivana Frydlova, Renata Slaba, Lenka Senohrabkova, Lenka Novakova, Jiri Hasek*

Institute of Microbiology of AS CR, v.v.i., Prague, Czech Republic

Abstract

In response to severe environmental stresses eukaryotic cells shut down translation and accumulate components of the translational machinery in stress granules (SGs). Since they contain mainly mRNA, translation initiation factors and 40S ribosomal subunits, they have been referred to as dominant accumulations of stalled translation preinitiation complexes. Here we present evidence that the robust heat shock-induced SGs of *S. cerevisiae* also contain translation elongation factors eEF3 (Yef3p) and eEF1Bγ2 (Tef4p) as well as translation termination factors eRF1 (Sup45p) and eRF3 (Sup35p). Despite the presence of the yeast prion protein Sup35 in heat shock-induced SGs, we found out that its prion-like domain is not involved in the SGs assembly. Factors eEF3, eEF1Bγ2 and eRF1 were accumulated and co-localized with Dcp2 foci even upon a milder heat shock at 42°C independently of P-bodies scaffolding proteins. We also show that eEF3 accumulations at 42°C determine sites of the genuine SGs assembly at 46°C. We suggest that identification of translation elongation and termination factors in SGs might help to understand the mechanism of the eIF2α factor phosphorylation-independent repression of translation and SGs assembly.

Citation: Grousl T, Ivanov P, Malcova I, Pompach P, Frydlova I, et al. (2013) Heat Shock-Induced Accumulation of Translation Elongation and Termination Factors Precedes Assembly of Stress Granules in *S. cerevisiae*. PLoS ONE 8(2): e57083. doi:10.1371/journal.pone.0057083

Editor: Mick F. Tuite, University of Kent, United Kingdom

Received October 11, 2012; **Accepted** January 17, 2013; **Published** February 25, 2013

Funding: This work was supported by the grants of the Czech Science Foundation 204/09/1924, P305/12/0480 and P305/10/P253, and RVO61388971. The funders had no role in study design, data collection and analysis, decision to publish, or preparation of the manuscript.

Competing Interests: The authors have declared that no competing interests exist.

* E-mail: hasek@biomed.cas.cz

¤ Current address: Department of Environmental Science, Stockholm University, Stockholm, Sweden

Introduction

Reactivity to environmental changes is a key property of all living organisms that enables them to survive and develop. Cells undergo adaptation to stress conditions via various mechanisms. To save energy, general translation is reduced and the expression of stress response-specific genes is triggered. New ribonucleoprotein (RNP) complexes are formed, through which the fate of mRNA molecules and translation machinery components is regulated.

Major accumulations of cytoplasmic RNP complexes that have been recognized in higher eukaryotes - processing bodies (P-bodies) and stress granules (SGs) have also been found in yeasts [1,2,3,4,5,6]. Whilst P-bodies are present even in unstressed cells and they become dominant upon stress, SGs are formed only in stressed cells. Besides translationally repressed mRNA molecules, P-bodies also contain proteins involved in mRNA degradation, translation repression, mRNA quality control and other functions (for a review, see [7,8]). However, nowadays it is evident that the function of P-bodies is far more complex than merely mRNA degradation [9,10,11,12] and is still not well understood (for a review, see [13]). The composition of SGs is influenced by the particular stress conditions and depends on the organism being subjected to the stress. It is generally accepted that major SGs components are stalled translation preinitiation complexes (48S), which contain molecules of mRNA, small ribosomal subunits and several translation initiation factors. Besides these, they may contain a few other factors, which could be found either in SGs or P-bodies [2,14]. Thus, P-bodies and SGs represent two distinct types of RNP assemblies, which can share some components and can be in spatial contact, but differ in their role in cell adaptation to environmental changes, which is realized via translation regulation and mRNA metabolism.

Analogous to mammalian cells, it is thought that yeast SGs take part in regulation of translation, sorting and storage of mRNA molecules, and the preservation of selected translation factors and mRNA molecules against an influence of a stress [10,14,15]. Recently, they have been shown to control TORC1 signaling [16]. Typical examples of yeast SGs are those containing eIF3 components. They are induced by robust heat shock [2], high concentrations of ethanol [3] or NaN_3 [17]. However, only the robust heat shock-induced SGs accumulate 40S ribosomal subunits. Based on the analyses of the strains from the GFP collection [18], none of the tested 60S markers formed foci upon robust heat shock indicating that 60S ribosomal subunits were not accumulated in these SGs [2]. Interestingly, these typical SGs containing 40S and eIF3 translation initiation factor have also been observed in fission yeast *S. pombe* affected by heat shock or glucose deprivation [4,19]. Other examples of RNP accumulations, which are thought to be functionally analogous to SGs, are

yeast EGP bodies [20], stress granules of glucose-deprived [1] or cold-stressed [6] *S. cerevisiae* cells.

Heat stress is an example of stress conditions resulting in the formation of either P-bodies or stress granules (SGs). In *S. cerevisiae* cells, whose temperature optimum for growth is between 25°C and 30°C, cultivation at 39°C triggers the assembly of P-bodies [21] and robust heat shock at 46°C leads to the formation of SGs [2]. Here we report on the identification of novel components of heat-induced SGs in yeast, translation elongation factors eEF3 (Yef3p) and eEF1Bγ2 (Tef4p) and translation termination factors eRF1 (Sup45p) and eRF3 (Sup35p). Despite the presence of the yeast prion protein Sup35, we proved that its prion-like domain is necessary neither for SGs assembly nor for its localization into SGs. Moreover, we showed that eEF3, eEF1Bγ2 and eRF1 factors accumulate even upon a milder heat shock at 42°C, possibly preparing a platform for assembly of genuine SGs at 46°C. Although RNP accumulations induced at 42°C contain some components of P-bodies, they depend neither on P-bodies scaffolding proteins nor on the Gcn2 kinase activity.

The Gcn2 kinase is so far the only known yeast kinase of α subunit of translation initiation factor 2 (eIF2α) [22]. This factor plays an essential role in translation initiation and its regulation. The eIF2 factor is a component of the "ternary complex", which brings the initiator tRNA to 40S ribosomal subunits. The GTP-bound to eIF2 is then hydrolyzed to GDP and the factor leaves the ribosome. The active, GTP-bound, form of eIF2 is recovered by its guanine nucleotide exchange factor eIF2B [23]. Under stress conditions, stress responsive kinases, e.g. Gcn2, phosphorylate α subunit of eIF2 factor [22]. Since the phosphorylated eIF2 factor has higher affinity for eIF2B [24], it leads to reduction of availability of eIF2B factor, eIF2-GTP and the "ternary complex". Thus, it results in inhibition of translation initiation, which is commonly link to an accumulation of stalled translation preinitiation complexes and stress granules assembly. Taken together, the phosphorylation of eIF2α factor is sufficient, but not necessary for SGs formation (for a review, see [14]). The eIF2α-phosphorylation independent mechanisms of SGs assembly have also been described from yeast to mammalian cells [2,25,26,27,28,29,30]. These mechanisms are mainly concerned with translation initiation factors, or are yet unknown [31].

Although, we found that assembly of heat-induced SGs at 46°C and RNP accumulations formed at 42°C are not driven by eIF2α phosphorylations, we also observed that the translation initiation factor eIF2α (Sui2p), which is not a component of the heat-induced SGs in *S. cerevisiae*, accumulates when SGs dissolve during the cell recovery from the stress. Altogether, our data might help to understand the eIF2α factor phosphorylation-independent signaling pathway of the SGs assembly and to reinforce the hypothesis that SGs are the sites where translation initiates after stress relief.

Materials and Methods

Yeast Strains and Growth Conditions

The *Saccharomyces cerevisiae* strains used in this study were derived either from the BY [32], S288C [18] or SEY6210 [33] backgrounds and are listed in Table 1. Yeast cultures were grown in YPD medium (1% yeast extract, 2% peptone, 2% glucose) or SC medium (0.17% YNB without amino acids and ammonium sulfate, 0.5% ammonium sulfate, 2% glucose, supplemented with a complete or appropriate mixture of amino acids) at 30°C. The corresponding solid media contained 2% agar. To select for auxotrophies, the respective amino acid was omitted from the dropout mix. To select for resistance to antibiotics, the appropriate antibiotic was added to the media. Standard methods were used for all DNA manipulations [34]. Strains and mutants expressing particular combinations of various GFP/RFP/mCherry fusion proteins from the sites on the chromosomes were generated by mating, sporulation on solid Fowell medium and subsequent spore dissection by Singer^{TM} micromanipulator. To perform the heat shock, cells were re-suspended in YPD medium preheated to 42°C or 46°C and incubated under shaking at the given temperature for additional 10 minutes. Cycloheximide (Sigma-Aldrich, USA) was added to the final concentration of 50 μg/ml when appropriate.

Plasmids

Plasmids pRP2037 and pRP1187 for *PGK1* mRNA localization by U1A-GFP fusion protein [5,9] were kindly provided by R. Parker (University of Arizona, USA). For generation of strains expressing only a C-terminal part of Sup35 protein and wild-type form of Sup35 protein as a control, plasmids pLewi0512 and pLewi0564 were used (a kind gift from E.I. Lewitin, Institute of Industrial Genetics, Russia).

Escherichia coli strain DH5α [F$^-$ *rec A1 supE44 endA1 hsdR17 (rk-, mk+) gyrA96 relA1 thi-1 Δ(lacIZYA-argF)U169 deoR (Φ80dΔ(lacZ) M15*] [35] was cultivated in LB medium (1% trypton, 0.5% yeast extract and 1% NaCl) and used for plasmids propagation.

Construction of Strains with Chromosome-derived Expression of mCherry Fusions

To create C-terminal genomic fusions of genes of interest, the mCherry integrative cassette containing mCherry fluorescent protein and the selection marker *nat*NT2 (nourseothricin) was used. The cassette was amplified using ORF-specific primers by PCR on the template plasmid pFM699 (kindly provided by M. Farkasovsky, Slovak Academy of Sciences, Slovakia). Purified PCR products were transformed into the appropriate cells and transformants were selected on YPD plates containing 100 μg/ml of nourseothricin (WERNER BioAgents, Germany). Correct integration of the cassette was confirmed by PCR, fluorescence microscopy and Western blotting.

Construction of *edc3Δlsm4ΔC* Mutant Strain

The mutant strain *edc3*Δ*lsm4*ΔC was constructed by a repeated one-step gene disruption technique [36]. The deletion cassettes loxP-*URA3*-loxP and loxP-*LEU2*-loxP were amplified from pUG72 and pUG73 respectively [37], using the ORF-specific primers. The mutant *lsm4*ΔC denotes a partial deletion of 97 C-terminal amino acids of Lsm4 protein [8].

Polysome Profile Analyses

Cells were grown to an OD_{600} ~1 and cycloheximide (CYH; Sigma-Aldrich, USA) was added to the culture to a final concentration of 50 μg/ml 5 min before harvesting. Chilled cells were washed in the GA buffer (20 mM Tris-HCl pH 7.5, 50 mM KCl, 10 mM $MgCl_2$, 1 mM DTT, and 5 mM NaF) containing 50 μg/ml CYH. Lysates were prepared in the GA buffer (supplemented with 1 tablet of Complete Mini EDTA-free Protease Inhibitor Mix (Roche, Switzerland)/10 ml of the buffer and 50 μg/ml of cycloheximide) using glass beads in Fastprep Bio101 (Savant Instruments, USA) at speed 5 for 20 s. Lysates were precleared by centrifugation at 826 × *g* for 5 min and at 13,224 × *g* for 10 min, and loaded on a 5–45% sucrose gradient. Gradients were ultracentrifuged at 260,500 × *g* at 4°C for 2.5 h. Fractions were collected from the top and A_{254} was recorded.

Table 1. Yeast strains.

Strain	Genotype	Source
BY4741	*MAT*a *his3Δ1 leu2Δ0 met15Δ0 ura3Δ0*	[32]
BY4742	*MAT*α *his3Δ1 leu2Δ0 lys2Δ0 ura3Δ0*	[32]
BY4743	*MAT* a/α *his3Δ1/his3Δ1 leu2Δ0/leu2Δ0 lys2Δ0/LYS2 MET15/met15Δ0 ura3Δ0/ura3Δ0*	[32]
S288C	*MAT*α *SUC2 gal2 mal mel flo1 flo8-1 hap1 ho bio1 bio6*	[56]
Sey6210	*MAT*α *leu2-3, 112 ura3-52 his3-Δ200 trp1-Δ901 lys2-801 suc2-Δ9*	[33]
Sey6210.1	*MAT*a *leu2-3,112 ura3-52 his3-Δ200 trp1-Δ901 lys2-801 suc2-Δ9*	[33]
CRY255	Sey6210; *MAT*α *RPG1-RFP::kan*MX4	[2]
CRY309	BY4741; *MAT*a *gcn2::kan*MX4	EUROSCARF
CRY412	S288C; *MAT*a *SUP35-GFP::HIS3*MX6	[18]
CRY423	S288C; *MAT*a *PAB1-GFP::HIS3*MX6	[18]
CRY437	S288C; *MAT*a *SUI2-GFP::HIS3*MX6	[18]
CRY462	S288C; *MAT*a *NGR1-GFP::HIS3*MX6	[18]
CRY510	S288C; *MAT*a *YEF3-GFP::HIS3MX6*	[18]
CRY521	S288C; *MAT*a *TIF11-GFP::HIS3MX6*	[18]
CRY528	Sey6210 × S288C; *MAT*α *RPG1-RFP::kan*MX4 *PAB1-GFP::HIS3*MX6	This study
CRY552	S288C; *MAT*a *EFT1-GFP::HIS3*MX6	[18]
CRY554	S288C; *MAT*a *TEF4-GFP::HIS3*MX6	[18]
CRY564	Sey6210 × S288C; *MAT*a *RPG1-RFP::kan*MX4 *DCP2-GFP::HIS3*MX6	[2]
CRY582	S288C × BY4742; *MAT*α *gcn2::kan*MX4	This study
CRY649	Sey6210 × S288C; *MAT*a *RPG1RFP::kan*MX4 *YEF3-GFP::HIS3*MX6	This study
CRY977	Sey6210 × S288C; *MAT*a *RPG1-RFP::kan*MX4 *DCP2-GFP::HIS3*MX6 *edc3::URA3 lsm4ΔC::LEU2*	[2]
CRY993	BY4743; *MAT*a/α *sup35::kan*MX4*/SUP35*	EUROSCARF
CRY998	BY4741 × BY4742; *MAT*α *sup35::kan*MX4+ pLewi0564 (Ura+)	This study
CRY1001	BY4741 × BY4742; *MAT*α *sup35::kan*MX4+ pLewi0512 (Ura+)	This study
CRY1007	BY4741 × BY4742 × S288C; *MAT*α *sup35::kan*MX4 *RPG1-GFP::HIS3*MX6+ pLewi0512 (Ura+)	This study
CRY1011	BY4741 × BY4742 × S288C; *MAT*a *sup35::kan*MX4 *RPG1-GFP::HIS3*MX6+ pLewi0564 (Ura+)	This study
CRY1035	Sey6210 × S288C; *MAT*a *RPG1-RFP::kan*MX4 *PUB1-GFP::HIS3*MX6 *edc3::URA3 lsm4ΔC::LEU2*	This study
CRY1041	Sey6210 × S288C; *MAT*α *RPG1-RFP::kan*MX4 *NGR1-GFP::HIS3*MX6 *edc3::URA3 lsm4ΔC::LEU2*	This study
CRY1043	BY4742; *MAT*α *edc3::URA3 lsm4ΔC::LEU2*	This study
CRY1146	S288C × BY4742; *MAT*α *YEF3-GFP::HIS3*MX6 *edc3::URA3 lsm4ΔC::LEU2*	This study
CRY1287	S288C; *MAT*a *YEF3-mCherry::nat*NT2 *NGR1-GFP::HIS3*MX6	This study
CRY1288	BY4742; *MAT*α *DCP2-mCherry:: nat*NT2	This study
CRY1289	BY4742; *MAT*α *NGR1-mCherry:: nat*NT2	This study
CRY1292	S288C × BY4742; *MAT*a *gcn2::kanMX YEF3-GFP::HIS3*MX6	This study
CRY1315	BY4742 × S288C; *MAT*a *YEF3-mCherry:: nat*NT2 *TEF4-GFP::HIS3*MX6	This study
CRY1332	Sey6210 × S288C; *MAT*a *RPG1-RFP::Kan*MX4 *SUI2-GFP::HIS3*MX6	This study
CRY1336	S288C × BY4742; *MAT*α *YEF3-GFP::HIS3*MX6 *gcn2::kan*MX4	This study
CRY1339	BY4742; *MAT*α *YEF3-mCherry:: nat*NT2	This study
CRY1364	Sey6210 × S288C; *MAT*a *RPG1-RFP::kan*MX4 *SUP35-GFP::HIS3*MX6	This study
CRY1516	S288C; *MAT*a *STM1-GFP::HIS3*MX6	[18]
CRY1552	S288C; *MAT*a *SUP45-GFP::HIS3*MX6	[18]
CRY1559	BY4742 × S288C; *MAT*α *YEF3-mCherry:: nat*NT2 *DCP2-GFP::HIS3*MX6	This study
CRY1618	BY4742 × Sey6210.1; *MAT*α *YEF3-mCherry:: nat*NT2+ pRP1187 (Trp+)+pPS2037 (Ura+)	This study
CRY1627	Sey6210 × S288C; *MAT*a/α *RPG1-RFP::kan*MX4 *SUP45-GFP::HIS3*MX6	This study
CRY1636	BY4742 × S288C; *MAT*α *DCP2-mCherry:: nat*NT2 *SUP45-GFP::HIS3*MX6	This study
CRY1638	BY4742 × S288C; *MAT*α *NGR1-mCherry:: nat*NT2 *SUP45-GFP::HIS3*MX6	This study
CRY1691	Sey6210 × S288C × BY4742; *MAT*a *RPG1-RFP::kan*MX4 *SUI2-GFP::HIS3*MX6 *gcn2::kan*MX4	This study
CRY1704	BY4741; *MAT*a *gcn2::kan*MX4	EUROSCARF
CRY1760	Sey6210 × S288C × BY4741; *MAT*a *RPG1-RFP::kan*MX4 *PAB1-GFP::HIS3*MX6 *stm1::kan*MX4	This study
CRY1764	S288C; *MAT*a *TEF1-GFP::HIS3*MX6	[18]

doi:10.1371/journal.pone.0057083.t001

Analyses of Protein Accumulations

Exponentially growing cells were heat-shocked at 46°C for 10 min and harvested. Cells were washed and resuspended in the lysis buffer [9] containing 50 mM Tris-HCl (pH 7.6), 50 mM NaCl, 5 mM $MgCl_2$, 0.1% NP-40, 1 mM β-mercaptoethanol and 1 tablet of Complete Mini EDTA-free Protease Inhibitor Mix (Roche, Switzerland)/10 ml of the buffer. The disruption of cells was carried out twice in a Fastprep Bio101 (Savant Instruments, USA) at speed 4 for 20 s. Cell debris were pelleted at 2,296 × *g* at 4°C for 10 minutes. The supernatant was centrifuged at 18,000 × *g* at 4°C for 10 minutes. Resulting pellets and supernatants were analyzed by SDS-PAGE and Western blotting for the presence of GFP-tagged fusion proteins.

Western Blot Analyses

Proteins resolved by SDS-PAGE were transferred to a Protran nitrocellulose membrane (Sigma-Aldrich, USA). The membrane blots were blocked with 3% non-fat milk in TBS-T buffer and incubated overnight with appropriate antibodies. Mouse monoclonal anti-GFP HRP-conjugated antibody (Santa Cruz Biotechnology, USA) was used at 1:2000. Rabbit polyclonal anti-Sup35 antibody was used at 1:2000. Donkey anti-rabbit IgG antibody conjugated with a horseradish peroxidase (GE Healthcare; England) was used as a secondary antibody.

Microscopy

The cells were inspected after washing with SC medium, mounting on coverslips and coating with a slice of 1.5% agarose in an appropriate medium. The distribution of various fusion proteins (fused to GFP or RFP or mCherry) was analyzed with a 100x PlanApochromat objective (NA = 1.4) using an Olympus IX-81 inverted microscope equipped with a Hammamatsu Orca/ER digital camera and an Olympus CellR^{TM} detection and analyzing system (GFP filter block U-MGFPHQ, exc. max. 488, em. max. 507; RFP filter block U-MWIY2, exc. max. 545–580, em. max. 610). Images were processed and merged using Olympus CellR^{TM} and Adobe CS5 software. The quantitative co-localization analyses were performed using NIH ImageJ software with the Co-localization Finder plugin, available at http://rsb.info.nih.gov/ij/plugins/. This software was used to determine the Pearson's correlation coefficient (R_r), which describes the extent of overlap between image pairs. It is a value between −1 and +1, with −1 being no overlap and +1 being perfect overlap of the two images. The time-lapse experiments were done using an ONIX microfluidic perfusion system (Cell Asic Corp., USA; http://www.cellasic.com).

In-gel Digestion and MALDI-TOF Mass Spectrometry

The spots of interest were cut from the CBB-stained SDS–PAGE gels, destained by a mixture of 100 mM ethylmorpholine acetate buffer and acetonitrile (1:1), and reduced with Tris(2-carboxyethyl)phosphine hydrochloride. Reduced cysteines were then alkylated with 50 mM iodoacetic acid. Gel pieces were washed three times with acetonitrile and water. Trypsin protease was added to the gel in the digestion buffer (50 mM ethylmorpholine acetate buffer, 10% acetonitrile, pH 8.3). After an overnight incubation, tryptic peptides were extracted from the gel by the addition of 80% acetonitrile, 0.1% trifluoroacetic acid.

Extracted peptides were desalted using a Peptide Microtrap in the off-line holder (MichromBioresources, USA). Each sample was spotted in one position of the 384-position ground steel MALDI plate (Bruker Daltonics, USA). α-Cyano-4-hydroxycinnamic acid was used as a matrix (Bruker Daltonics). Samples were ionized by matrix-assisted laser desorption ionization (MALDI) using a Dual II ion source (Bruker Daltonics). Mass spectra were acquired in an APEX-Qe Fourier transformation mass spectrometry instrument equipped with a 9.4 T superconducting magnet (Bruker Daltonics). The cell was opened for 4 ms; accumulation time was set to 0.2 s, and one experiment consisted of the average of four spectra. The acquisition data set size was set to 512,000 points, with the mass range starting at m/z 600 atomic mass units. The instrument was externally calibrated using Bruker Daltonics calibration standard II. The spectra were processed by Data Analysis 4.0 software (Bruker Daltonics) and searched with the Mascot search engine (http://www.matrixscience.com) against the data base (UniProt Knowledgebase; http://www.ebi.ac.uk/uniprot) created from all known *S. cerevisiae* proteins.

Results

Translation Elongation Factor eEF3 (Yef3p) is a Novel Component of Heat-induced SGs of *S. cerevisiae*

In our previous work, we described that formation of the robust heat shock-induced stress granules (SGs) is promoted by P-bodies in *S. cerevisiae* [2]. In addition, we also described that these SGs are formed even in the *edc3*Δ*lsm4*ΔC mutant, which is unable to form visible P-bodies under glucose deprivation [8]. Therefore, we used the *edc3*Δ*lsm4*ΔC mutant in our recent experiments to identify additional components of SGs in heat-shocked cells. We applied a biochemical approach combined with mass spectrometry analyses. We stressed the exponentially growing *edc3*Δ*lsm4*ΔC mutant cells either at 42°C or at 46°C for 10 minutes. The protein samples from the heat-shocked cells were prepared by differential centrifugation according to the protocol we used previously [2] and proteins in the pellet were separated by SDS-PAGE. A 116-kD protein appeared to accumulate predominantly in the pellet of the mutant cells heat-shocked at 46°C (Fig. 1A). The protein band was cut out of the gel and subjected to enzymatic digestion in suspension followed by the mass spectrometry analysis, which identified only peptides of the translation elongation factor eEF3 (Yef3p) (Table 2). This result was further confirmed by the Western blot analysis of pelleted proteins prepared by differential centrifugation of the lysate from the wild-type cells expressing Yef3-GFP (Fig. 1B). To perform microscopic analyses of heat-shocked cells, we used either the Yef3-GFP strain from the GFP collection [18] or a newly prepared Yef3-mCherry expressing strain. The distribution of both fusion proteins in wild-type cells was uniformly cytosolic at 30°C (Fig. 1C). They both were accumulated in cytoplasmic foci after heat-shock at 46°C for 10 minutes. In heat-shocked cells harboring the *edc3*Δ*lsm4*ΔC deletion and the Yef3-GFP fusion, we observed a similar pattern of the fluorescent foci-containing Yef3-GFP as found in wild-type cells (Fig. 1C).

To investigate whether these Yef3-containing foci were identical to previously identified heat-induced SGs, we prepared a new strain co-expressing Yef3-GFP together with the stress granule marker Rpg1-RFP. We observed that both proteins co-localized in SGs of heat-shocked cells (Fig. 2A). Very high values of the Pearsons correlation coefficient (R_r), over 0.9, confirmed the high degree of this co-localization. Similar results were obtained in experiments with the strains co-expressing Yef3-mCherry and other constituents of heat-induced SGs, Ngr1-GFP or Dcp2-GFP proteins (Fig. 2B). The presence of the Yef3 protein accumulations in heat-shocked cells of the *gcn2*Δ mutant indicated that their assembly is also independent of the eIF2α factor phosphorylation, as we reported previously for

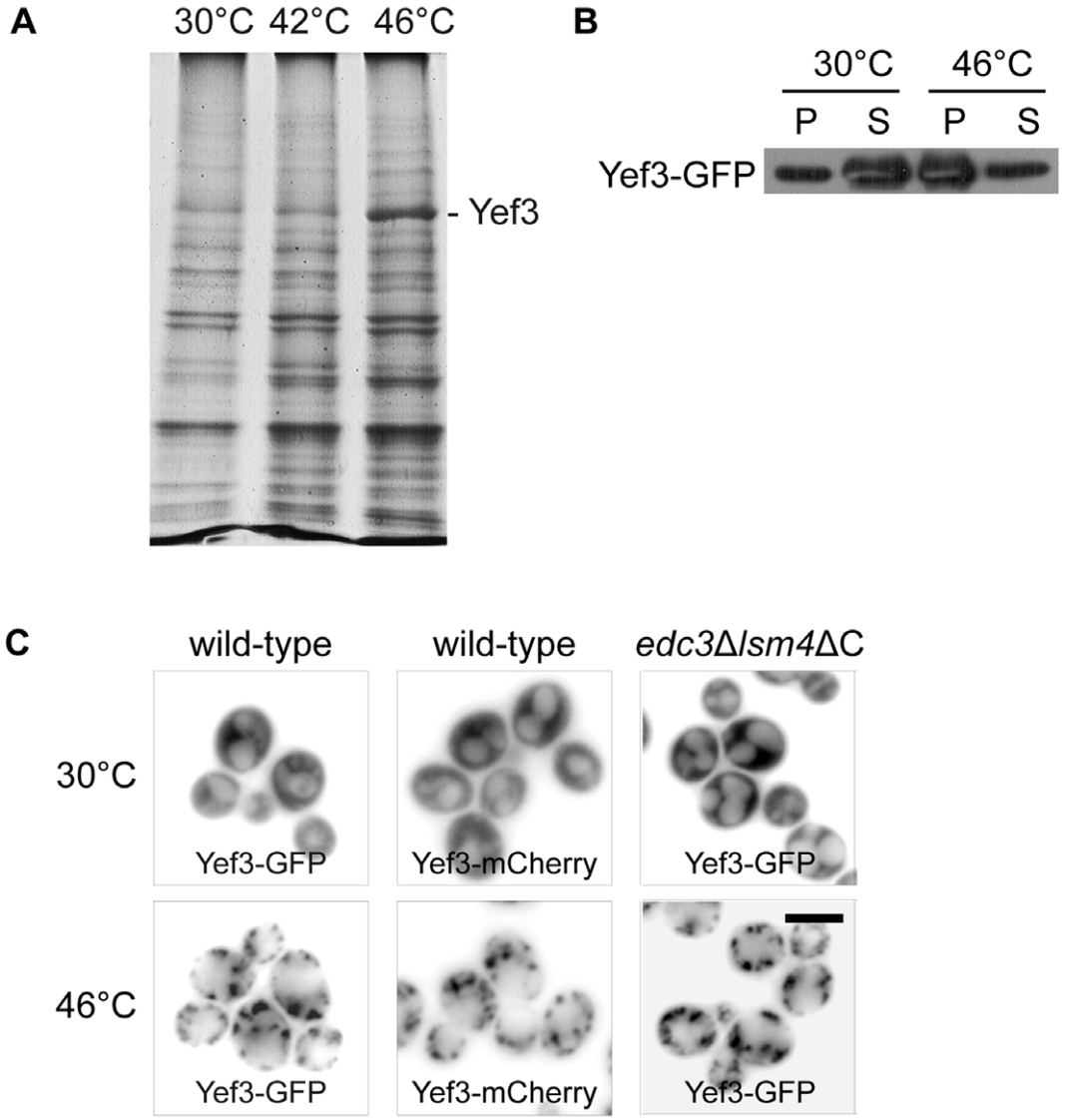

Figure 1. Translation elongation factor eEF3 (Yef3p) accumulates in foci upon robust heat shock. (A) Pellet fractions from the *edc3*Δ*lsm4*ΔC cell (CRY1043 strain) lysates taken upon control (30°C) and heat shock (42°C and 46°C) conditions were separated by SDS-PAGE and stained with Coomassie Brilliant Blue. Yef3 protein, identified by MS analysis, is enriched in the pellet fraction from the cells heat-shocked at 46°C for 10 minutes. (B) Pellet and supernatant fractions from the lysates of cells expressing Yef3-GFP (CRY510 strain) were analyzed by SDS-PAGE and Western blotting. Samples were prepared as described elsewhere [2]. The Yef3-GFP fusion protein was accumulated in the pellet fraction of heat-shocked cells. (C) The Yef3 fusions were accumulated at cytoplasmic foci in wild-type cells (CRY510 and CRY1339 strains) as well as in the *edc3*Δ*lsm4*ΔC mutant cells (CRY1146 strain) heat-shocked at 46°C for 10 minutes. Scale bar 4 μm.
doi:10.1371/journal.pone.0057083.g001

accumulations of eIF3a (Rpg1p/Tif32p) [2] (Fig. 2C). We conclude that the translation elongation factor eEF3 (Yef3p) is a novel component of the heat-induced SGs in *S. cerevisiae*.

SGs also Contain Translation Factors eEF1Bγ2 (Tef4p), eRF1 (Sup45p) and eRF3 (Sup35p)

Since we found that heat-induced SGs contain the translation elongation factor eEF3, we wanted to know whether other translation factors are also present. Using the strains from the GFP collection [18], we analyzed the distribution of some other translation factors and found that the elongation factor eEF1Bγ2 (Tef4p) together with the termination factors eRF3 (Sup35p) and eRF1 (Sup45p) also accumulate in distinct cytoplasmic foci under heat shock at 46°C (Fig. 3A). Other microscopic analyses using the particular strains from the GFP collection [18] revealed that other translation factors, elongation factor eEF1A (Tef1p), elongation factor eEF2 (Eft1p) and initiation factor eIF1A (Tif11p), remained uniformly cytosolic when the robust heat shock was applied (Fig. 3B).

To co-localize Tef4, Sup45 and Sup35 heat-induced foci with SGs, we prepared a strain co-expressing Tef4-GFP and Yef3-mCherry fusion proteins and strains co-expressing Sup45-GFP or Sup35-GFP fusion proteins together with the stress granule marker Rpg1-RFP. As shown in Fig. 3C, there is a near-perfect overlap of accumulated Tef4-GFP and Yef3-mCherry fusion proteins upon robust heat shock. Similarly, Sup35-GFP or Sup45-GFP significantly overlapped with the accumulated Rpg1-RFP in heat-shocked cells (Fig. 3C). In addition, similar results were obtained in the strains co-expressing either Sup45-

Table 2. MS identification of Yef3 (eEF3) protein.

Identified peptides: sequence	start – end
K.ALLPHLTNAIVETNK.W	128–142
R.MPELIPVLSETMWDTKK.E	168–184
K.ATETVDNKDIER.F	197–208
K.LVEDPQVIAPFLGK.L	276–289
K.SNFATIADPEAR.E	296–307
K.IVVEYIAAIGADLIDER.I	360–376
K.AKDILDEFR.K	400–408
K.DILDEFR.K	402–408
K.DILDEFRK.R	402–409
R.YGICGPNGCGKSTLMR.A	459–474
R.YGICGPNGCGKSTLMR.A	459–474
R.TVYVEHDIDGTHSDTSVLDFVFESGVGTK.E	492–520
K.AYEELSNTDLEFKFPEPGYLEGVK.T	637–660
K.FPEPGYLEGVK.T	650–660
K.QHAFAHIESHLDK.T	738–750
K.TPSEYIQWR.F	751–759
R.FQTGEDRETMDR.A	760–771
R.IAGIHSR.R	797–803
R.IAGIHSRR.K	797–804
K.MVAEVDMKEALASGQFRPLTR.K	852–872
K.EALASGQFRPLTR.K	860–872
K.ALKEFEGGVIIITHSAEFTK.N	938–957
K.EFEGGVIIITHSAEFTK.N	941–957
K.LSSAELRK.K	1014–1021

ORF translation sequence of Yef3 protein:

(matched peptides shown in bold)

MSDSQQSIKV	LEELFQKLSV	ATADNRHEIA	SEVASFLNGN	IIEHDVPEHF
FGELAKGIKD	KKTAANAMQA	VAHIANQSNL	SPSVEPYIVQ	LVPAICTNAG
NKDKEIQSVA	SETLISIVNA	VNPVAIK**ALL**	**PHLTNAIVET**	**NK**WQEKIAIL
AAISAMVDAA	KDQVALR**MPE**	**LIPVLSETMW**	**DTKK**EVKAAA	TAAMTK**ATET**
VDNKDIERFI	PSLIQCIADP	TEVPETVHLL	GATTFVAEVT	PATLSIMVPL
LSRGLNERET	GIKRKSAVII	DNMCK**LVEDP**	**QVIAPFLGK**L	LPGLK**SNFAT**
IADPEAREVT	LRALKTLRRV	GNVGEDDAIP	EVSHAGDVST	TLQVVNELLK
DETVAPRFK**I**	**VVEYIAAIGA**	**DLIDER**IIDQ	QAWFTHITPY	MTIFLHEKK**A**
KDILDEFRKR	AVDNIPVGPN	FDDEEDEGED	LCNCEFSLAY	GAKILLNKTQ
LRLKRARR**YG**	**ICGPNGCGKS**	**TLMR**AIANGQ	VDGFPTQEEC	R**TVYVEHDID**
GTHSDTSVLD	**FVFESGVGTK**	EAIKDKLIEF	GFTDEMIAMP	ISALSGGWKM
KLALARAVLR	NADILLLDEP	TNHLDTVNVA	WLVNYLNTCG	ITSITISHDS
VFLDNVCEYI	INYEGLKLRK	YKGNFTEFVK	KCPAAK**AYEE**	**LSNTDLEFKF**
PEPGYLEGVK	TKQKAIVKVT	NMEFQYPGTS	KPQITDINFQ	CSLSSRIAVI
GPNGAGKSTL	INVLTGELLP	TSGEVYTHEN	CRIAYIK**QHA**	**FAHIESHLDK**
TPSEYIQWRF	**QTGEDRETMD**	**R**ANRQINEND	AEAMNKIFKI	EGTPRR**IAGI**
HSRRKFKNTY	EYECSFLLGE	NIGMKSERWV	PMMSVDNAWI	PRGELVESHS
K**MVAEVDMKE**	**ALASGQFRPL**	**TR**KEIEEHCS	MLGLDPEIVS	HSRIRGLSGG
QKVKLVLAAG	TWQRPHLIVL	DEPTNYLDRD	SLG**ALSKALK**	**EFEGGVIIIT**
HSAEFTKNLT	EEVWAVKDGR	MTPSGHNWVS	GQGAGPRIEK	KEDEEDKFDA
MGNKIAGGKK	KKK**LSSAELR**	**K**KKKERMKKK	KELGDAYVSS	DEEF

doi:10.1371/journal.pone.0057083.t002

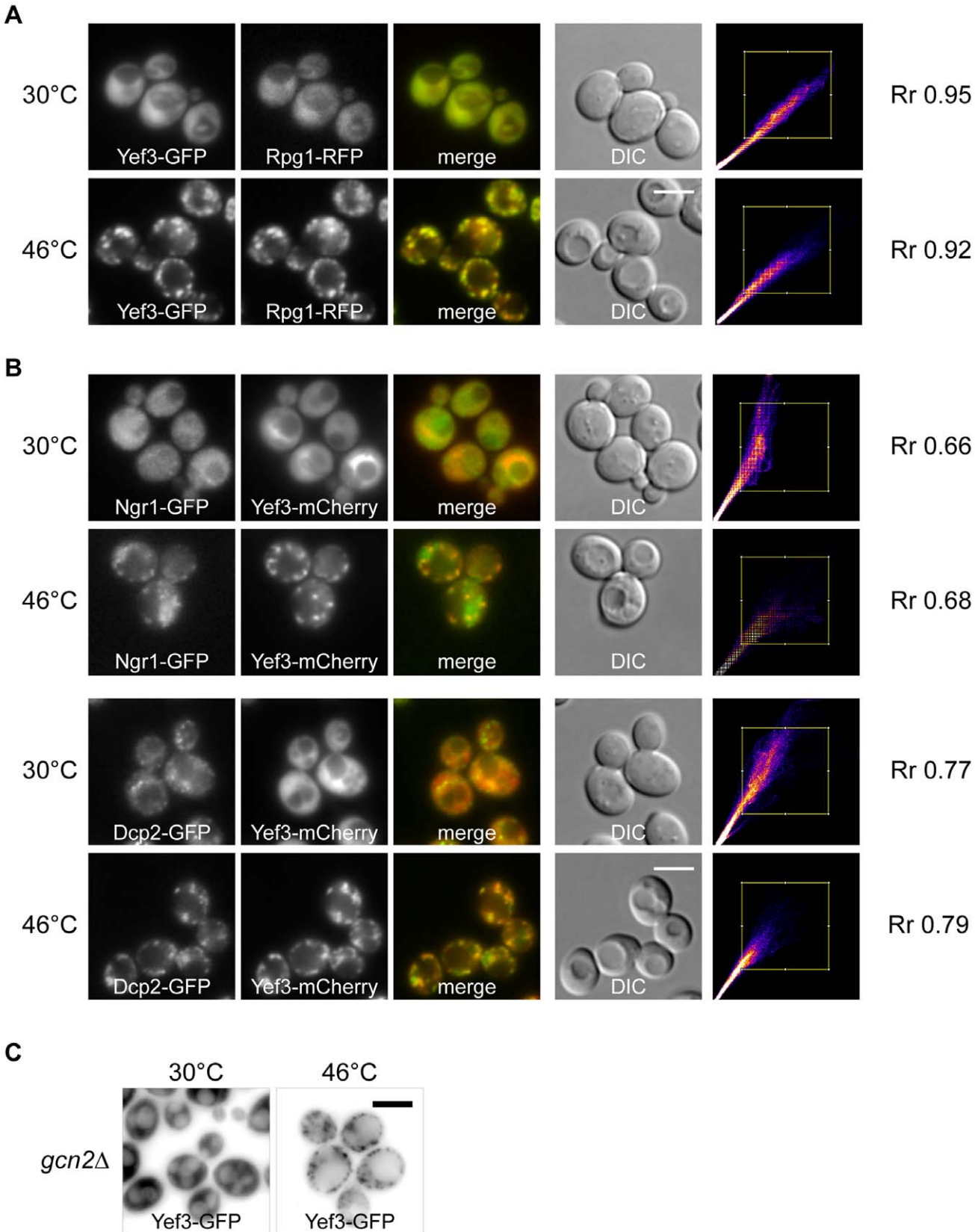

Figure 2. Heat shock-induced stress granules contain translation elongation factor eEF3 (Yef3p). (A) The distribution of fusion proteins Yef3-GFP and Rpg1-RFP (CRY649 strain) was uniformly cytosolic at 30°C. Accumulations of Yef3-GFP fusion protein completely co-localized with accumulations of the stress granule marker protein Rpg1-GFP in cells heat-shocked at 46°C for 10 minutes. The Scatter plot produced by colocalization analysis software shows colocalized pixels along the diagonal. Very high values of the Pearsons correlation coefficient (R_r), over 0.9,

confirmed the high degree of this co-localization. (B) Localization of theYef3-mCherry fusion protein with Ngr1-GFP (CRY1287 strain) and Dcp2-GFP (CRY1559 strain) fusion proteins under control conditions (30°C) and in heat-shocked cells at 46°C for 10 minutes. Yef3-mCherry protein co-localized with heat-induced accumulations of stress granules marker proteins Dcp2-GFP and Ngr1-GFP. (C) Yef3-GFP accumulates in cytoplasmic foci in both, wild-type (CRY510 strain) and *gcn2*Δ (CRY1292 strain), cells heat-shocked at 46°C. Scale bar 4 μm.
doi:10.1371/journal.pone.0057083.g002

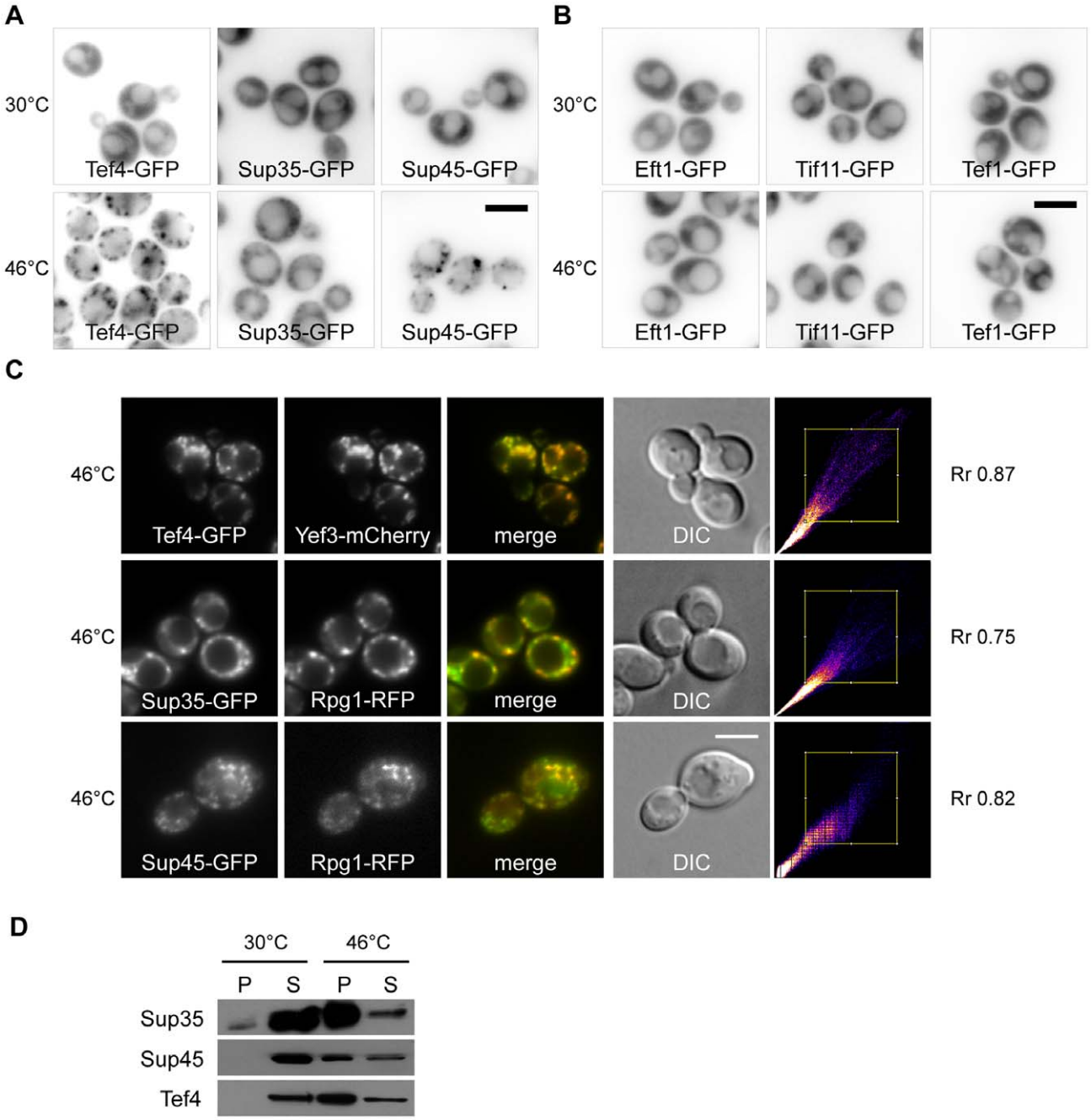

Figure 3. Factors eEF1Bγ2 (Tef4p), eRF1 (Sup45p) and eRF3 (Sup35p) are novel components of stress granules. (A) The distribution of Tef4-GFP (CRY554 strain), Sup35-GFP (CRY412 strain) and Sup45-GFP (CRY1552 strain) proteins was analyzed in control (30°C) and heat-shocked (46°C) cells. All of these fusion proteins accumulated in discrete cytoplasmic foci in heat-shocked cells. (B) Subcellular localization of Eft1-GFP (eEF2) (CRY552 strain), Tif11-GFP (eIF1A) (CRY521 strain) and Tef1-GFP (eEF1A) (CRY1764 strain) fusion proteins upon control and heat shock conditions. The distribution of Eft1-GFP, Tif11-GFP and Tef1-GFP remained diffusely cytosolic even upon the stress condition. (C) Tef4-GFP fusion protein co-localized with accumulations of the Yef3-mCherry fusion protein (CRY1315 strain). Similarly, Sup35-GFP and Sup45-GFP co-localized with the stress granule marker protein Rpg1-RFP in cells heat-shocked at 46°C for 10 minutes (strains CRY1364; CRY1627 strains). High values of the Pearsons correlation coefficient (R_r) confirmed the high degree of this co-localization. Scale bar 4 μm. (D) Pellet and supernatant fractions from the appropriate cell lysates (strains CRY554; CRY412; CRY1552 strains) were analyzed by SDS-PAGE and Western blotting. Samples were prepared as described elsewhere [2]. All tested fusion proteins were clearly accumulated in the pellet fraction of cells heat-shocked at 46°C for 10 minutes.
doi:10.1371/journal.pone.0057083.g003

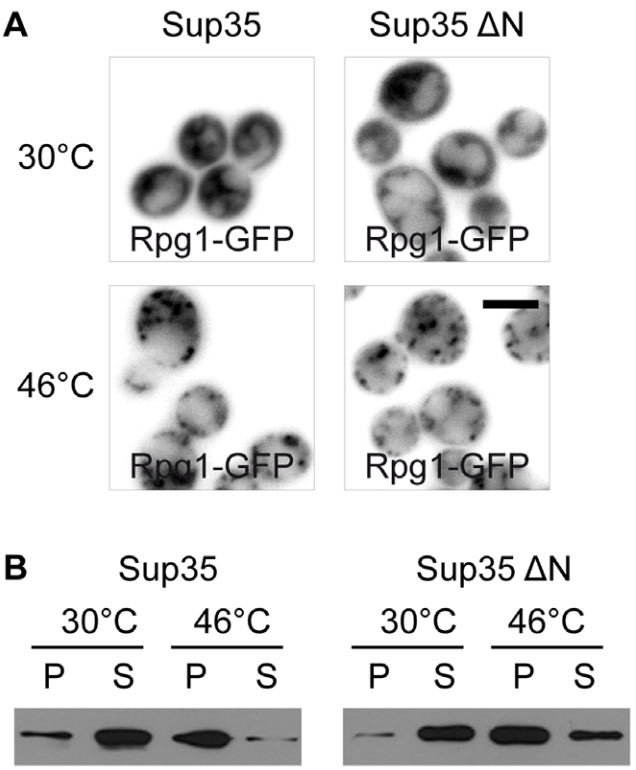

Figure 4. Full length Sup35 protein is not necessary for SGs assembly and its localization into SGs. (A) The distribution of Rpg1-GFP fusion protein under control (30°C) and heat shock (46°C) conditions in either the wild-type strain (Sup35p; CRY1011 strain) or the strain expressing only the N-terminal truncated form of Sup35 protein (Sup35ΔN; CRY1007 strain). SGs (Rpg1-GFP) were formed even in the mutant strain suggesting that the N-terminal part of Sup35 protein is dispensable for the SGs formation. Scale bar 4 μm. (B) Pellet and supernatant fractions from the wild-type (CRY998 strain) and the Sup35 N-terminal truncated mutant strains (CRY1001 strain) were analyzed by SDS-PAGE and Western blotting using the anti-Sup35 antibody. Samples were prepared as described elsewhere [2]. The N-terminal truncated form of Sup35 protein was enriched in the pellet fraction of heat-shocked cells, as well as the wild-type form of Sup35 protein, suggesting that only Sup35 C-terminal part is sufficient to localize this protein to the heat-induced stress granules.
doi:10.1371/journal.pone.0057083.g004

GFP and Dcp2-mCherry or Sup45-GFP and Ngr1-mCherry fusions (Fig. S1).

Changes in the subcellular distribution of Tef4-GFP, Sup35-GFP and Sup45-GFP fusion proteins upon robust heat shock were confirmed by SDS-PAGE and the Western blot analysis of samples prepared by differential centrifugation (Fig. 3D). In agreement with the results of microscopic analyses, the tested proteins were found to be enriched in the pellet fraction of heat-shocked cells. We thus established eEF1γ2 (Tef4p), eRF1 (Sup45p) and eRF3 (Sup35p) factors to be novel constituents of SGs induced by robust heat shock in *S. cerevisiae*.

The N-terminal Prion-like Domain of Sup35 Protein is not Involved in SGs Assembly

As described above, we identified the translation termination factor eRF3 (Sup35p) as a constituent of SGs induced by robust heat shock at 46°C. Interestingly, this protein belongs to known yeast prion proteins and its N-terminal part is indispensable for [PSI+] prion formation and maintenance [38,39]. Since some proteins with prion-like domains have been referred to as affecting development of SGs in mammalian cells [40], we wanted to understand whether the prion-induction domain of Sup35 protein affects accumulation of Rpg1/eIF3a, the SGs marker protein. We constructed the strain expressing only the essential C-terminal part of Sup35 protein together with Rpg1-GFP. As a control, we used the strain of the same genetic background co-expressing the wild-type form of Sup35p and the Rpg1-GFP fusion protein. We observed Rgp1-GFP accumulated in SGs of both, wild-type and the mutant cells heat-shocked at 46°C for 10 minutes (Fig. 4A) suggesting that assembly of heat-induced SGs does not require the N-terminal part of Sup35 protein. In addition, using differential centrifugation followed by SDS-PAGE and Western blotting we observed that even in the absence of the Sup35 N-terminal domain the truncated protein was still accumulated in SGs of the cells heat-shocked at 46°C (Fig. 4B). This indicates that the full length Sup35 protein can be accumulated in SGs in a non-prion form. We conclude that the prion-induction domain of Sup35 protein is not necessary for SG assembly and the C-terminal part of this protein is sufficient to recruit the whole Sup35 protein to SGs.

Translation Elongation Factor eEF3 (Yef3p) Accumulates in RNP Complexes Even at 42°C

Despite the fact that eEF3 factor (Yef3p) was not significantly enriched in the pellet fraction of the cells heat-shocked at 42°C (see Fig. 1A), we also analyzed the distribution of this protein by fluorescence microscopy under these stress conditions. Surprisingly, Yef3-GFP or Yef3-mCherry accumulated in cytoplasmic foci even upon heat shock at 42°C (Fig. 5A). It should be noted that Yef3-mCherry fusion protein forms fewer granules in comparison to Yef3-GFP protein under heat shock at 42°C. The accumulations of eEF3 (Yef3-GFP) after heat shock at 42°C for 10 minutes were transient and dissolved after releasing cells from the stress conditions (Fig. 5B).

We also analyzed distribution of other newly identified components of SGs, e.g. Tef4, Sup45 and Sup35 proteins, upon the heat shock at 42°C. Despite we did not see accumulation of Sup35-GFP, we were able to observe formation of visible assemblies of Tef4-GFP and Sup45-GFP under these stress conditions (Fig. 5C).

Subsequent microscopic analyses of strains co-expressing Tef4-GFP with Yef3-mCherry, Dcp2-GFP with Yef3-mCherry, Sup45-GFP with Dcp2-mCherry and Ngr1-GFP with Yef3-mCherry from the chromosomal sites confirmed that all these proteins co-localized in distinct foci in cells heat-shocked at 42°C for 10 minutes (Fig. 5D). Similar results were obtained for the strains co-expressing Ngr1-GFP with Dcp2-mCherry and Pub1-GFP with Dcp2-RFP fusion proteins (data not shown).

To determine whether the Yef3-containing foci formed at 42°C comprise mRNA, we used the *PGK1* mRNA/U1A-GFP detection reporter system [9]. Initially, we observed that fine granules of *PGK1* mRNA (U1A-GFP) were present even under control temperature in a majority of cells. The heat shock at 42°C induced accumulation of some of these granules into larger clusters. We observed co-localization of the *PGK1* mRNA (U1A-GFP) clusters with accumulations of Yef3-mCherry fusion protein under these heat shock conditions (Fig. 6A). We used the "Co-localization Finder" plugin (ImageJ) to express statistically the overlaps. The value of the Pearson's correlation coefficient (R_r) for both cultures about 0.5 indicates co-localization, but also means that there is always a portion of Yef3 translation elongation factor which is not directly associated with the mRNA-U1A-GFP and vice versa. We

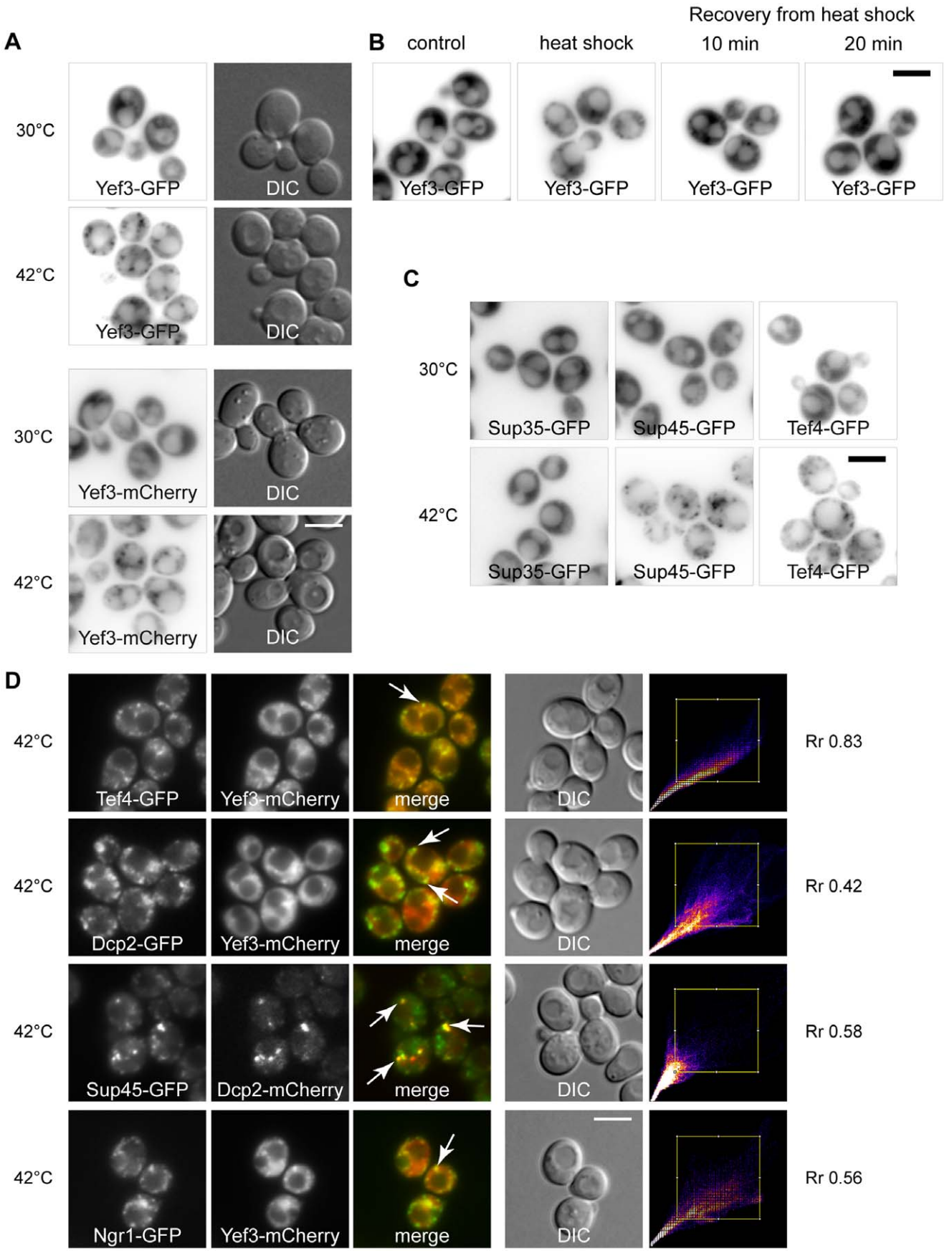
A
30°C
Yef3-GFP
DIC
42°C
Yef3-GFP
DIC
30°C
Yef3-mCherry
DIC
42°C
Yef3-mCherry
DIC
B
control
heat shock
Recovery from heat shock
10 min
20 min
Yef3-GFP
Yef3-GFP
Yef3-GFP
Yef3-GFP
C
30°C
Sup35-GFP
Sup45-GFP
Tef4-GFP
42°C
Sup35-GFP
Sup45-GFP
Tef4-GFP
D
42°C
Tef4-GFP
Yef3-mCherry
merge
DIC
Rr 0.83
42°C
Dcp2-GFP
Yef3-mCherry
merge
DIC
Rr 0.42
42°C
Sup45-GFP
Dcp2-mCherry
merge
DIC
Rr 0.58
42°C
Ngr1-GFP
Yef3-mCherry
merge
DIC
Rr 0.56

Figure 5. Translation elongation and termination factors accumulate in the same foci at 42°C. (A) The distribution of Yef3-GFP or Yef3-mCherry fusion protein was analyzed in wild-type cells (CRY510 strain: CRY1339 strain) heat-shocked at 42°C for 10 minutes. Whereas the Yef3-GFP and Yef3-mCherry fusion protein were uniformly cytosolic at 30°C, they formed discrete cytoplasmic foci in the cells heat-shocked at 42°C for 10 minutes. (B) Distribution of the Yef3-GFP protein (CRY510 strain) was analyzed in control, heat-shocked (at 42°C) and recovering cells. Yef3-GFP accumulations were dissolved within 20 minutes of the cell recovery from the stress. (C) The distribution of Sup35-GFP (CRY412 strain), Sup45-GFP (CRY1552 strain) and Tef4-GFP (CRY554 strain) was analyzed under control conditions at 30°C and under heat shock at 42°C. Whereas Sup35-GFP protein remained uniformly cytosolic even upon the heat shock at 42°C, Sup45-GFP and Tef4-GFP proteins accumulated into discrete cytoplasmic foci (D) Yef3-mCherry fusion protein was co-localized either with Tef4-GFP (CRY1315 strain), Dcp2-GFP (CRY1559 strain) or Ngr1-GFP (CRY1287 strain) fusion proteins, as well as Sup45-GFP fusion protein was co-localized with Dcp2-mCherry fusion protein (CRY1636 strain), in cells heat-shocked at 42°C.
doi:10.1371/journal.pone.0057083.g005

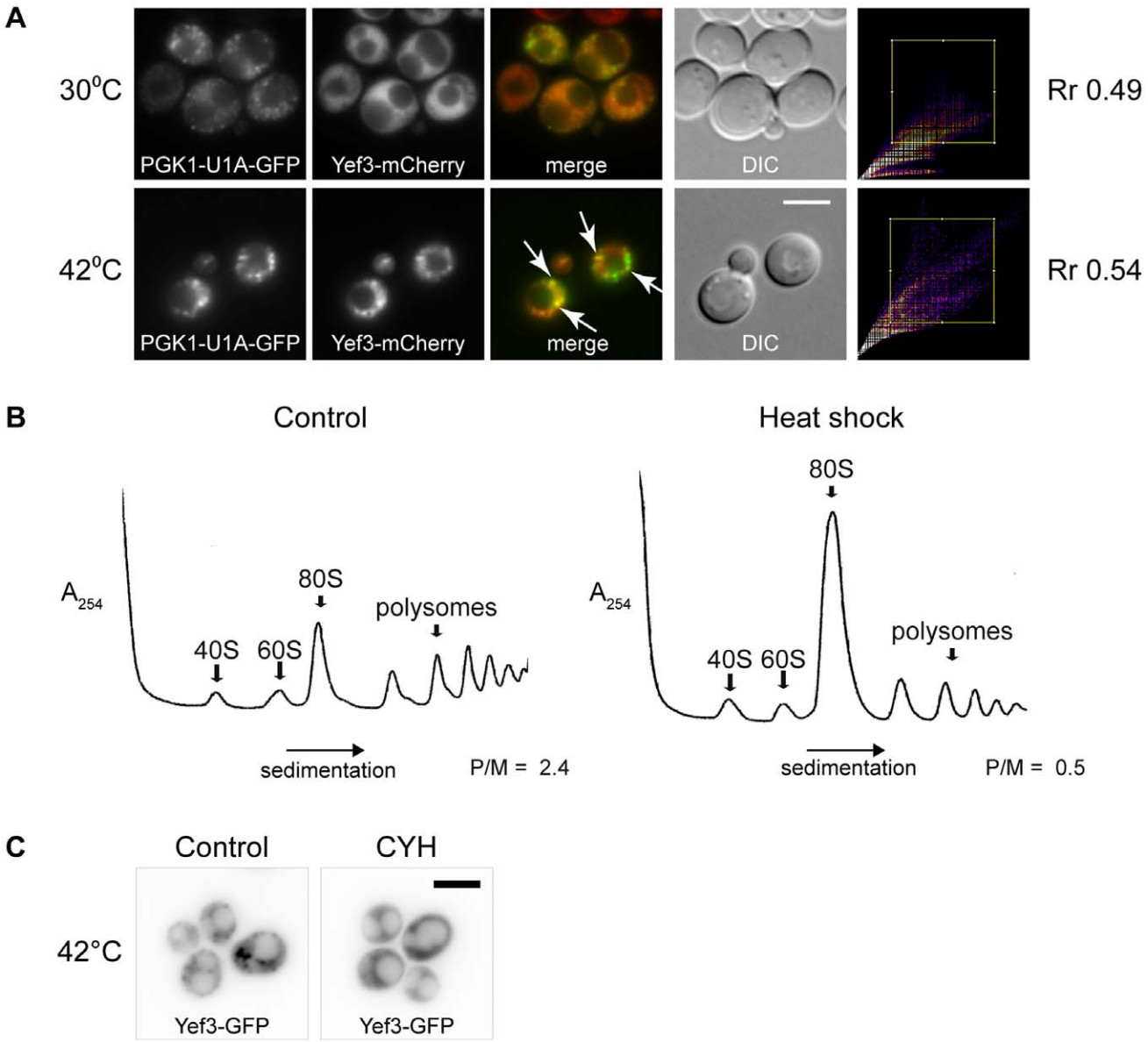

Figure 6. Heat shock at 42°C alters translation and triggers accumulation of mRNA in Yef3 foci. (A) Distribution of *PGK1* mRNA (*PGK1* mRNA/U1A-GFP reporter system) at 30°C or upon heat shock at 42°C was analyzed in cells expressing Yef3-mCherry fusion protein (CRY1618 strain). Fine granules of *PGK1* mRNA (U1A-GFP) were present at 30°C in a majority of cells. The heat shock at 42°C induced an accumulation of some of these granules into larger clusters and formations of Yef3 foci. Arrows point to obviously overlapping signals of both fusions. Scale bar 4 μm. (B) Polysome profiles of wild-type strain (BY4741) at permissive temperature and after heat shock at 42°C for 10 minutes. Translation profile was altered in heat-shocked cells. P/M stands for polysome/monosome ratio. (C) Distribution of Yef3-GFP (CRY510 strain) was analyzed in cells heat-shocked at 42°C for 10 minutes with or without preincubation in the presence of cycloheximide (CYH). When this drug was added before the heat shock, no accumulations of Yef3-GFP protein were formed. Scale bar 4 μm.
doi:10.1371/journal.pone.0057083.g006

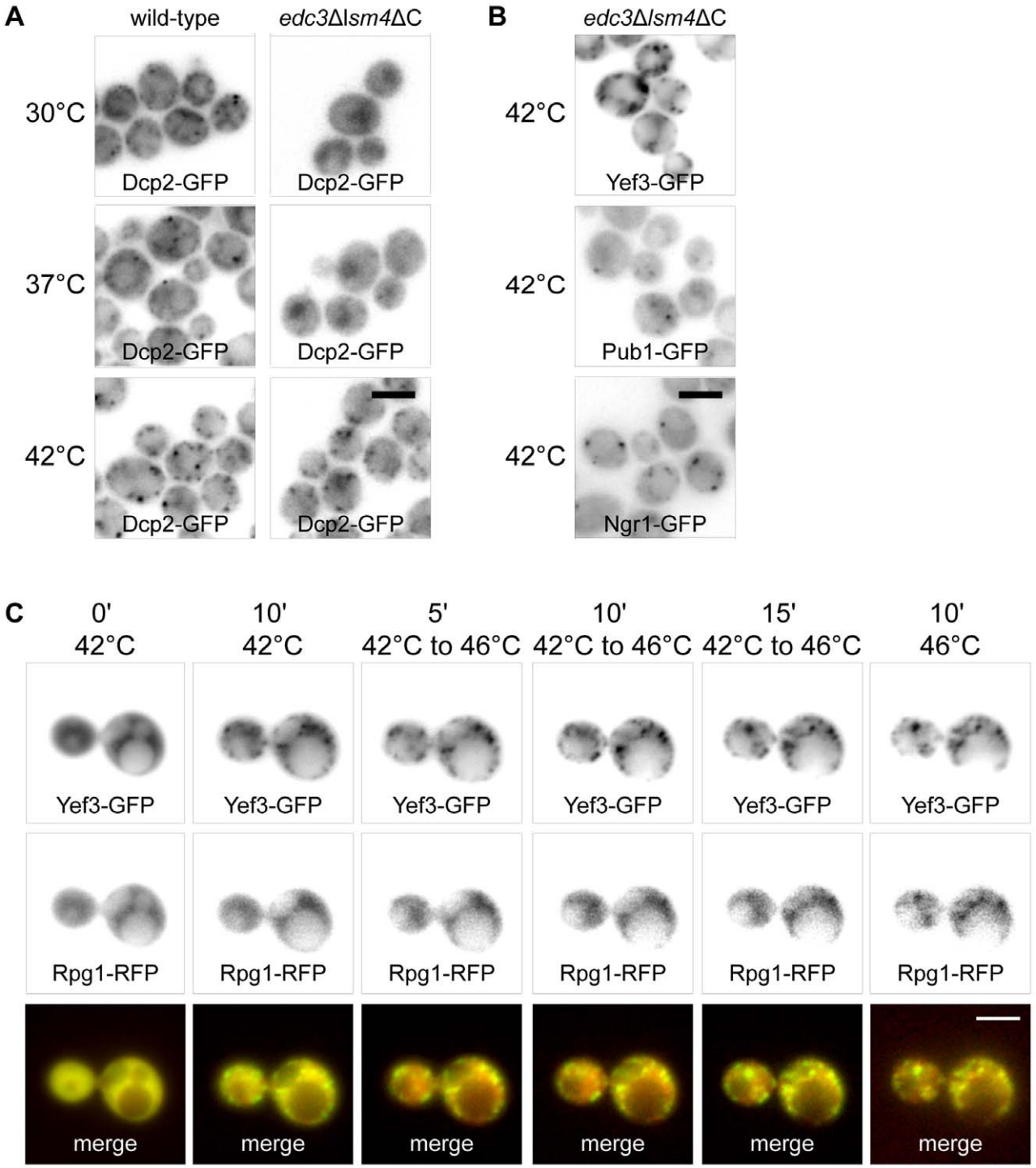

Figure 7. RNP accumulations formed at 42°C serve as ''seeds'' for genuine SGs. (A) Distribution of Dcp2-GFP was analyzed in wild-type (CRY564 strain) and *edc3*Δ*lsm4*ΔC mutant (CRY977 strain) cells after incubation at 30°C, 37°C and 42°C for 10 minutes. These wild-type cells exhibited increasing number of enlarged accumulations of the Dcp2-GFP fusion protein corresponding to raising temperatures of the heat shock. In contrast, *edc3*Δ*lsm4*ΔC mutant cells did not exhibit any cytoplasmic accumulations of the Dcp2-GFP fusion protein upon incubation at 30°C or 37°C. However, these mutant cells displayed accumulations of Dcp2-GFP upon heat shock at 42°C for 10 minutes. (B) The distribution of fusion proteins Pub1-GFP, Ngr1-GFP and Yef3-GFP was analyzed in *edc3*Δ*lsm4*ΔC mutant cells (CRY1035, CRY1041 and CRY1146 strains) either at 30°C or upon heat shock at 42°C for 10 minutes. All of these proteins accumulated in the mutant cells at 42°C, thus independently of P-body scaffolding proteins Edc3 and Lsm4. (C) Time lapse experiment using the cells co-expressing Yef3-GFP and Rpg1-RFP fusion proteins (CRY649 strain) showing the formation of Yef3-GFP foci after 10 minutes at 42°C, accumulation of Rpg1-RFP protein during the temperature rise from 42°C to 46°C and after 10 minutes at 46°C. Yef3-GFP foci were first formed at 42°C, whereas the localization of the Rpg1-RFP protein was still uniformly cytoplasmic at this temperature. During heating from 42°C to 46°C and upon cultivation at 46°C, the Rpg1-RFP protein only accumulated at the preformed Yef3-GFP foci. Scale bar 4 μm.
doi:10.1371/journal.pone.0057083.g007

supposed that the translation polysome profiles of the heat-shocked cells would be altered at 42°C. Indeed, as shown in Fig. 6B, the polysomal fraction was smaller and the 80S peak enlarged for cells heat-shocked at 42°C comparing the polysome profile of non-stressed cells. This suggested that mRNA molecules leave the active translation cycle and accumulate in cytoplasmic Yef3-containing RNP complexes. To support these results, we performed experiments in which mRNA was trapped in polysomes after cycloheximide (CYH) pretreatment. As expected, Yef3-containing accumulations were not assembled in cells pretreated with CYH and heat-shocked at 42°C for 10 minutes (Fig. 6C). This confirms that free mRNA outside the ribosome (polysome) is a prerequisite for the formation of RNP accumulations upon heat shock at 42°C.

We published earlier [2] that formation of heat-induced SGs and translation arrest accompanying robust heat shock are independent of Gcn2 kinase. In accordance with these findings, we observed that formation of Yef3-containing foci at 42°C and the alteration of polysome profile seen at 42°C are also Gcn2 independent (Fig. S2).

Accumulations of RNP Complexes Formed at 42°C Determine Sites for SGs Assembled at 46°C

To analyze the RNP accumulations formed at 42°C in detail, we used the *edc3*Δ*lsm4*ΔC mutant, which is unable to form visible P-bodies [8]. We prepared appropriate *edc3*Δ*lsm4*ΔC mutant strains expressing GFP fusion variants of some proteins found to accumulate in joint assemblies under heat shock at 42°C (see above), e.g. Yef3p, Dcp2p, Ngr1p and Pub1p. We found that in contrast to wild-type cells, the *edc3*Δ*lsm4*ΔC mutant did not exhibit any accumulations of the Dcp2-GFP fusion protein under control conditions at 30°C or upon heat shock at 37°C (Fig. 7A). These cells only displayed the Dcp2-GFP signal in the nuclear region. However, the mutant cells displayed distinct accumulations of Dcp2-GFP under heat shock at 42°C. We conclude that these Dcp2-GFP accumulations at 42°C do not depend on P-bodies scaffolding proteins Edc3 and Lsm4. Interestingly, we found that also accumulations of other proteins Ngr1-GFP, Pub1-GFP and Yef3-GFP at 42°C was independent on Edc3 and Lsm4 proteins (Fig. 7B). The distribution pattern of these protein accumulations in the mutant was similar to that of wild-type cells. We conclude that Dcp2-containing accumulations at 42°C, similarly to other components of SGs, do not require P-bodies scaffolding proteins.

The similarity of RNP accumulations formed at 42°C to SGs formed at 46°C indicated that they are structurally related. We performed a time-lapse experiment using the strain co-expressing Yef3-GFP with the SGs marker protein Rpg1-RFP (Fig. 7C). The cells were pre-heated to 42°C and then continuously heated up to 46°C. The Yef3-GFP fusion protein was accumulated during the initial cultivation at 42°C and also later on. In contrast, the Rpg1-RFP fusion protein began to accumulate around Yef3-GFP foci only after raising the temperature above 42°C, with most focused accumulations being observed at 46°C. We conclude that the RNP accumulations formed at 42°C serve as "seeds" for genuine SGs assembled upon robust heat shock at 46°C.

Translation Initiation Factor eIF2α Subunit is Recruited to Heat-induced SGs Upon a Stress Relief

In contrast to P-bodies, the composition of SGs suggests that SGs might be sites where translation initiates during the cell recovery from a stress. In our previous work [2], we described that α subunit of the translation initiation factor eIF2 (Sui2p) is not a constituent of the robust heat shock-induced SGs in *S. cerevisiae*. Here we analyzed distribution of the Sui2 protein in cells recovering from the heat shock using a strain co-expressing Sui2-GFP fusion protein with the stress granule marker Rpg1-RFP. In contrast to the cells heat-shocked at 46°C, where distribution of Sui2-GFP was uniformly cytosolic, the cells recovering from the heat shock displayed accumulations of Sui2-GFP overlapping with dissolving SGs (Rpg1-RFP) (Fig. 8A).

To analyze whether accumulation of Sui2-GFP on SGs during the recovery from the stress is dependent on a phosphorylation status of Sui2p, we used a new strain carrying Sui2-GFP and Rpg1-RFP proteins together with the *gcn2* deletion. We found that Sui2-GFP accumulated on dissolving SGs even in the absence of the Gcn2 kinase (Fig. 8B). It means that Sui2p accumulated on SGs is present also in its non-phosphorylated form, thus translation competent. Our data thus support the hypothesis that SGs serve as sites to initiate translation after a stress relief.

Discussion

It is widely accepted that stress granules (SGs) are composed of stalled translation preinitiation complexes (48S) containing mRNA, small ribosomal subunits and some translation initiation factors [15,41]. Here we provide evidence that the heat-induced SGs formed at 46°C in *S. cerevisiae* also contain certain translation elongation and translation termination factors. Some of them, elongation factors eEF3 and eEF1Bγ2 and the termination factor eRF1 accumulate already at 42°C on Dcp2 foci independently of P-bodies scaffolding proteins. We also showed, on the example of eEF3 factor, that an accumulation of the protein at 42°C is independent on the Gcn2 kinase activity. However, these foci still determine sites for assembly of SGs upon heat shock at 46°C. Our data suggest that assembly of these SGs might be controlled by translation elongation and termination factors released from ongoing translation. Furthermore, recruitment of the key translation initiation factor eIF2α (Sui2p) to dissolving SGs points to the recovery of translation at these sites after stress relief.

Although SGs are referred to as stalled translation preinitiation complexes, it is generally accepted that the composition of SGs varies depending on organisms and cell types, as well as on intensity and type of the stress [42]. For example, SGs induced by a high concentration of ethanol in *S. cerevisiae* contain only the eIF3c/Nip1 subunit of the eIF3 complex [3] and SGs induced by a prolonged glucose deprivation do not harbor the eIF3 complex at all [1]. With respect to the intensity of the stress, treatment with a low concentration of NaN_3 does not affect the distribution of eIF3a (Rpg1p/Tif32p) [2] but at higher concentration this drug induces eIF3a accumulation in SGs [17]. We show here that SGs induced by the robust heat shock in *S. cerevisiae* contain translation elongation factors eEF3 (Yef3p) and eEF1Bγ2 (Tef4p) together with translation termination factors eRF1 (Sup45p) and eRF3 (Sup35p). These factors have never been observed in SGs of any other eukaryotic cell. However, the termination factors have been found to accumulate in P-bodies [1,43]. Those authors have concluded that presence of translation termination factors in P-bodies is coupled to the P-bodies assembly. A similar role could be suggested for presence of these factors in heat-induced SGs.

The proteins with self-aggregation (prion-like) domain, like TIA-1 or TIAR in mammalian cells, have been described to influence dynamics of SGs [40]. A newly identified component of the heat-induced SGs in *S.cerevisiae*, Sup35p, possesses a prion-like domain at the N-terminus. Sup35p can thus convert into the prion form, known as [PSI+]. The N-terminal part of the protein is indispensable for the prion formation and maintenance [38,39]. Similarly to a situation in mammalian cells [40] we found that

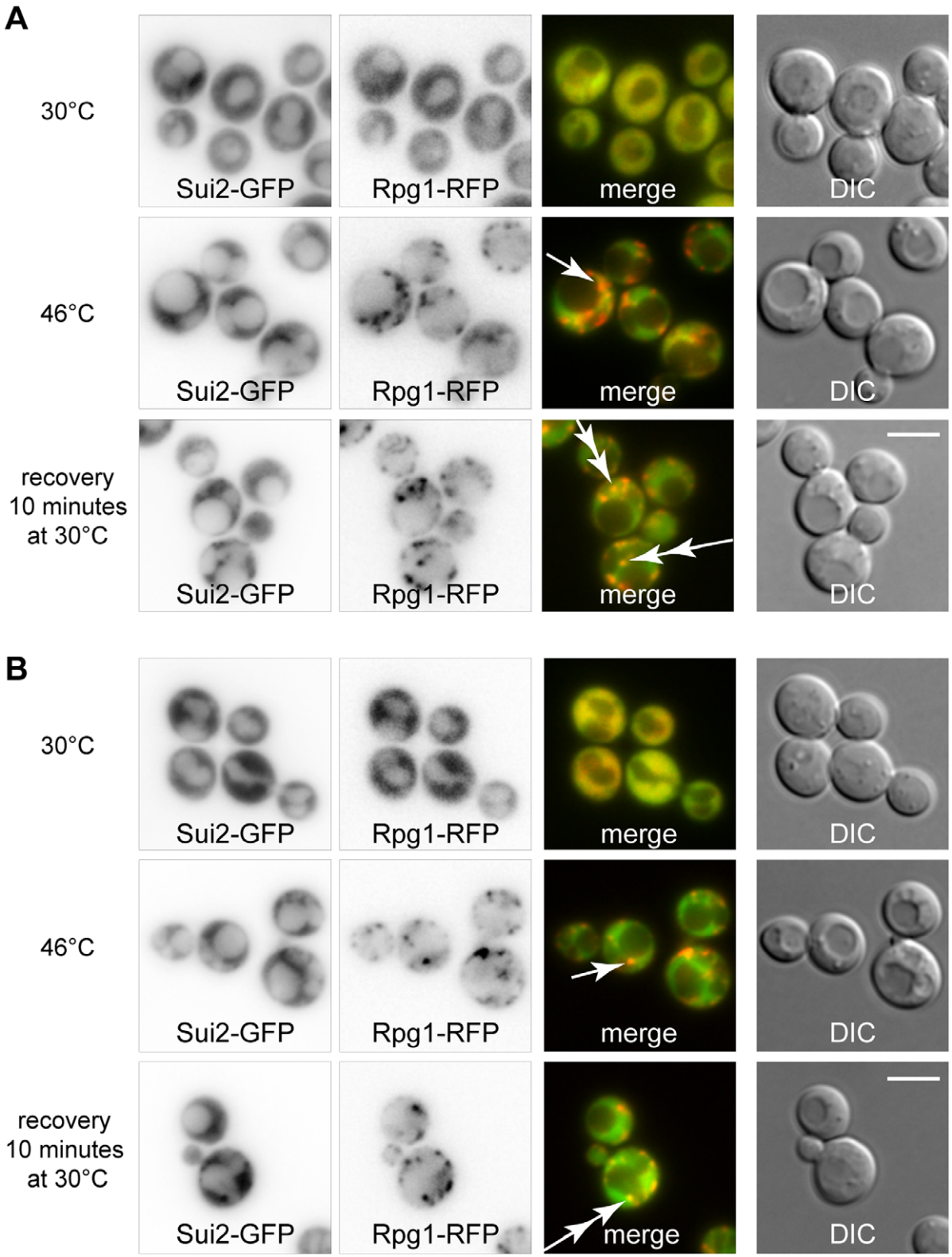

Figure 8. Sui2p associates with dissolving SGs in cells recovering from the heat shock. (A) The localization of fusion proteins Sui2-GFP and Rpg1-RFP was analyzed in cells (CRY1332 strain) cultivated at 30°C or heat-shocked at 46°C for 10 minutes or cultivated after heat shock for additional 10 minutes. Sui2-RFP protein was not accumulated in stress granules (Rpg1-GFP) of heat-shocked cells (single arrow). Sui2 protein began to accumulate with stress granules during the cell recovery phase after cultivation of the heat-shocked cells at 30°C for additional 10 minutes (double arrows). (B) The same situation as in (A), but in the *gcn2*Δ strain (CRY1691 strain). Scale bar 4 μm.
doi:10.1371/journal.pone.0057083.g008

rather a non-prion part of Sup35p is responsible for accumulation of the protein in SGs. However, observations that SGs are formed even in the absence of the N-terminal prion-like domain of Sup35p indicate that unlike in mammals, the assembly of heat-induced SGs in *S. cerevisiae* is not driven by these "prion" structural elements. This hypothesis is also supported by our earlier findings that heat-induced SGs are formed even in the absence of yeast orthologs of mammalian TIA-1 and TIAR proteins, Ngr1 and Pub1 proteins in *S. cerevisiae* [2].

Translation termination factors eRF1 (Sup45p) and eRF3 (Sup35p) are responsible for effective termination of translation [44]. In addition, they seem to be required for an effective function of the fungal-specific elongation factor eEF3 (Yef3p) [45] in recycling of the translation posttermination complexes after the release of newly synthetized peptide chains [46,47]. In this respect, identification of elongation and termination factors in heat-induced SGs may indicate that these SGs are composed of translation posttermination complexes stalled before the ribosome recycling step. However, we did not observe any accumulation of several essential proteins of the 60S ribosomal subunits under robust heat shock [2] and Grousl et al. (unpublished data). In addition, all the published information on recycling of the translation posttermination complexes comes from in vitro experiments only. Therefore, it is currently unclear, how recycling is catalyzed in vivo and the reasons for presence of the translation elongation and the termination factors in robust heat shock-induced SGs remain to be elucidated.

Whereas different roles for SGs and P-bodies in cell survival upon heat stress conditions could be suggested, both accumulations are always closely spatially and functionally intertwined. In *S. cerevisiae* cells, P-bodies promote formation of SGs [1,2]. The assembly of P-bodies is connected with changes in expression profiles and adaptation to changed environmental conditions, when the translation of certain transcripts is inhibited and, on the other hand, the translation of new transcripts is induced [11]. They are present in cells even under non-stress conditions and they enlarge under various stresses, such as a heat shock at 39°C [21] and 42°C [48]. However, one of the major components of P-bodies, Dcp2p that is engaged in mRNA decapping [5,9,10], is also a component of the robust heat shock-induced SGs, which may form independently of the P-bodies scaffolding proteins Edc3 and Lsm4 [2]. On the contrary to glucose-deprived cells [1,8] and cells heat-shocked at 37°C, we show here that Dcp2 foci formed in cells heat-shocked at 42°C do not depend on these scaffolds. These Dcp2 accumulations do not contain translation initiation factors and still serve as sites for assembly of SGs upon continuous and more robust heat stress. They might be considered as "premature SGs", as well as Dcp2-containing structures related to P-bodies.

The stress-induced phosphorylation of translation initiation factor eIF2α is the best characterized mechanism of stress granule assembly [14,15]. However, there are other ways, how to induce SGs or influence their dynamics. Apart influencing other translation initiation factors, they concern the metabolism of polyamines or hexosamines and the stress-induced tRNA derivates [29,31,49,50]. Moreover, since eIF2α-phosphorylation independent mechanisms of SGs assembly prevail in lower eukaryotes, it seems that these are evolutionary older. We show here that accumulations of translation elongation factor eEF3 (Yef3p) on Dcp2 foci at 42°C precede assembly of eIF3-containing SGs in cells heat-shocked at 46°C. This suggests that the translation elongation phase is affected first in the stressed cells. It is conceivable that there might be a shortage of the eEF3 factor due to its sequestration into cytoplasmic foci at 42°C. This may cause an alteration of kinetics of the translation elongation, which results in a deceleration of translation initiation. Such regulation of translation at the elongation step has also been proposed as a possible function of the Stm1 protein, which is able to stall ribosomes after the 80S complex formation *in vitro* and to promote decapping of a subset of mRNA [51]. Moreover, Stm1p has been shown to regulate interaction of eEF3 factor with ribosomes and to play a complementary role to eEF3 in translation under nutrient stress conditions [52]. Interestingly, we did not observe an accumulation of Stm1-GFP fusion protein neither upon heat shock at 42°C nor under heat shock at 46°C (Figure S3). Additionally, we did not see any effect of the *stm1*Δ on assembly of SGs in cells heat-shocked at 46°C (Figure S4). Therefore, the roles of Stm1 protein and eEF3 factor in the Gcn2-independent signaling and translation repression resulting in SGs assembly in heat-shocked cells remain elusive.

Meanwhile assembly of P-bodies is generally connected with reprogramming of cells to new growth conditions, SGs are formed in response to severe stresses when the translation of housekeeping genes is completely shut down. Although SGs are thought to be sites where mRNA molecules are sorted, selected, and together with translation factors, sheltered from the effects of a stress [15,53], the fate of SGs components after a stress relief is mainly unknown [42]. However, it is conceivable that at least some SGs protein components may also return back to the active translation. In this respect, our observation of accumulation of the key translation initiation factor eIF2α (Sui2p) on dissolving SGs during cell recovery from the heat stress suggests that SGs may help cells to effectively recover after a stress relief. To recover, a fast restart of translation is facilitated by increasing a local concentration of translation initiation and elongation components in SGs, where only the key regulator, eIF2α factor (Sui2p), is missing and recruited after a stress relief only. There is a supporting evidence from mammalian cells where a phospho-variant of the eIF2α factor subunit was found to be recruited to disassembling SGs and considered as important for SGs disassembly [15]. On the contrary, we found that the eIF2α factor (Sui2p) accumulation on SGs does not depend on the phosphorylation status of this factor. It implies that the eIF2α factor is recruited to dissolving SGs also in its unphosphorylated state, thus translation competent. Taken together, it reinforces the hypothesis that SGs serve as sites where translation is effectively initiated at the time of a stress relief.

We showed here that a portion of the key translation initiation factor eIF2α (Sui2p) is recruited to dissolving SGs, but some of the Sui2-GFP foci did not co-localize with SGs markers in these cells. We suggest that these particular Sui2-GFP foci may represent the eIF2B bodies [54]. In accordance with our assumption that translation is restored on dissolving SGs, the eIF2B bodies should also be formed under recovery from the stress. The eIF2B bodies most probably serve as sites, where guanine nucleotide exchange of the eIF2α factor takes place and the eIF2α-GDP form is converted to the translation competent eIF2α-GTP form. The eIF2B bodies would then help to regenerate efficiently the translation competent form of the eIF2α factor as suggested previously [55]. The eIF2α-GTP form would then be recruited to sites on dissolving SGs.

Altogether, our data support the current view that the composition of stress granules depends on the type and the intensity of the applied stress. We confirmed that formation of yeast heat shock-induced SGs is not dependent on the translation initiation arrest caused by phosphorylation of eIF2α and we propose that translation machinery in heat shocked-cells seems to be primarily modulated at the level of translation elongation since also some translation elongation and termination factors accumulate within SGs. Our data further indicate that SGs reflect the sites

where translation initiates after a stress relief. We also show that RNP accumulations formed upon heat shock at 42°C and containing translation elongation and termination factors may develop into genuine SGs upon robust heat shock at 46°C. Although we confirmed that all these accumulations depend on mRNA released from translation, links between heat-induced repression of translation and SGs assembly still remain to be elucidated.

Supporting Information

Figure S1 Factor eRF1 (Sup45p) co-localizes with Dcp2 and Ngr1 proteins in stress granules. (A) The subcellular distribution of Sup45-GFP and Dcp2-mCherry (CRY1636 strain) or (B) Sup45-GFP and Ngr1-mCherry (CRY1638) fusion proteins under heat shock at 46°C. Both pairs of proteins co-localize within stress granules. Values of the Pearsons correlation coefficient (R_r) over 0.5 confirmed the co-localization. Scale bar 4 μm.
(TIF)

Figure S2 An accumulation of eEF3 factor and an alteration of polysome profile at 42°C are *gcn2*Δ independent. (A) The distribution of Yef3-GFP protein in *gcn2*Δ strain (CRY1336 strain) at 30°C and under heat shock at 42°C. The protein accumulates in the same extend as the wild-type strain (compare with Figure 5) upon the heat shock. (B) Polysome profiles of *gcn2*Δ strain (CRY309 strain) at permissive temperature and after heat shock at 42°C for 10 minutes. Translation profile was altered in heat-shocked cells. P/M stands for polysome/monosome ratio.
(TIF)

Figure S3 Subcellular distribution of Stm1-GFP fusion protein is not altered upon heat shock at 42°C and 46°C. The distribution of Stm1-GFP fusion protein (CRY1516 strain) remains diffusely cytosolic under all tested conditions. Scale bar 4 μm.
(TIF)

Figure S4 Deletion of the *STM1* gene does not affect assembly of heat-induced SGs. (A) The distribution of Pab1-GFP and Rpg1-RFP proteins in wild-type cells (CRY528 strain) at 30°C and upon heat shock at 46°C for 10 minutes. Both proteins are accumulated in stress granules. (B) The *stm1*Δ mutant (CRY1760 strain) displayed a similar pattern of stress granules as the wild-type cells. Scale bar 4 μm.
(TIF)

Acknowledgments

We are grateful to Alan G. Hinnebusch (NICH & HDNIH, USA) for a critical reading of the manuscript and helpful comments. Technical assistance by J. Serbouskova is gratefully acknowledged. We are grateful to M. Farkasovsky (Slovak Academy of Sciences, Slovakia), R. Parker (University of Arizona, USA) and E.I. Lewitin (Institute of Industrial Genetics, Russia) for providing plasmids.

Author Contributions

Conceived and designed the experiments: JH PI TG. Performed the experiments: TG PI RS. Analyzed the data: JH PI TG. Contributed reagents/materials/analysis tools: IM IF LS LN PP. Wrote the paper: TG JH.

References

1. Buchan JR, Muhlrad D, Parker R (2008) P bodies promote stress granule assembly in Saccharomyces cerevisiae. J Cell Biol 183: 441–455.
2. Grousl T, Ivanov P, Frydlova I, Vasicova P, Janda F, et al. (2009) Robust heat shock induces eIF2alpha-phosphorylation-independent assembly of stress granules containing eIF3 and 40S ribosomal subunits in budding yeast, Saccharomyces cerevisiae. J Cell Sci 122: 2078–2088.
3. Kato K, Yamamoto Y, Izawa S (2011) Severe ethanol stress induces assembly of stress granules in Saccharomyces cerevisiae. Yeast 28: 339–347.
4. Nilsson D, Sunnerhagen P (2011) Cellular stress induces cytoplasmic RNA granules in fission yeast. RNA 17: 120–133.
5. Sheth U, Parker R (2003) Decapping and decay of messenger RNA occur in cytoplasmic processing bodies. Science 300: 805–808.
6. Hofmann S, Cherkasova V, Bankhead P, Bukau B, Stoecklin G (2012) Translation suppression promotes stress granule formation and cell survival in response to cold shock. Mol Biol Cell 23: 3786–3800.
7. Eulalio A, Behm-Ansmant I, Izaurralde E (2007) P bodies: at the crossroads of post-transcriptional pathways. Nat Rev Mol Cell Biol 8: 9–22.
8. Decker CJ, Teixeira D, Parker R (2007) Edc3p and a glutamine/asparagine-rich domain of Lsm4p function in processing body assembly in Saccharomyces cerevisiae. J Cell Biol 179: 437–449.
9. Brengues M, Teixeira D, Parker R (2005) Movement of eukaryotic mRNAs between polysomes and cytoplasmic processing bodies. Science 310: 486–489.
10. Balagopal V, Parker R (2009) Polysomes, P bodies and stress granules: states and fates of eukaryotic mRNAs. Curr Opin Cell Biol 21: 403–408.
11. Arribere JA, Doudna JA, Gilbert WV (2011) Reconsidering movement of eukaryotic mRNAs between polysomes and P bodies. Mol Cell 44: 745–758.
12. Parker R (2012) RNA Degradation in Saccharomyces cerevisae. Genetics 191: 671–702.
13. Balagopal V, Fluch L, Nissan T (2012) Ways and means of eukaryotic mRNA decay. Biochim Biophys Acta.
14. Anderson P, Kedersha N (2008) Stress granules: the Tao of RNA triage. Trends Biochem Sci 33: 141–150.
15. Anderson P, Kedersha N (2002) Stressful initiations. J Cell Sci 115: 3227–3234.
16. Takahara T, Maeda T (2012) Transient Sequestration of TORC1 into Stress Granules during Heat Stress. Mol Cell 47: 242–252.
17. Buchan JR, Yoon JH, Parker R (2011) Stress-specific composition, assembly and kinetics of stress granules in Saccharomyces cerevisiae. J Cell Sci 124: 228–239.
18. Huh WK, Falvo JV, Gerke LC, Carroll AS, Howson RW, et al. (2003) Global analysis of protein localization in budding yeast. Nature 425: 686–691.
19. Dunand-Sauthier I, Walker C, Wilkinson C, Gordon C, Crane R, et al. (2002) Sum1, a component of the fission yeast eIF3 translation initiation complex, is rapidly relocalized during environmental stress and interacts with components of the 26S proteasome. Mol Biol Cell 13: 1626–1640.
20. Hoyle NP, Castelli LM, Campbell SG, Holmes LE, Ashe MP (2007) Stress-dependent relocalization of translationally primed mRNPs to cytoplasmic granules that are kinetically and spatially distinct from P-bodies. J Cell Biol 179: 65–74.
21. Cowart LA, Gandy JL, Tholanikunnel B, Hannun YA (2010) Sphingolipids mediate formation of mRNA processing bodies during the heat-stress response of Saccharomyces cerevisiae. Biochem J 431: 31–38.
22. Proud CG (2005) Semin Cell Dev Biol 16: 3–12.
23. Hinnebusch AG (2005) eIF2alpha kinases provide a new solution to the puzzle of substrate specificity. Nat Struct Mol Biol 12: 835–838.
24. Pavitt GD, Ramaiah KV, Kimball SR, Hinnebusch AG (1998) eIF2 independently binds two distinct eIF2B subcomplexes that catalyze and regulate guanine-nucleotide exchange. Genes Dev 12: 514–526.
25. Dang Y, Kedersha N, Low WK, Romo D, Gorospe M, et al. (2006) Eukaryotic initiation factor 2alpha-independent pathway of stress granule induction by the natural product pateamine A. J Biol Chem 281: 32870–32878.
26. Mazroui R, Sukarieh R, Bordeleau ME, Kaufman RJ, Northcote P, et al. (2006) Inhibition of ribosome recruitment induces stress granule formation independently of eukaryotic initiation factor 2alpha phosphorylation. Mol Biol Cell 17: 4212–4219.
27. Kramer S, Queiroz R, Ellis L, Webb H, Hoheisel JD, et al. (2008) Heat shock causes a decrease in polysomes and the appearance of stress granules in trypanosomes independently of eIF2{alpha} phosphorylation at Thr169. J Cell Sci 121: 3002–3014.
28. Farny NG, Kedersha NL, Silver PA (2009) Metazoan stress granule assembly is mediated by P-eIF2alpha-dependent and -independent mechanisms. Rna 15: 1814–1821.
29. Emara MM, Ivanov P, Hickman T, Dawra N, Tisdale S, et al. (2010) Angiogenin-induced tRNA-derived stress-induced RNAs promote stress-induced stress granule assembly. J Biol Chem 285: 10959–10968.
30. Emara MM, Fujimura K, Sciaranghella D, Ivanova V, Ivanov P, et al. (2012) Hydrogen peroxide induces stress granule formation independent of eIF2alpha phosphorylation. Biochem Biophys Res Commun 423: 763–769.
31. Simpson CE, Ashe MP (2012) Adaptation to stress in yeast: to translate or not? Biochem Soc Trans 40: 794–799.
32. Brachmann CB, Davies A, Cost GJ, Caputo E, Li J, et al. (1998) Designer deletion strains derived from Saccharomyces cerevisiae S288C: a useful set of strains and plasmids for PCR-mediated gene disruption and other applications. Yeast 14: 115–132.

33. Robinson JS, Klionsky DJ, Banta LM, Emr SD (1988) Protein sorting in Saccharomyces cerevisiae: isolation of mutants defective in the delivery and processing of multiple vacuolar hydrolases. Mol Cell Biol 8: 4936–4948.
34. Sambrook J, Russell DW (2001) Molecular cloning: a laboratory manual (3rd ed.). Cold Spring Harbor, NY: Cold Spring Harbor Laboratory.
35. Sambrook J, Fritsch EF, Maniatis T (1989) Molecular cloning : a laboratory manual. Cold Spring Harbor, N.Y.: Cold Spring Harbor Laboratory.
36. Rothstein R (1991) Targeting, disruption, replacement, and allele rescue: integrative DNA transformation in yeast. Methods Enzymol 194: 281–301.
37. Gueldener U, Heinisch J, Koehler GJ, Voss D, Hegemann JH (2002) A second set of loxP marker cassettes for Cre-mediated multiple gene knockouts in budding yeast. Nucleic Acids Res 30: e23.
38. Ter-Avanesyan MD, Dagkesamanskaya AR, Kushnirov VV, Smirnov VN (1994) The SUP35 omnipotent suppressor gene is involved in the maintenance of the non-Mendelian determinant [psi+] in the yeast Saccharomyces cerevisiae. Genetics 137: 671–676.
39. Derkatch IL, Chernoff YO, Kushnirov VV, Inge-Vechtomov SG, Liebman SW (1996) Genesis and variability of [PSI] prion factors in Saccharomyces cerevisiae. Genetics 144: 1375–1386.
40. Gilks N, Kedersha N, Ayodele M, Shen L, Stoecklin G, et al. (2004) Stress granule assembly is mediated by prion-like aggregation of TIA-1. Mol Biol Cell 15: 5383–5398.
41. Kimball SR, Horetsky RL, Ron D, Jefferson LS, Harding HP (2003) Mammalian stress granules represent sites of accumulation of stalled translation initiation complexes. Am J Physiol Cell Physiol 284: C273–284.
42. Anderson P, Kedersha N (2009) Stress granules. Curr Biol 19: R397–398.
43. Dori D, Choder M (2007) Conceptual modeling in systems biology fosters empirical findings: the mRNA lifecycle. PLoS One 2: e872.
44. Alkalaeva EZ, Pisarev AV, Frolova LY, Kisselev LL, Pestova TV (2006) In vitro reconstitution of eukaryotic translation reveals cooperativity between release factors eRF1 and eRF3. Cell 125: 1125–1136.
45. Chakraburtty K (2001) Translational regulation by ABC systems. Res Microbiol 152: 391–399.
46. Kurata S, Nielsen KH, Mitchell SF, Lorsch JR, Kaji A, et al. (2010) Ribosome recycling step in yeast cytoplasmic protein synthesis is catalyzed by eEF3 and ATP. Proc Natl Acad Sci U S A 107: 10854–10859.
47. Pisarev AV, Skabkin MA, Pisareva VP, Skabkina OV, Rakotondrafara AM, et al. (2010) The role of ABCE1 in eukaryotic posttermination ribosomal recycling. Mol Cell 37: 196–210.
48. Scarcelli JJ, Viggiano S, Hodge CA, Heath CV, Amberg DC, et al. (2008) Synthetic Genetic Array Analysis in Saccharomyces cerevisiae Provides Evidence for an Interaction Between RAT8/DBP5 and Genes Encoding P-Body Components. Genetics 179: 1945–1955.
49. Zou T, Rao JN, Liu L, Xiao L, Cui YH, et al. (2012) Polyamines inhibit the assembly of stress granules in normal intestinal epithelial cells regulating apoptosis. Am J Physiol Cell Physiol 303: C102–111.
50. Li CH, Ohn T, Ivanov P, Tisdale S, Anderson P (2010) eIF5A promotes translation elongation, polysome disassembly and stress granule assembly. PLoS One 5: e9942.
51. Balagopal V, Parker R (2011) Stm1 modulates translation after 80S formation in Saccharomyces cerevisiae. RNA 17: 835–842.
52. Van Dyke N, Pickering BF, Van Dyke MW (2009) Stm1p alters the ribosome association of eukaryotic elongation factor 3 and affects translation elongation. Nucleic Acids Res 37: 6116–6125.
53. Buchan JR, Parker R (2009) Eukaryotic stress granules: the ins and outs of translation. Mol Cell 36: 932–941.
54. Campbell SG, Hoyle NP, Ashe MP (2005) Dynamic cycling of eIF2 through a large eIF2B-containing cytoplasmic body: implications for translation control. J Cell Biol 170: 925–934.
55. Campbell SG, Ashe MP (2006) Localization of the translational guanine nucleotide exchange factor eIF2B: a common theme for GEFs? Cell Cycle 5: 678–680.
56. Mortimer RK, Johnston JR (1986) Genealogy of principal strains of the yeast genetic stock center. Genetics 113: 35–43.

Figure S1

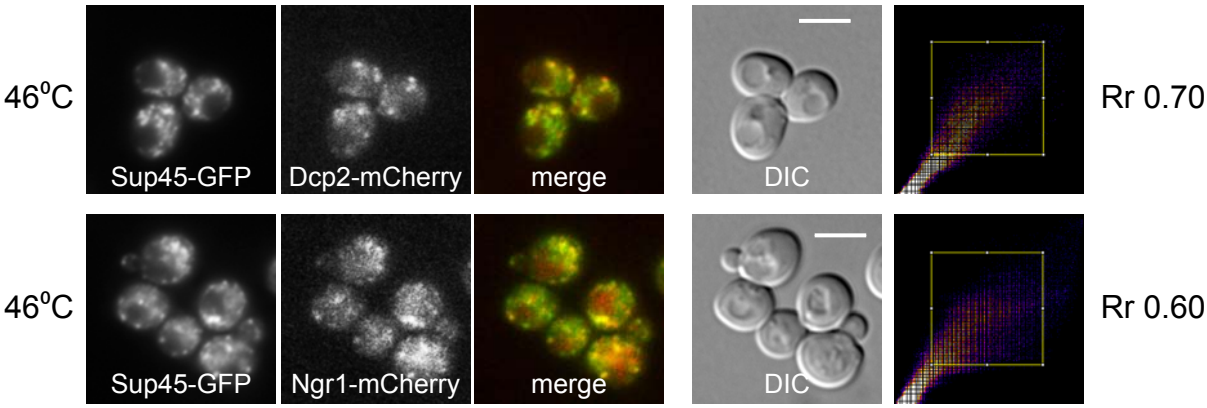

Figure S1

Factor eRF1 (Sup45p) co-localizes with Dcp2 and Ngr1 proteins in stress granules. (A) The subcellular distribution of Sup45-GFP and Dcp2-mCherry (CRY1636 strain) or (B) Sup45-GFP and Ngr1-mCherry (CRY1638) fusion proteins under heat shock at 46°C. Both pairs of proteins co-localize within stress granules. Values of the Pearson's correlation coefficient (R_r) over 0.5 confirmed the co-localization. Scale bar 4 μm.

Figure S2

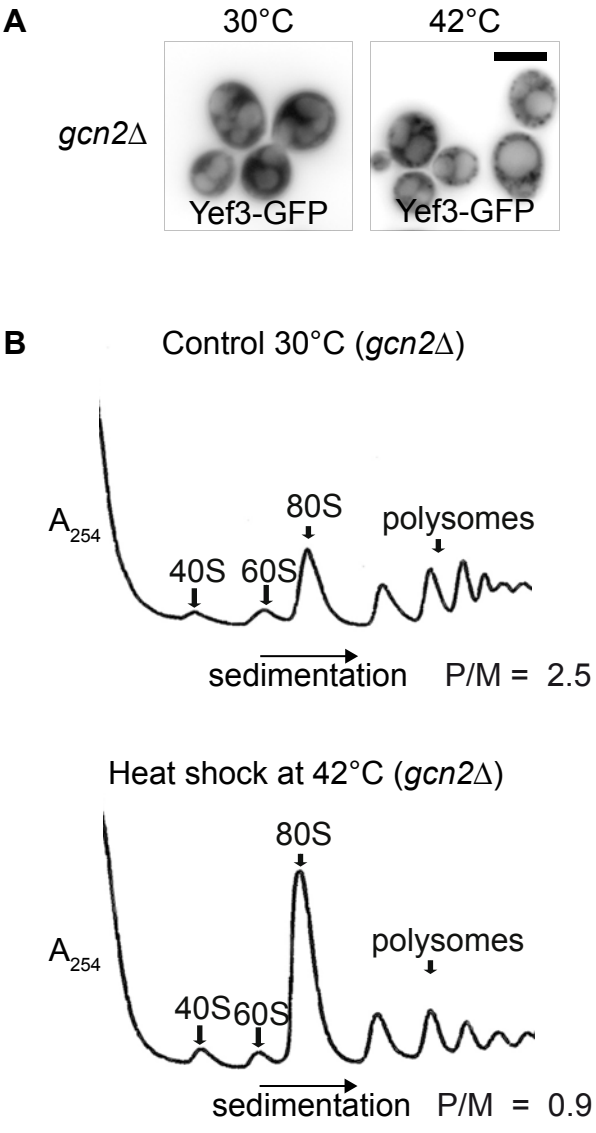

Figure S2

An accumulation of eEF3 factor and an alteration of polysome profile at 42°C are *gcn2*Δ independent. (A) The distribution of Yef3-GFP protein in *gcn2*Δ strain (CRY1336 strain) at 30°C and under heat shock at 42°C. The protein accumulates in the same extend as the wild-type strain (compare with Figure 5) upon the heat shock. (B) Polysome profiles of *gcn2*Δ strain (CRY309 strain) at permissive temperature and after heat shock at 42°C for 10 minutes. Translation profile was altered in heat-shocked cells. P/M stands for polysome/monosome ratio.

Figure S3

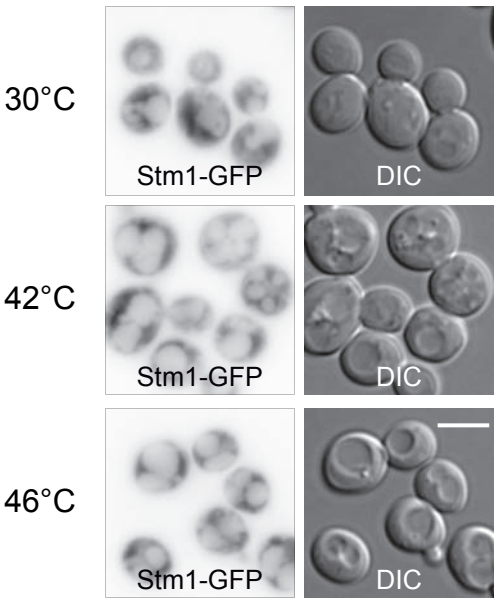

Figure S3

Subcellular distribution of Stm1-GFP fusion protein is not altered upon hea shock at 42°C and 46°C. The distribution of Stm1-GFP fusion protein (CRY1516 strain) remains diffusely cytosolic under all tested conditions. Scale bar 4 μm.

Figure S4

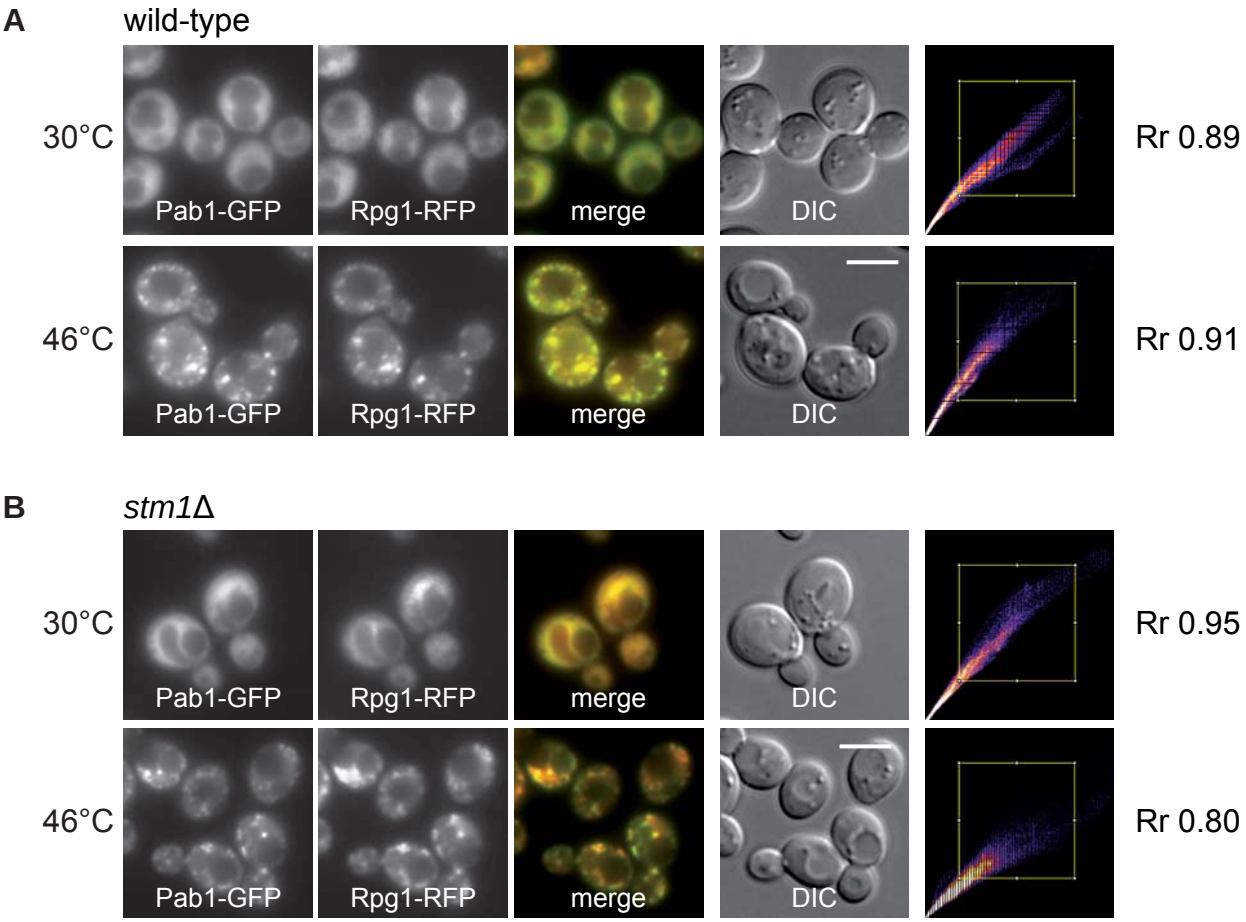

Figure S4

Deletion of the *STM1* gene does not affect assembly of heat-induced SGs. (A) The distribution of Pab1-GFP and Rpg1-RFP proteins in wild-type cells (CRY528 strain) at 30°C and upon heat shock at 46°C for 10 minutes. Both proteins are accumulated in stress granules. (B) The *stm1*Δ mutant (CRY1760 strain) displayed a similar pattern of stress granules as the wild-type cells. Scale bar 4 μm.

Paper 3

The paper *Mmi1, the yeast homologue of mammalian TCTP, associates with stress granules in heat-shocked cells and modulates proteasome activity* by Rinnerthaler et al., focuses mainly on yeast microtubule and mitochondria interacting protein 1 (Mmi1).

The main message of the paper is a discovery of new roles of Mmi1 protein in cells of *Saccharomyces cerevisiae*. Mmi1 protein is an ortholog of mammalian translation controlled tumor protein (TCTP), which is intensively studied for its therapeutical potential. A research on Mmi1 could help also to that of TCTP due to their evolutionary conserved protein structures and shared cellular functions. Authors of the paper showed that the Mmi1 protein is associated with heat-induced stress granules (SGs) upon robust heat shock. Concurrently, deletion of *mmi1* (*tma19*) gene confers resistance to the stress indicating role of this protein in heat shock stress response, possibly through the association with SGs. However, deletion of *mmi1* gene does not influence dynamics of the SGs, at least in tested parameters. The domain analyses of Mmi1 protein revealed which parts of the proteins are responsible for its localization into different subcellular compartments. The rest of the paper is dedicated to nuclear localization of Mmi1 and its interconnection with the proteasome degradation pathway.

Authors of the paper performed variety of methodologies, as are electron and live cell fluorescence microscopy, proteasome activity assays, protein structure prediction analyses and certain genetic and biochemical methods.

The idea of the paper is to present new data about yeast ortholog of mammalian TCTP protein, Mmi1. It concerns domain localization analyses of the protein, a characterization of the deletion phenotype and discovered connections with heat-induced stress granules and the proteasomal degradation system. Based on these data, authors declare hypothesis about a function of Mmi1, as a regulator of protein degradation upon stress conditions.

OPEN ACCESS Freely available online

PLOS ONE

Mmi1, the Yeast Homologue of Mammalian TCTP, Associates with Stress Granules in Heat-Shocked Cells and Modulates Proteasome Activity

Mark Rinnerthaler[1☯], Renata Lejskova[2☯], Tomas Grousl[2], Vendula Stradalova[3], Gino Heeren[1¤], Klaus Richter[1], Lore Breitenbach-Koller[1], Jan Malinsky[3], Jiri Hasek[2]*, Michael Breitenbach[1]*

1 Department Cell Biology, Division Genetics, University of Salzburg, Salzburg, Austria, **2** Laboratory of Cell Reproduction, Institute of Microbiology of AS CR, v.v.i., Prague, Czech Republic, **3** Microscopy Unit, Institute of Experimental Medicine of AS CR, v.v.i., Prague, Czech Republic

Abstract

As we have shown previously, yeast Mmi1 protein translocates from the cytoplasm to the outer surface of mitochondria when vegetatively growing yeast cells are exposed to oxidative stress. Here we analyzed the effect of heat stress on Mmi1 distribution. We performed domain analyses and found that binding of Mmi1 to mitochondria is mediated by its central alpha-helical domain (V-domain) under all conditions tested. In contrast, the isolated N-terminal flexible loop domain of the protein always displays nuclear localization. Using immunoelectron microscopy we confirmed re-location of Mmi1 to the nucleus and showed association of Mmi1 with intact and heat shock-altered mitochondria. We also show here that *mmi1*Δ mutant strains are resistant to robust heat shock with respect to clonogenicity of the cells. To elucidate this phenotype we found that the cytosolic Mmi1 holoprotein re-localized to the nucleus even in cells heat-shocked at 40°C. Upon robust heat shock at 46°C, Mmi1 partly co-localized with the proteasome marker Rpn1 in the nuclear region as well as with the cytoplasmic stress granules defined by Rpg1 (eIF3a). We co-localized Mmi1 also with Bre5, Ubp3 and Cdc48 which are involved in the protein de-ubiquitination machinery, protecting protein substrates from proteasomal degradation. A comparison of proteolytic activities of wild type and *mmi1*Δ cells revealed that Mmi1 appears to be an inhibitor of the proteasome. We conclude that one of the physiological functions of the multifunctional protein module, Mmi1, is likely in regulating degradation and/or protection of proteins thereby indirectly regulating the pathways leading to cell death in stressed cells.

Citation: Rinnerthaler M, Lejskova R, Grousl T, Stradalova V, Heeren G, et al. (2013) Mmi1, the Yeast Homologue of Mammalian TCTP, Associates with Stress Granules in Heat-Shocked Cells and Modulates Proteasome Activity. PLoS ONE 8(10): e77791. doi:10.1371/journal.pone.0077791

Editor: Sandy D. Westerheide, University of South Florida, United States of America

Received March 20, 2013; **Accepted** September 4, 2013; **Published** October 28, 2013

Funding: This work was supported by the grants P305/12/0480 (Czech Science Foundation, CSF), 7AMB12ATOO2 and RVO61388971 (to JH), by grant OeAD Aktion CZ 11/2012 (to MR), by grants S9302-B05 (FWF Austria) and 512020 MIMAGE (EC, Brussels) (to MB) and by grant P302/11/0146 (CSF) (to JM). The funders had no role in study design, data collection and analysis, decision to publish, or preparation of the manuscript.

Competing Interests: The authors have declared that no competing interests exist.

* E-mail: hasek@biomed.cas.cz (JH); michael.breitenbach@sbg.ac.at (MB)

☯ These authors contributed equally to this work.

¤ Current address: Department of Laboratory Medicine, Paracelsus Medical University, Salzburg, Austria

Introduction

The literature covering the highly conserved eukaryotic protein generally called TCTP (for "translationally controlled tumor protein"), has been reviewed recently [1]. In growing cells, this small (18 kD) and water-soluble protein is expressed at a high level. The protein was first isolated and described from human tumor cells [2]. Then it has been intensively investigated because of its role in the control of cell division and as an anti-apoptotic agent [3]. It was even studied as a possible drug target for tumor therapy [4]. TCTP is also a tubulin binding protein [5] [6] and acts as a histamine-releasing factor after non-classical secretion [7]. After 32 years of research since its discovery [2], and about 150 papers dealing with TCTP, the physiological role of this small and versatile protein is still not completely clear, mostly due to the multiplicity of its proposed functions and cellular localizations [1]. The structure of *Sch. pombe* TCTP was determined by X-ray crystallography and the solution structure was determined by high field NMR [8], later followed by several more TCTP structures. These structures were found to be highly homologous among each other just like the sequences of the proteins. However, they are not structurally homologous to other protein domains of known function and therefore do not give strong clues about the biochemical function of this protein family.

The literature contains many indications that TCTP/Mmi1 is a stress sensor and stress-response regulator. A stress-induced up-regulation of TCTP expression was reported in many organisms and included a broad variety of harmful stresses such as oxidative stress [9,10], heat stress [4], exposure to Ca^{2+} [4] or heavy metals [11]. In this context TCTP is an important decision-maker between life and death due to its anti-apoptotic features. Although the anti-apoptotic features of TCTP have been already reported by preventing etoposide-induced apoptosis in HeLa cells [3], the detailed mode of this TCTP function is still not clear. TCTP itself is interacting with two other anti-apoptotic proteins (Bcl-xl and Mcl-1) and could in this way stabilize these two interactors [12–

14]. Binding of TCTP to the mitochondria and thereby inhibiting the dimerization of BAX (that is a prerequisite for permeabilization of the outer mitochondrial membrane) is in discussion [15]. Another hypothesis is based on the fact that TCTP is a calcium binding protein [16]. Therefore, TCTP by binding cytoplasmic calcium ions could protect the cells from apoptosis [17]. In yeast there is also growing evidence that Mmi1 could have anti-apoptotic features. In this respect, overexpression of Mmi1 was shown to modulate resistance to arsenite [18], which has been shown to induce apoptosis [19].

We have previously published [6] that the *S. cerevisiae* TCTP, named by us Mmi1 (for "microtubule and mitochondria interacting"), plays a role in the stress response of the yeast cell. We showed that on oxidative stress, Mmi1 rapidly changes localization from the cytoplasm to the outer surface of the mitochondria. In addition, the *MMI1* deletion mutant is viable and sensitive to microtubule-destabilizing drugs like are benomyl and nocodazole. In the present communication we are showing that this mutant also exhibits a strong resistance to an otherwise lethal heat shock. To elucidate this phenotype, we performed functional analyses of Mmi1 domains fused with GFP. Here we show that the alpha-helical central domain (V-domain) of Mmi1associates with mitochondria under all conditions, even in non-stressed cells. Similarly, the N-terminal flexible loop domain of the protein localizes to the nucleus. We conclude that these domains could contain the appropriate signals for recognizing the mitochondrial surface, and the nuclear envelope, respectively. We also found that after an intermediate heat-shock treatment (40°C) a significant part of Mmi1 is re-localized to the nuclear region. Upon robust heat stress at 46°C, Mmi1 partially overlaps with the proteasome (Rpn1) in the nucleus and also co-localizes in cytoplasm with Rpg1 (eIF3a), which is a known component of yeast stress granules (SGs) [20]. After the end of a non-lethal heat stress, stress granules disappear, and the stored translational pre-initiation complexes probably serve to restart protein synthesis [21]. In this respect, TCTP has been also identified as a regulator of the translation factor eEF1A when protein synthesis is restarted in stressed human cells [22]. Additionally, we show that Mmi1 interacts with the de-ubiquitination machinery of the cell and modulates the activity of proteasome. Therefore, we suggest that the protein might be one of key players in the stress response of yeast.

Materials and Methods

Yeast strains, media and culture conditions

All strains used in this study are based on the *S. cerevisiae* strains BY4741 (*MATa his3Δ1 leu2Δ0 met15Δ0 ura3Δ0*), BY4742 (*MATα his3Δ1 leu2Δ0 lys2Δ0 ura3Δ0*) [23] and SEY6210 (*MATα leu2-3, 112 ura3-52 his3-Δ200 trp1-Δ901 lys2-801 suc2-Δ9*) [24]. The strains used and created in this study are summarized in Table 1. Yeast cells were either grown in complex medium (YPD) (1% (w/v) yeast extract, 2% (w/v) peptone and 2% (w/v) D-glucose) or synthetic complete glucose medium (SC-glucose) (2% (w/v) D-glucose, 0.17% (w/v) yeast nitrogen base without amino acids, 0.5% ammonium sulphate and 10 ml of complete dropout mixture (0.2% Arg, 0.1% His, 0.6% Ile, 0.6% Leu, 0.4% Lys, 0.1% Met, 0.6% Phe, 0.5% Thr, 0.4% Trp, 0.1% Ade, 0.4% Ura, 0.5% Tyr) per liter). Solid media were made by adding 2% (w/v) agar. Selection for plasmids was achieved by leaving out the appropriate amino acid from the dropout media. Strains with the desired marker combinations were created by mating of the appropriate parent strains, diploid selection, sporulation in liquid or solid Fowell medium and spore dissection using a Singer MSM micromanipulator. Survival of heat shock conditions was measured by pre-growing cultures at 30°C to mid-exponential phase, transferring the cultures to 46°C for 10, 40, 70 and 100 min, plating appropriate dilutions of the cells on YPD plates and counting the colonies (clonogenicity) after an additional incubation at 30°C for two to three days. The cell survival rate [in %] was normalized to the survival value at time zero.

Before inducing a robust heat shock, overnight cultures were diluted in YPD or SC medium to an $OD_{600} = 0.1$ and were grown to mid-exponential phase ($\sim OD_{600} = 0.8$) in flasks with constant agitation at 30°C. To perform the heat shock, cells were re-suspended either in YPD or SC medium preheated to 37°C, 40°C, 41°C, 42°C or 46°C and incubated under shaking at the given temperature for an additional 10 min. Cycloheximide (Sigma-Aldrich, USA) was added to the final concentration of 50 μg/ml when appropriate.

For growth curves an overnight culture was diluted to an $OD_{600} = 0.1$ in SC medium. Each 90 min a sample was taken and the OD_{600} was measured using the Hitachi U-3000 spectrophotometer. The doubling time was calculated with the online available "Doubling Time" tool [25] (www.doubling-time.com/compute.php).

Cloning experiments

The centromeric vector pUG35 (Hegemann J.H., unpublished) was used for this study. For PCR amplifications the Phusion® High-Fidelity DNA Polymerase (NEB, Ipswich, MA) was used. All restriction enzymes were provided by either Promega (Mannheim, Germany), NEB (Ipswich, MA) or Thermo Scientific (Waltham, MA). The cloning strategies, sequence of primers (obtained from Eurofins-MWG-OPERON (Ebersberg, Germany)), enzymes used for cloning and the target vectors are summarized in Table 2. All constructs were sequenced by Eurofins-MWG-OPERON.

Construction of expression strains with chromosomally integrated RFP gene fusions

In this study chromosomally integrated C-terminal RFP fusion-proteins were created. Integration cassettes containing RFP as well as kanMX4 were amplified via PCR from the template plasmid pRFPKanMX [26] using the primers summarized in Table 3. An aliquot of 1 μg of the PCR product was transformed into BY4741 or BY4742 wild type cells, chromosomal integration was selected by plating the cells on YPD plates containing 200 μg/ml G418 (Geneticin, Sigma Aldrich, USA). Integration of the cassette in the correct chromosomal region, creating an RFP fusion, was controlled by PCR using the antisense-primer RFP200N (CTTGGAGCCGTACTGGAA) and a gene specific primer as summarized in Table 3.

Deletion of *MMI1*

A *MMI1* deletion cassette harboring the *SAT1* gene (conferring nourseothricin resistance) was PCR amplified from the template plasmid pSDS4 [27] using the primers MMI1 SAT1 sense (GGGTCTCAGTTGCGGTTAGCAGATTAACACAGAACA-TACTATAGACAAATGATCCAGCGTCAAAACT) and MMI1 SAT1 antisense (TACTCTCAAATTCAAATACAAAA-TACGAAAATTTTTCTAATTTCGCTAGACTGCAGAGG-TAAACCC). The PCR product was transformed into the yeast cells and chromosomal integrations replacing the native *MMI1* gene with the *SAT1* gene were selected by plating the cells on YPD plates containing 100 μg/ml nourseothricin (NTC, Werner BioAgents, Germany). Integration at the correct chromosomal sites was controlled by PCR using the primers Sat1 control

Table 1. Yeast strains used in this study.

Strain	Genotype	Source
BY4741	*MAT*a *his3Δ1 leu2Δ0 met15Δ0 ura3Δ0*	[23]
BY4742	*MAT*α *his3Δ1 leu2Δ0 lys2Δ0 ura3Δ0*	[23]
BY4743	*MAT* a/α *his3Δ1/his3Δ1 leu2Δ0/ leu2Δ0 lys2Δ0/LYS2 MET15/met15Δ0 ura3Δ0/ura3Δ0*	[23]
Sey6210	*MAT*α *leu2-3, 112 ura3-52 his3-Δ200 trp1-Δ901 lys2-801 suc2-Δ9*	[24]
Sey6210.1	*MAT*a *leu2-3,112 ura3-52 his3-Δ200 trp1-Δ901 lys2-801 suc2-Δ9*	[24]
CRY255	Sey6210; *MAT*α *RPG1::RFP::KanMX4*	[20]
CRY410	BY4741; *MATa RPG1::GFP::HIS3MX6*	[54]
CRY411	BY4741; *MATa DCP2::GFP::HIS3MX6*	[54]
CRY423	BY4741; *MATa PAB1::GFP::HIS3MX6*	[54]
CRY430	BY4741; *MAT*a *PUB1::GFP::HIS3MX6*	[54]
CRY527	*MAT*α *RPG1::RFP::KanMX4 PAB1::GFP::HIS3MX6* (segregant from the crossing CRY255 X CRY423)	[21]
CRY564	*MAT*a *RPG1::RFP::KanMX4 DCP2::GFP::HIS3MX6* (segregant from the crossing CRY255 X CRY411)	[21]
CRY1060	CRY527; *MAT*α *RPG1::RFP::KanMX4 PAB1::GFP::HIS3MX6 mmi1::nat*NT2	This study
CRY1062	CRY564; *MAT*a *RPG1::RFP::KanMX4 DCP2::GFP::HIS3MX6 mmi1::nat*NT2	This study
CRY1081	BY4741; *MAT*a *CDC48::GFP::HIS3MX6*	[54]
CRY1103	BY4741; *MAT*a *MMI1::GFP::HIS3MX6*	[54]
CRY1107	BY4741; *MAT*a *mmi1::KanMX4*	Euroscarf
CRY1161	BY4741; *MAT*a *RPN1::RFP::KanMX4*	This study
CRY1226	BY4742; *MATa MMI1::GFP::HIS3MX6*	This study
CRY1231	*MAT*a *RPN1::RFP::KanMX4 MMI1::GFP::HIS3MX6* (segregant from the crossing CRY1161x CRY1226)	This study
CRY1307	BY4742; *MAT*α *MMI1::RFP::KanMX4*	This study
CRY1308	*MAT*a *MMI1::RFP::KanMX4 CDC48::GFP::HIS3MX6* (segregant from the crossing CRY1307x CRY1081)	This study
CRY1309	*MAT*α *MMI1::RFP::KanMX4 RPG1::GFP::HIS3MX6* (segregant from the crossing CRY1307x CRY410)	This study
CRY1399	BY4741; *MAT*a *UBP3::GFP::HIS3MX6*	[54]
CRY1400	BY4741; *MATa BRE5::GFP::HIS3MX6*	[54]
CRY1696	*MAT*a *MMI1::RFP::KanMX4 UBP3::GFP::HIS3MX6* (segregant from the crossing CRY1307 x CRY1399)	This study
CRY1698	*MAT*a *MMI1::RFP::KanMX4 BRE5::GFP::HIS3MX6* (segregant from the crossing CRY1307x CRY1400)	This study
CRY1837	BY4742; *MAT*α [pUG35]	This study
CRY1838	BY4742; *MAT*α [pUG35-*MMI1-GFP*]	This study
CRY1839	BY4742; *MAT*α [pUG35-*(V)MMI1-GFP*] [pYX142-mtRFPm]	This study
CRY1842	BY4742; *MAT*α [pUG35-*(N+V)MMI1-GFP*]	This study
CRY1844	CRY1307; *MAT*α *MMI1::RFP::KanMX4* [pUG35-*ACO1-GFP*]	This study
CRY1924	BY4742; *MAT*α [pUG35-*(N)MMI1-GFP*] [pYX142-mtRFPm]	This study
CRY1967	*MAT*a *MMI1::RFP::KanMX4 PUB1::GFP::HIS3MX6* (segregant from the crossing CRY1307x CRY430)	This study
CRY1981	BY4742; *MAT*α *mmi1::KanMX4*	Euroscarf

doi:10.1371/journal.pone.0077791.t001

Table 2. Primers used for cloning.

Primer	Sequence	Cloning site	Source	Target	Resulting Vector
SP/MMI1 P1	CGGGATCCATGATTATTTACAAGGATATC	BamHI	pUG35-*MMI1*	pUG35	pUG35- (N)*MMI1*
ASP/MMI1 P1	CGGAATTCAGCGGTTTGTTGTAGACG	EcoRI	pUG35-*MMI1*	pUG35	pUG35- (N)*MMI1*
SP/MMI1 P2	CGGGATCCATGTTCCGTCTACAACAAACCGCTTTTG	BamHI	pUG35-*MMI1*	pUG35	pUG35- (V)*MMI1*
ASP/MMI1 P2	CGGAATTCTGGGTCCATGGATTCACC	EcoRI	pUG35-*MMI1*	pUG35	pUG35- (V)*MMI1*
SP/MMI1 P3	CGGGATCCATGGAGTTCTTCACTGGTGAA	BamHI	pUG35-*MMI1*	pUG35	pUG35-(C)*MMI1*
ASP/MMI1 P3	GGAATTCGATCTTTTCTTCCACA	EcoRI	pUG35-*MMI1*	pUG35	pUG35-(C)*MMI1*
SP/MMI1 P1	CGGGATCCATGATTATTTACAAGGATATC	BamHI	pUG35-*MMI1*	pUG35	pUG35- (N+V)*MMI1*
ASP/MMI1 P2	CGGAATTCTGGGTCCATGGATTCACC	EcoRI	pUG35-*MMI1*	pUG35	pUG35- (N+V)*MMI1*

doi:10.1371/journal.pone.0077791.t002

Table 3. Primers used for chromosomal integration of RFP-tags.

Primer	Sequence	Source	Resulting Strain
SP/RPN1	TTGAGGGCGTAGTAATTTTAAAGAAGAACCCTGACTATCGTGAAGAGGAGGGAG-CAGGGGCGGGTGC	pRFPKanMX	CRY1161
ASP/RPN1	AAATGGTTTTGAATTTTTCCTATTCTGGTTGATATTGCCCAAAAGCTATTCCCCCTCGA-GGTCGACGGTATCG	pRFPKanMX	CRY1161
RPN1 control	CTGGATTACGCAATCCACTC	pRFPKanMX	CRY1161
SP/MMI1	CCATTTGTTGCCATCTGGAAGCACGGTATTGTGGAAGAAAAGATCGGAGCAG-GGGCGGGTGC	pRFPKanMX	CRY1307
ASP/MMI1	CAAATTCAAATACAAAATACGAAAATTTTTCTAATTTCGCTAGACCCCCTCGAG-GTCGACGGTATCG	pRFPKanMX	CRY1307
MMI1 control	CCGCTTTTGACAAGAAGTCC	pRFPKanMX	CRY1307

doi:10.1371/journal.pone.0077791.t003

(CGACCGAAAGCAAATAAGAACAAAA) and YKL056cA (CGCATTTCTCGTAGAATTGATATTT).

Structure prediction

The structure of Mmi1 protein was predicted using the fully automated protein structure homology-modeling SWISS-Model server (http://swissmodel.expasy.org/) [28,29].

Fluorescence microscopy

The cells were inspected after washing with SC medium, mounting on coverslips and coating with a slice of 1.5% agarose in an appropriate medium. The distribution of various fusion proteins (fused to GFP or RFP) was analyzed with a 100× PlanApochromat objective (NA = 1.4) using an Olympus IX-81 inverted microscope equipped with a Hammamatsu Orca/ER digital camera and an Olympus CellR^{TM} detection and analyzing system (GFP filter block U-MGFPHQ, exc. max. 488, em. max. 507; RFP filter block U-MWIY2, exc. max. 545-580, em. max. 610; DAPI filter block U-MNUA2, exc. max. 360–370, em. max. 420–460). Images were processed and merged using Olympus Xcellence RT^{TM} and Adobe CS5 software. They represent individual optical slices obtained by Z-axis optical sectioning using the Olympus CellR^{TM} system. The quantitative co-localization analyses were performed using NIH ImageJ software with the Co-localization Finder plugin, available at http://rsb.info.nih.gov/ij/plugins/. This software was used to determine the Pearson's correlation coefficient (R_r), which describes the extent of co-localization between image pairs. It is a value between -1 and +1, with negative values indicating the exclusion and positive values indicating co-localization (positive correlation) of the two images. The average values of R_r were obtained by the analysis of six images containing altogether approximately 400 cells from three independent experiments. To analyze the effect of various temperatures on distribution of Mmi1-GFP we also used an Olympus BX60 microscope equipped with a 100× PlanApochromat objective (NA = 1.4), Fluoview cooled CCD camera and an Olympus detection system (HQ-set GFP/EGFP filter block, exc. max. 470, em. max. 525; DAPI filter block U-MNUA, exc. max. 360-370, em. max. 420). Images were processed and merged using Olympus analySIS and Adobe CS5 software. For staining DNA the living cells were incubated with Hoechst 33342 (Life Technologies, USA) at a final concentration of 10 μg/ml either for 20 min at 30°C, 37°C and 40°C or during the last minute of heat shock at 42°C or 46°C.

Electron microscopy

Living yeast cells (overnight culture) were diluted 1:30 in YPD medium, let grow at 30°C for 4 hours and then heat-shocked at 46°C for 10 min. Afterwards, the cells were processed as described previously [11]. In brief: cells were filtered, loaded in a flat specimen carrier (Leica, 1.2 mm cavity diameter) and frozen in the Leica EM PACT high-pressure freezer. Frozen samples were freeze-substituted in acetone supplemented with 0.1% uranyl acetate and 1% water in a Leica AFS machine and then embedded in HM20 resin. Ultrathin sections (60 nm) were cut with Ultracut S ultramicrotome equipped with a diamond knife (35°; Diatome, Biel, Switzerland) and placed on formvar-coated gilded nickel (or copper) grids. After on-section immunogold labeling, the sections were contrasted with a saturated aqueous solution of uranyl acetate for 1 hour, washed, air-dried and examined in a FEI Morgagni 268(D) transmission electron microscope at 80 kV. Images were captured with Megaview II CCD camera.

On-section immunogold labeling

Sections on formvar-coated grids were blocked in 5% BSA in PBS for 30 minutes, and then incubated for 1 hour on droplets of primary antibody diluted 1:20 in 1% BSA/PBS. The primary antibody used was rabbit anti-GFP (Fitzgerald Industries International, USA), pre-adsorbed over night at 4°C against an acetone powder made from a non-GFP expressing yeast strain at concentration of 10 mg/ml. In addition, the diluted antibody was also pretreated with 0.5 mg/ml purified yeast mannan for 30 minutes just before the labeling procedure to suppress the non-specific cell wall binding [30]. Afterwards, the grids were washed on droplets of PBS for 10 minutes, and incubated with secondary antibody for 2 hours (ultra small goat anti-rabbit IgG-gold; Aurion; diluted 1:100). In controls, the primary antibody was omitted. After three washes in PBS, the grids were post-fixed in 8% glutaraldehyde for 15 minutes, washed on droplets of distilled water, silver-enhanced (Aurion, Hatfield, USA), air-dried and contrasted.

Proteasome activity measurements

To measure proteasome activity, we used the 20S Proteasome Activity Assay Kit (Millipore, Billerica, USA). Yeast cell lysates were prepared from 40 ml cultures grown in YPD medium at 30°C to mid-exponential phase (OD600 = 0.8). Cultures were divided into two parts. One part of the cell culture (control) was cultivated at 30°C for 10 min. The second part (HS) was cultivated at 46°C for 10 min. The following steps were performed

at 4°C. Cells were harvested by centrifugation (1650× g for 5 min) and resuspended in the lysis buffer (50 mM Tris, pH 7.5, 0.5 mM EDTA, 5 mM $MgCl_2$, 50 mM NaCl, 1 mM DTT, 0.1% NP-40, 2% glycerol). Cells were broken by vortexing with sterile glass beads. The cell extract was centrifuged (50× g for 10 min) to remove unbroken cells. The supernatants were adjusted to the same level of protein concentration. For the measurement, an aliquot of 50 µg of the total protein was used. The measurement was performed according to the manufacturer's protocol using Tecan Infinite R 200 PRO multimode plate reader in the fluorescence mode.

Results and Discussion

Identification of functional domains in the Mmi1 protein structure

The yeast protein Mmi1 as well as its mammalian homologue TCTP (translationally-controlled tumor protein) has been found to be primarily localized to the cytoplasm [6] [31]. In a previous study we demonstrated that under oxidative stress Mmi1 changes distribution and localizes to the surface of mitochondria [6]. This finding has been confirmed in many follow-up studies including yeast and higher eukaryotes [15]. Surprisingly, it has been also shown that mammalian TCTP re-localizes to the nucleus in hydrogen peroxide-stressed cells [32], in cancer cells [33] and upon de-phosphorylation [34]. However, a nuclear localization of this protein has not been reported in yeast yet.

This small highly conserved protein has a very distinct three-dimensional structure. A structure prediction derived by homology modeling, based on published X-ray and NMR data of Mmi1 homologs is shown in Figure 1A. This structure is similar to all published and experimentally determined TCTP structures. According to this data Mmi1 harbors three clearly distinguishable domains defined as follows: I) an N-terminal flexible loop domain (here named N-domain, blue); II) a central two-helical domain (here named V-domain; green); III) and a C-terminal β-stranded core domain (here named C-domain, red) [1]. These three domains are highlighted in the amino acid sequence shown in Figure 1B. Overlaps between the partial clones (see below) of the first and the second, and the second and the third part of the protein, respectively, are highlighted in yellow.

Because Mmi1/TCTP fulfills a multitude of functions and can be found in various organelles depending on growth or stress conditions, we wanted to learn if possible localization signals are located in any of the three domains. The parts of the *MMI1* ORF corresponding to the three domains were PCR cloned and expressed as C-terminal GFP fusion proteins in the yeast vector pUG35 (for details see Materials and Methods). In parallel experiment and similarly to data published previously [6], unstressed exponentially growing yeast cells displayed a uniformly cytosolic distribution of the full length Mmi1-RFP (chromosomal) (Figure 1C upper). Its co-localization with Aco1-GFP (marker of mitochondria; [35]) and fluorescent dye Hoechst 33342 (labeling of DNA) did not show any significant overlaps under these conditions. In cells heat-shocked at 46°C for 10 min, a partial co-localization of Mmi1 with the nuclear DNA and partial overlaps with altered mitochondria were observed (Figure 1C, lower).

Concerning the Mmi1 domain analyses, the N-terminal part of the protein, expressed as a 70 amino acid partial clone C-terminally fused to GFP, displayed nuclear localization under control and heat shock conditions (Figure 1D, the experiment at 30°C is shown). It is documented by complete co-localization with Hoechst 33342-stained DNA, with only a minor fraction of the N-terminal Mmi1 part located in the cytoplasm. This predominant nuclear localization became more obvious when cells from the same culture reached early stationary phase (data not shown). No mitochondrial location of this Mmi1 mutant variant could be seen either at 30°C or at 46°C as evidenced by co-expressing a mitochondrial marker MITO-RFP (pXY142 mtRFPm) [36] in the cells and fluorescence microscopic examination. The middle domain (V-domain) of the protein was expressed as a C-terminal GFP fusion protein (amino acids 71–138, with added N-terminal methionine) and is shown in Figure 1E. This domain was found to be localized to mitochondria independently of temperature as evidenced by comparison with distribution of MITO-RFP. We conclude from these results that the V-domain possibly can direct the Mmi1 holoprotein to the mitochondrial surface.

Interestingly fusion of the N-terminal domain and the V-domain (consisting of the first 138 amino acids of the protein and only lacking the C-terminal domain) was uniformly cytosolic in unstressed cells (Figure 1F, 30°C), but apparently in cytoplasmic accumulations and in nuclei in cells heat-shocked at 46°C for 10 minutes (Figure 1F, 46°C). Our interpretation is that (a) structural detail(s) which are not contained in the smaller partial clones, but are displayed by the N+V fusion protein, perhaps near the boundary of the two domains, are responsible for the regulation of the protein's transfer to the different compartments of the cell upon heat shock.

Immunogold electron microscopy confirmed a partial re-localization of Mmi1 to the nucleus in heat-shocked cells

To extend the results obtained with fluorescence microscopy we applied the immunoelectron microscopy technique on wild-type (WT) cells expressing the Mmi1-GFP fusion from the chromosomal site. We used high pressure freezing fixation followed by freeze substitution, low temperature resin embedding and incubation of ultrathin resin sections with the specific anti-GFP-antibody. The Mmi1-GFP fusion protein was then visualized with the secondary antibody conjugated with ultra small gold particles enhanced with silver intensification method. As expected, Mmi1-GFP was predominantly detected in the cytoplasm in unstressed cells. An association of Mmi1 with the mitochondria was also detected under these conditions (Figure 2A, B). After robust heat shock (46°C for 10 min) the protein accumulated in the nucleus (Figure 2C, D). In addition, the cytoplasmic pool of the protein was often detected in clusters, possibly corresponding to stress granules. The numbers shown in Figure 2E were obtained by counting immunogold signals in over two hundred cells at 30°C as well as after heat shock at 46°C. Compared to the fluorescence microscopy results shown in Figure 1C and in the fluorescence micrographs to follow, we note that the nuclear localization is not confined only to the nuclear periphery, but the prominent signals are found throughout the nucleus. This is not in contradiction to the important results showing localization at the proteasome and the de-ubiquitination complex (see below). In only partial consistence with fluorescence microscopy, our quantitative electron microscopy results confirmed that a portion of Mmi1 possibly associates with mitochondria under all conditions tested. However, our data did not confirm an accumulation of Mmi1 at the outer surface of mitochondria in stressed cells, which was found after oxidative stress at 3 mM H_2O_2 previously [6].

Mmi1 affects growth and heat shock resistance of yeast

One of the "day jobs" of Mmi1 has been clearly attributed to the ribosome. It has been shown that Mmi1 is associated with ribosomal subunits and *MMI1* deletion has to cope with a decreased protein synthesis rate associated with an altered polysome profile [37]. As can be seen in Figure 3A, this decrease

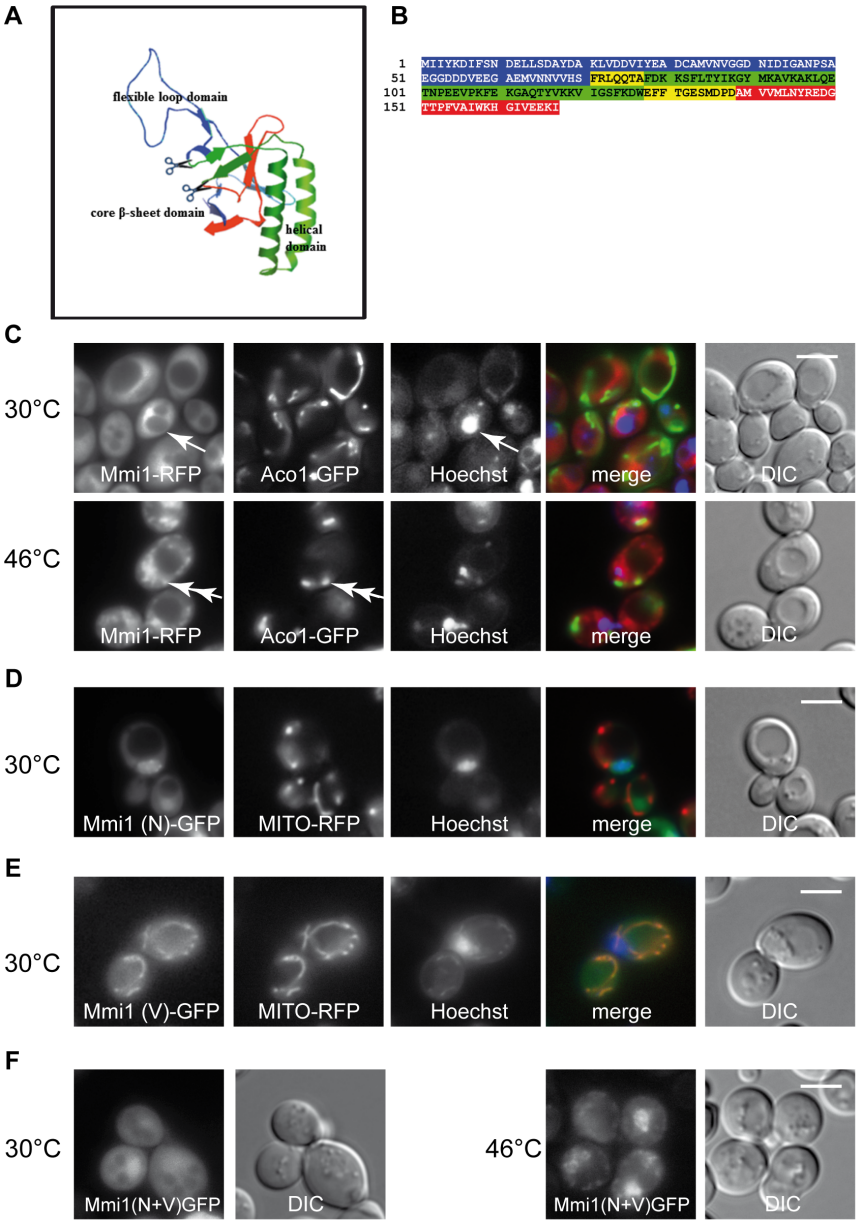

Figure 1. Mmi1 localization studies. (A) Structure prediction of Mmi1 with Swissmodel (http://swissmodel.expasy.org/). (B) Amino acid sequence of the open reading frame of MMI1. Three domains which are obvious in structure (A) are color-marked here. Blue is the N-terminal domain, (Mmi1(N)); green is the middle V-domain (Mmi1(V)) which is characterized by two large alpha helices; red is the C-terminal domain, which contains two short beta sheets and which is not shown in the fluorescence pictures. The three domains were cloned separately including the respective overlapping sequences (yellow) adding a start methionine where necessary and fused C-terminally with GFP as described in Materials and Methods. (C) Mmi1-RFP expressed from its chromosomal locus compared with the mitochondrial marker Aco1-GFP expressed from plasmid pUG35 in strain CRY1844 and the nuclear stain Hoechst 33342. In control cells, Mmi1-RFP was excluded from the nucleus (arrow points to nucleus). After heat shock, Mmi1 accumulates in the nucleus and partially overlaps with mitochondria (double arrow). (D) Mmi1(N)-GFP compared with MITO-RFP and Hoechst 33342 in strain CRY1924. The N-terminal domain is nuclear at all temperatures. It is shown here at 30°C. (E) Mmi1(V)-GFP co-expressed with MITO-RFP and Hoechst 33342 staining in strain CRY1839. The V-domain is mitochondrial at all temperatures. It is shown here at 30°C. (F) Mmi1(N+V) is cytoplasmic at 30°C, and nuclear after heat shock with a part of the proteins forming cytoplasmic granules (strain CRY1842). It appears that the combination of the two domains has re-gained heat shock-dependent regulation of Mmi1 subcellular localization. Scale bar 4 μm.
doi:10.1371/journal.pone.0077791.g001

in protein synthesis in the *mmi1*Δ strain is likely connected with a decrease in growth rate. The wild type (WT) control strain has a doubling time of 135 min ($R^2 = 0.9925$), whereas the *mmi1*Δ strain shows a doubling time of 145 min ($R^2 = 0.9994$). The decrease in growth rate is reversed if oxidative stress is applied. Already a concentration of 1 mM H_2O_2 leads to an increase of the doubling time to 272 min in the WT strain ($R^2 = 0.9303$), whereas the *mmi1*Δ strain shows a nearly unaltered growth rate with a doubling time of 145 min ($R^2 = 0.9946$). A concentration of 3 mM H_2O_2 completely abolishes the growth in the WT cells, whereas the *mmi1*Δ strain shows at least marginal growth. In general it can be stated that in times of oxidative stress a loss of Mmi1 seems to be beneficial. Previously, we showed [6] that the *mmi1*Δ strain has a prolonged replicative lifespan. Later on, it was confirmed by the

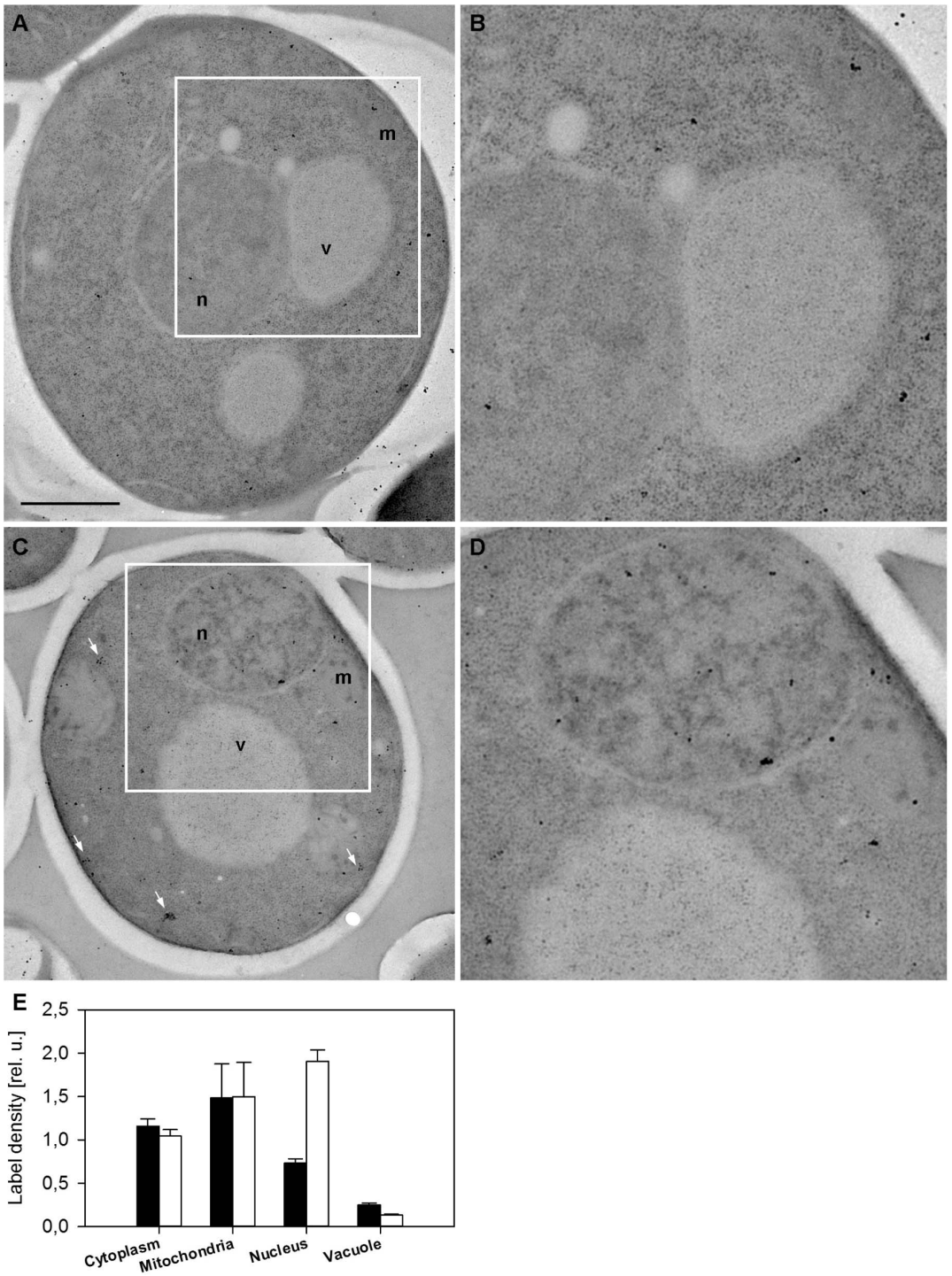

Figure 2. Electron microscopy of Mmi1-GFP. Exponentially growing cells expressing Mmi1-GFP from the chromosomal locus (strain CRY1103) were processed for immunogold labeling (see Materials and Methods for details) either prior to (A, B, full bars in E) or immediately following the 10 min long heat shock at 46°C (C, D, empty bars in E). Representative examples of whole cell sections (A, C) and detailed views in negative contrast allowing for identification of individual gold particles (B, D) are presented. Mitochondria (m), the cytosol (c), the nucleus (n) and vacuoles (v) are marked. Cytoplasmic clusters of gold particles frequently observed in heat-shocked cells are highlighted (arrows). Scale bar 1 μm. Density of the immunogold labeling (number of the gold particles per the area of the corresponding cellular compartment) was counted by analyzing 237 cells. Relative errors of both the measured quantities were determined as SDs from random repetitions of measurements on identical images. Relative error of the ratio was calculated as a sum of these relative errors. Gold particle densities are plotted relative to the average density (gold particles per cell), equal to 1. In total, 105 untreated and 132 heat-shocked cells (4868 and 7565 gold particles, respectively) were analyzed. A significant enrichment of Mmi1 in the nucleus after heat shock was found.
doi:10.1371/journal.pone.0077791.g002

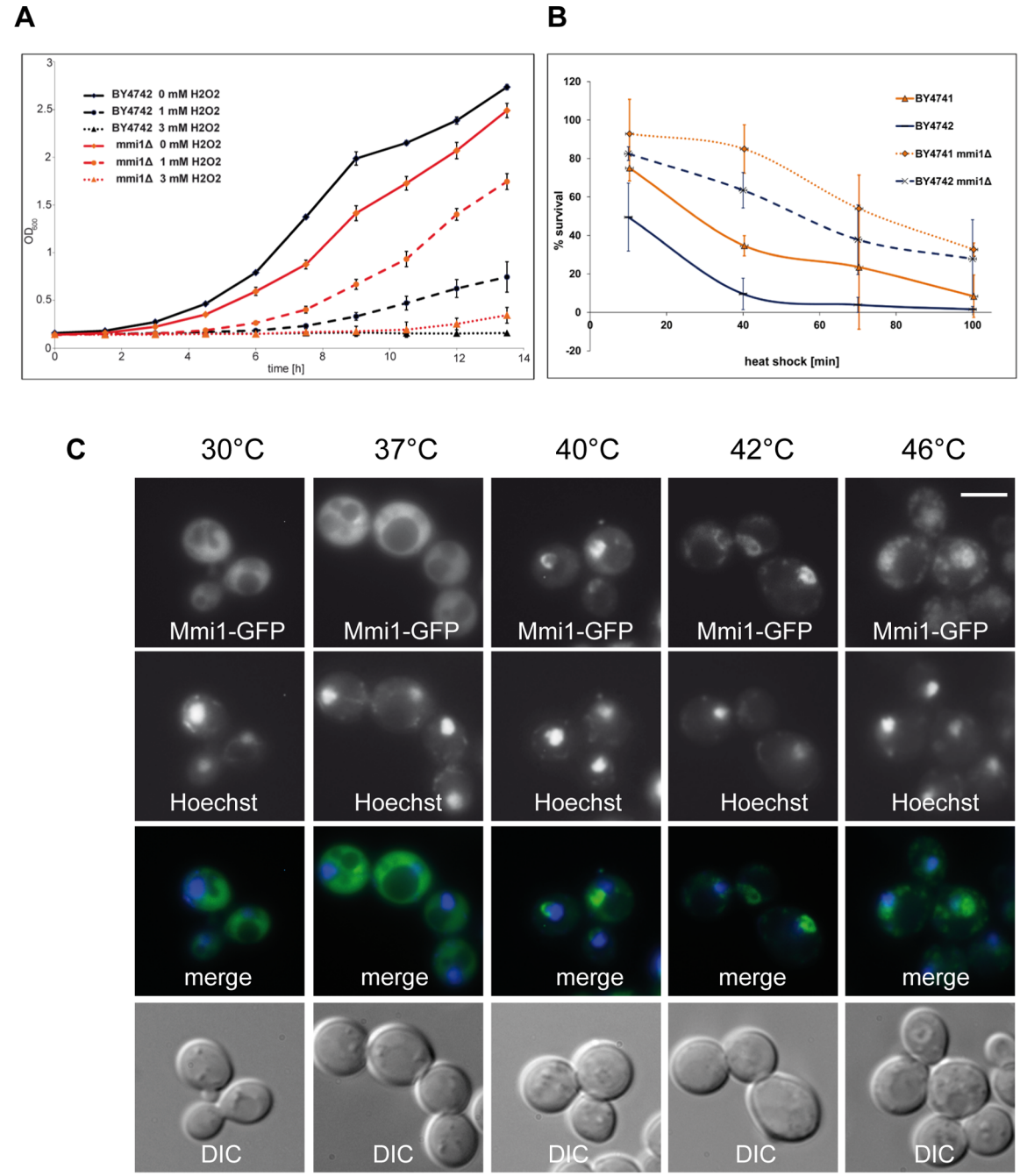

Figure 3. Mmi1 in times of stress. (A) Growth curves of BY4742 wild type (WT) cells as well as *mmi1*Δ cells in the BY4742 strain (strain CRY1981) with and without the addition of 1 mM and 3 mM hydrogen peroxide. (B) Survival of WT and *mmi1*Δ cells of both mating types (strains BY4741, BY4742, CRY1107, CRY1981) after a temperature shift from 30°C to 46°C for time periods of up to 100 min. Note the very marked increase of heat shock resistance of the deletion mutants. Error bars denote standard deviations of the mean obtained form 3 independent repeats of the experiment. (C) Changes of Mmi1-GFP distribution after a temperature shift from 30°C to 37°C, 40°C, 42°C and 46°C for 10 min each (strain CRY1838). Scale bar 4 μm. The figures show transfer of Mmi1 to part of the nuclear compartment at intermediate temperatures and transfer to both the nucleus and cytoplasmic granules upon 10 min heat shock at 46°C.
doi:10.1371/journal.pone.0077791.g003

Kaeberlein laboratory [38]. Because yeast old mother cells develop oxidative stress and contain a high level of ROS [39], the reason for the longevity phenotype of the *mmi1*Δ strain is very probably its oxidative stress resistance.

As we have shown above (see Figure 2), the heat shock at 46°C induced the most prominent shift from the cytoplasm to the nucleus. Therefore we analyzed the survival of WT and *mmi1*Δ strains after incubation at 46°C for various times as described in Materials and Methods. This analysis has been repeated three times and the result is shown in Figure 3B. The two haploid WT strains from the EUROSCARF collection [23] showed essentially complete killing after 80–120 min exposure to the stress conditions. However, the two haploid *mmi1*Δ strains survived to about 50% under conditions where nearly 100% of the WT cells were

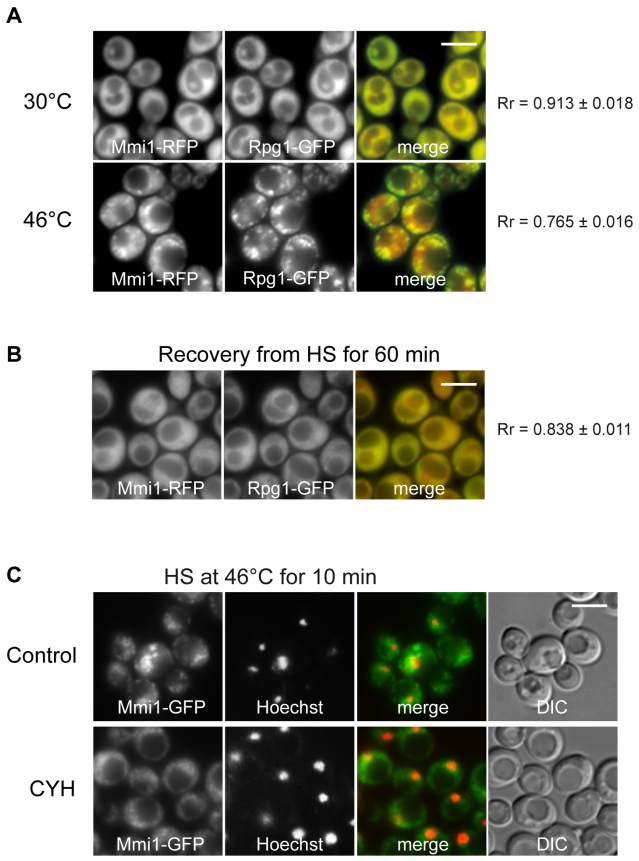

Figure 4. Mmi1 co-localizes with stress granules. (A) Distribution of Mmi1-RFP and the stress granule marker Rpg1-GFP co-expressed from the chromosome sites (strain CRY1309) was analyzed in cells before and after heat shock at 46°C for 10 min where the two proteins were co-localized to a high degree in cytoplasmic granules (B) During recovery from heat shock both proteins returned to their uniform "unstressed" cytoplasmic location. (C) Cells expressing Mmi1-GFP from the chromosomal locus (strain CRY1226) were heat-shocked at 46°C for 10 min in the absence (Control) or in the presence of cycloheximide (CYH; 50 μg/ml). The nuclear DNA was stained with Hoechst 33342. Cycloheximide affected formation of large Mmi1 cytoplasmic accumulations but did not prevent the translocation of Mmi1 to the nucleus. Scale bar 4 μm.
doi:10.1371/journal.pone.0077791.g004

dead. This indicates that the presence of Mmi1 strongly affects the survival rate at 46°C.

Figure 3C shows the WT cells with the plasmid-derived Mmi1-GFP at four different temperatures for 10 min each. Co-staining with Hoechst 33342 indicates the cells' nuclei. These pictures clearly show that after a mild heat shock (40°C and 42°C) the protein is predominantly nuclear. Although the localization at the nuclear region is obvious, the match is not 100%. It appears that the nuclear location of Mmi1 is not completely coincident with the nuclear DNA shown by Hoechst 33342 staining but rather concerns part of the nucleus and/or the nuclear periphery. After a heat shock at 42°C or 46°C the protein was accumulated also in cytoplasmic granules.

Mmi1 associates with the stress granules in heat-stressed cells

To analyze cytoplasmic accumulations of Mmi1 in heat shocked cells and to test their possible association with heat-induced stress granules, we constructed a new strain co-expressing Mmi1-RFP

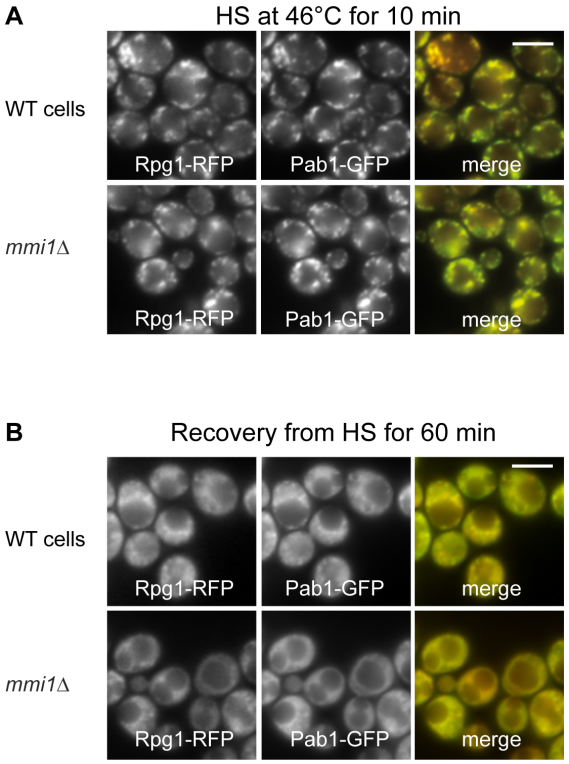

Figure 5. Deletion of *MMI1* gene does not affect SGs assembly and dissolution. We compared the distribution of stress granules markers Pab1-GFP and Rpg1-RFP fusion proteins produced from sites on chromosomes in wild type (strain CRY527) and *mmi1*Δ (strain CRY1060) cells. (A) Stress granule formation after robust heat shock was not influenced at all by the absence of Mmi1 in the *mmi1*Δ deletion strain. (B) In the same strains that were used in (A) recovery from heat shock was observed for 60 min (shown) and 120 min. As shown, absence of Mmi1 had no influence on the dissolution of stress granules during recovery from the heat shock. Scale bar 4 μm.
doi:10.1371/journal.pone.0077791.g005

and the stress granule marker Rpg1-GFP (eIF3a) from chromosomal sites. Figure 4A shows that Mmi1 granules described above coincide with the stress granule marker Rpg1 (eIF3a). We conclude that, besides Mmi1 translocation to the nucleus, the protein also associates with stress granules (SGs) after robust heat shock. Figure 4B shows that after 60 min recovery from the heat shock both, Mmi1-RFP and Rpg1-GFP, proteins have returned to their original uniformly cytosolic distribution. The formation of SGs is affected by cycloheximide which apparently prevents the dissolution of polysomes and the liberation of mRNA required for the formation of the SGs [20]. To show dependency of Mmi1 accumulation on ribosome-free mRNA availability, we added cycloheximide for 10 min before performing robust heat shock in medium containing cycloheximide (Figure 4C). We found that cycloheximide affected formation of large Mmi1 accumulations but did not prevent the translocation of Mmi1 to the nucleus (determined by staining of DNA with Hoechst 33342). However, a fraction of Mmi1 still visibly accumulates in the cytoplasm even under cycloheximide treatment. It may suggest that Mmi1, besides its association with SGs, fulfills additional role in the cytoplasm of heat-shocked cells. Nevertheless, the partial dependency on mRNA further supports our findings that Mmi1 associates with SGs under stress conditions.

Next, we wanted to test whether Mmi1 was necessary for proper SGs dynamics. We constructed a new strain with deletion of the

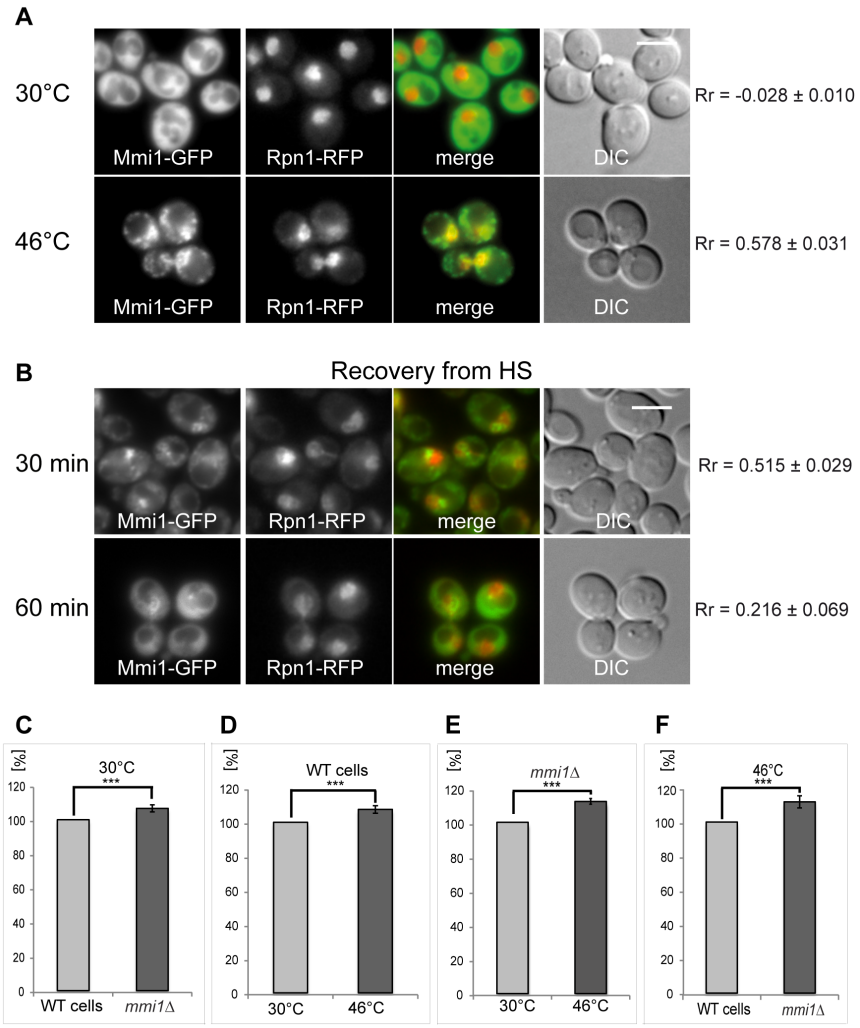

Figure 6. Co-localization of Mmi1 with proteasomes. (A) Both fusion proteins Mmi1-GFP and Rpn1-RFP were expressed from the chromosomal sites (strain CRY1231) and co-localized in control (30°C) and 10 min heat-shocked cells (46°C). Control cells at 30°C displayed almost no overlaps of the two fusion proteins. This was confirmed by a negative value of the Pearsons correlation coefficient (R_r). However, the cells heat-shocked at 46°C for 10 min displayed co-localization of both fusion proteins at the nuclear region. (B) In cells recovering from the heat stress, Mmi1 granules were dissolving during the time indicated whereas partial Mmi1-GFP location in the nuclear region remained detectable. However, decreased values of Rr in cells recovering from the heat shock for 60 min indicate continuous separation of the Mmi1-GFP and the Rpn1-RFP signals. Scale bar 4 μm. (C, D, E, F) We measured proteasomal proteolytic activity in low speed (50× g) supernatants prepared from cells either of the wild type strain (WT; strain CRY564) or the *mmi1Δ* strain (strain CRY1062), growing at 30°C or heat-shocked at 46°C for 10 min. Error bars indicate standard errors of eleven independent experiments. (C) A small but highly significant (p = 0.005) increase of 6.7% in proteasomal activity of the *mmi1Δ* strain was observed at 30°C. (D) Influence of the heat shock treatment on proteasomal activity in WT cells. A modest but significant (p = 0.003) increase of 7.6% in proteasomal activity was observed in WT cells. (E) Influence of the heat shock treatment on proteasomal activity in *mmi1Δ cells*. An 12.2% increase in proteasomal activity with high significance (p = 1. E-5) was observed. (F) Comparison of the WT and *mmi1Δ* strains after heat shock at 46°C. A large and significant (p = 0.007) increase of 11.8% in the proteasomal activity of the *mmi1Δ* strain was observed after heat-shock. We conclude that heat shock results in increase of the proteasomal activity and a presence of Mmi1 displays an inhibitory function in regulation of the proteasomal activity which is most pronounced after heat-shock.
doi:10.1371/journal.pone.0077791.g006

MMI1 gene and co-expressing Pab1-GFP (another SGs marker which binds to the polyA tail of mRNA) together with Rpg1-RFP from chromosomal sites. We observed a normal formation and distribution of SGs (Figure 5A), as well as SGs dissolution during the 60 min recovery of cells from the heat shock (Figure 5B). We conclude that Mmi1 is not directly required for SGs formation or dissolution.

The formation of stress granules (SGs) via P-bodies is a general phenomenon [20,40,41] that apparently serves to store components of the protein synthesis machinery under conditions where growth is impossible due to stress prohibiting translation, arresting growth and cell cycle progression, and possibly protecting cells from death [20] [21] [42]. To test whether Mmi1 associates with SGs also upon other stresses than robust heat shock, we constructed a new strain co-expressing Mmi1-RFP with the stress granule marker Pub1-GFP [41]. We analyzed distribution of both fusion proteins in cells after 95 min glucose starvation (Figure S1). While Pub1-GFP was already observed in detectable accumulations corresponding to SGs, Mmi1-RFP remained uniformly cytosolic. Our results suggest that Mmi1 is not an essential component of SGs and its association with SGs requires robust stresses like the heat shock at 46°C for 10 min.

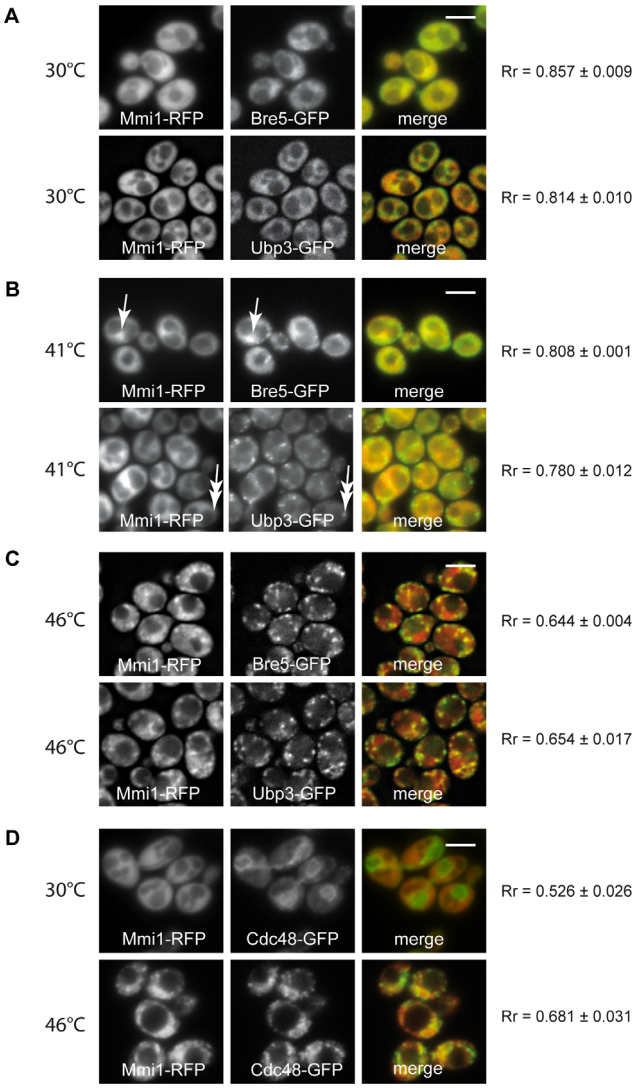

Figure 7. Mmi1 and the de-ubiquitination complex. Mmi1-RFP was tested for co-localization with either Bre5-GFP, or Ubp3-GFP (A – C) after a heat shock in strains CRY1698 and CRY1696, co-expressing particular fusion proteins from chromosomal sites. (A) Unstressed cells displayed uniformly cytosolic distribution of the fusion proteins. (B) In cells heat-shocked at 41°C for 10 min, co-localization of Mmi1-RFP with Bre5-GFP was observed in the nuclear region (arrows). In these cells, Ubp3-GFP was already accumulated in cytoplasmic granules whereas Mmi1-RFP remained uniformly cytosolic (double arrows). (C) Robust heat shock induced the accumulation of Bre5-GFP and Ubp3-GFP fusion proteins together with Mmi1-RFP in cytoplasmic granules but not with Mmi1-RFP accumulations in the nuclear region. (D) After a robust heat shock at 46°C, extensive co-localization of Mmi1 with Cdc48 in cytoplasmic granules was observed (strain CRY1308). Scale bars 4 µm.
doi:10.1371/journal.pone.0077791.g007

Mmi1 associates with the proteasome and the de-ubiquitination machinery in heat-stressed cells

Mmi1 was found as a direct possible interactor of proteasomal components Rpn1, Rpt5, Rpn10 [43] and Rpn11 [43,44] in high throughput studies. This also could mean that Mmi1 associates with the proteasome and may assist the degradation machinery under the heat shock conditions applied. To further elucidate accumulation of Mmi1 at the nuclear region of heat-shocked cells we tested for co-localization of Mmi1 with Rpn1, which is a non-ATPase subunit of the base subcomplex of the 26S proteasome [45]. As shown in Figure 6A, Mmi1-GFP (cytoplasmic) and the proteasomal structural component, Rpn1-RFP (nuclear), when expressed from the chromosome under the cognate promoter, are not obviously co-localized in unstressed cells. This fact is confirmed by very low value ($R_r = -0.028$) of the Pearsons correlation coefficient (R_r). It suggests that under normal growth conditions these two proteins mainly localize to different cellular regions. However, after robust heat shock, Mmi1 is re-localized to cytoplasmic granules on the one hand, and to the nucleus on the other hand. In the nucleus, Mmi1-GFP and Rpn1-RFP proteins show co-localization.

We further studied recovery from the heat shock in the strain expressing both fusion proteins (Figure 6B). As expected, after 30 min and even more clearly after 60 min Rpn1 is nuclear, but Mmi1 gradually returns to its diffusely cytoplasmic location. Accordingly, the degree of overlaps between the two proteins is substantially diminished with time of recovery. To elucidate functional consequences of the co-localization, we measured proteasomal proteolytic activities of WT and *mmi1*Δ strains. We performed several experiments comparing this activity in low speed supernatants of the cells growing either at 30°C or upon heat shock at 46°C for 10 min. In eleven biological replicas of this experiment it was shown that at the low temperature (30°C) the deletion of *MMI1* gene had a small but significant effect on the proteolytic activity of the proteasome (Figure 6C). In addition, we found that the WT cells heat-shocked at 46°C for 10 min displayed also a slight but significant increase of the proteasomal activity compared to WT cells grown at 30°C (Figure 6D). Similarly, a comparison of proteasome actvity of *mmi1Δ* cells at 30°C with the same cells at 46°C showed a strong and significant difference (Figure 6E). Comparing analyses of the WT with the *mmi1*Δ cells after robust heat shock revealed strong and significant increase of the proteasomal activity in the mutant (Figure 6F). Our data suggest that Mmi1 has some inhibitory activity on the proteasome under all conditions tested but the strongest effect is seen after the robust heat shock. Comparing these biochemical data with our fluorescence microscopy observations, we can conclude that redistribution of Mmi1 to the de-ubiquitination machinery upon heat shock (see below) might be partially linked to this inhibitory effect.

Additionally, Mmi1 was also found to interact with other components of the protein degradation machinery, in particular Bre5 and Ubp3 [46–48]. The auxiliary protein Bre5 interacts with ubiquitin-specific protease Ubp3 forming a de-ubiquitination complex. We therefore tested this interaction in our heat-shocked *S. cerevisiae* cells. We constructed new strains co-expressing Mmi1-RFP and either Bre5-GFP or Ubp3-GFP from chromosomal sites. In unstressed cells all three fusion proteins were cytosolic (Figure 7A). Mild heat stress (41°C) resulted in a co-localization Mmi1 with Bre5 at the nucleus, whereas at this temperature Ubp3 was predominantly found in cytoplasmic granules but not in the nuclear region (Figure 7B). Robust heat stress resulted in a granular pattern showing prominent overlap between Mmi1-RFP, Bre5-GFP as well as Ubp3-GFP in association with SGs but not in the nuclear region (Figure 7C). We tentatively interpret these findings to indicate that Ubp3 may be an early marker of SGs and Bre5 is at first fulfilling a function at the proteasome and then leaves the proteasome to become a part of SGs. In heat-shocked cells, we also co-localized Mmi1 with the AAA-ATPase Cdc48, which was found to be a functional interaction partner of Ubp3 and to be active in various processes of protein degradation [49] [50] [51]. We found that accumulations of both proteins overlapped in cytoplasmic granules to a very high degree

(Figure 7D). This finding is important for the understanding of the multifunctional protein module, Mmi1, in the context of the results presented so far. In a *cdc48* temperature sensitive mutant at the non-permissive temperature yeast cells undergo apoptosis and transfer Mmi1 efficiently to the outer surface of the mitochondria [6]. Our data underscore the link between Mmi1 and the protein degradation machinery which is needed during the heat stress response.

Conclusion and functional interpretation

We would like to propose a unifying hypothesis which is not contradicting the experimental results presented here and could explain the heat shock resistance of the *mmi1*Δ cells. The translocation of Mmi1 to the proteasome and to the de-ubiquitination machinery which is located independently of the proteasome could have to do with a partial inhibition of protein degradation under these conditions. The wild type Mmi1 protein is according to our hypothesis taking away the proteasomal activity which is increased after a robust heat shock and needed for cell survival [52]. Thereby Mmi1 compromises cell survival and its absence in in the *mmi1*Δ mutant under heat stress can increase survival of the cells to a large degree, as shown in Figure 3. It could also tentatively explain the increased replicative lifespan of the *mmi1*Δ mutant [6]. This function in the proteasomal protein degradation machinery is underscored by numerous co-localization results with proteins of the proteasome and the de-ubiquitination complex. The complex serves to modulate protein degradation by removing the polyubiquitin chains from proteins which would otherwise be degraded. We have therefore, using the versatile yeast genetic system, discovered a new and important function of the small multifunctional protein module, Mmi1. The function probably applies to most if not all eukaryotic cells, given the very high degree of sequence conservation of Mmi1 and the TCTP of higher eukaryotic cells. Testing this new function further is now a promising possibility. Mmi1 is a true "jack of all trades" and many additional functions still to be discovered are hinted at by the additional locations which we have demonstrated here the protein occurs throughout the nucleus depending on stress and always in a possible association with mitochondria (see Figure 2). Mmi1 may also associate with the specific kind of stress granules (SGs) which are formed in yeast upon robust heat shock. They are thought to be a storage form of various proteins which are needed for restarting growth and the cell cycle, but the role of Mmi1 related to SGs remains to be further elucidated.

We think that this amazing multitude of functions and locations of a small protein is by no means the exception in the eukaryotic world. As the number of genes of eukaryotic cells and organisms is very small compared to the functions to be fulfilled and the proteins to be discovered, we can speculate that in many cases, in a combinatorial way, one protein has to fulfill a number of different functions by interacting with different partners, perhaps also triggered by different posttranslational modifications. This latter point has not been studied for human TCTP or yeast Mmi1 (with the exception of glutathionylation [53] or de-phosphorylation [34]), and is also very worth studying.

We suggest that Mmi1 is involved both in the protection of proteins (in particular proteins of the translation machinery which are known components of SGs) and in their degradation, depending on the timing and intensity of the heat stress applied (compare in Figure 3C). The evidence presented here results in a working hypothesis which can unify at least some of the Mmi1 functions which are involved in the stress response of yeast cells. A presumed chaperone function of Mmi1/TCTP [4] would also fit very well into this general picture.

Supporting Information

Figure S1 Co-localization of Mmi1 with the stress granule marker Pub1 in glucose-deprived cells. The cells co-expressing Mmi1-RFP with Pub1-GFP from chromosomal sites (strain CRY1967) were analyzed by fluorescence microscopy after a 95 min of cultivation in the synthetic medium without glucose. While Pub1-GFP became accumulated in stress granules in glucose-deprived cells, Mmi1-RFP remained uniformly cytosolic. We conclude that glucose starvation does not result in rearrangement of subcellular Mmi1 localization and accumulation in stress granules. Scale bar, 4 μm.
(TIF)

Acknowledgments

Technical assistance by J. Serbouskova, D. Janoskova, P. Vesela and L. Novakova is gratefully acknowledged. We are grateful to J.M. Shaw (Univ. Utah, U.S.A.) for providing pYX142-mtRFPm plasmid.

Author Contributions

Conceived and designed the experiments: MR JH MB TG. Performed the experiments: MR JH GH TG RL VS. Analyzed the data: MR MB JH KR LBK JM. Contributed reagents/materials/analysis tools: JM. Wrote the paper: MR MB JH.

References

1. Bommer UA (2012) Cellular Function and Regulation of the Translationally Controlled Tumour Protein TCTP. The Open Allergy Journal 5: 19–32.
2. Thomas G, Thomas G, Luther H (1981) Transcriptional and translational control of cytoplasmic proteins after serum stimulation of quiescent Swiss 3T3 cells. Proc Natl Acad Sci U S A 78: 5712–5716.
3. Li F, Zhang D, Fujise K (2001) Characterization of fortilin, a novel antiapoptotic protein. J Biol Chem 276: 47542–47549.
4. Gnanasekar M, Rao KVN, Chen L, Narayanan RB, Geetha M, et al. (2002) Molecular characterization of a calcium binding translationally controlled tumor protein homologue from the filarial parasites Brugia malayi and Wuchereria bancrofti. Molecular and Biochemical Parasitology 121: 107–118.
5. Gachet Y, Tournier S, Lee M, Lazaris-Karatzas A, Poulton T, et al. (1999) The growth-related, translationally controlled protein P23 has properties of a tubulin binding protein and associates transiently with microtubules during the cell cycle. Journal of Cell Science 112: 1257–1271.
6. Rinnerthaler M, Jarolim S, Heeren G, Palle E, Perju S, et al. (2006) MMI1 (YKL056c, TMA19), the yeast orthologue of the translationally controlled tumor protein (TCTP) has apoptotic functions and interacts with both microtubules and mitochondria. Biochim Biophys Acta 1757: 631–638.
7. Macdonald SM, Rafnar T, Langdon J, Lichtenstein LM (1995) Molecular-Identification of an Ige-Dependent Histamine-Releasing Factor. Science 269: 688–690.
8. Thaw P, Baxter NJ, Hounslow AM, Price C, Waltho JP, et al. (2001) Structure of TCTP reveals unexpected relationship with guanine nucleotide-free chaperones. Nat Struct Biol 8: 701–704.
9. Rupec RA, Poujol D, Kaltschmidt C, Messer G (1998) Isolation of a hypoxia-induced cDNA with homology to the mammalian growth-related protein p23. Oncology Research 10: 69–74.
10. Yan Y, Weaver VM, Blair IA (2005) Analysis of protein expression during oxidative stress in breast epithelial cells using a stable isotope labeled proteome internal standard. Journal of Proteome Research 4: 2007–2014.
11. Schmidt I, Fahling M, Nafz B, Skalweit A, Thiele BJ (2007) Induction of translationally controlled tumor protein (TCTP) by transcriptional and post-transcriptional mechanisms. Febs Journal 274: 5416–5424.
12. Zhang D, Li F, Weidner D, Mnjoyan ZH, Fujise K (2002) Physical and functional interaction between myeloid cell leukemia 1 protein (MCL1) and fortilin - The potential role of MCL1 as a fortilin chaperone. Journal of Biological Chemistry 277: 37430–37438.

13. Liu H, Peng HW, Cheng YS, Yuan HS, Yang-Yen HF (2005) Stabilization and enhancement of the antiapoptotic activity of Mcl-1 by TCTP. Molecular and Cellular Biology 25: 3117–3126.
14. Yang Y, Yang F, Xiong ZY, Yan Y, Wang XM, et al. (2005) An N-terminal region of translationally controlled tumor protein is required for its antiapoptotic activity. Oncogene 24: 4778–4788.
15. Susini L, Besse S, Duflaut D, Lespagnol A, Beekman C, et al. (2008) TCTP protects from apoptotic cell death by antagonizing bax function. Cell Death and Differentiation 15: 1211–1220.
16. Haghighat NG, Ruben L (1992) Purification of Novel Calcium-Binding Proteins from Trypanosoma-Brucei - Properties of 22-Kilodalton, 24-Kilodalton and 38-Kilodalton Proteins. Molecular and Biochemical Parasitology 51: 99–110.
17. Graidist P, Yazawa M, Tonganunt M, Nakatomi A, Lin CCJ, et al. (2007) Fortilin binds Ca2+ and blocks Ca2+-dependent apoptosis in vivo. Biochemical Journal 408: 181–191.
18. Takahashi T, Yano T, Zhu JX, Hwang GW, Naganuma A (2010) Overexpression of FAP7, MIG3, TMA19, or YLR392c confers resistance to arsenite on Saccharomyces cerevisiae. Journal of Toxicological Sciences 35: 945–946.
19. Du L, Yu Y, Li Z, Chen J, Liu Y, et al. (2007) Tim18, a component of the mitochondrial translocator, mediates yeast cell death induced by arsenic. Biochemistry (Mosc) 72: 843–847.
20. Grousl T, Ivanov P, Frydlova I, Vasicova P, Janda F, et al. (2009) Robust heat shock induces eIF2alpha-phosphorylation-independent assembly of stress granules containing eIF3 and 40S ribosomal subunits in budding yeast, Saccharomyces cerevisiae. Journal of Cell Science 122: 2078–2088.
21. Grousl T, Ivanov P, Malcova I, Pompach P, Frydlova I, et al. (2013) Heat Shock-Induced Accumulation of Translation Elongation and Termination Factors Precedes Assembly of Stress Granules in S. cerevisiae. Plos One 8: e57083.
22. Cans C, Passer BJ, Shalak V, Nancy-Portebois V, Crible V, et al. (2003) Translationally controlled tumor protein acts as a guanine nucleotide dissociation inhibitor on the translation elongation factor eEF1A. Proceedings of the National Academy of Sciences of the United States of America 100: 13892–13897.
23. Brachmann CB, Davies A, Cost GJ, Caputo E, Li J, et al. (1998) Designer deletion strains derived from Saccharomyces cerevisiae S288C: a useful set of strains and plasmids for PCR-mediated gene disruption and other applications. Yeast 14: 115–132.
24. Robinson JS, Klionsky DJ, Banta LM, Emr SD (1988) Protein Sorting in Saccharomyces-Cerevisiae - Isolation of Mutants Defective in the Delivery and Processing of Multiple Vacuolar Hydrolases. Molecular and Cellular Biology 8: 4936–4948.
25. Roth V (2006) Kernel fisher discriminants for outlier detection. Neural Computation 18: 942–960.
26. Malinska K, Malinsky J, Opekarova M, Tanner W (2003) Visualization of protein compartmentation within the plasma membrane of living yeast cells. Molecular Biology of the Cell 14: 4427–4436.
27. Lettner T, Zeidler U, Gimona M, Hauser M, Breitenbach M, et al. (2010) Candida albicans AGE3, the Ortholog of the S. cerevisiae ARF-GAP-Encoding Gene GCS1, Is Required for Hyphal Growth and Drug Resistance. Plos One 5: e11993.
28. Arnold K, Bordoli L, Kopp J, Schwede T (2006) The SWISS-MODEL workspace: a web-based environment for protein structure homology modelling. Bioinformatics 22: 195–201.
29. Kiefer F, Arnold K, Kunzli M, Bordoli L, Schwede T (2009) The SWISS-MODEL Repository and associated resources. Nucleic Acids Research 37: D387–D392.
30. Rossanese OW, Soderholm J, Bevis BJ, Sears IB, O'Connor J, et al. (1999) Golgi structure correlates with transitional endoplasmic reticulum organization in Pichia pastoris and Saccharomyces cerevisiae. Journal of Cell Biology 145: 69–81.
31. Arcuri F, Papa S, Carducci A, Romagnoli R, Liberatori S, et al. (2004) Translationally controlled tumor protein (TCTP) in the human prostate and prostate cancer cells: Expression, distribution, and calcium binding activity. Prostate 60: 130–140.
32. Rid R, Onder K, Trost A, Bauer J, Hintner H, et al. (2010) H2O2-dependent translocation of TCTP into the nucleus enables its interaction with VDR in human keratinocytes: TCTP as a further module in calcitriol signalling. Journal of Steroid Biochemistry and Molecular Biology 118: 29–40.
33. Ma YP, Zhu WL (2012) Cytoplasmic and Nuclear Localization of TCTP in Normal and Cancer Cells. Biochemistry Research International 2012 1–4.
34. Diraison F, Hayward K, Sanders KL, Brozzi F, Lajus S, et al. (2011) Translationally controlled tumour protein (TCTP) is a novel glucose-regulated protein that is important for survival of pancreatic beta cells. Diabetologia 54: 368–379.
35. Klinger H, Rinnerthaler M, Lam YT, Laun P, Heeren G, et al. (2010) Quantitation of (a)symmetric inheritance of functional and of oxidatively damaged mitochondrial aconitase in the cell division of old yeast mother cells. Exp Gerontol 45: 533–542.
36. Westermann B, Neupert W (2000) Mitochondria-targeted green fluorescent proteins: convenient tools for the study of organelle biogenesis in Saccharomyces cerevisiae. Yeast 16: 1421–1427.
37. Fleischer TC, Weaver CM, McAfee KJ, Jennings JL, Link AJ (2006) Systematic identification and functional screens of uncharacterized proteins associated with eukaryotic ribosomal complexes. Genes Dev 20: 1294–1307.
38. Managbanag JR, Witten TM, Bonchev D, Fox LA, Tsuchiya M, et al. (2008) Shortest-Path Network Analysis Is a Useful Approach toward Identifying Genetic Determinants of Longevity. Plos One 3.
39. Laun P, Pichova A, Madeo F, Fuchs J, Ellinger A, et al. (2001) Aged mother cells of Saccharomyces cerevisiae show markers of oxidative stress and apoptosis. Mol Microbiol 39: 1166–1173.
40. Anderson P, Kedersha N (2008) Stress granules: The Tao of RNA triage. Trends in Biochemical Sciences 33: 141–150.
41. Buchan JR, Muhlrad D, Parker R (2008) P bodies promote stress granule assembly in Saccharomyces cerevisiae. Journal of Cell Biology 183: 441–455.
42. Takahara T, Maeda T (2012) Stress granules: the last refuge of TORC1? Cell Cycle 11: 3707–3708.
43. Guerrero C, Milenkovic T, Przulj N, Kaiser P, Huang L (2008) Characterization of the proteasome interaction network using a QTAX-based tag-team strategy and protein interaction network analysis. Proceedings of the National Academy of Sciences of the United States of America 105: 13333–13338.
44. Kaake RM, Milenkovic T, Przulj N, Kaiser P, Huang L (2010) Characterization of Cell Cycle Specific Protein Interaction Networks of the Yeast 26S Proteasome Complex by the QTAX Strategy. Journal of Proteome Research 9: 2016–2029.
45. Hanna J, Finley D (2007) A proteasome for all occasions. Febs Letters 581: 2854–2861.
46. Ossareh-Nazari B, Bonizec M, Cohen M, Dokudovskaya S, Delalande F, et al. (2010) Cdc48 and Ufd3, new partners of the ubiquitin protease Ubp3, are required for ribophagy. Embo Reports 11: 548–554.
47. Hoppins S, Collins SR, Cassidy-Stone A, Hummel E, DeVay RM, et al. (2011) A mitochondrial-focused genetic interaction map reveals a scaffold-like complex required for inner membrane organization in mitochondria. Journal of Cell Biology 195: 323–340.
48. Costanzo M, Baryshnikova A, Bellay J, Kim Y, Spear ED, et al. (2010) The Genetic Landscape of a Cell. Science 327: 425–431.
49. Verma R, Aravind L, Oania R, McDonald WH, Yates JR, et al. (2002) Role of Rpn11 metalloprotease in deubiquitination and degradation by the 26S proteasome. Science 298: 611–615.
50. Stolz A, Hilt W, Buchberger A, Wolf DH (2011) Cdc48: a power machine in protein degradation. Trends in Biochemical Sciences 36: 515–523.
51. Heo JM, Livnat-Levanon N, Taylor EB, Jones KT, Dephoure N, et al. (2010) A Stress-Responsive System for Mitochondrial Protein Degradation. Molecular Cell 40: 465–480.
52. Riezman H (2004) Why do cells require heat shock proteins to survive heat stress? Cell Cycle 3: 61–63.
53. Shenton D, Grant CM (2003) Protein S-thiolation targets glycolysis and protein synthesis in response to oxidative stress in the yeast Saccharomyces cerevisiae. Biochemical Journal 374: 513–519.
54. Huh WK, Falvo JV, Gerke LC, Carroll AS, Howson RW, et al. (2003) Global analysis of protein localization in budding yeast. Nature 425: 686–691.

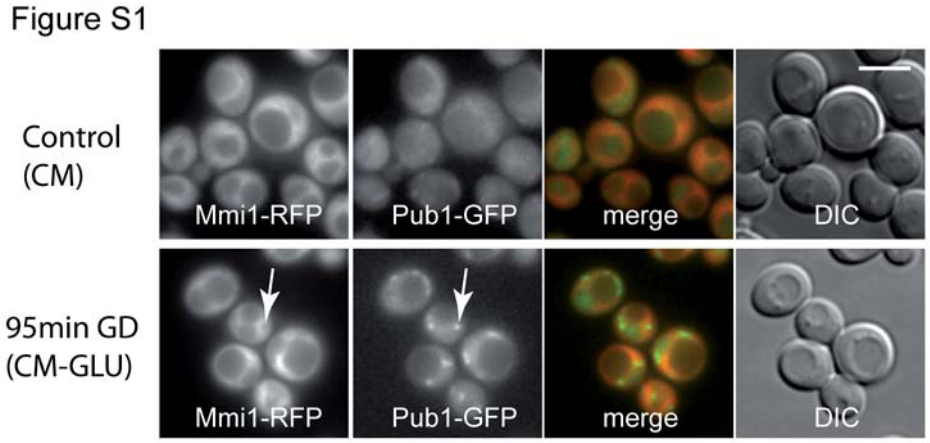

Figure S1

Co-localization of Mmi1 with the stress granule marker Pub1 in glucose-deprived cells. The cells co-expressing Mmi1-RFP with Pub1-GFP from chromosomal sites (strain CRY1967) were analyzed by fluorescence microscopy after a 95 min of cultivation in the synthetic medium without glucose. While Pub1-GFP became accumulated in stress granules in glucose-deprived cells, Mmi1-RFP remained uniformly cytosolic. We conclude that glucose starvation does not result in rearrangement of subcellular Mmi1 localization and accumulation in stress granules. Scale bar, 4 μm.

Paper 4

The paper *Yno1p/Aim14p, a NADPH-oxidase ortholog, controls extramitochondrial reactive oxygen species generation, apoptosis, and actin cable formation in yeast* by Rinnerthaler et al., focuses on newly discovered yeast NADPH oxidase enzyme, Yno1.

The main message of the paper is an identifying and further characterization of the first NOX (*NADPH oxidase*) enzyme in yeast *Saccharomyces cerevisiae*. NOX enzymes have been found, so far, in animals, plants and certain fungi, but have not been found in hemiascomycetous yeasts, until now. These enzymes are engaged in oxidative biosynthesis, cellular signalling and also in defence against pathogens. As a result of their action, superoxide radical anion (O_2^-) is produced. The superoxide is then metabolised to other *Reactive Oxygen Species* (ROS), as are H_2O_2, hydroxyl radical (OH^-) and others.

Authors identified *aim14* gene of *S. cerevisiae* to be partially sequentially similar to human NOX2 gene. Aim14 protein was seen to be related to ferric reductases that are connected with iron ion metabolism. However, Rinnerthaler et al. proved that Aim14, which was later on renamed to Yno1, has no ferric reductase activity. Instead of this, Yno1 was shown to produce superoxide in a NADPH-dependent manner. Moreover, an over-expression of Yno1 leads to elevated production of ROS and consequently to Yca1-dependent apoptosis. The ROS production in Yno1-overproducing strain is not dependent on the mitochondrial respiratory chain. On the contrary, a deletion of *yno1* confers less sensitivity to external oxidative stress, in a form of H_2O_2. With the respect to mentioned data, authors claim that Yno1 is genuine yeast NADPH oxidase. The *yno1* deletion also shows sensitivity to actin cytoskeleton-destabilizing drugs, as are wiskostatin or latrunculin B. It suggests that one of Yno1 functions may lie in regulation of actin cytoskeleton dynamics via production of ROS. Finally, Yno1 protein was localized to endoplasmic reticulum by usage of fluorescence microscopy.

Authors of the paper performed variety of methodologies including an iron and ROS detection assays, live cell imaging fluorescence microscopy, electron microscopy, microsomes purification, phylogenetic analyses and certain genetic and biochemical methods.

The paper deals with identification and further characterization of Yno1 enzyme, which is the first proved NADPH oxidase in *S. cerevisiae* and in hemiascomycetous yeasts at all. Authors showed that Aim14 / Yno1 does not have ferric reductase activity. Instead, Yno1 has been shown to be involved in production of ROS, dependently on NADPH and independently on the mitochondrial respiratory chain. The protein was localized to

endoplasmic reticulum and its absence was shown to be connected with resistance to oxidative stress and sensitivity to actin cytoskeleton-destabilizing drugs. With the respect to the fact that ROS have multiple roles in cell metabolism and they are also in relation with aging and various pathologies, authors of the paper believe that discovery of non-mitochondrial source of ROS in *S. cerevisiae* will help in better understanding of mentioned processes even in evolutionary higher organisms.

Yno1p/Aim14p, a NADPH-oxidase ortholog, controls extramitochondrial reactive oxygen species generation, apoptosis, and actin cable formation in yeast

Mark Rinnerthaler[a], Sabrina Büttner[b], Peter Laun[a], Gino Heeren[c], Thomas K. Felder[c], Harald Klinger[a], Martin Weinberger[d], Klaus Stolze[e], Tomas Grousl[f], Jiri Hasek[f], Oldrich Benada[f], Ivana Frydlova[f], Andrea Klocker[a], Birgit Simon-Nobbe[a], Bettina Jansko[a], Hannelore Breitenbach-Koller[a], Tobias Eisenberg[b], Campbell W. Gourlay[g], Frank Madeo[b], William C. Burhans[d,1], and Michael Breitenbach[a,1]

[a]Department of Cell Biology, Division of Genetics, University of Salzburg, 5020 Salzburg, Austria; [b]Department of Molecular Biosciences, University of Graz, 8010 Graz, Austria; [c]Department of Laboratory Medicine, Paracelsus Medical University, 5020 Salzburg, Austria; [d]Department of Molecular and Cellular Biology, Roswell Park Cancer Institute, Buffalo, NY 14263; [e]Department of Biomedical Sciences, University of Veterinary Medicine, 1210 Vienna, Austria; [f]Laboratory of Cell Reproduction, Institute of Microbiology of the Academy of Sciences of the Czech Republic, v.v.i. 14220 Prague 4, Czech Republic; and [g]Department of Biosciences, University of Kent, Canterbury Kent CT2 7NJ, United Kingdom

Edited by Irwin Fridovich, Duke University Medical Center, Durham, NC, and approved April 16, 2012 (received for review January 30, 2012)

The large protein superfamily of NADPH oxidases (NOX enzymes) is found in members of all eukaryotic kingdoms: animals, plants, fungi, and protists. The physiological functions of these NOX enzymes range from defense to specialized oxidative biosynthesis and to signaling. In filamentous fungi, NOX enzymes are involved in signaling cell differentiation, in particular in the formation of fruiting bodies. On the basis of bioinformatics analysis, until now it was believed that the genomes of unicellular fungi like *Saccharomyces cerevisiae* and *Schizosaccharomyces pombe* do not harbor genes coding for NOX enzymes. Nevertheless, the genome of *S. cerevisiae* contains nine ORFs showing sequence similarity to the catalytic subunits of mammalian NOX enzymes, only some of which have been functionally assigned as ferric reductases involved in iron ion transport. Here we show that one of the nine ORFs (YGL160W, AIM14) encodes a genuine NADPH oxidase, which is located in the endoplasmic reticulum (ER) and produces superoxide in a NADPH-dependent fashion. We renamed this ORF *YNO1* (yeast NADPH oxidase 1). Overexpression of *YNO1* causes YCA1-dependent apoptosis, whereas deletion of the gene makes cells less sensitive to apoptotic stimuli. Several independent lines of evidence point to regulation of the actin cytoskeleton by reactive oxygen species (ROS) produced by Yno1p.

cell cycle | integral membrane reductase | wiskostatin | latrunculin

Reactive oxygen species (ROS) have multiple roles in physiology and pathophysiology, in particular during aging and induction of programmed cell death. This includes also non-mitochondrial sources, besides the long-studied mitochondrially generated ROS. These findings can be viewed as important additions to the classical "free radical theory of aging" (1) and theories developed thereafter (2, 3).

In higher organisms, among others, at least two major sources of superoxide other than mitochondria are known. On the one hand, xanthine oxidase, an enzyme in the catabolism of purines, which catalyses the oxidation of hypoxanthine to xanthine and to uric acid, produces superoxide (4). On the other hand, NADPH oxidases (NOX) catalyze the production of superoxide from oxygen and NADPH (5).

The NADPH oxidase superfamily of membrane-located enzymes of higher cells has been known for a decade (for review, ref. 5). Whereas the human NOX2 was discovered early on, other NOX (Nox1/3/4/5) as well as dual oxidase (DUOX) (Duox1/2) enzymes (displaying two domains: a NADPH oxidase domain and a peroxidase domain) have been found relatively recently in human cells. The human NOX2 was discovered as a defense enzyme of neutrophils and macrophages, which produce a burst of superoxide ($O_2^{\cdot -}$) as a first line of defense against invading microorganisms. Although X-ray or NMR structure determinations are not available, we know from indirect evidence and bioinformatics that the catalytic subunit of the macrophage enzyme contains six transmembrane helices, is located in the plasma membrane, and produces superoxide in a vectorial way to the lumen of the phagosome, which is topologically outside the cytoplasmic space of the cell. In fact, all known NOX enzymes are membrane bound and deliver superoxide in a vectorial way. Not all NOX enzymes are located in the plasma membrane, however. For instance, human NOX4 was reported to be localized in the endoplasmic reticulum (ER), the nucleus, or in the mitochondria in several conflicting reports (6, for review, ref. 7). The NADPH oxidases require three different redox cofactors, namely two tightly bound b-type hemes, $FADH_2$ and NADPH, which are bound by the dehydrogenase domain (5, 6). The general structural and mechanistic features of the NOX catalytic subunit seem to be relatively well conserved between the different NOX enzymes; however, they are regulated in different ways, either through regulatory subunits or by calcium ions. Calcium-dependent regulation is assumed and in some cases verified by experiments to occur via EF-hand motifs, which are present in NOX5 and the DUOX enzymes (8).

The immediate product (presumed or directly measured) of NOX (and DUOX) enzymes is the superoxide radical anion, which is, however, metabolized to other ROS molecules (peroxynitrite, H_2O_2, hypochlorite, and hydroxyl radical) relevant for defense in the case of NOX2 (9). The other NOX enzymes serve more specialized metabolic functions. A signaling function of ROS (superoxide and hydrogen peroxide) originating from NOX enzymes is increasingly discussed in the literature (5).

Fungal NOX enzymes of the NOXA, -B, and -C subfamilies and their physiological roles were discovered relatively recently (10, for review, ref. 11). The filamentous fungi *Podospora anserina*, *Neurospora crassa* (12) and the social amoeba *Dictostelium discoideum* (13) could be shown to express NADPH oxidases that actively produce superoxide (14). The deletion of *PaNOX1* has no influence on growth, but completely blocks fruiting body formation (14). Fungal NOX enzymes mostly produce ROS as second messengers for coordination of multicellular communication

Author contributions: M.R., S.B., P.L., G.H., T.K.F., H.K., M.W., K.S., T.G., J.H., O.B., I.F., A.K., B.S.-N., B.J., H.B.-K., T.E., C.W.G., F.M., and M.B. designed research; M.R., S.B., P.L., G.H., T.K.F., H.K., M.W., K.S., T.G., J.H., O.B., I.F., A.K., B.S.-N., B.J., H.B.-K., T.E., C.W.G., and F.M. performed research; M.R., S.B., P.L., G.H., T.K.F., H.K., K.S., T.G., J.H., O.B., I.F., A.K., B.S.-N., B.J., H.B.-K., T.E., C.W.G., F.M., W.C.B., and M.B. analyzed data; and M.R., W.C.B., and M.B. wrote the paper.

The authors declare no conflict of interest.

This article is a PNAS Direct Submission.

Freely available online through the PNAS open access option.

[1]To whom correspondence may be addressed. E-mail: wburhans@buffalo.edu or michael.breitenbach@sbg.ac.at.

This article contains supporting information online at www.pnas.org/lookup/suppl/doi:10.1073/pnas.1201629109/-/DCSupplemental.

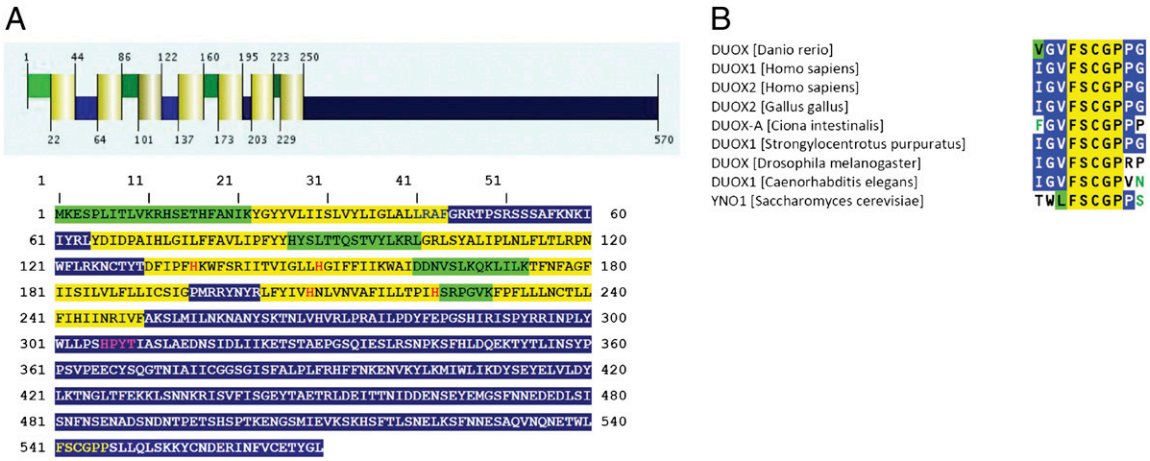

Fig. 1. Bioinformatic predictions for Yno1p (YGL160W). (*A*) Prediction of secondary structure for Yno1p obtained with the Phillius transmembrane prediction algorithm as described in *SI Materials and Methods*. The transmembrane helices are highlighted in yellow; the luminal regions, which reside presumably in the lumen of the ER, are highlighted in green; and the cytoplasmic regions are highlighted in blue. The four conserved histidine residues responsible for coordinating the two heme groups are marked with red letters. The NADPH binding site is marked with yellow letters and the FAD binding site is highlighted with purple letters. (*B*) Sequence alignment of the nicotinamide binding site of dual oxidases (DUOX) from various organisms. The sequence "FSCGP" is specific for DUOX enzymes and for Yno1p.

(14). However, in hemiascomycetous yeasts no gene or enzyme has been assigned as a superoxide-generating NADPH oxidase up to now (10, 15).

In this work we present evidence that the yeast *Saccharomyces cerevisiae* produces a NADPH oxidase encoded by the ORF, YGL160W (*AIM14*). We show that this enzyme exhibits all biochemical properties of a fungal NADPH oxidase and have therefore renamed it *YNO1* (yeast NADPH oxidase 1). Overexpression leads to production of ROS causing Yca1p-dependent apoptosis. Deletion of the gene confers resistance against apoptotic stimuli and hypersensitivity to wiskostatin and latrunculin B, indicating a role of Yno1p in regulation of the actin cytoskeleton.

Results and Discussion

Yeast Genome Codes for a Putative NADPH Oxidase Homolog: Yno1p. The common structural features of the NOX/integral membrane reductase (IMR) superfamily include in the N-terminal part six or seven transmembrane helices, two of which contain two strictly conserved histidine residues responsible for coordinating two spectroscopically nonidentical b-type heme groups. The C-terminal cytoplasmic globular domain contains binding sites for $FADH_2$ and NADPH (Fig. 1*A*). Position-specific iterated (PSI)-BLAST analyses with the sequence of the catalytic subunit of the human NOX2 against the yeast genome showed that all features of NOX enzymes could be found in yeast ferric reductases, which are, like NADPH oxidases, proven flavocytochromes b_{558} (16). We conclude that within the large NOX protein superfamily functional diversity developed and a new function (ferric reductase or, more generally, IMR) arose (11). Among the yeast *FRE* subfamily the closest homolog to human NOX enzymes was found to be the yeast ORF YGL160W, bearing 32.1% sequence similarity (16.6% identity) to *NOX5*. The binding site for the nicotinamide moiety of NADPH in *YNO1* is identical with the corresponding sequences of the DUOX enzymes (Fig. 1*B*).

In a phylogenetic tree of the NOX/IMR superfamily, *FRE1–FRE7* cluster together, whereas the closely related sequences of *FRE8* and *YNO1* are located somewhat farther away from the FRE genes and show a closer relationship to the animal NOX5 sequences (Fig. S1). A ferric reductase function has been shown for *FRE1–FRE4* (17), and iron- (or copper)-dependent transcriptional control was found for *FRE1–FRE7* (18, 19). *FRE8* and *YNO1* cluster together and are neither transcriptionally controlled by iron nor is the deletion dependent on increased iron for growth (18).

Yno1p Does Not Function as a Ferric Reductase. To test for the possibility that Yno1p might have ferric reductase activity that aids iron uptake leading to superoxide production, we determined total iron as well as soluble iron in strains overexpressing *YNO1* and compared the results with controls carrying the empty vector (Fig. S2). Clearly, overexpression of *YNO1* did not lead to a significant accumulation of iron in the cells. Microsomes isolated from a strain overexpressing *YNO1*, which showed a high level of NADPH oxidase activity (see below) were only weakly active irrespective of the presence or absence of Yno1p when tested for iron reductase activity (20) (Fig. S3). Taken together, the iron reductase activity measurements, iron uptake data, phylogenetic tree construction, and the transcriptional regulation data cited above do not support a ferric reductase function for Yno1p.

Yno1p Produces Superoxide Anions. To clarify whether the proteins encoded by *YNO1* or any one of the eight yeast *FRE* genes has the capacity to produce superoxide ($O2^{\bullet-}$), as would be expected of a genuine NADPH oxidase, all nine genes were cloned into

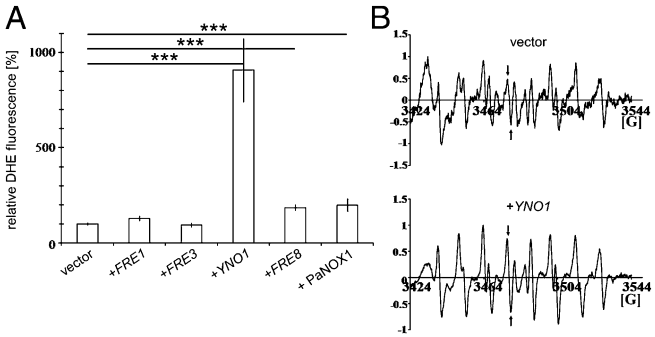

Fig. 2. (*A*) Quantitative determination of fluorescence in live yeast strains overexpressing putative NADPH oxidases after galactose induction and in controls. ROS production was determined by measuring oxidized DHE in BY4741 cells transformed with: the pYES2 vector, pYES2-*FRE1*, pYES2-*FRE3*, pYES2-*YNO1*, pYES2-*FRE8*, and pYES2-*PaNOX1*. See Table S1 for determination of statistical significance. (*B*) Results of in vivo ESR measurements using the spin trap, DEPMPO (22). Lines marked with arrows are specific for the superoxide adduct. *Upper* spectrum corresponds to BY4741 transformed with the empty vector. *Lower* spectrum was obtained after galactose induction of pYES2-*YNO1*. Both spectra were recorded with three biological replicas each. Comparing the signal intensities of the superoxide-specific bands shows that they are significantly different with a two-tailed *P* value of 0.0057.

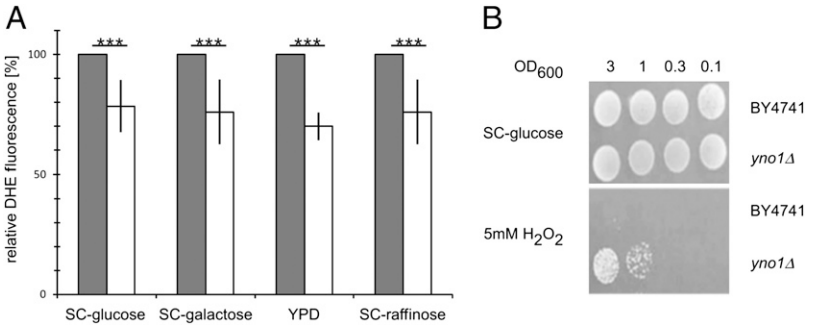

Fig. 3. (*A*) ROS production in WT (gray bars) and *yno1Δ* (open bars) cells. Four different growth media were used as indicated. In each of the four experiments, a statistically significant loss of ~20% activity was consistently observed in *yno1Δ* compared with WT cells. (*B*) *yno1Δ* cells exhibit marked resistance to 5mM H_2O_2, which completely inhibits growth of WT cells. Serial dilutions of WT and *yno1Δ* cells were spotted on SC −glucose and SC −glucose +5 mM H_2O_2 media and scored after 2 d.

the expression vector pCM297 under the control of a tightly regulated but relatively weak doxycyline-inducible promoter (19, 21). All these constructs were transformed into the yeast strain BY4741, which was grown to midexponential phase. Thereafter, 100 mg/L doxycyline was added to induce the expression of the genes to be tested. After 6 and 16 h, respectively, the superoxide levels were measured by dihydroethidium (DHE) assay. Compared with the wild-type strain BY4741, which was transformed with the empty vector pCM297, *YNO1* was the only one of the yeast genes tested that gave a small but significant positive signal indicated by a 50% increased oxidation of DHE (Fig. S4).

For further experiments, the yeast *YNO1* as well as the *PaNOX1* gene (positive control) and the *FRE1*, *FRE3*, and *FRE8* genes were subcloned into the expression vector pYES2, harboring the strong GAL1 promoter to induce high expression of the selected genes. Expression of these constructs confirmed the results obtained by expression in pCM297. Overexpressing *YNO1* led to an approximately five- to ninefold increase of the ROS level. The control strain with *PaNOX1* showed a twofold increase in fluorescence signal intensity, as did the *FRE8* ORF. *FRE1* and *FRE3* showed a ROS level comparable to the wild-type strain expressing the empty vector (Fig. 2*A*).

The DHE assay is very sensitive but not absolutely specific for superoxide (21). Therefore, we also performed ESR measurements for a more direct detection of superoxide with the spin trap 5-(Diethoxyphosphoryl)-5-methyl-1-pyrroline N-oxide (DEPMPO), which forms a stable radical adduct, the resonance spectrum of which is specific for superoxide (22). ESR spectra were recorded in vivo at room temperature. Wild-type cells overexpressing the empty vector only produce signals with DEPMPO at background level. However, cells of a strain overexpressing *YNO1* produced a strong signal characteristic of the superoxide radical anion (Fig. 2*B* and Table S1).

Using the same DHE fluorescence assay as described above, the *yno1Δ* strain also was tested under the same conditions after growth on YPD, SC −glucose, SC −raffinose, and SC −galactose. Reproducibly and significantly, the deletion strain produced a signal that was about 20% weaker than that of an untransformed WT strain (Fig. 3*A*). This indicates that Yno1p contributes about 20% to the total ROS production under exponential growth conditions and that other sources of ROS also exist. We hypothesized that the deletion strain could be resistant to externally applied oxidative stress. Ten-microliter aliquots of the deletion strain and the WT strain in different dilutions were spotted on SC plates containing hydrogen peroxide, diamide, or tert-butyl hydroperoxide. Indeed, the deletion strain showed a higher resistance than the wild-type strain against hydrogen peroxide (Fig.

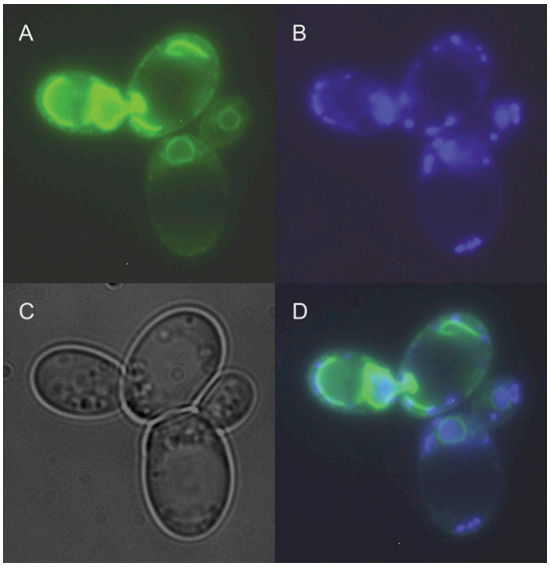

Fig. 4. Fluorescence micrograph of two live cells with large daughters from midlog phase growth on rich media. (*A*) Localization of the Yno1–eGFP fusion protein. (*B*) Nuclear and mitochondrial DNA stained with DAPI. (*C*) The same cells visualized by phase contrast microscopy. (*D*) Overlay of *A*–*C*. The perinuclear location of the fusion protein is clearly visible.

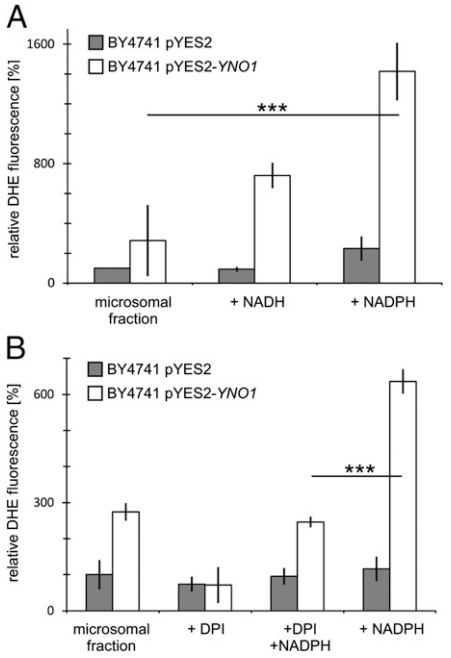

Fig. 5. ROS measurements by DHE fluorescence in purified microsomes. (Gray bars) Microsomes from a strain containing only the vector (vector control). (Open bars) Strain expressing Yno1p under galactose control. (*A*) NADPH oxidase activity detected in the microsomal fraction in the presence of NADPH; a weaker activity is detected with NADH. (*B*) NADPH-dependent activity is inhibited by adding DPI. Residual DHE oxidation in the absence of added NADPH is also inhibited by DPI.

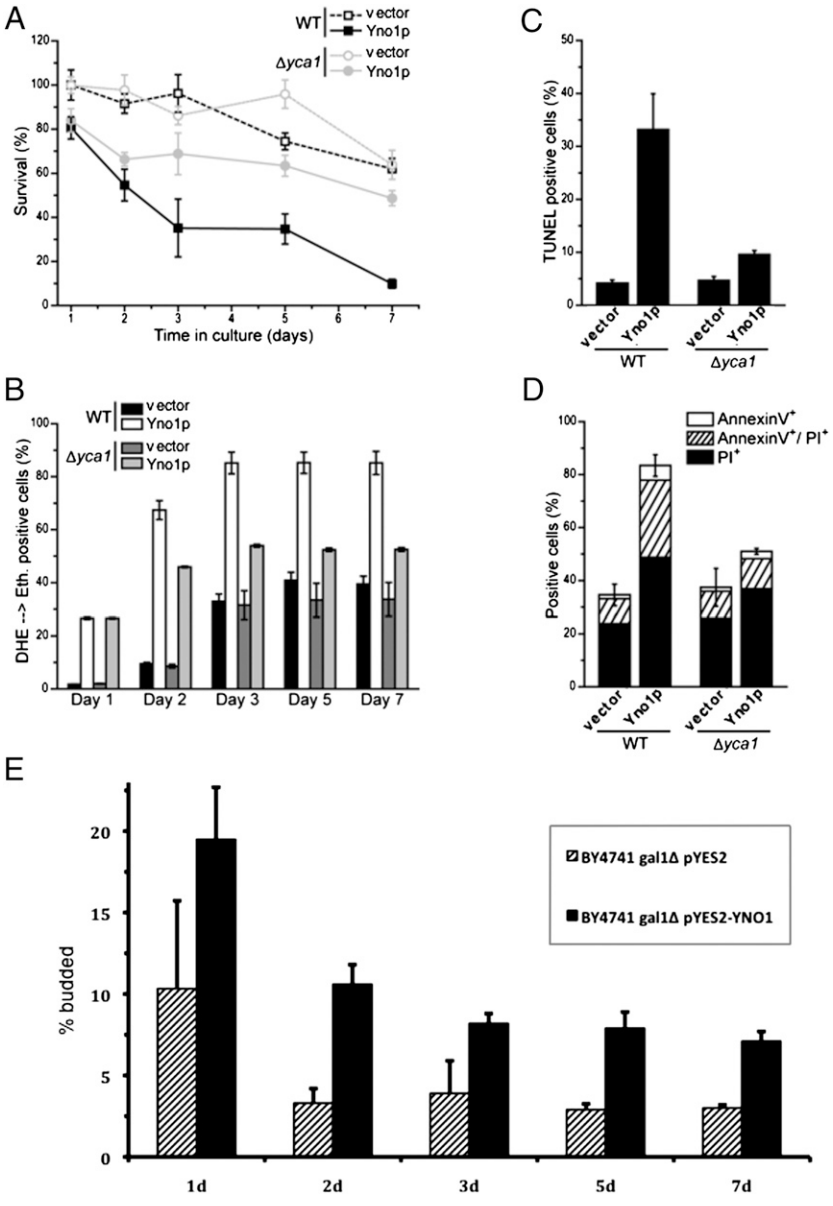

Fig. 6. Survival, apoptotic phenotype, and bud index of stationary phase cells overexpressing *YNO1*. Cells were pregrown in SC raffinose; expression of *YNO1* from the pYES2 plasmid was induced by 3% (wt/vol) galactose, and survival, apoptotic phenotypes, and bud index in stationary phase were determined. (*A*) Chronological aging (survival in stationary phase) over 7-d culture in spent medium and its inhibition by inactivation of *YCA1*. (*B*) ROS production measured over time in stationary phase for the same cells described in *A*. Up until day 2, ROS production in the *yca1Δ*, *YNO1* overexpression strain was high, although apoptotic phenotypes are low (*A*, *C*, and *D*). Later in stationary phase, the *yca1Δ* strain displayed a lower ROS level. (*C*) TUNEL measurements in the same four strains on day 2 of stationary phase. TUNEL$^+$ cells indicating DNA strand breaks are more numerous in the strain overexpressing *YNO1*, but reduced in number when *YCA1* is deleted. (*D*) Measurements of staining with AnnexinV and propidium iodide (PI) in the same four strains in stationary phase (day 2). Overexpression of *YNO1* led to high-level staining with both AnnexinV and PI, which indicates the existence of apoptotic as well as necrotic cells. Staining was not elevated if *YCA1* was deleted. (*E*) Determination of bud index (% budded cells) in stationary phase. Overexpression of *YNO1* was induced by shifting from medium containing 2% (wt/vol) raffinose to medium containing 2% (wt/vol) raffinose +3% (wt/vol) galactose, growing the cells to stationary phase and keeping them in spent medium for 7 d. Cells transformed with the empty vector were used as controls. After 3 d, ~8% of cells in stationary cultures overexpressing *YNO1* remained budded, in contrast to the ~3% budded cells detected in controls.

3*B*). The deletion strain showed no change in sensitivity on plates containing diamide or tert-butyl hydroperoxide (Fig. S5).

Yno1p-Mediated Production of Superoxide Depends on NADPH in Vivo. We wanted to test whether the high superoxide signal in the *YNO1* overexpressing strain was dependent on the NADPH level of the cells. In *S. cerevisiae*, *ZWF1* codes for glucose-6-phosphate dehydrogenase, an enzyme catalyzing the first and rate-limiting step of the pentose phosphate pathway, a reaction that generates NADPH. Cells lacking *ZWF1* show a reduced level of NADPH (23). A *zwf1Δ* strain overexpressing *YNO1* showed no increase in ROS compared with wild type or the deletion strain carrying the empty vector, indicating that Yno1p activity very probably is NADPH dependent in vivo (Fig. S6).

Yno1p Localizes to the Perinuclear ER. Previous studies of NADPH oxidases in human cells indicate that NOX enzymes are localized in various membranes such as the plasma membrane, ER, or the mitochondrial membranes (6, 7). To determine subcellular localization of Yno1p, we constructed a C-terminal fusion protein of Yno1p and eGFP expressed under the control of the constitutive *MET25* promoter in the pUG35 vector. In cells expressing the fusion protein, a clear perinuclear GFP signal was observed (Fig. 4; compare with ref. 24). Simultaneously expressing HDEL-RFP (25) showed colocalization of Yno1-GFP with HDEL-RFP in the perinuclear ER (Fig. S7).

To biochemically localize the enzyme activity in cells of a strain overexpressing the full-length nonfusion Yno1p under galactose control, cells were broken with glass beads and fractions were obtained by differential centrifugation. DHE fluorescence assays were performed as described above to measure superoxide anions in microsomal fractions (100,000 × *g* pellet) from cells transformed with the empty vector and from cells overexpressing *YNO1*. Microsomes were characterized by electron microscopy (Fig. S8). As shown in Fig. 5, the microsomal fraction contains the Yno1p enzyme activity, which is NADPH dependent in vitro and is inhibited by diphenyleneiodonium chloride (DPI) (26), indicating a genuine NADPH oxidase and confirming the results seen with the Yno1–eGFP fusion protein. The microsomes displayed a residual activity with NADH as cofactor. Note that some flavocytochromes b, like the human NOX2 enzyme, also show a weak affinity for NADH, whereas NOX4 and NOX5 are specific for NADPH (27). The microsomes show a small residual NADPH-dependent activity that was not inhibited by DPI, which

is likely due to the presence of microsomal oxidoreductases other than Yno1p. When we compared the specific activity of Yno1p (DHE fluorescence counts divided by protein amount) in the supernatant of the 4,500 × *g* centrifugation with the activity in the purified microsomes, we observed a significant enrichment (*SI Results*), indicating that the majority of the enzyme is located in microsomes. All other fractions obtained except the 18,000 × *g* supernatant containing microsomes showed reduced levels of DHE fluorescence (Fig. S9).

***YNO1* Overexpression Causes Cell Death Depending on the Yeast Caspase *YCA1*.** To investigate the impact of Yno1p on yeast cell physiology, we first tested cell growth (Fig. S10). Compared with WT, a *yno1* deletion strain exhibited normal growth on standard media (synthetic complete, SC) (Fig. S10*A*). Overexpression of Yno1p resulted in a substantial slowing of growth (Fig. S10*B*), which was caused by induction of apoptosis and necrosis, as shown below. However, growth was not altered by overexpression of *YNO1* in a *yca1Δ* strain (28, 29), indicating that cell death by *YNO1* overexpression depends on a functional Yca1p caspase (Fig. S10*C*).

Next we tested apoptotic and necrotic markers in the same strains just discussed (Fig. 6). The results show that clonogenicity over 7-d culture in stationary phase decreased substantially when Yno1p was expressed, indicating increased chronological aging. However, this effect was substantially dampened by deleting *YCA1* (Fig. 6*A*), confirming the results seen in the growth curves of Fig. S10. Measuring apoptotic and necrotic markers showed that the cells were rescued from both forms of death by the *YCA1* deletion (Fig. 6 *C* and *D*), although ROS production was still high in the *yca1Δ* strain overexpressing *YNO1* at day 2 (Fig. 6*B*). This latter effect was time dependent and at the end of the survival curve (day 7), ROS production in the *yca1Δ YNO1* overexpressing strain appeared to be lower. Microscopic images of the apoptotic markers examined are shown in Fig. S11. Taken together, the results shown in Fig. 6 and Figs. S10 and S11 establish that Yca1p acts downstream of the ROS produced by Yno1p.

We next tested the budding index in stationary WT cells with or without overexpression of Yno1p. As shown in Fig. 6*E*, after 3 d, the WT exhibited a low number of budded cells, but in the *YNO1* overexpressing strain, cells began new cell cycles despite the absence of nutrients. This is consistent with the lethal effect of *YNO1* overexpression and suggests that the ROS produced by Yno1p creates a signal that starts a new cell cycle.

ROS Production by Yno1p Is Independent of the Mitochondrial Respiratory Chain and Does Not Contribute to ER Stress. We wanted to determine whether the remarkable increase in ROS production in *YNO1* overexpressing strains required a functional respiratory chain. The deletion of *AFO1* (30), a mitochondrial ribosomal protein, leads to cells completely devoid of mitochondrial DNA (ρ^0), which also display a very low level of ROS, in contrast to standard ρ^0 strains isolated after treatment with ethidium bromide. This strain was therefore ideally suited for this measurement. The results indicate that a functional respiratory chain (which is absent in ρ^0 strains) is not needed for ROS production by Yno1p (Fig. S12*A*).

Tunicamycin induces ER stress and a high level of ROS in WT yeast (31) that can lead to apoptosis. As shown in Fig. S12*B*, this effect is independent of Yno1p. Therefore, Yno1p is not a significant contributor to ER stress. This finding is also consistent with the observation that a *yno1Δ* strain shows neither resistance nor sensitivity to the reductant dithiothreitol (DTT), which leads to an accumulation of unfolded proteins in the ER and causes ER stress (Fig. S13). We conclude that ROS production by Yno1p is not related to mitochondrial respiration and mitochondrial ROS production. We also conclude that the direct influence of Yno1p on mitochondria and vice versa is weak or absent in this case, in contrast to higher cells where a cross-talk between NOX enzymes and mitochondria has been described (32). Furthermore, the production of ROS by this ER membrane-localized enzyme is independent of the ROS production due to ER stress and the accumulation of unfolded proteins in the ER.

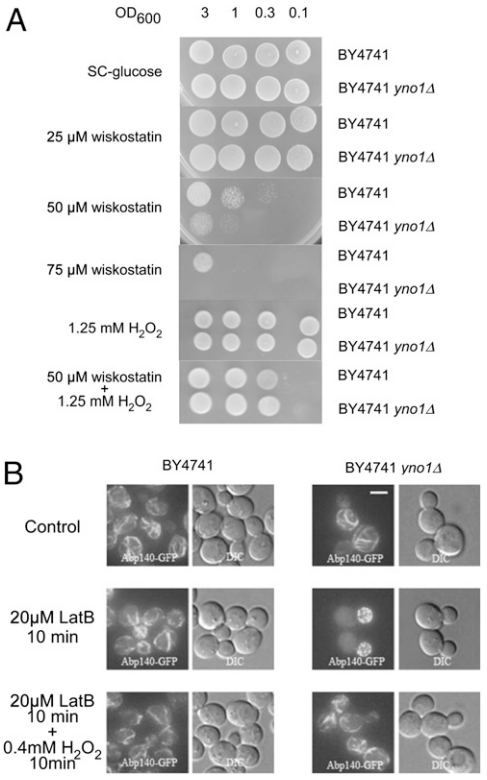

Fig. 7. (*A*) Deletion of *yno1* caused hypersensitivity to wiskostatin, which was suppressed by external exposure to H_2O_2. Dilutions of WT and *yno1Δ* strains were spotted onto SC −glucose, SC −glucose +wiskostatin, and SC −glucose +wiskostatin +H_2O_2. Addition of a low nontoxic amount of H_2O_2 to the media enabled the hypersensitive cells of the deletion strain to grow in the presence of an otherwise inhibitory concentration of wiskostatin. (*B*) F-Actin was visualized with Abp140-GFP; deletion of *yno1* caused hypersensitivity to latrunculin B (inhibitor of F-actin cable elongation) at a concentration of 20 μM, which does not inhibit F-actin cable elongation in the WT. H_2O_2 reversed inhibition of actin cables by latrunculin B. Thus, ROS produced by Yno1p are required for F-actin regulation.

Interaction of the Yno1p-Produced ROS with the Nucleation and Elongation Step in the Biosynthesis of F-Actin Cables. Previous whole genome screening (33) identified the *yno1Δ* strain as hypersensitive to wiskostatin and showed synthetic lethality of *yno1Δ* with a heterozygous deletion of *act1*, the only actin-encoding gene on the haploid genome of yeast (34). Wiskostatin is a drug that interacts with Wiskott-Aldrich syndrome protein (WASP), thereby preventing the nucleation of F-actin cables. We confirmed this high-throughput result and also determined that a nontoxic concentration of H_2O_2 partially reverses the toxic effect of wiskostatin (Fig. 7*A*). Note that H_2O_2 does not oxidize wiskostatin under the conditions used.

Additional inhibitors of the actin cytoskeleton have been identified (33), including latrunculin B, an inhibitor of F-actin cable elongation (35). After a 10-min incubation with 20 μM latrunculin B, the *yno1Δ* mutant completely lost F-actin cables, but not F-actin patches (in the daughter cell at this stage of the cell cycle). Under the same conditions, WT cells remain completely normal in appearance. The effect of latrunculin B on the mutant was efficiently reversed by adding a low concentration of H_2O_2, which did not inhibit cell growth (Fig. 7*B*). We conclude that Yno1p functionally interacts with F-actin by producing ROS and that the function of *YNO1* in this interaction very probably is to supply H_2O_2 generated via its primary product, superoxide. This conclusion is strengthened by the fact that in the mammalian system, ROS created by NOX have been shown to regulate the actin cytoskeleton (36).

Concluding Remarks. We show here that Yno1p of *S. cerevisiae* is a NADPH oxidase, which produces superoxide and indirectly H_2O_2. Two of the nine *S. cerevisiae* members of the NOX/IMR superfamily, Fre8p and Yno1p, the protein described in this communication, cluster together at a location different from the other seven Fre enzymes in phylogenetic trees constructed by two different methods (ref. 11, this paper, and Fig. S1). Yno1p and Fre8p are also different from Fre1-7p because they show no involvement in iron reduction and uptake. Another distinctive feature of Yno1p is that overproduction of this protein, but not overproduction of Fre1-Fre7p leads to slow growth as determined in a whole genome screen (37) and in this study (Fig. S10). Slow growth of these strains can be explained by apoptotic and necrotic cell death.

Additional criteria for identification of Yno1p as a genuine NADPH oxidase are its inhibition by DPI, dependence on NADPH, and sequence information that predicts seven transmembrane helices, four conserved histidine residues that can coordinate two heme b groups, and a globular C-terminal region containing binding sites for FAD and NADPH (Fig. 1). *FRE8* overexpression leads to weak but significant superoxide production, whereas the other seven *FRE* genes after overexpression yield a level of ROS equal to the WT or uninduced yeast cells.

Strong (albeit indirect) evidence points to a physiological function of Yno1p in the regulation of the cell's actin cytoskeleton. The *yno1Δ* mutant shows hypersensitivity to wiskostatin, which inhibits F-actin cable nucleation, and to latrunculin B, which inhibits F-actin cable elongation. In both cases, the phenotype can be rescued by addition of a relatively small nontoxic concentration of H_2O_2. This indicates that the function missing in *yno1Δ* cells is production of ROS that have a role in signaling. How is this possible considering that there are many other sources of ROS in the cell? Although the answer to this interesting question must await future research, it could be related to compartmentalization of different kinds of ROS in space and time during the cell cycle. This possibility is consistent with the observation that overexpression of *YNO1* causes a significant increase of budded cells in stationary phase.

Materials and Methods

Strains BY4741 (*MATα his3 Δ1 leu2Δ0 ura3Δ0 met15Δ0*) and the respective knockout in the *YNO1* gene (European Saccharomyces Cerevisiae Archive for Functional Analysis) were grown in SC medium (20) with 2% (wt/vol) glucose as carbon source and used for most of the experiments. Overexpression of the *YNO1* and its homologs was accomplished by cloning it as a PmeI/PmeI fragment into the galactose-inducible pYES2 yeast expression plasmid (Invitrogen) and growing the strains on 3% galactose. For visualizing the actin cytoskeleton, the genomic integration of ABP140–eGFP in strain SEY (*MATa his3 Δ200 leu2-3112 ura3-52 trp1-Δ901 lys2-801 suc2Δ9*) was used. Latrunculin B (Sigma) was added to a final concentration of 20 μM to cultivation media. Fluorescence microscopy was performed using an Olympus IX-71 inverted microscope equipped with Hamamatsu Orca/ER digital camera and the Cell R detection system. ROS (superoxide) determination was performed in vivo with DHE in an Anthos Zenyth 3100 plate reader as described previously (20). Apoptotic markers and chronological lifespan were determined as described in ref. 27. A more detailed description of the materials and methods, including statistical analysis, is given in *SI Materials and Methods*.

ACKNOWLEDGMENTS. We thank Dan Kosman for his help with ferric reductase determinations and Philippe Silar for supplying the *PaNOX1* cDNA. This work was supported by Austrian Science Fund (FWF) Grants S9302-B05 (to M.B.), T414-B09 (to S.B.), S9304-B05, LIPOTOX, DK-MCD W 1226-B18 and P23490-B12 (to F.M.); P24381-B20 (to F.M. and T.E.); the European Commission (Brussels) Role of Mitochondria in Conserved Mechanisms of Aging (MIMAGE) Project (Contract 512020, to M.B.) and a National Cancer Institute Support Grant (P30CA016056) to Roswell Park Cancer Institute; and the Medical Research Council (United Kingdom) for Career Development Fellowship 78573 (to C.W.G). J.H. and O.B. were supported by CSF204/09/1924, MEB 060902, 7AMB12ATOO2; and T.G. and I.F. were supported by LC545 (Czech Republic).

1. Harman D (1956) Aging: A theory based on free radical and radiation chemistry. *J Gerontol* 11:298–300.
2. Harman D (1972) The biologic clock: The mitochondria? *J Am Geriatr Soc* 20:145–147.
3. Harman D (1991) The aging process: Major risk factor for disease and death. *Proc Natl Acad Sci USA* 88:5360–5363.
4. Porras AG, Olson JS, Palmer G (1981) The reaction of reduced xanthine oxidase with oxygen. Kinetics of peroxide and superoxide formation. *J Biol Chem* 256:9006–9103.
5. Nauseef WM (2008) Biological roles for the NOX family NADPH oxidases. *J Biol Chem* 283:16961–16965.
6. Krause KH (2004) Tissue distribution and putative physiological function of NOX family NADPH oxidases. *Jpn J Infect Dis* 57:S28–S29.
7. Block K, Gorin Y, Abboud HE (2009) Subcellular localization of Nox4 and regulation in diabetes. *Proc Natl Acad Sci USA* 106:14385–14390.
8. Kawahara T, Lambeth JD (2007) Molecular evolution of Phox-related regulatory subunits for NADPH oxidase enzymes. *BMC Evol Biol* 7:178.
9. Valko M, et al. (2007) Free radicals and antioxidants in normal physiological functions and human disease. *Int J Biochem Cell Biol* 39:44–84.
10. Takemoto D, Tanaka A, Scott B (2007) NADPH oxidases in fungi: Diverse roles of reactive oxygen species in fungal cellular differentiation. *Fungal Genet Biol* 44: 1065–1076.
11. Grissa I, Bidard F, Grognet P, Grossetete S, Silar P (2010) The Nox/Ferric reductase/Ferric reductase-like families of Eumycetes. *Fungal Biol* 114:766–777.
12. Cano-Domínguez N, Alvarez-Delfín K, Hansberg W, Aguirre J (2008) NADPH oxidases NOX-1 and NOX-2 require the regulatory subunit NOR-1 to control cell differentiation and growth in Neurospora crassa. *Eukaryot Cell* 7:1352–1361.
13. Lardy B, et al. (2005) NADPH oxidase homologs are required for normal cell differentiation and morphogenesis in Dictyostelium discoideum. *Biochim Biophys Acta* 1744:199–212.
14. Malagnac F, Lalucque H, Lepère G, Silar P (2004) Two NADPH oxidase isoforms are required for sexual reproduction and ascospore germination in the filamentous fungus Podospora anserina. *Fungal Genet Biol* 41:982–997.
15. Kawahara T, Quinn MT, Lambeth JD (2007) Molecular evolution of the reactive oxygen-generating NADPH oxidase (Nox/Duox) family of enzymes. *BMC Evol Biol* 7:109.
16. Shatwell KP, Dancis A, Cross AR, Klausner RD, Segal AW (1996) The FRE1 ferric reductase of Saccharomyces cerevisiae is a cytochrome b similar to that of NADPH oxidase. *J Biol Chem* 271:14240–14244.
17. Georgatsou E, Alexandraki D (1994) Two distinctly regulated genes are required for ferric reduction, the first step of iron uptake in Saccharomyces cerevisiae. *Mol Cell Biol* 14:3065–3073.
18. Georgatsou E, Alexandraki D (1999) Regulated expression of the Saccharomyces cerevisiae Fre1p/Fre2p Fe/Cu reductase related genes. *Yeast* 15:573–584.
19. Martins LJ, Jensen LT, Simon JR, Keller GL, Winge DR (1998) Metalloregulation of FRE1 and FRE2 homologs in Saccharomyces cerevisiae. *J Biol Chem* 273:23716–23721.
20. Wyman S, Simpson RJ, McKie AT, Sharp PA (2008) Dcytb (Cybrd1) functions as both a ferric and a cupric reductase in vitro. *FEBS Lett* 582:1901–1906.
21. Klinger H, et al. (2010) Quantitation of (a)symmetric inheritance of functional and of oxidatively damaged mitochondrial aconitase in the cell division of old yeast mother cells. *Exp Gerontol* 45:533–542.
22. Stolze K, Udilova N, Nohl H (2000) Spin trapping of lipid radicals with DEPMPO-derived spin traps: Detection of superoxide, alkyl and alkoxyl radicals in aqueous and lipid phase. *Free Radic Biol Med* 29:1005–1014.
23. Ralser M, et al. (2007) Dynamic rerouting of the carbohydrate flux is key to counteracting oxidative stress. *J Biol* 6:10.
24. Loewen CJ, Young BP, Tavassoli S, Levine TP (2007) Inheritance of cortical ER in yeast is required for normal septin organization. *J Cell Biol* 179:467–483.
25. Friedman JR, et al. (2011) ER tubules mark sites of mitochondrial division. *Science* 334: 358–362.
26. O'Donnell BV, Tew DG, Jones OT, England PJ (1993) Studies on the inhibitory mechanism of iodonium compounds with special reference to neutrophil NADPH oxidase. *Biochem J* 290:41–49.
27. Bedard K, Krause KH (2007) The NOX family of ROS-generating NADPH oxidases: Physiology and pathophysiology. *Physiol Rev* 87:245–313.
28. Madeo F, et al. (2002) A caspase-related protease regulates apoptosis in yeast. *Mol Cell* 9:911–917.
29. Khan MA, Chock PB, Stadtman ER (2005) Knockout of caspase-like gene, YCA1, abrogates apoptosis and elevates oxidized proteins in *Saccharomyces cerevisiae*. *Proc Natl Acad Sci USA* 102:17326–17331.
30. Heeren G, et al. (2009) The mitochondrial ribosomal protein of the large subunit, Afo1p, determines cellular longevity through mitochondrial back-signaling via TOR1. *Aging (Albany NY)* 1:622–636.
31. Hauptmann P, et al. (2006) Defects in N-glycosylation induce apoptosis in yeast. *Mol Microbiol* 59:765–778.
32. Desouki MM, Kulawiec M, Bansal S, Das GM, Singh KK (2005) Cross talk between mitochondria and superoxide generating NADPH oxidase in breast and ovarian tumors. *Cancer Biol Ther* 4:1367–1373.
33. Hillenmeyer ME, et al. (2008) The chemical genomic portrait of yeast: Uncovering a phenotype for all genes. *Science* 320:362–365.
34. Haarer B, Viggiano S, Hibbs MA, Troyanskaya OG, Amberg DC (2007) Modeling complex genetic interactions in a simple eukaryotic genome: Actin displays a rich spectrum of complex haploinsufficiencies. *Genes Dev* 21:148–159.
35. Spector I, Shochet NR, Kashman Y, Groweiss A (1983) Latrunculins: Novel marine toxins that disrupt microfilament organization in cultured cells. *Science* 219:493–495.
36. San Martín A, Griendling KK (2010) Redox control of vascular smooth muscle migration. *Antioxid Redox Signal* 12:625–640.
37. Sopko R, et al. (2006) Mapping pathways and phenotypes by systematic gene overexpression. *Mol Cell* 21:319–330.

Supporting Information

Rinnerthaler et al. 10.1073/pnas.1201629109

SI Results

Specific Activity of Yno1p. Yeast WT cells transformed either with the empty plasmid pYES2 or with pYES2-*YNO1* and grown with galactose as carbon source to induce expression of the insert were broken up as described in *SI Materials and Methods*. Microsomes were prepared and reactive oxygen species (ROS) production and protein content were determined in the 2,000 × *g* supernatant and in the purified microsome fraction (100,000 × *g* pellet). The increase in specific activity (ROS production/micrograms of protein) comparing the two fractions was 4.49-fold for WT cells without overexpression of Yno1p, and 1.86-fold for WT cells overexpressing Yno1p. Experiments were done three times with very similar results. The smaller purification factor for the overexpression strain is due to its larger Yno1 protein content in the microsomes.

SI Materials and Methods

Phylogenetic Tree. The phylogenetic tree was built with 94 full-length sequences of known NADPH oxidases and ferric reductases, on the basis of the nearest neighbor joining method (1) with the program AlignX as part of the Vector NTI Advance10 Suite (Invitrogen). The tree was displayed with the Interactive Tree Of Life (http://itol.embl.de/index.shtml).

Determination of Free Iron. The free iron concentration was measured according to ref. 2. Briefly, 70 μL of the cleared cell lysate was mixed with 100 μL 1 M Tris-HCl pH 7.4, 60 μL 10% (wt/vol) SDS, 20 μL 1 M sodium dithionite, 100 μL of 100 mM bathophenantroline, and 650 μL H_2O. The mixture was incubated for 5 min at 20 °C and pelleted for 5 min at 10,000 × *g*. The absorption spectra of the supernatant was then measured between 500 and 700 nm, with an absorption peak at 540 nm, representing the measured Fe^{2+}-bathophenantroline complex. A calibration curve was obtained using appropriate $FeSO_4$ concentrations.

Determination of Total Iron by Atomic Absorption Spectrometry. Total iron concentration was determined by graphite furnace atomic absorption spectrophotometry using an instrument (Perkin-Elmer; 5000 Zeeman) equipped with an electrothermal atomization unit (HGA-500) and an automatic sample injector (AS-40). The absorption at 248.3 nm (0.2 nm, low slit) from an iron hollow cathode lamp was measured. A total of 20 μL of sample was injected in a pyrolytical graphite tube. The area under the atomization signal peak was integrated by the instrument. All final samples contained 0.01 M HNO_3 to prevent the absorption of trace metal onto the cup wall.

DNA Manipulations and Cloning Techniques. All genes were first cloned into the mammalian expression vector pcDNA3.1/HYGRO(−) (Invitrogen), then subcloned into different plasmids.

The following yeast shuttle vectors were used in this study: For GFP fusions the centromeric vector pUG35 was used (3). For overexpression experiments the galactose-inducible plasmid pYES2 (Invitrogen) and the doxycycline-inducible vector pCM297 (4) were used.

PCR products were amplified with the KOD polymerase (Novagen). Restriction enzymes were obtained from Fermentas. All constructs were sequenced at Eurofins MWG Operon. The inserts *FRE1*, *FRE4*, and YGL160W were subcloned from the plasmid pCDNA3.1/HYGRO(−) into the vector pCM297 with PmeI. *FRE8* was cloned from pGEM-T into plasmid pCDNA3.1/HYGRO(−) and pCM297 with NotI. pCDNA3.1/HYGRO(−)–*FRE3* was cut with KpnI, the sticky end was blunted with the Klenow polymerase, then cut with BamHI and cloned into the vector pCM297 linearized with BamHI and HpaI. FRE7 was cut out from the plasmid pCDN3.1/HYGRO(−) and cloned into the vector pCM297 with EcoRI. The ORF YGL160W was cut out from pCM297 and cloned into pYES2 with BamHI. *FRE1* was excised from pCDNA3.1/HYGRO(−) with SacI and cloned into the vector pYES2. *PaNOX1* and *PaNOX2* were cut out from the vector pFL61 with NotI and cloned into pCM297. *PaNOX1* was subcloned from pCM297 to vector pYES2 with NotI.

SI Spot Tests

The sensitivity or resistance of a *YNO1* deletion strain was tested by spotting yeast cells on SC −glucose plates containing various concentrations of oxidants, the reductant dithiothreitol (DTT) or wiskostatin: menadione (0.05–0.35 mM), diamide(1–2 mM), *tert*-butyl hydrogen peroxide (0.8–2 mM), H_2O_2 (1–5 mM), wiskostatin (10–50 μM), and DTT (10–50 mM). Both WT and Δ*yno1* strains were grown to stationary phase in liquid SC −glucose and were then diluted to the following OD_{600} values: 3.0, 1.0, 0.3, and 0.1. Ten-microliter aliquots were spotted onto the appropriate plates. The strains were incubated for 3 d at 28 °C.

Electron Microscopy. Sediments were dissolved in 10 μL of appropriate buffer. Five-microliter drops were applied onto glow-discharge–activated (5) formvar/carbon grids and let to adsorb for 30 s. After that, the grids were negatively stained with 2% (wt/vol) uranyl acetate. Samples were viewed in Philips CM100 electron microscope at 80 kV. Digital images were recorded using a slow-scan MegaViewII camera.

Protein Determination. Microsomal pellet was resuspended in 250 mM sucrose, 50 mM Tris pH 4.5, 22 mg/mL octyl-β-D-glucopyranoside (Sigma) were added, incubated for 10 min, and 20 μL of this solution was added to 1 mL of Bradford reagent (Pierce), incubated for 5 min in the dark, and absorbance at 595 nm was measured. Calibration curve was prepared with bovine serum albumine.

Preparation of Yeast Microsomes. A total of 4×10^9 cells of each strain to be tested were pelleted at 1,000 × *g* for 3 min at 4 °C and resuspended in 10 mL 250 mM sucrose, 50 mM Tris-HCl, pH 4.5. Three mL of glass beads (0.25 to 0.5 mm diameter; Merck) were added and the cells were broken in a bead beater (FastPrep-24; MP Biomedical) and transferred to precooled Sorvall SS34 centrifuge tubes and cetrifuged at 2,000 × *g* for 10 min to remove unbroken cells and cell walls. The supernatant was centrifuged at 18,500 × *g* for 10 min at 4 °C to pellet mitochondria. The supernatant was centrifuged at 100,000 × *g* for 2 h in a Sorvall Ultra Pro-80 centrifuge (TH-641 swing-out rotor) and the pellet containing the microsomal fraction (see also electron microscopy) was resuspended in 1 mL 250 mM sucrose, 50 mM Tris-HCl, pH 4.5.

ROS Measurements of Microsomal Fractions. Ninety microliters of the microsomal fraction was mixed with 90 μL of a 10 μg/mL dihydroethidium (DHE) solution in a black microwell plate (Nunc). Appropriate coenzymes and/or inhibitors were added and after a 15-min incubation in the dark at 28 °C the fluorescence was measured in an Anthos Zenyth 3100 (Anthos Labtec Instruments) plate reader with an excitation wavelength of 485 nm and an emission wavelength of 595 nm. Depending on the experiment, 200 μM NADPH or 100 μM NADH was added. To

test inhibition of the NADPH oxidase activity of Yno1p, the microsomal fraction was preincubated with 100 μM diphenyleneiodonium chloride (DPI); Sigma) for 30 min after which treatment NADPH was added.

Endoplasmic Reticulum (ER) Stress. ER stress was induced by the addition of tunicamycin (Sigma) to a final concentration of 10 μg/mL (stock: 1 mg/mL in DMSO) and incubation for 8 h at 37 °C under constant agitation.

Statistical Analysis. Data are reported as mean values of at least three independent determinations and presented as mean ± SD. Statistical analyses were performed using the two-tailed Student *t* test. Significant difference at the *95, **99, and ***99.9% levels.

1. Saitou N, Nei M (1987) The neighbor-joining method: A new method for reconstructing phylogenetic trees. *Mol Biol Evol* 4:406–425.
2. Molik S, Lill R, Mühlenhoff U (2007) Methods for studying iron metabolism in yeast mitochondria. *Methods Cell Biol* 80:261–280.
3. Hegemann JH, et al. (1999) A fast method to diagnose chromosome and plasmid loss in Saccharomyces cerevisiae strains. *Yeast* 15(10B):1009–1019.
4. Klinger H, et al. (2010) Quantitation of (a)symmetric inheritance of functional and of oxidatively damaged mitochondrial aconitase in the cell division of old yeast mother cells. *Exp Gerontol* 45:533–542.
5. Benada O, Pokorný V (1990) Modification of the Polaron sputter-coater unit for glow-discharge activation of carbon support films. *J Electron Microsc Tech* 16:235–239.

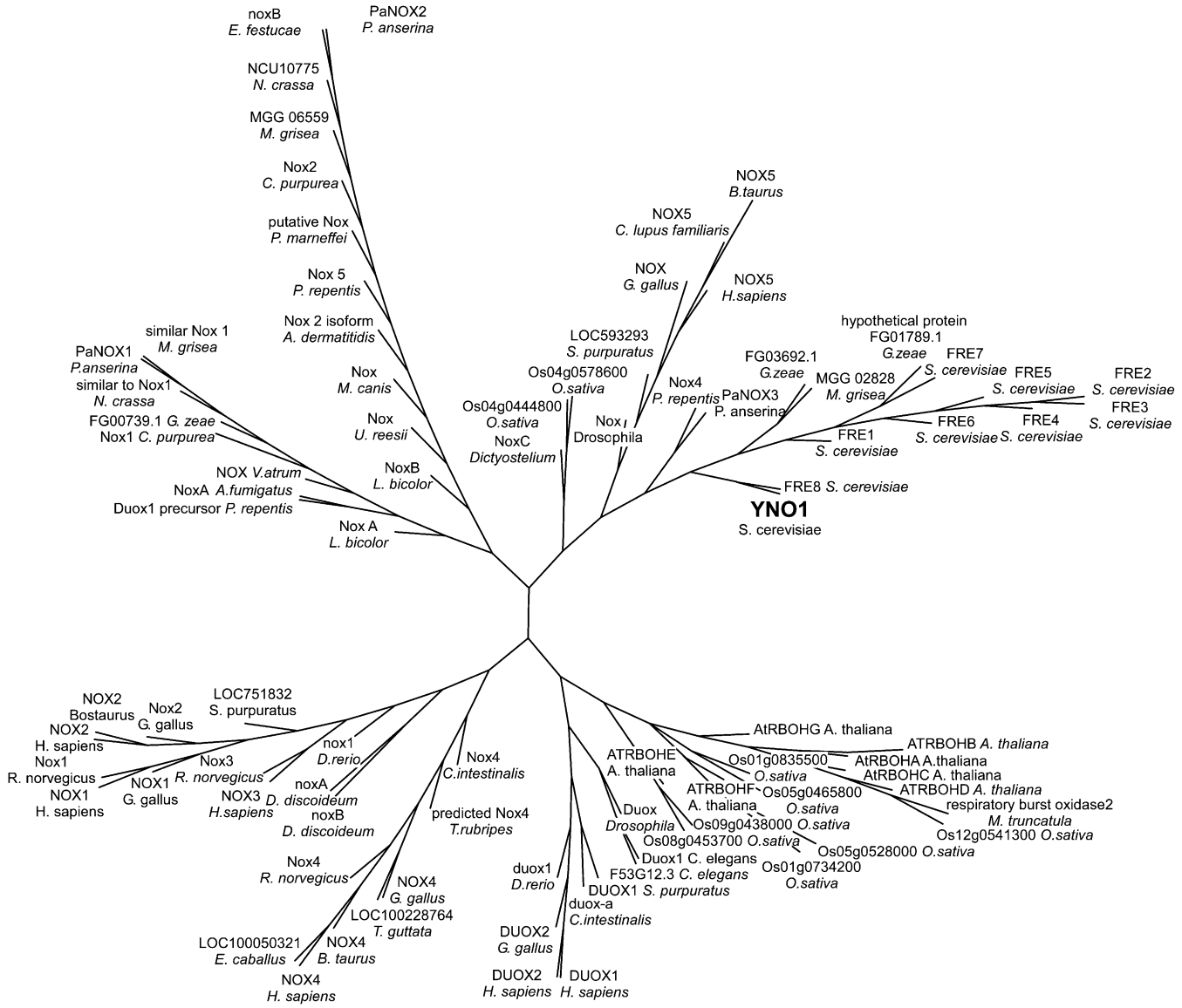

Fig. S1. Phylogenetic tree of NOX enzymes and ferric reductases. Among the nine homologs of this protein superfamily, *FRE1–FRE7* are grouped as very close neighbors, whereas *FRE8* and *YNO1* together cluster at a different location. The closest homolog to *YNO1* is *FRE8*, which is not a ferric reductase (1). Among the fungal members of this protein superfamily, *YNO1* is most closely related to fungal NOXC, and the closest relationship to mammalian NADPH oxidases is to NOX5.

1. De Freitas JM, Liba A, Meneghini R, Valentine JS, Gralla EB (2000) Yeast lacking Cu-Zn superoxide dismutase show altered iron homeostasis. Role of oxidative stress in iron metabolism. *J Biol Chem* 275:11645–11649.

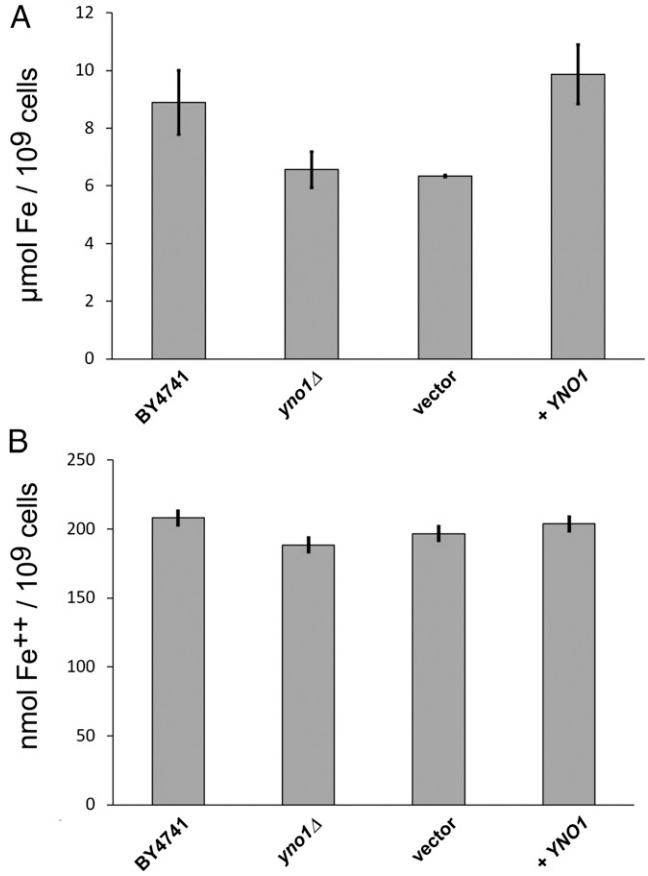

Fig. S2. Iron measurements. (*A*) Total iron measurement with atomic absorption spectroscopy. Total iron concentrations were slightly but not significantly increased when the *YNO1* overexpressing strain was compared with the BY4741 WT strain. (*B*) Measurement of free ferrous iron with bathophenantroline. No significant difference between all four measured cultures could be detected.

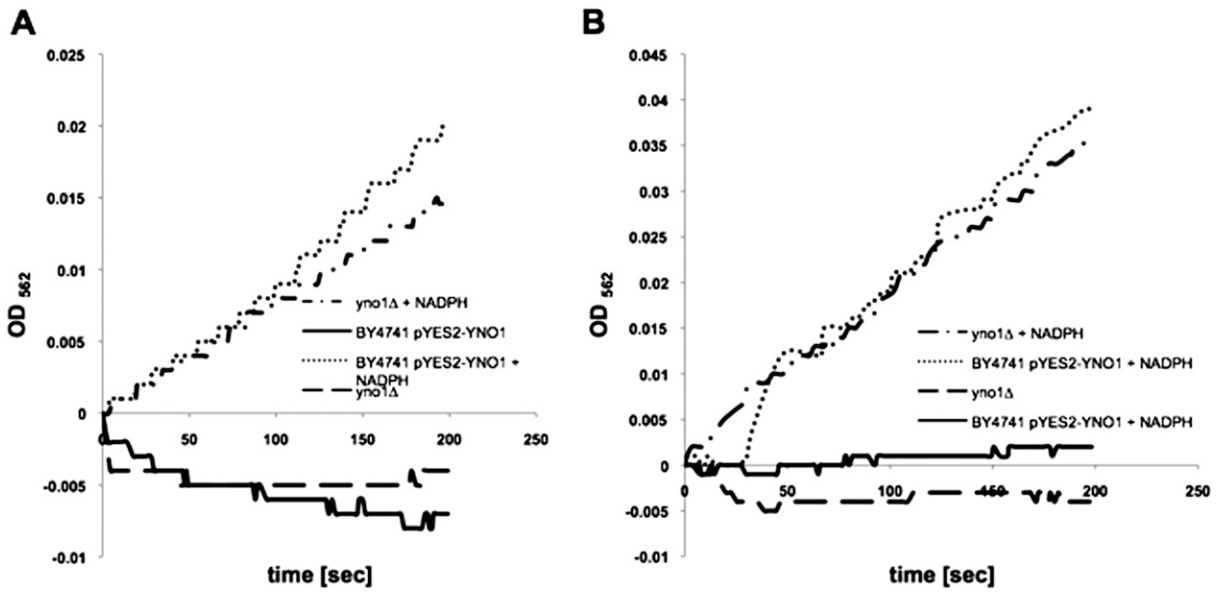

Fig. S3. Determination of ferric reductase activity in yeast microsomes. Two independent experiments are shown measuring ferric reductase activities of microsomes of a strain overexpressing *YNO1* or being deleted for *YNO1*. Conditions were exactly as described by ref. 1 using the buffer described and titrated to pH 6.0. Absorption was normalized by subtraction of blanks. *Upper* curves in each experiment were obtained with the overexpression strain and the deletion strain, respectively, and are very similar, indicating that the small change in arbitrary units over the course of a few minutes is due to a background activity of the microsomes, not to Yno1p. The values obtained were 0.01 and 0.02 arb. units/min. The specific activity of the background ferric reductase was 16 nmol/min × mg protein in experiment A and 27 nmol/min × mg protein in experiment B. *Lower* curves were obtained by leaving out NADPH, showing that the small background activity does depend on NADPH.

1. Wyman S, Simpson RJ, McKie AT, Sharp PA (2008) Dcytb (Cybrd1) functions as both a ferric and a cupric reductase in vitro. *FEBS Lett* 582:1901–1906.

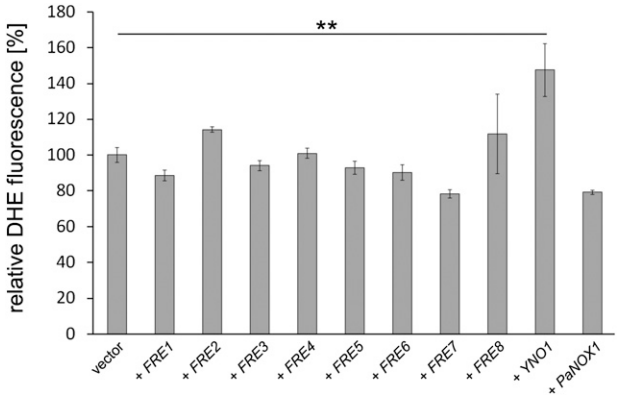

Fig. S4. DHE measurements of the nine members of the NOX/IMR protein family in *Saccharomyces cerevisiae*. All seven putative ferric reductases (*FRE1–FRE7*), *YNO1*, *FRE8*, and *PaNOX1* were cloned into the expression vector pCM297 (4). Expression was induced by the addition of 100 mg/L doxycyline. Only the Yno1p overexpressing strain showed an approximately 50% increase in superoxide levels.

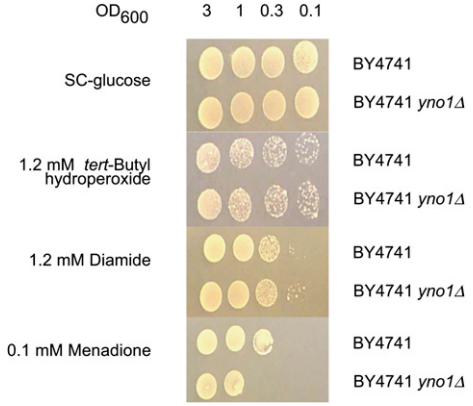

Fig. S5. Wild-type cells and cells deleted for *YNO1* were spotted onto plates containing either *tert*-butylhydroperoxide, diamide, or menadione. The *yno1*Δ deletion mutant was slightly sensitive to menadione, whereas on plates containing *tert*-butyl-hydroperoxide or diamide no difference in growth was observed.

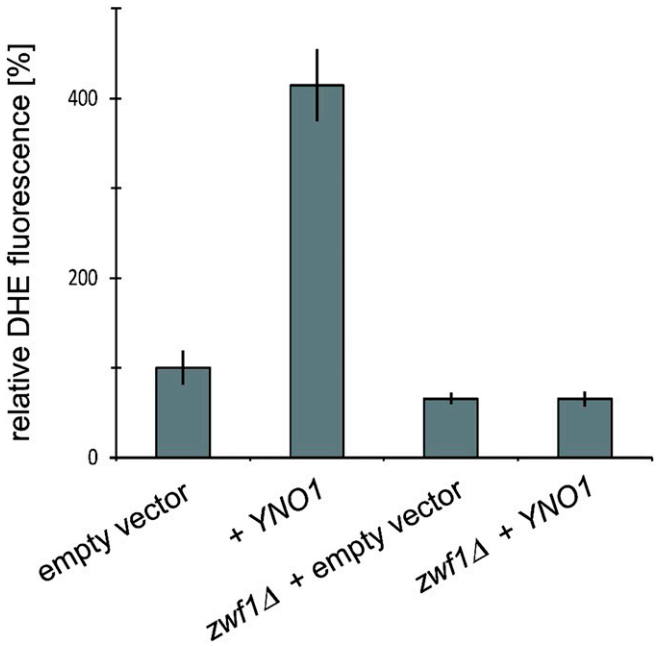

Fig. S6. ROS measurements by DHE fluorescence in the BY4741 background testing the influence of the *zwf1* deletion. Deletion of *zwf1* allows normal growth in the absence of stress. Overexpression of *YNO1* in a *zwf1Δ* strain did not lead to an increase in ROS levels compared with controls, showing that intracellular NADPH is required for ROS production through Yno1p.

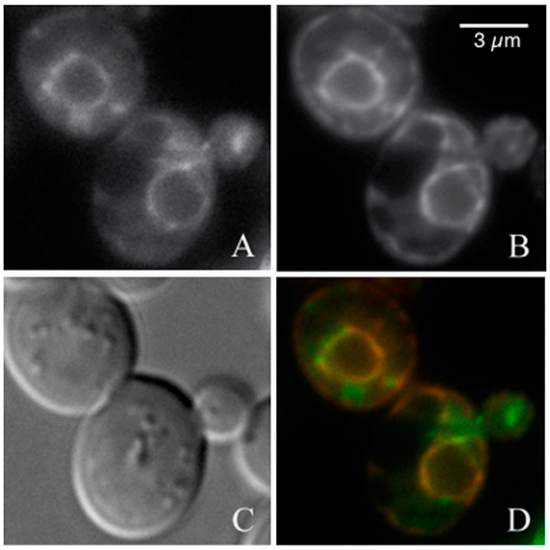

Fig. S7. Two budded yeast cells expressing YNO1-GFP as well as HDEL-RFP (1) were analyzed by fluorescence microscopy as described in *Materials and Methods*. (*A*) YNO1–eGFP stain, (*B*) HDEL-RFP stain, (*C*) phase contrast, and (*D*) overlay of *A*–*C*. Colocalization of both fluorescent markers in the perinuclear ER can be seen. A small part of the YNO1–eGFP is located in the cytoplasm.

1. Friedman JR, et al. (2011) ER tubules mark sites of mitochondrial division. *Science* 334:358–362.

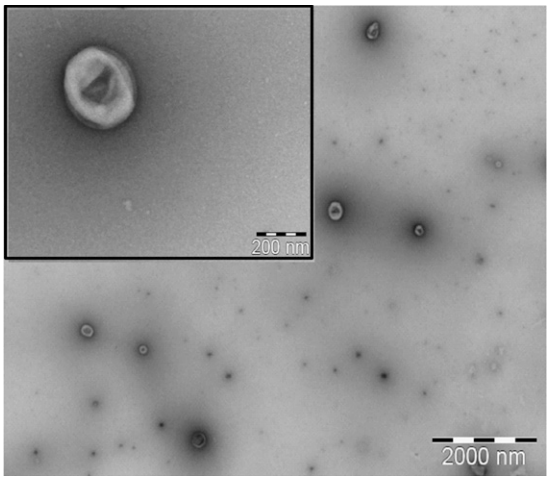

Fig. S8. Transmission electron microscopy of the osmotically stabilized microsomal fraction was performed as described in *SI Materials and Methods*. Microsomes appeared as closed membrane vesicles with diameters between 50 and 200 nm.

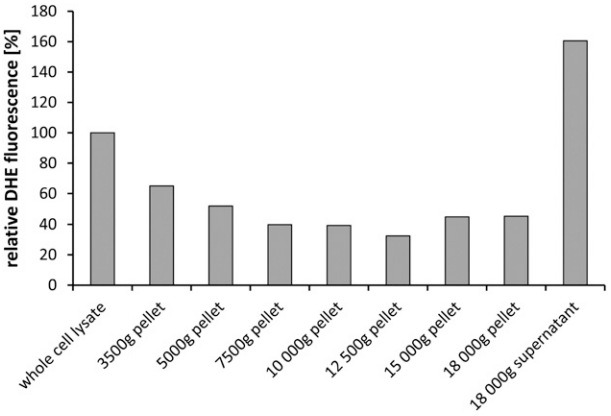

Fig. S9. Cell fractions obtained by differential centrifugation were tested for ROS production after addition of 200 μM NADPH. An increased level in DHE oxidation could only be detected in the microsome-containing 18,000 × *g* supernatant, confirming the results of the ER localization of Yno1p–eGFP. The cells were broken with glass beads in 250 mM sucrose, 50 mM Tris-HCl, pH 4.5, all fractions (pellets were resuspended in 250 mM sucrose, 50 mM Tris-HCl, pH 4.5) were adjusted to equal volumes before ROS measurements.

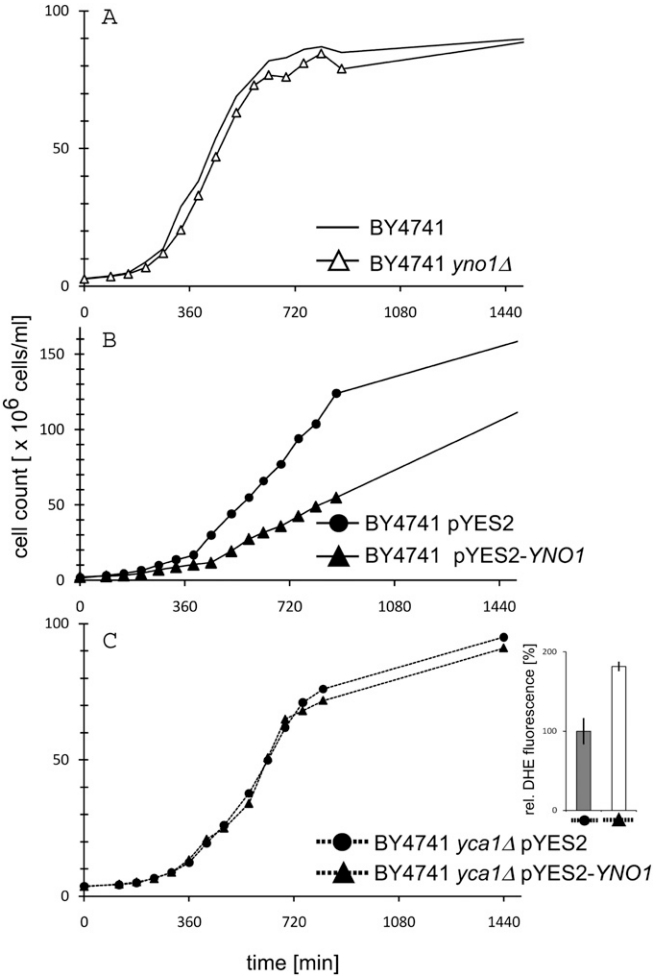

Fig. S10. Growth curves of WT, *yno1Δ*, and *yca1Δ* strains overexpressing YNO1 under galactose control or in the absence of *YNO1* overexpression (vector control). (*A*) WT and *yno1Δ* strain show identical growth kinetics. (*B*) Overexpression of Yno1p substantially slows the growth of BY4741. (*C*) Deletion of the yeast metacaspase, *YCA1*, does not prohibit ROS production in cells overexpressing *YNO1* (*Inset*) but rescues growth kinetics.

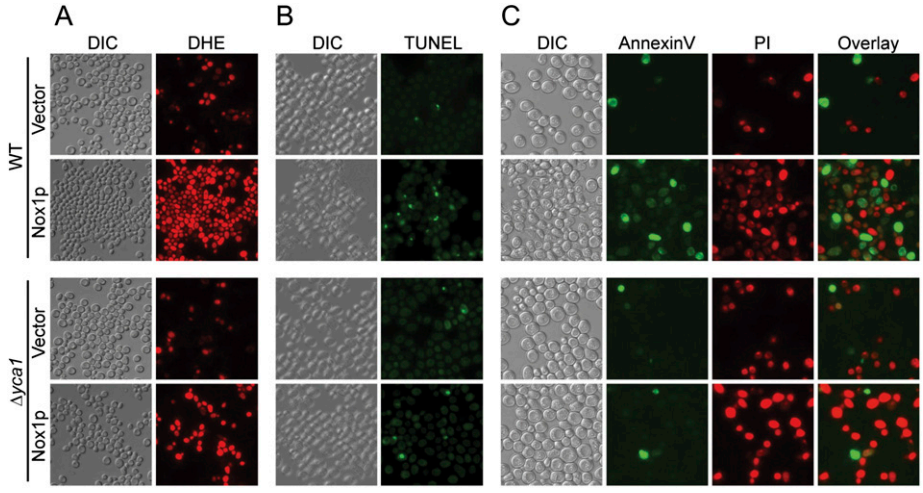

Fig. S11. Examples of the actual fluorescence microscopic determinations of DHE (*A*), TUNEL (*B*), Annexin V, and propidium iodide (PI) (*C*) in four strains (BY4741 pYES2, BY4741 pYES2-*YNO1*, yca1Δ pYES2, and yca1Δ pYES2-*YNO1*). Note that cells staining positively with AnnexinV as well as with PI (late apoptotic) occurred infrequently, but necrotic cells (PI^+) were frequent. Apoptotic markers were prominent in the WT strain overexpressing Yno1, but nearly absent in a strain deleted for YCA1, whereas ROS levels were high in both strains.

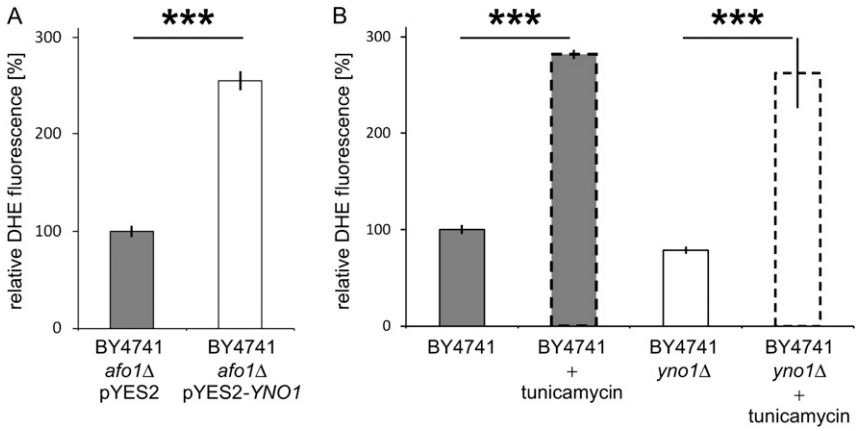

Fig. S12. (*A*) ROS production through *YNO1* overexpression occurred in the *afo1Δ* strain in the same amount as in the control, showing that ROS production through Yno1 is independent of the mitochondrial respiratory chain. (*B*) ROS determinations in BY4741 and *yno1Δ* strains in the presence and absence of tunicamycin (which induces ER stress concomitant with a high level of ROS (1). The fact that tunicamycin induces the same high level of ROS also in an *yno1Δ* strain shows that ER stress is independent of Yno1.

1. Hauptmann P, et al. (2006) Defects in N-glycosylation induce apoptosis in yeast. *Mol Microbiol* 59:765–778.

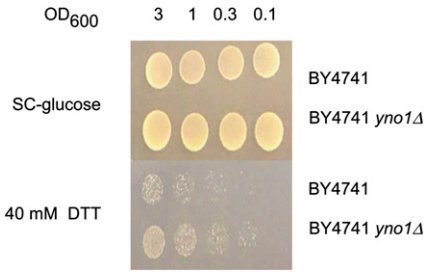

Fig. S13. To test the possible involvement of YNO1 in counteracting reductive stress, wild-type cells and *yno1Δ* cells were spotted on plates containing 40 mM DTT. On these plates, both strains showed similar growth, showing that the deletion of *YNO1* cannot increase reductive stress, which acts primarily through protein aggregation in the ER (1).

1. Trotter EW, Grant CM (2002) Thioredoxins are required for protection against a reductive stress in the yeast Saccharomyces cerevisiae. *Mol Microbiol* 46:869–878.

Table S1. Mean peak intensities (areas under the peaks marked with arrows) and SDs of the superoxide-specific ESR peaks in the two spectra shown in Fig. 2*B*

	BY4741 pYES2	BY4741 pYES2-*YNO1*
Mean	23510.33	79517.67
SD	4626.44	8685.24
SEM	2671.08	5014.42

Three biological replicas each; arbitrary units.

6. Discussion

The single steps of gene expression, as are transcription, RNA processing and transport, translation and RNA decay, are realized by multiprotein and nucleoprotein complexes. Some of these complexes tend to cluster or assemble into high-ordered structures under certain conditions. For example, under a stress, mRNA molecules with their associated proteins accumulate to stress granules (SGs) and processing bodies (PBs). However, a formation of "granules" or "particles" is not limited only to components of mRNA metabolism. Assemblies of metabolic enzymes, cytoskeleton constituents and others can be found in eukaryotic and even prokaryotic cells. Since the phenomenon of accumulation into high-ordered structures is evolutionary conserved from prokaryotes, through lower eukaryotes (yeasts), up to mammals, it is most likely that there is specific physiological functions for these assemblies. We are just at the beginning of understanding this phenomenon. Nowadays, various accumulations and assemblies within the cell are being described and concurrently, dynamics properties of these granules or particles and their possible functions in cellular metabolism are proposed. Nevertheless, the detailed understanding of these entities is still elusive.

It seems that conserved mechanism evolved for assembly of protein complexes into multicomplex accumulations. Certain proteins possess unique domain or domains which are able to self-assemble and dimerize or multimerize the protein or the protein complex into higher-ordered structures. Examples of these proteins are yeast Lsm4 protein with its C-terminal Q/N-rich (glutamine / asparagine) domain, which is engaged in assembly of PBs. Equally, mammalian TIA-1 and TIAR proteins, with their glutamine-rich prion-related domains, promoting assembly of SGs. Despite undeniable, but still rather unknown, physiological function of multicomplex accumulations, there is also "dark side" of the phenomenon. Mentioned proteins with their domains may spin out of control and may irreversibly aggregate, due to various reasons. These aggregates constitute a stress for the cell and it may subsequently lead to pathology. One of the most known examples of such noxious aggregates is represented by prions. Therefore, the understanding of the essence of both protein complex and nucleoprotein complex accumulations, as are stress granules and others, definitely help not only to our better knowledge of entire cellular metabolism, but it helps even in dealing with such pathologies, as are prion and neurodegenerative diseases.

Heat-induced stress granules of *Saccharomyces cerevisiae* are core theme of my PhD thesis. Despite SGs are, in general, extensively studied separately or in relationship with either PBs, signalling pathways or other cellular processes, missing parts in understanding of their dynamics and involvement in cellular metabolism still exist. Here, the characterization of heat-induced SGs of *S. cerevisiae* is presented. Firstly, heat stress effects on the yeast translation and mRNA metabolism is discussed, followed by a description of currently valid model of dynamic relationship among certain messenger ribonucleoprotein complexes (mRNPs) integrated in the "mRNA cycle". Concurrently, present knowledge about connection between translation inhibition and SGs assembly is submitted. Secondly, robust heat shock-induced SGs are described in the context of other yeast SGs. For the third, data about yeast heat-induced SGs are presented with a focus on their relationship to PBs, on dynamics of their assembly and on possible models of translation alterations leading to their formation. Taken together, a comprehensive view on the yeast translation under a heat stress and on heat-induced SGs of *S. cerevisiae* is submitted. In the next part, newly discovered connections of Mmi1 / Tma19 protein to both yeast heat-induced SGs and protein degradation machinery are presented. A possible role for this SGs-associated protein in heat stress response is suggested. Finally, an impact of a stress on protein homeostasis in general is discussed. Special attention is paid to the yeast NADPH oxidase enzyme family member and *Reactive Species*-producer, Yno1 protein, and to its predicted roles in the yeast metabolism.

Heat stress and translation

Yeast *Saccharomyces cerevisiae*, as well as other living organisms, needs to adapt to changing environmental conditions. One of a factor influencing the being of this single cell and non-motile living form is temperature. *S. cerevisiae* is a mesophilic organism, meaning that its temperature optimum for growth is between 25°C and 30°C. An exposure to temperature of about 37°C and higher triggers multiple changes in cell physiology, including alteration of genes expression profiles and translation. Whereas the yeast cells are able to adapt to heat stress at 37°C and resume growth (for a review see (Morano, Grant et al. 2012)), the cells heat shocked at 46°C inhibit growth and during prolonged treatment at given temperature become die ((Rinnerthaler, Lejskova et al. 2013) (Cherkasov, Hofmann et al. 2013) and our unpublished data). In terms of translations, cultivation at 37°C leads to transient and weak inhibition of translation initiation and, together with simultaneous gene expression reprogramming, synthesis of stress-responsive proteins is triggered ((Meier,

Deloche et al. 2006) (Yamamoto and Izawa 2013) and for a review see (Estruch 2000)). Neither assembly of microscopically visible processing bodies (PBs) nor stress granules (SGs) has been documented upon this stress[2] (Brengues, Teixeira et al. 2005) (Kilchert, Weidner et al. 2010) (Yamamoto and Izawa 2013). In contrast, multiple aspects of mRNA metabolism are affected upon cultivation at 46°C (for details see *Review of Literature*). Among these effects, translation is massively inhibited, mRNP complexes (mRNPs) are remodelled and redirected from translation cycle to stress-induced mRNPs accumulations, which are SGs (Grousl, Ivanov et al. 2009). The dynamics of mRNPs "movement" among active translation, SGs and even PBs, under both stress conditions and right after that, is described in the proposed "mRNA cycle" model.

The "mRNA cycle"

As we showed in the report Grousl et al., 2009, robust heat shock at 46°C has dramatic effect on translation and polysome profile of *S. cerevisiae* (Grousl, Ivanov et al. 2009). A fraction of polysomes completely disappears and 80S/monosome peak is significantly enriched indicating inhibition of translation initiation. It is in conformity with effects of other stresses, as are glucose deprivation or azide treatment (Ashe, De Long et al. 2000) (Buchan, Yoon et al. 2011). It was documented that under such stress conditions, mRNA molecules (mRNAs) leave active translation and accumulate in other types of cytoplasmic messenger ribonucleoprotein complexes (mRNPs). Processing bodies and stress granules are the most common examples of such complex accumulations. Herein, the fate of mRNAs is further determined. Translationally repressed mRNAs can be, either stored for later usage, degraded or sent back to active translation. The "mRNA cycle" model has been proposed for the transition and remodelling of distinct mRNPs among different states and subcellular locations (see also *Review of Literature*).

In spite of mRNAs are translationally repressed in both SGs and PBs, the function of these entities in the "mRNA cycle" is different. Whereas SGs are thought to be sites where mRNAs are stored for later usage in translation, PBs are primarily linked to mRNA decay. However, this basic view is continually supplemented by additional data and thus, nowadays, it is evident that SGs do not serve only as a transient depository of mRNAs and that PBs are not only linked to mRNA decay. SGs have been shown to sequestrate even proteins which

[2] It was reported that under combination of heat stress at 37°C together with ethanol stress (5% v/v), SGs and PBs are formed (Yamamoto and Izawa 2013).

play roles in cellular signalling pathways and in other metabolic processes connecting SGs with such actions as are cell fate (survival / apoptosis) decision, immune response, cell adhesion and others (for reviews see (Anderson and Kedersha 2008) and (Kedersha and Anderson 2009)). PBs are, beyond mRNA decay, engaged in such processes as are translation repression, mRNA storage, mRNA quality control and mRNA-mediated gene silencing (for a review see (Eulalio, Behm-Ansmant et al. 2007)). Moreover, the very nature of mRNA decay in PBs is still under a debate. In connection, it was shown, on the one hand, that mRNA degradation intermediates accumulate in PBs (Sheth and Parker 2003), but, on the other hand, abolishment of assembly of microscopically visible PBs does not influence mRNA decay rates (Eulalio, Behm-Ansmant et al. 2007). It is plausible that mRNA decay truly occurs in mRNP complexes which constitute PBs, but accumulation of these mRNP complexes into high-ordered and microscopically visible structures is not essential for mRNA degradation.

Back to the "mRNA cycle" model, certain mRNP complexes can be remodelled and mRNA molecules with some associated protein factors can thus move between different subcellular functional locations. Such an example is mRNAs transition from translating polysomes to SGs or PBs. In addition, mRNA can be sent back to active translation from PBs (Brengues, Teixeira et al. 2005) and it is expected that even from SGs. However, the former case seems not to be universally valid (Arribere, Doudna et al. 2011). Whether mRNA molecules are able to move even from SGs to PBs is currently unknown, but it is assumed (Kedersha and Anderson 2009) (Buchan and Parker 2009). According to a hypothesis, SGs represents transient stage on mRNA route from PBs back to translation process (Brengues and Parker 2007). However, the increasing body of evidence suggests that SGs can be formed even independently on PBs (Hoyle, Castelli et al. 2007) (Shah, Zhang et al. 2013). It seems likely that SGs are assembled either dependently or independently on PBs regarding type, intensity and the speed of onset of a stress. In this respect, robust heat shock represents a kind of stress which can induce SGs independently of PBs (Grousl, Ivanov et al. 2009). On the other hand, for example, glucose deprivation triggers formation of SGs in conjunction with PBs (Buchan, Muhlrad et al. 2008). Taken in general, milder stresses, which slightly and temporary attenuate translation in the cell, usually result in PBs appearance. Upon continuing stress or under an increase of its intensity, SGs may subsequently also appear, usually in conjunction with and more or less dependently on pre-existing PBs. Whereas robust alteration of translation profile, which is manifested by block of global translation and complete or almost complete loss of active translation, is preferentially linked to immediate SGs assembly,

independently on the presence of PBs ((Arribere, Doudna et al. 2011) and for reviews see (Anderson and Kedersha 2002) and (Buchan and Parker 2009)).

Taken together, the "mRNA cycle" model proposes possible dynamic inter-connection among translation process and stress-responsive mRNPs accumulations, as are SGs and PBs. Whether this model is universal for all of mRNA molecule species or not needs to be further established. Equally, with the respect to current knowledge, specific nature of every applied stress must be taken into account when considering particular steps of the "mRNA cycle". Either way, we are still far from complete and detailed understanding of particular stress effects on translation and mRNA metabolism.

Stress granules assembly-coupled translation inhibition

Regulation of translation offers possibility to rapidly balance changed protein demands under mild cellular environment perturbations. Similarly, translation regulation enables to safe cell energy and material resources by shut down of global protein synthesis and simultaneously to engage stress-specific translation program under severe stresses.

Translation initiation stage seems to be effective step to regulate entire translation process and indeed, regulatory mechanisms targeting translation initiation are widely utilized across eukaryotic kingdom. Equally, inhibition of translation initiation and formation of stalled translation pre-initiation complexes are viewed as general mechanism to induce SGs formation. The model is based on various observations from various organisms. Firstly, stresses which result in phosphorylation of eIF2 factor, and in its consequences in both, lower availability of the initiator ternary complex and translation initiation inhibition (for a detail see *Review of Literature*), trigger SGs assembly. The eIF2 phosphorylation is sufficient to promote SGs formation (in mammalian cells) (Kedersha, Gupta et al. 1999) (Kimball, Horetsky et al. 2003). Secondly, alterations in translation initiation dynamics elsewhere than on the level of eIF2 factor also elicit SGs assembly. Inhibition of eIF4A and eIF4G factors functions are the examples (Dang, Kedersha et al. 2006) (Mazroui, Sukarieh et al. 2006). For the third, polysome profile analyses demonstrate that translation profile is markedly altered with characteristics for inhibition of translation initiation upon stresses capabled to induce SGs (e.g. (Kedersha, Chen et al. 2002) (Grousl, Ivanov et al. 2009)). Finally, the composition of SGs reassembles mRNA "closed loop" structure (for details see *Review of Literature*) stalled in translation initiation process (Kedersha, Chen et al. 2002) (Kimball, Horetsky et al. 2003) (Grousl, Ivanov et al. 2009) (Yamamoto and Izawa 2013).

However, yeast SGs fit to this model only partially. Despite phosphorylation of eIF2 is a well-known mechanism to induce mammalian SGs (Kedersha, Gupta et al. 1999), with the exception of glucose deprivation-induced SGs of *S. cerevisiae*, all of other known the yeast SGs form independently on eIF2 factor phosphorylation (see also *Review of Literature*). *S. cerevisiae*, unlike higher eukaryotes, possess only one kinase (Gcn2) which phosphorylates eIF2 factor (Proud 2005). It was proved by the usage of *gcn2Δ* strains or eIF2 factor mutants that SGs can be induced even in the mutant background, thus without eIF2 phosphorylation (Grousl, Ivanov et al. 2009) (Buchan, Yoon et al. 2011) (Kato, Yamamoto et al. 2011). However, it was shown, on the example of heat stress-induced SGs, that eIF2 factor is, in the presence of Gcn2 kinase, actually phosphorylated under a heat stress (Grousl, Ivanov et al. 2009). It raises possibility that stress-induced phosphorylation of eIF2 factor might naturally contribute to SGs formation even in yeast cells. Nevertheless, the main regulatory and signalling points of SGs assembly reside elsewhere.

In addition to eIF2 factor, an engagement of other translation initiation factors has been shown to influence translation process under a stress and eventually SGs formation. It was shown that drugs inhibiting function of eIF4A helicase provoke inhibition of translation and subsequent SGs formation in mammalian cells (Dang, Kedersha et al. 2006) (Mazroui, Sukarieh et al. 2006). Similarly, glucose depletion leads to release of eIF4A factor from translation pre-initiation complexes and inhibition of translation initiation in the yeast cells (Castelli, Lui et al. 2011). Fusel alcohols directly target yeast eIF2B factor and inhibit its enzyme activity (Ashe, Slaven et al. 2001). In consequence, it leads to reduction of the initiator ternary complex concentration and inhibition of translation. The mode of operation reassembles that of eIF2 factor phosphorylation, but, in this case, eIF2B factor is directly involved. Concerning heat stress, an effect of eIF4E-binding protein Eap1 on the yeast heat stress response was documented. eIF4E-binding proteins are competitive inhibitors of eIF4E factor which is engaged in translation initiation. In mammalian cells, eIF4E-binding protein association with eIF4E is regulated by TOR (Target of Rapamycin) pathway. However in the yeast, the regulation is not so clear and it is still not completely understood (for a review see (Simpson and Ashe 2012)). Nevertheless, Eap1 protein has been shown to influence heat stress response suggesting involvement of eIF4E-binding proteins and eIF4E itself in the process (Meier, Deloche et al. 2006).

Under certain conditions, regulation of post-initiation stages of translation enters the game, too. These mechanisms may provide a fine-tuning of translation program under specific growth conditions and stresses or can possibly be the main translation regulatory force. Such

an example is documented by an evidence of translating ribosome stalling by Stm1 protein. This protein is capable to stall ribosome right after 80S ribosome formation and is proposed to play regulatory role in translation under nutrient deprivation stress (Van Dyke, Baby et al. 2006) (Van Dyke, Pickering et al. 2009) (Balagopal and Parker 2011). Other evidence about regulation of translation elongation comes from research on oxidative stress effects on translation. Attenuation of elongating ribosomes along with enrichment of polysomes on mRNAs were observed upon yeast cell exposure to high dose of hydrogen peroxide (Shenton, Smirnova et al. 2006). In both just mentioned cases of translation elongation regulation, those authors believe that stalling translation in elongation phase offers source of "ready-to-use" transcripts, already engaged in translation, for a subsequent recovery from a stress. It is worth to note that possible regulation of translation upon robust heat stress must operate differently, because, in this case, mRNAs do not stay with ribosomes, but leave translation apparatus and accumulate in SGs. Nevertheless, the presence of translation elongation and termination factors in heat-induced SGs of *S. cerevisiae* opens up a possibility that the translation phases in which these factors are engaged are primary targets for translation regulation under heat stress (see *the next* chapter).

Heat stress-induced stress granules

It was reported that stress granules are formed in higher eukaryotes' cells under various conditions including heat stress (for a review see (Anderson and Kedersha 2006)). In fission yeast *Schizosaccharomyces pombe*, SG-like structures were observed upon treatment at 42°C (Dunand-Sauthier, Walker et al. 2002). However, SGs or SGs-analogous structures have not been primarily observed at this temperature in *S. cerevisiae*[3] (Grousl, Ivanov et al. 2009). Therefore, we increase temperature of heat shock to 46°C and found that granules which reassemble in composition and dynamics SGs of higher eukaryotes appear in the yeast cytoplasm (Grousl, Ivanov et al. 2009). On the contrary to, up to that time, the only known yeast SGs of glucose deprived cells, heat-induced SGs contain typical SGs components represented by translation initiation factor eIF3 and small ribosomal subunit. With the respect to widely accepted hypothesis that SGs are mainly formed by stalled translation pre-initiation complexes, heat-induced SGs contain also mRNA molecule, poly(A) binding protein Pab1 and translation initiation factor eIF4G. All of aforementioned components, together with

[3] Until the report Grousl et al., 2013.

eIF4E factor (also component of SGs), are constituents of translation pre-initiation complexes on "closed loop" structured mRNA molecule (for details see *Review of Literature*). Other factors engaged in translation initiation are not present in the SGs (e.g. eIF2) or its presence has not been analyzed (e.g. eIF1, eIF1A).

The composition of yeast SGs varies depending on applied stress. Only some of them contain core translation pre-initiation components (see *Review of Literature*). Heat-stress induced SGs are example of such of them (Grousl, Ivanov et al. 2009). However, additional constituents of the SGs somehow undermine, at the present time, widely accepted hypothesis about SGs as primarily mRNPs accumulations of stalled translation pre-initiation complexes. Finding that translation elongation and termination factors are present in heat-induced SGs of *S. cerevisiae* opened the question about function of these factors within SGs (Grousl, Ivanov et al. 2013). One possible explanation is that translation is primarily modulated on the level of elongation upon heat stress. The alteration in translation elongation dynamics subsequently leads to global translation shut down accompanied by a block in translation initiation processes as in universal regulatory point of translation. However, physical presence of elongation and termination factors in SGs seems not to be essential for this scenario. Alternative roles of the identified factors in translation post-termination processes (see *Review of Literature*) bring another hypothesis about their connection to heat-induced SGs. Translation elongation factor eEF3 together with both release factors eRF1 and eRF3 have been shown to participate in releasing of ribosome-bound mRNA and tRNA molecules from the ribosome after the end of a protein synthesis (Kurata, Nielsen et al. 2010). The presence of just these factors in the SGs can be pointing to connection between SGs and translation post-termination process. In other words, it may suggest that alteration in translation post-termination dynamics under heat stress can lead to assembly of SGs. However, the hypothesis about interconnection of SGs and translation post-termination has a couple of inconsistence. It is important to mention that the exact mechanism of translation post-termination is still not completely clear. Alternative hypothesis about the process exists, which operates with other factor than eEF3, namely with Rli1 protein (Shoemaker and Green 2011). It is for sure that further research is essential for better knowledge of this stage of translation. Another inconsistence concerns the fact that the large ribosomal subunit (60S), which is a component of post-termination complexes, does not translocate to the SGs upon heat stress ((Grousl, Ivanov et al. 2009) (Grousl, Ivanov et al. 2013). Thus, according to the present hypotheses, it is not possible that heat-induced SGs represent genuine translation post-termination complexes. The possibility where a release of translation elongation and termination factors

from active translation and their subsequent accumulation in mRNPs assemblies is a consequence of primarily translation initiation inhibition cannot be excluded, too.

Translation elongation and termination factors contained in heat-induced SGs may also serve as structural elements or directly as scaffolds of the SGs. This possibility is supported by the fact that under milder heat stress (at 42°C), which is unable to induce genuine SGs and when translation is not as affected as under robust heat stress, only some SGs components accumulate into visible cytoplasmic foci and eEF3 with eRF1 are present among these factors (Grousl, Ivanov et al. 2013). Translation elongation and termination factors have never been observed in any SGs of any organism and cell type. Nevertheless, the release factors have been found within PBs in stationary phase of growth and under glucose deprivation in yeasts (Dori and Choder 2007) (Buchan, Muhlrad et al. 2008). A role of these factors in PBs assembly has been proposed. Similar function for translation elongation and termination factors in heat stress-induced SGs assembly can be also suggested.

As well as composition of SGs varies depending on certain stresses, protein factors required for SGs assembly differ among applied stresses. In mammalian cells, it was proved that TIA-1 and TIAR proteins play essential role in SGs formation (Kedersha, Gupta et al. 1999) (Gilks, Kedersha et al. 2004). In the yeast cells, a formation of heat stress-induced SGs is, however, independent on these structural elements, which are Pub1 (ortholog of TIA-1) and Ngr1 (ortholog of TIAR) (Grousl, Ivanov et al. 2009). Similarly, newly discovered heat-induced SGs constituent, eRF3 / Sup35, has been shown to do not influence assembly and dynamics of the SGs. Sup35 protein possesses prion-like domain, which is able to convert the protein into its prion form [PSI+] (Ter-Avanesyan, Dagkesamanskaya et al. 1994) (Derkatch, Chernoff et al. 1996). Unlike in yeast case, these self-assemble domains have been reported to drive assembly of mammalian SGs (Gilks, Kedersha et al. 2004). Equally to heat-induced SGs, formation of other known yeast SGs is independent on either Pub1 or Ngr1, with the exception of Pub1 and glucose deprivation-induced SGs. Those SGs are also structurally dependent on Pbp1, which is ortholog of mammalian Ataxin-2, and on eIF4G factor being again an exception among yeast SGs (Buchan, Muhlrad et al. 2008). For the third, SGs assembly of glucose deprived cells have been identified to be dependent on otherwise scaffolds of PBs, Lsm4 and Edc3 proteins (Buchan, Muhlrad et al. 2008) (Decker, Teixeira et al. 2007). Neither heat stress-induced nor azide treatment-induced SGs need these proteins for their assembly (Grousl, Ivanov et al. 2009) (Buchan, Yoon et al. 2011). On the contrary, azide-induced SGs are structurally linked to translation repressors Dhh1, Pat1 and Scd6 (Buchan, Yoon et al. 2011) (Rajyaguru, She et al. 2012). Taken together, it seems that SGs

composition and dynamics properties relay on *modus operandi* of particular stress and thus likely reflect involvement of different signalling pathways and mechanisms of SGs assembly.

Heat stress is able, as other stresses, induced either PBs or SGs regarding intensity of the stress. It was shown that *S. cerevisiae* cells cultivated at 39°C trigger formation of PBs but not SGs (Cowart, Gandy et al. 2010). Interestingly, when applied combined heat stress at 37°C with mild ethanol stress (5% v/v), SGs are formed (Yamamoto and Izawa 2013). Otherwise, the crucial temperature for the yeast metabolism to induced PBs and / or SGs seems to be 42°C. At this temperature, PBs, represented by Dcp2 and Xrn1 proteins, have been observed (Scarcelli, Viggiano et al. 2008). However, under these conditions, the PBs extensively co-localize with so called REGs (RNA export granules). These granules contain Rat8 protein, mRNA exporting receptor Mex67, mRNA itself and may harbour stress granule marker protein Pab1 (for details see (Scarcelli, Viggiano et al. 2008)). Moreover, we found that formation of Dcp2 accumulations at 42°C is independent on PBs scaffolds Edc3 and Lsm4 and that Dcp2 co-localizes, at the time, with stress granule markers Ngr1, Pub1 and also with other heat-induced SGs constituents, eEF3 and eRF1 factors. Finally, we proved that the joint mRNPs accumulations formed at 42°C are continuously transformed into fully-developed SGs upon increasing temperature from 42°C to 46°C (Grousl, Ivanov et al. 2013). With the respect to the aforementioned data, it can be anticipated that depending on an onset of the stress, either SGs are formed independently on PBs upon severe heat shocks or PBs are remodelled to SGs during slowly increasing temperature (see also *The "mRNA cycle"* chapter).

According to widely and at the present time accepted hypothesis, mRNAs and components of translation machinery contained within SGs are returned back to active translation after stress relief. Nevertheless, the direct proof about this has not been submitted, yet. Assuming that SGs are composed mostly of stalled translational pre-initiation complexes, they actually represent cytoplasmic sites where translation machinery is inactive, but locally concentrated. When the stress alleviates, SGs may thus confer platform for efficient restoration of translation, as was proposed even before (Parker and Sheth 2007). Our finding that a key translation initiation component, eIF2α (Sui2) factor, (for details see *Review of Literature*) accumulates on dissolving SGs during recovery from heat stress supports aforementioned hypothesis (Grousl, Ivanov et al. 2013). Nevertheless, the process of re-entry of SGs components back to active translation is not operating for 100%, as well as in the case of other biological and even mechanical processes. Under certain conditions, e.g. prolonged stress, SGs can be targeted to vacuole for degradation by process called granulophagy

(Buchan, Kolaitis et al. 2013). Since SGs are put into context with neurodegenerative diseases, as are amylotrophic lateral sclerosis, frontotemporal dementia and others (for a review see (Vanderweyde, Youmans et al. 2013)), Buchan et al. suggest that inappropriate degradation of SGs by granulophagy may be related to such pathologies.

Summary of the heat-induced stress granules part

Stress granules and also processing bodies play important, although still not completely and in detail understood, role in regulation of translation, mRNA turnover and consequently in many physiological processes. The relationship between these two types of mRNPs accumulations and their exact roles in the "mRNA cycle" are also still not completely clear. The research on *Saccharomyces cerevisiae* helps in answering raised questions. By the usage of heat-induced SGs as a model system for SGs research, we contributed to findings that SGs phenomenon is spread across eukaryotic kingdom and thus belongs to evolutionary conserved part of cell stress response. In terms of the "mRNA cycle" model, we showed that SGs can be assembled either independently on pre-existing PBs under robust and sudden stresses or that SGs are remodelled from PBs upon prolonged and intensity-increasing stresses. Heat-induced SGs, as well as other the yeast SGs, utilize signalling cascades controlling their assembly which seem to be evolutionary older than those of higher eukaryotes. However, the exact mechanism of the yeast SGs assembly is mostly unknown. The finding that heat-induced SGs contain, besides expected translation initiation factors, also translation elongation and termination factors may provide clue to elucidate SGs assembly mechanism. Even if it is shown that these translation factors are not the primary mediators of heat stress effects on translation process, it still could be possible that the factors are structural cornerstones of the SGs formation process. The beneficial function of SGs in cell survival was many times proved. We supported this hypothesis by finding that SGs serve as local depositories of translation machinery components which are mobilized after a stress relief and thus help to efficient restoration of translation. However, SGs may also spin out of control and as deleterious aggregates can contribute to various cell pathologies. Despite we proved that the yeast prion protein (eRF3/Sup35/[PSI+]) does not play essential role in heat-induced SGs dynamics, its presence in the SGs points to the connection between SGs and neurodegenerative and other *unfolded protein* diseases. Taken together, we hope that further study of heat-induced stress granules of *S. cerevisiae* will help in better understanding not

only of yeast SGs, but also of functions, dynamics and possible relation to various pathologies of higher eukaryotes‘ SGs, including those of mammals.

Heat stress-induced SGs-associated protein - Mmi1

Stress granules as sites of local accumulation of translation machinery components concentrate also proteins which are not directly linked to translation. In higher eukaryotes, those comprise proteins engaged in multiple aspects of mRNA metabolism, as are pre-mRNA splicing, mRNA silencing or mRNA decay. In addition, proteins involved in cell growth, development, adhesion, cellular signalling and even others are present in SGs (for a review see (Anderson and Kedersha 2008)). In yeasts, SGs harbour also additional and stress-specific components. They include translation repressors and mRNA decay factors Dhh1 and Dcp2, mRNA processing and exporting factors Hrp1 and Gbp2 or protein kinase Ksp1 (Grousl, Ivanov et al. 2009) (Buchan, Muhlrad et al. 2008) (Mitchell, Jain et al. 2013).

Another example of protein sequestered by SGs is Mmi1 / Tma19, which was found to be in association with heat stress-induced SGs of *S. cerevisiae* (Rinnerthaler, Lejskova et al. 2013). The protein was first identified in screen for ribosome-associated proteins and found to influence protein synthesis rates, possibly via translation initiation (Fleischer, Weaver et al. 2006). Afterwards, Mmi1 connection to microtubules and mitochondria has been found and Mmi1 role as stress response modulator has been proposed (Rinnerthaler, Jarolim et al. 2006). Concerning heat stress, *mmi1Δ* strain is sensitive to mild heat stress at 37°C (Sinha, David et al. 2008). Whether the thermosensitive phenotype of *mmi1Δ* strain at 37°C is directly linked to its function in translation or not, remains to be established. Surprisingly, we found that the same strain is more resistant to robust heat shock at 46°C, illustrated on increased survival rate in comparison to wild-type strain under the stress (Rinnerthaler, Lejskova et al. 2013). These seemingly contradictory results can be explained by qualitatively distinct responses of the cell to mild and robust heat stresses (see the *Heat stress and translation* chapter).

With the respect to documented Mmi1 function in translation and to its association with heat shock-induced SGs, it is possible that observed phenotypes of *mmi1Δ* strain are directly linked to Mmi1 function in heat-stress translation regulation. However, following this hypothesis, Mmi1 would have to fulfil, at least, two distinct translation functions depending on intensity of heat stress (37°C or 46°C). Moreover, Mmi1 engagement in robust heat stress

response does not probably directly involve assembly and disassembly of SGs, because Mmi1 absence does not alter these SGs dynamic properties (Rinnerthaler, Lejskova et al. 2013).

Alternatively, a structural and functional link between Mmi1 and protein degradation machinery may take part in Mmi1 functioning in heat stress response. Additionally to Mmi1 association with heat-induced SGs, the protein has been shown to co-localize either with proteasomal marker Rpn1 in nuclear region or with de-ubiquitination factors in cytosol under conditions of a heat stress. Moreover, one of Mmi1 functions in the cell seems to be modulation of proteasomal activity (Rinnerthaler, Lejskova et al. 2013). In particular, Mmi1 inhibits proteasomal activity both, under non-stressed conditions and, in combination with the effect of heat stress, also under the heat stress. However, since Mmi1 influences proteasomal activity even under non-stress conditions, this process is not essentially linked to mentioned changes of Mmi1 localization pattern upon heat stress conditions. The fact that Mmi1 co-localizes also with chaperone Cdc48 upon heat stress (Rinnerthaler, Lejskova et al. 2013) and that Cdc48 has been proposed to play a role in turnover of no-more needed SGs (Buchan, Kolaitis et al. 2013) opens a possibility that Mmi1 mediates just this protective SGs removal (see also the *Heat stress-induced stress granules* chapter).

Interestingly, component of fission yeast eIF3 translation initiation complex, Sum1 (Tif34 in *S. cerevisiae*), which is a constituent of fission yeast SGs, has been found to display physical and genetic interaction with the proteasomal complex (Dunand-Sauthier, Walker et al. 2002), similarly as Mmi1 in the budding yeast (see above). In addition, orthologs of factors engaged in protein de-ubiquitination in *S. cerevisiae*, Bre5 and Ubp3 which has been identified to associate with Mmi1 upon heat stress, are localized to or influence SGs of both *Sch. pombe* and mammals (Rinnerthaler, Lejskova et al. 2013) (Wang, Wen et al. 2012) (Ohn, Kedersha et al. 2008) (Tourriere, Chebli et al. 2003). These data imply that the connection between SGs and protein degradation pathways is evolutionary conserved.

Recently, it has been shown that heat-induced SGs of *S. cerevisiae* co-accumulate with misfolded protein aggregates, which are formed due to heat stress (Cherkasov, Hofmann et al. 2013). The interconnection is believed to co-ordinate cellular heat stress response. In detail, protein folding status of the cell controls translation machinery via molecular chaperons, which are required for disassembly of SGs and thus for restoration of translation. This particular mode of co-regulation of translation and protein homeostasis seems to be evolutionary conserved among lower eukaryotes but not, for example, in mammals (Cherkasov, Hofmann et al. 2013).

Taken together, despite newly discovered connection of Mmi1 with heat-induced stress granules and protein degradation system, precise roles of the protein in these cellular processes under heat stress remain unclear and they are subjects for further research. Nevertheless, with the respect to multiple functions of Mmi1 / TCTP protein family members in higher eukaryotes including mammals (see *Review of Literature*), newly discovered data about the yeast agent are the next piece in elucidating complex role of Mmi1 / TCPT family proteins in cell metabolism.

Nox enzymes and Yno1 of S. cerevisiae

One of possible effects of a stress on the cell is damaging of cellular components, as are proteins, nucleic acids and lipids. Stress responsive expression program is engaged to alleviate impacts of such a stress on cell homeostasis. However, the damaged molecules must be also properly removed to avoid their possible further noxious effects. On the level of translation process and translation machinery *per se*, this protective degradation system is documented by granulophagy of stress granules (see the *Heat stress-induced stress granules* chapter). Beside alterations of translation profile and translation process itself, protein homeostasis is targeted even more directly under stress conditions. Proteins conformation, stability and even integrity are influenced by a stress. One of major contributors to proteins damaging under various stresses are so called – Reactive Species (RS) (see also *Review of Literature*). However, RS are not only unwanted and deleterious by-products of cell metabolism and mediators of a stress. They serve also as signalling molecules and together with cellular antioxidant defence systems co-regulate cell fate.

Reactive Species had been found to hold signalling functions in development of multicellular organisms including fungi (for a review see (Takemoto, Tanaka et al. 2007)) and it was thus believed that NOX enzymes had appeared in evolution for certain purposes of multicellular metabolism. Alternatively, NOX enzymes were thought to be lost in evolution resulting in their lack in unicellular organisms as are *S. cerevisiae* or *Sch. pombe* (Lalucque and Silar 2003). From the time when the first NOX enzyme was found in filamentous fungus *Podospora anserine* (Lalucque and Silar 2003), members of the protein family were further identified across fungi kingdom (for a review see (Takemoto, Tanaka et al. 2007)). However, strictly only fungi species with multicellular structures, as is fruiting body, were among the identified. It supports the hypothesis that NOX enzymes possess multicellular-specific

functions. Surprisingly, genuine NADPH oxidase has been now found in unicellular hemiascomycetous fungus *Saccharomyces cerevisiae* (Rinnerthaler, Buttner et al. 2012). It is the first evidence about presence of NOX enzyme in hemiascomycetous fungi and, to my knowledge, in solely unicellular organisms at all.

The identification of NOX enzyme in *S. cerevisiae* raises many questions. What is exact role for NADPH oxidase in unicellular eukaryotic cell? Are there additional NOX enzymes in *S. cerevisiae* or in other unicellular organisms? How the yeast NADPH oxidase is regulated and to which signalling cascades is connected? The answers for all of these questions are subjects for further research. Nevertheless, first evidences about yeast NADPH oxidase of *S. cerevisiae*, Yno1, and its involvement in cellular metabolism exist. After what NADPH oxidase activity and production of superoxide were proved for Yno1, the protein has been suggested to participate in regulation of actin cytoskeleton dynamics and also in signalling to programmed cell death (Rinnerthaler, Buttner et al. 2012). The previous finding that deletion of *yno1* gene displays synthetic haploinsuficient phenotype with actin (*act1*) gene (Haarer, Viggiano et al. 2007) was enriched by the finding that the strain carrying deletion of *yno1* gene is sensitive to actin-destabilizing drugs (Rinnerthaler, Buttner et al. 2012). These data suggest a connection of RS production, e.g. by NOX enzymes, and actin cytoskeleton dynamics, as it was proposed even for higher eukaryotes ((San Martin and Griendling 2010) and references therein). Additionally, *yno1* deletion strain is less sensitive to apoptotic stimuli. Consistently, overproduction of Yno1 leads to Yca1-dependent apoptosis of the yeast cells (Rinnerthaler, Buttner et al. 2012). The role of Yno1 in RS-mediated yeast aging and apoptosis is supported by the evidence which interconnects production of RS (especially ROS) by Yno1 and dysfunctional mitochondria. When mitochondrial cytochrome c oxidase activity is impaired, the organelle accumulates Ras2 signalling molecule on its outer membrane. Consequently, it leads to suppression of ERAD-mediated degradation of Yno1 and in aberrant production of ROS by the protein. In conclusion, the hypothesis where dysfunctional mitochondria serve as a signalling platform rather than producer of ROS and where the later activity is adopted by Yno1 is established (Leadsham, Sanders et al. 2013). Those authors also suggest that mentioned mechanism of mitochondria-based Ras signalling which influences ROS production by Yno1 leads to aberrant accumulation of ROS, loss of redox homeostasis and accelerated aging of the cell. The recent report provides more straightforward evidence about another physiological function of Yno1 protein. Production of superoxide by Yno1 was shown to take part in inhibition of mitochondrial respiration under presence of glucose. A process of the inhibition is mediated by a superoxide dismutase

enzyme (Sod1) which utilizes superoxide produced by Yno1 and, in turn, stabilizes casein kinases, which are required for repression of respiration (Reddi and Culotta 2013).

Despite it was believed for a long time that NOX (NADPH oxidase) enzymes are present only in multicellular organisms, a member of this protein family has been recently identified in unicellular yeast *S. cerevisiae* (Rinnerthaler, Buttner et al. 2012). The first reports about functions of Yno1 in the yeast metabolism suggest that the protein probably participates in similar RS-related processes to those of higher eukaryotes' cells. These processes include regulation of actin cytoskeleton dynamics, cell aging and apoptosis or co-regulation of crucial metabolic pathways. It opens a possibility to use this model organism to study NOX-related processes and possibly to undercover missing parts in NOX enzymes functioning in higher eukaryotes. However, the identification of Yno1 as the yeast NADPH oxidase is only the first step on the road.

Summary of the Mmi1 and Yno1 part

The unexpected ability of stress granules to sequestrate protein factors which are not directly engaged in translation or mRNA-related processes interconnects both SGs and regulation of translation with broad range of cellular processes. Association of Mmi1 protein with heat-induced SGs of *S. cerevisiae* probably does not play a role in heat stress response mediated by SGs *per se*, but rather may take part in proposed and evolutionary conserved connection of SGs and protein degradation system. Despite Mmi1 influence on the proteasomal function is, in general, independent on heat stress, it is plausible that an association of Mmi1 with SGs and concurrently with protein degradation system under heat stress has its physiological, but yet unknown, consequences.

The protein homeostasis is not influenced solely by alteration of translation process under a stress. Proteins themselves are direct targets for deleterious effects of certain stresses. One of major mediators of such stresses are *Reactive Species* (RS). However, RS participate not only in pathological, but even in physiological processes in the cell and thus constitute indispensable part of cell metabolism. Discovery of a NADPH oxidase (NOX) enzyme family member in yeast *S. cerevisiae*, Yno1 protein, has the potential to contribute to more complex knowledge about these RS-producers and their roles in cell metabolism not only in the yeast, but also in higher eukaryotes.

7. Conclusion

We identified and further characterized heat-induced stress granules (SGs) of yeast *Saccharomyces cerevisiae*. Concerning this, our research contributed to general knowledge of SGs phenomenon. It was proved by us and others that SGs are evolutionary conserved across eukaryotic kingdom and therefore, they very likely constitute the indispensable part of cellular stress response. There is also an effort to assign particular function and position of SGs in the "mRNA cycle". However, the general model of the “mRNA cycle” should be always accommodated by intensity, duration and speed of onset of a stress. In connection, roles of SGs or processing bodies (PBs) in translation regulation and mRNA turnover are stress-specific. Whereas PBs can be engaged in mRNA storage, mRNA degradation or in return of mRNA molecules to active translation under certain conditions, stress granules adopt some of these functions under other stresses. Moreover, we experimentally supported and identified with the hypothesis where SGs serve also as a platform for efficient restoration of translation process after a stress relief.

The SGs composition may reflect a mechanism of their assembly and an engagement of different signalling pathways. We and others showed that dynamic properties and a composition of SGs are stress-specific. In addition, we proved that, as well as other lower eukaryotes, *S. cerevisiae* utilizes eIF2α-phosphorylation independent and probably evolutionary old pathway(s) for SGs assembly. In addition, on the basis of dynamic properties of heat-induced SGs and their specific composition, we suggest possible models for regulation of the yeast translation under a heat stress. The further research towards elucidating this mechanism and exact mechanism of heat-induced SGs assembly is promising in respect to SGs involvement in entire cellular metabolism and also in certain pathologies. Other promising field of heat-induced SGs research concerns analysing proposed interconnection of the SGs to other cellular structures, as is the cytoskeleton or the mitochondria, which may shed more light to SGs functioning in the cell.

Despite we have not yet clarified role of *microtubule and mitochondria interacting protein 1* (Mmi1) in observed connection of heat-induced SGs to the mitochondria, we proved that Mmi1 is a SGs-associated protein. Concurrently, we proposed a role for Mmi1 in heat stress response connecting sequestration of the protein in the SGs and its effect on protein degradation system of the cell. Since Mmi1 belongs to evolutionary conserved protein family and physiological functions of its human ortholog TCTP in broad range of metabolic processes are still not completely known, further research on Mmi1 of *S. cerevisiae* promises

to enrich knowledge about this protein family members in general and about their roles in the eukaryotic cell.

In an effort to analyse effects of *Reactive Species*-producers on heat-induced stress granules and on cell physiology in general, we contributed to identification and further characterization of the first known member of NOX (NADPH oxidase) enzyme family in yeast *S. cerevisiae*. Since NOX enzymes as *Reactive Species*-producers participate in various cellular processes and they were believed to be specific for multicellular organisms, the discovery of Yno1 protein in the unicellular yeast may bring new evidences not only about its functioning in the yeast metabolism, but also about roles of NOX enzymes in higher eukaryotes.

References

Anderson, P. and N. Kedersha (2002). "Stressful initiations." J Cell Sci 115(Pt 16): 3227-34.

Anderson, P. and N. Kedersha (2006). "RNA granules." J Cell Biol 172(6): 803-8.

Anderson, P. and N. Kedersha (2008). "Stress granules: the Tao of RNA triage." Trends Biochem Sci 33(3): 141-50.

Arimoto, K., H. Fukuda, et al. (2008). "Formation of stress granules inhibits apoptosis by suppressing stress-responsive MAPK pathways." Nat Cell Biol 10(11): 1324-32.

Arribere, J. A., J. A. Doudna, et al. (2011). "Reconsidering movement of eukaryotic mRNAs between polysomes and P bodies." Mol Cell 44(5): 745-58.

Ashe, M. P., S. K. De Long, et al. (2000). "Glucose depletion rapidly inhibits translation initiation in yeast." Mol Biol Cell 11(3): 833-48.

Ashe, M. P., J. W. Slaven, et al. (2001). "A novel eIF2B-dependent mechanism of translational control in yeast as a response to fusel alcohols." EMBO J 20(22): 6464-74.

Balagopal, V., L. Fluch, et al. (2012). "Ways and means of eukaryotic mRNA decay." Biochim Biophys Acta 1819(6): 593-603.

Balagopal, V. and R. Parker (2009). "Polysomes, P bodies and stress granules: states and fates of eukaryotic mRNAs." Current Opinion in Cell Biology 21(3): 403-408.

Balagopal, V. and R. Parker (2011). "Stm1 modulates translation after 80S formation in Saccharomyces cerevisiae." RNA 17(5): 835-42.

Bommer, U. A. (2012). "Cellular Function and Regulation of the Translationally Controlled Tumour Protein TCTP." The Open Allergy Journal 5: 19-32.

Bommer, U. A. and B. J. Thiele (2004). "The translationally controlled tumour protein (TCTP)." Int J Biochem Cell Biol 36(3): 379-85.

Brengues, M. and R. Parker (2007). "Accumulation of polyadenylated mRNA, Pab1p, eIF4E, and eIF4G with P-bodies in Saccharomyces cerevisiae." Mol Biol Cell 18(7): 2592-602.

Brengues, M., D. Teixeira, et al. (2005). "Movement of eukaryotic mRNAs between polysomes and cytoplasmic processing bodies." Science 310(5747): 486-9.

Buchan, J. R., R. M. Kolaitis, et al. (2013). "Eukaryotic stress granules are cleared by autophagy and Cdc48/VCP function." Cell 153(7): 1461-74.

Buchan, J. R., D. Muhlrad, et al. (2008). "P bodies promote stress granule assembly in Saccharomyces cerevisiae." J Cell Biol 183(3): 441-55.

Buchan, J. R. and R. Parker (2009). "Eukaryotic stress granules: the ins and outs of translation." Mol Cell 36(6): 932-41.

Buchan, J. R., J. H. Yoon, et al. (2011). "Stress-specific composition, assembly and kinetics of stress granules in Saccharomyces cerevisiae." J Cell Sci 124(Pt 2): 228-39.

Campbell, S. G., N. P. Hoyle, et al. (2005). "Dynamic cycling of eIF2 through a large eIF2B-containing cytoplasmic body: implications for translation control." J Cell Biol 170(6): 925-34.

Castelli, L. M., J. Lui, et al. (2011). "Glucose depletion inhibits translation initiation via eIF4A loss and subsequent 48S preinitiation complex accumulation, while the pentose phosphate pathway is coordinately up-regulated." Mol Biol Cell 22(18): 3379-93.

Cowart, L. A., J. L. Gandy, et al. (2010). "Sphingolipids mediate formation of mRNA processing bodies during the heat-stress response of Saccharomyces cerevisiae." Biochem J 431(1): 31-8.

Dang, Y., N. Kedersha, et al. (2006). "Eukaryotic initiation factor 2alpha-independent pathway of stress granule induction by the natural product pateamine A." J Biol Chem 281(43): 32870-8.

Davidson, J. F., B. Whyte, et al. (1996). "Oxidative stress is involved in heat-induced cell death in Saccharomyces cerevisiae." Proc Natl Acad Sci U S A 93(10): 5116-21.

Decker, C. J., D. Teixeira, et al. (2007). "Edc3p and a glutamine/asparagine-rich domain of Lsm4p function in processing body assembly in Saccharomyces cerevisiae." J Cell Biol 179(3): 437-49.

DeLeo, F. R., J. B. Burritt, et al. (2000). "Processing and maturation of flavocytochrome b558 include incorporation of heme as a prerequisite for heterodimer assembly." J Biol Chem 275(18): 13986-93.

Derkatch, I. L., Y. O. Chernoff, et al. (1996). "Genesis and variability of [PSI] prion factors in Saccharomyces cerevisiae." Genetics 144(4): 1375-86.

Dori, D. and M. Choder (2007). "Conceptual modeling in systems biology fosters empirical findings: the mRNA lifecycle." Plos One 2(9): e872.

Dunand-Sauthier, I., C. Walker, et al. (2002). "Sum1, a component of the fission yeast eIF3 translation initiation complex, is rapidly relocalized during environmental stress and interacts with components of the 26S proteasome." Mol Biol Cell 13(5): 1626-40.

Estruch, F. (2000). "Stress-controlled transcription factors, stress-induced genes and stress tolerance in budding yeast." FEMS Microbiol Rev 24(4): 469-86.

Eulalio, A., I. Behm-Ansmant, et al. (2007). "P bodies: at the crossroads of post-transcriptional pathways." Nat Rev Mol Cell Biol 8(1): 9-22.

Eulalio, A., I. Behm-Ansmant, et al. (2007). "P-body formation is a consequence, not the cause, of RNA-mediated gene silencing." Mol Cell Biol 27(11): 3970-81.

Farny, N. G., N. L. Kedersha, et al. (2009). "Metazoan stress granule assembly is mediated by P-eIF2alpha-dependent and -independent mechanisms." RNA 15(10): 1814-21.

Finegold, A. A., K. P. Shatwell, et al. (1996). "Intramembrane bis-heme motif for transmembrane electron transport conserved in a yeast iron reductase and the human NADPH oxidase." J Biol Chem 271(49): 31021-4.

Fleischer, T. C., C. M. Weaver, et al. (2006). "Systematic identification and functional screens of uncharacterized proteins associated with eukaryotic ribosomal complexes." Genes Dev 20(10): 1294-307.

Georgatsou, E. and D. Alexandraki (1999). "Regulated expression of the Saccharomyces cerevisiae Fre1p/Fre2p Fe/Cu reductase related genes." Yeast 15(7): 573-84.

Gilks, N., N. Kedersha, et al. (2004). "Stress granule assembly is mediated by prion-like aggregation of TIA-1." Mol Biol Cell 15(12): 5383-98.

Gregio, A. P., V. P. Cano, et al. (2009). "eIF5A has a function in the elongation step of translation in yeast." Biochem Biophys Res Commun 380(4): 785-90.

Grousl, T., P. Ivanov, et al. (2009). "Robust heat shock induces eIF2 alpha-phosphorylation-independent assembly of stress granules containing eIF3 and 40S ribosomal subunits in budding yeast, Saccharomyces cerevisiae." Journal of Cell Science 122(12): 2078-2088.

Grousl, T., P. Ivanov, et al. (2013). "Heat Shock-Induced Accumulation of Translation Elongation and Termination Factors Precedes Assembly of Stress Granules in S. cerevisiae." Plos One 8(2): e57083.

Gutierrez, E., B. S. Shin, et al. (2013). "eIF5A promotes translation of polyproline motifs." Mol Cell 51(1): 35-45.

Haarer, B., S. Viggiano, et al. (2007). "Modeling complex genetic interactions in a simple eukaryotic genome: actin displays a rich spectrum of complex haploinsufficiencies." Genes Dev 21(2): 148-59.

Herruer, M. H., W. H. Mager, et al. (1988). "Mild temperature shock affects transcription of yeast ribosomal protein genes as well as the stability of their mRNAs." Nucleic Acids Res 16(16): 7917-29.

Hess, D. C., C. L. Myers, et al. (2009). "Computationally driven, quantitative experiments discover genes required for mitochondrial biogenesis." PLoS Genet 5(3): e1000407.

Hinnebusch, A. G. (2005). "eIF2alpha kinases provide a new solution to the puzzle of substrate specificity." Nat Struct Mol Biol 12(10): 835-8.

Hinnebusch, A. G. (2005). "Translational regulation of GCN4 and the general amino acid control of yeast." Annu Rev Microbiol 59: 407-50.

Hinnebusch, A. G. and J. R. Lorsch (2012). "The mechanism of eukaryotic translation initiation: new insights and challenges." Cold Spring Harb Perspect Biol 4(10).

Hinojosa-Moya, J., B. Xoconostle-Cazares, et al. (2008). "Phylogenetic and structural analysis of translationally controlled tumor proteins." J Mol Evol 66(5): 472-83.

Hofmann, S., V. Cherkasova, et al. (2012). "Translation suppression promotes stress granule formation and cell survival in response to cold shock." Mol Biol Cell 23(19): 3786-3800.

Hood, H. M., D. E. Neafsey, et al. (2009). "Evolutionary roles of upstream open reading frames in mediating gene regulation in fungi." Annu Rev Microbiol 63: 385-409.

Hoyle, N. P., L. M. Castelli, et al. (2007). "Stress-dependent relocalization of translationally primed mRNPs to cytoplasmic granules that are kinetically and spatially distinct from P-bodies." J Cell Biol 179(1): 65-74.

Huang, H. T., J. Maruyama, et al. (2013). "Aspergillus oryzae AoSO Is a Novel Component of Stress Granules upon Heat Stress in Filamentous Fungi." PLoS One 8(8): e72209.

Chakraburtty, K. (2001). "Translational regulation by ABC systems." Res Microbiol 152(3-4): 391-9.

Cherkasov, V., S. Hofmann, et al. (2013). "Coordination of Translational Control and Protein Homeostasis during Severe Heat Stress." Curr Biol 23(24): 2452-62.

Iwaki, A., T. Kawai, et al. (2013). "Biomass conversion inhibitors furfural and 5-hydroxymethylfurfural induce formation of messenger RNP granules and attenuate translation activity in Saccharomyces cerevisiae." Appl Environ Microbiol 79(5): 1661-7.

Iwaki, A., S. Ohnuki, et al. (2013). "Vanillin inhibits translation and induces messenger ribonucleoprotein (mRNP) granule formation in saccharomyces cerevisiae: application and validation of high-content, image-based profiling." PLoS One 8(4): e61748.

Jones, B. L., J. Vanloozen, et al. (2013). "Stress granules form in Brachionus manjavacas (Rotifera) in response to a variety of stressors." Comp Biochem Physiol A Mol Integr Physiol 166(2): 375-84.

Jud, M. C., M. J. Czerwinski, et al. (2008). "Large P body-like RNPs form in C. elegans oocytes in response to arrested ovulation, heat shock, osmotic stress, and anoxia and are regulated by the major sperm protein pathway." Dev Biol 318(1): 38-51.

Kamath, A. and K. Chakraburtty (1989). "Role of yeast elongation factor 3 in the elongation cycle." J Biol Chem 264(26): 15423-8.

Kato, K., Y. Yamamoto, et al. (2011). "Severe ethanol stress induces assembly of stress granules in Saccharomyces cerevisiae." Yeast 28(5): 339-47.

Kedersha, N. and P. Anderson (2009). "Regulation of translation by stress granules and processing bodies." Prog Mol Biol Transl Sci 90: 155-85.

Kedersha, N., S. Chen, et al. (2002). "Evidence that ternary complex (eIF2-GTP-tRNA(i)(Met))-deficient preinitiation complexes are core constituents of mammalian stress granules." Mol Biol Cell 13(1): 195-210.

Kedersha, N., M. R. Cho, et al. (2000). "Dynamic shuttling of TIA-1 accompanies the recruitment of mRNA to mammalian stress granules." J Cell Biol 151(6): 1257-68.

Kedersha, N. L., M. Gupta, et al. (1999). "RNA-binding proteins TIA-1 and TIAR link the phosphorylation of eIF-2 alpha to the assembly of mammalian stress granules." J Cell Biol 147(7): 1431-42.

Kilchert, C., J. Weidner, et al. (2010). "Defects in the secretory pathway and high Ca2+ induce multiple P-bodies." Mol Biol Cell 21(15): 2624-38.

Kim, B., H. J. Cooke, et al. (2012). "DAZL is essential for stress granule formation implicated in germ cell survival upon heat stress." Development 139(3): 568-78.

Kimball, S. R., R. L. Horetsky, et al. (2003). "Mammalian stress granules represent sites of accumulation of stalled translation initiation complexes." Am J Physiol Cell Physiol 284(2): C273-84.

Kramer, S., R. Queiroz, et al. (2008). "Heat shock causes a decrease in polysomes and the appearance of stress granules in trypanosomes independently of eIF2(alpha) phosphorylation at Thr169." J Cell Sci 121(Pt 18): 3002-14.

Kurata, S., K. H. Nielsen, et al. (2010). "Ribosome recycling step in yeast cytoplasmic protein synthesis is catalyzed by eEF3 and ATP." Proc Natl Acad Sci U S A 107(24): 10854-9.

Kwon, S., Y. Zhang, et al. (2007). "The deacetylase HDAC6 is a novel critical component of stress granules involved in the stress response." Genes Dev 21(24): 3381-94.

Lalucque, H. and P. Silar (2003). "NADPH oxidase: an enzyme for multicellularity?" Trends Microbiol 11(1): 9-12.

Lambeth, J. D. (2007). "Nox enzymes, ROS, and chronic disease: an example of antagonistic pleiotropy." Free Radic Biol Med 43(3): 332-47.

Lambeth, J. D., T. Kawahara, et al. (2007). "Regulation of Nox and Duox enzymatic activity and expression." Free Radic Biol Med 43(3): 319-31.

Leadsham, J. E., G. Sanders, et al. (2013). "Loss of Cytochrome c Oxidase Promotes RAS-Dependent ROS Production from the ER Resident NADPH Oxidase, Yno1p, in Yeast." Cell Metab 18(2): 279-86.

Li, B., C. R. Nierras, et al. (1999). "Transcriptional elements involved in the repression of ribosomal protein synthesis." Mol Cell Biol 19(8): 5393-404.

Li, C. H., T. Ohn, et al. (2010). "eIF5A Promotes Translation Elongation, Polysome Disassembly and Stress Granule Assembly." Plos One 5(3).

Lodish, H., A. Berk, et al. (2003). "Molecular Cell Biology, 5th edition" Freeman, W. H. & Company ISBN: 0716743663

Malys, N. and J. E. McCarthy (2011). "Translation initiation: variations in the mechanism can be anticipated." Cell Mol Life Sci 68(6): 991-1003.

Mateyak, M. K. and T. G. Kinzy (2010). "eEF1A: thinking outside the ribosome." J Biol Chem 285(28): 21209-13.

Mazroui, R., R. Sukarieh, et al. (2006). "Inhibition of ribosome recruitment induces stress granule formation independently of eukaryotic initiation factor 2alpha phosphorylation." Mol Biol Cell 17(10): 4212-9.

Meier, K. D., O. Deloche, et al. (2006). "Sphingoid base is required for translation initiation during heat stress in Saccharomyces cerevisiae." Mol Biol Cell 17(3): 1164-75.

Mitchell, S. F., S. Jain, et al. (2013). "Global analysis of yeast mRNPs." Nat Struct Mol Biol 20(1): 127-33.

Morano, K. A., C. M. Grant, et al. (2012). "The response to heat shock and oxidative stress in Saccharomyces cerevisiae." Genetics 190(4): 1157-95.

Murphy, M. P. (2009). "How mitochondria produce reactive oxygen species." Biochem J 417(1): 1-13.

Nauseef, W. M. (2008). "Biological roles for the NOX family NADPH oxidases." J Biol Chem 283(25): 16961-5.

Nilsson, D. and P. Sunnerhagen (2011). "Cellular stress induces cytoplasmic RNA granules in fission yeast." RNA 17(1): 120-33.

Nonhoff, U., M. Ralser, et al. (2007). "Ataxin-2 interacts with the DEAD/H-box RNA helicase DDX6 and interferes with P-bodies and stress granules." Mol Biol Cell 18(4): 1385-96.

Ohn, T., N. Kedersha, et al. (2008). "A functional RNAi screen links O-GlcNAc modification of ribosomal proteins to stress granule and processing body assembly." Nat Cell Biol 10(10): 1224-31.

Parker, R. (2012). "RNA degradation in Saccharomyces cerevisae." Genetics 191(3): 671-702.

Parker, R. and U. Sheth (2007). "P bodies and the control of mRNA translation and degradation." Mol Cell 25(5): 635-46.

Pavitt, G. D., K. V. Ramaiah, et al. (1998). "eIF2 independently binds two distinct eIF2B subcomplexes that catalyze and regulate guanine-nucleotide exchange." Genes Dev 12(4): 514-26.

Pisarev, A. V., M. A. Skabkin, et al. (2010). "The role of ABCE1 in eukaryotic posttermination ribosomal recycling." Mol Cell 37(2): 196-210.

Planta, R. J. (1997). "Regulation of ribosome synthesis in yeast." Yeast 13(16): 1505-18.

Proud, C. G. (2005). "eIF2 and the control of cell physiology." Semin Cell Dev Biol 16(1): 3-12.

Rajyaguru, P., M. She, et al. (2012). "Scd6 targets eIF4G to repress translation: RGG motif proteins as a class of eIF4G-binding proteins." Mol Cell 45(2): 244-54.

Reddi, A. R. and V. C. Culotta (2013). "SOD1 integrates signals from oxygen and glucose to repress respiration." Cell 152(1-2): 224-35.

Rinnerthaler, M., S. Buttner, et al. (2012). "Yno1p/Aim14p, a NADPH-oxidase ortholog, controls extramitochondrial reactive oxygen species generation, apoptosis, and actin cable formation in yeast." Proc Natl Acad Sci U S A 109(22): 8658-63.

Rinnerthaler, M., S. Jarolim, et al. (2006). "MMI1 (YKL056c, TMA19), the yeast orthologue of the translationally controlled tumor protein (TCTP) has apoptotic functions and interacts with both microtubules and mitochondria." Biochim Biophys Acta 1757(5-6): 631-8.

Rinnerthaler, M., R. Lejskova, et al. (2013). "Mmi1, the yeast homologue of Mammalian TCTP, associates with stress granules in heat-shocked cells and modulates proteasome activity." PLoS One 8(10): e77791.

Saavedra, C., K. S. Tung, et al. (1996). "Regulation of mRNA export in response to stress in Saccharomyces cerevisiae." Genes Dev 10(13): 1608-20.

Saavedra, C. A., C. M. Hammell, et al. (1997). "Yeast heat shock mRNAs are exported through a distinct pathway defined by Rip1p." Genes Dev 11(21): 2845-56.

Saini, P., D. E. Eyler, et al. (2009). "Hypusine-containing protein eIF5A promotes translation elongation." Nature 459(7243): 118-21.

San Martin, A. and K. K. Griendling (2010). "Redox control of vascular smooth muscle migration." Antioxid Redox Signal 12(5): 625-40.

Scarcelli, J. J., S. Viggiano, et al. (2008). "Synthetic genetic array analysis in Saccharomyces cerevisiae provides evidence for an interaction between RAT8/DBP5 and genes encoding P-body components." Genetics 179(4): 1945-55.

Shah, K. H., B. Zhang, et al. (2013). "Processing body and stress granule assembly occur by independent and differentially regulated pathways in Saccharomyces cerevisiae." Genetics 193(1): 109-23.

Shenton, D., J. B. Smirnova, et al. (2006). "Global translational responses to oxidative stress impact upon multiple levels of protein synthesis." J Biol Chem 281(39): 29011-21.

Sheth, U. and R. Parker (2003). "Decapping and decay of messenger RNA occur in cytoplasmic processing bodies." Science 300(5620): 805-808.

Shoemaker, C. J. and R. Green (2011). "Kinetic analysis reveals the ordered coupling of translation termination and ribosome recycling in yeast." Proc Natl Acad Sci U S A 108(51): E1392-8.

Simpson, C. E. and M. P. Ashe (2012). "Adaptation to stress in yeast: to translate or not?" Biochem Soc Trans 40(4): 794-9.

Sinha, H., L. David, et al. (2008). "Sequential elimination of major-effect contributors identifies additional quantitative trait loci conditioning high-temperature growth in yeast." Genetics 180(3): 1661-70.

Takahara, T. and T. Maeda (2012). "Transient sequestration of TORC1 into stress granules during heat stress." Mol Cell 47(2): 242-52.

Takemoto, D., A. Tanaka, et al. (2007). "NADPH oxidases in fungi: diverse roles of reactive oxygen species in fungal cellular differentiation." Fungal Genet Biol 44(11): 1065-76.

Ter-Avanesyan, M. D., A. R. Dagkesamanskaya, et al. (1994). "The SUP35 omnipotent suppressor gene is involved in the maintenance of the non-Mendelian determinant [psi+] in the yeast Saccharomyces cerevisiae." Genetics 137(3): 671-6.

Thaw, P., N. J. Baxter, et al. (2001). "Structure of TCTP reveals unexpected relationship with guanine nucleotide-free chaperones." Nat Struct Biol 8(8): 701-4.

Thompson, D. M., C. Lu, et al. (2008). "tRNA cleavage is a conserved response to oxidative stress in eukaryotes." RNA 14(10): 2095-103.

Thompson, D. M. and R. Parker (2009). "Stressing out over tRNA cleavage." Cell 138(2): 215-9.

Tourriere, H., K. Chebli, et al. (2003). "The RasGAP-associated endoribonuclease G3BP assembles stress granules." J Cell Biol 160(6): 823-31.

Uniacke, J. and W. Zerges (2008). "Stress induces the assembly of RNA granules in the chloroplast of Chlamydomonas reinhardtii." J Cell Biol 182(4): 641-6.

Van Dyke, N., J. Baby, et al. (2006). "Stm1p, a ribosome-associated protein, is important for protein synthesis in Saccharomyces cerevisiae under nutritional stress conditions." J Mol Biol 358(4): 1023-31.

Van Dyke, N., B. F. Pickering, et al. (2009). "Stm1p alters the ribosome association of eukaryotic elongation factor 3 and affects translation elongation." Nucleic Acids Res 37(18): 6116-25.

Vanderweyde, T., K. Youmans, et al. (2013). "Role of Stress Granules and RNA-Binding Proteins in Neurodegeneration: A Mini-Review." Gerontology 59(6): 524-33.

Wang, C. Y., W. L. Wen, et al. (2012). "Analysis of stress granule assembly in Schizosaccharomyces pombe." RNA 18(4): 694-703.

Weber, C., L. Nover, et al. (2008). "Plant stress granules and mRNA processing bodies are distinct from heat stress granules." Plant J 56(4): 517-30.

Wells, S. E., P. E. Hillner, et al. (1998). "Circularization of mRNA by eukaryotic translation initiation factors." Mol Cell 2(1): 135-40.

Wen, W. L., A. L. Stevenson, et al. (2010). "Vgl1, a multi-KH domain protein, is a novel component of the fission yeast stress granules required for cell survival under thermal stress." Nucleic Acids Res 38(19): 6555-66.

Yamamoto, Y. and S. Izawa (2013). "Adaptive response in stress granule formation and bulk translational repression upon a combined stress of mild heat shock and mild ethanol stress in yeast." Genes Cells.

Yu, L., M. T. Quinn, et al. (1998). "Gp91(phox) is the heme binding subunit of the superoxide-generating NADPH oxidase." Proc Natl Acad Sci U S A 95(14): 7993-8.

Zavialov, A. V., V. V. Hauryliuk, et al. (2005). "Splitting of the posttermination ribosome into subunits by the concerted action of RRF and EF-G." Mol Cell 18(6): 675-86.